Production and preservation of archaeal glycerol dibiphytanyl glycerol tetraethers as intact polar lipids in marine sediments: Implications for their use in microbial ecology and TEX_{86} paleo-thermometry

SABINE KERSTIN LENGGER

Image on Cover: Martin Waugh

ISBN 978-94-6203-385-6

Oh! speculators on things, boast not of knowing the things that nature ordinarily brings about; but rejoice if you know the end of those things which you yourself devise.

The Notebooks of Leonardo Da Vinci, Chapter XIX, 1205

Production and preservation of archaeal glycerol dibiphytanyl glycerol tetraethers as intact polar lipids in marine sediments: Implications for their use in microbial ecology and TEX_{86} paleothermometry

Productie en preservatie van archaeale glycerol dibiphytanyl glycerol tetraethers als intakte polaire lipiden in mariene sedimenten: Implicaties voor hun toepassing in microbiële ecologie en TEX_{86} paleotemperatuurbepalingen

(met een samenvatting in het Nederlands)

Proefschrift

ter verkrijging van de graad van doctor aan de Universiteit Utrecht op gezag van de rector magnificus, prof. dr. G. J. van der Zwaan, ingevolge het besluit van het college voor promoties in het openbaar te verdedigen op donderdag 11 juli 2013 des ochtends te 12.45 uur

door

Sabine Kerstin Lengger

geboren op 22 april 1983 te Leoben, Oostenrijk

Promotoren: Prof. dr. ir. S. Schouten
Prof. dr. ir. J. S. Sinninghe Damsté

The research presented in this thesis was financially supported by the Darwin Center for Biogeosciences and the Royal NIOZ Netherlands Institute for Sea Research, an institution of the NWO Netherlands Organisation for Scientific Research.

Table of Contents

1. Introduction

Part I. Degradation and preservation of IPL-GDGTs.

2. Comparison of extraction and work up techniques for analysis of core and intact polar tetraether lipids from sedimentary environments

   Sabine K. Lengger, Ellen C. Hopmans, Jaap S. Sinninghe Damsté, Stefan Schouten

   Organic Geochemistry **47** (2012) 34-40.

3. Intact polar and core glycerol dibiphytanyl glycerol tetraether lipids in the Arabian Sea oxygen minimum zone. Part II: Selective preservation and degradation in sediments and consequences for the TEX_{86}

   Sabine K. Lengger, Ellen C. Hopmans, Gert-Jan Reichart, Klaas G.J. Nierop, Jaap S. Sinninghe Damsté, Stefan Schouten

   Geochimica et Cosmochimica Acta **98** (2012) 244-258.

4. Impact of oxygen exposure time and deep water column production on GDGT abundance and distribution in surface sediments in the Arabian Sea: Implications for the TEX_{86} paleothermometer

   Sabine K. Lengger, Ellen C. Hopmans, Jaap S. Sinninghe Damsté and Stefan Schouten

   In preparation for *Geochimica et Cosmochimica Acta*.

5. **FOSSILIZATION AND DEGRADATION OF ARCHAEAL INTACT POLAR TETRAETHER LIPIDS IN DEEPLY-BURIED MARINE SEDIMENTS (PERU MARGIN)**

   Sabine K. Lengger , Ellen C. Hopmans, Jaap S. Sinninghe Damsté and Stefan Schouten

   In preparation for *Geobiology*.

6. **DIFFERENTIAL DEGRADATION OF INTACT POLAR AND CORE GLYCEROL DIALKYL GLYCEROL TETRAETHER LIPIDS UPON POST-DEPOSITIONAL OXIDATION**

   Sabine K. Lengger, Mariska Kraaij, Marianne Baas, Rik Tjallingii, Jan-Berend Stuut, Ellen C. Hopmans, Jaap S. Sinninghe Damsté and Stefan Schouten

   Submitted to *Organic Geochemistry*.

PART II. STABLE ISOTOPE PROBING EXPERIMENTS INVESTIGATING *IN SITU* PRODUCTION OF ARCHAEAL GDGTS.

7. **NO DIRECT ROLE OF ARCHAEA IN DEEP SEA BENTHIC ORGANIC CARBON PROCESSING**

   Sabine K. Lengger, Markus M. Moeseneder, Lara Pozzato, Barry Thornton, Ursula Witte, Leon Moodley, Jack J. Middelburg, Jaap S. Sinninghe Damsté and Stefan Schouten

   Submitted to *PLoS ONE*.

8. **LACK OF ^{13}C-LABEL INCORPORATION SUGGESTS LOW TURNOVER RATES OF THAUMARCHAEAL INTACT POLAR TETRAETHER LIPIDS IN SEDIMENTS FROM THE ICELAND SHELF**

   Sabine K. Lengger, Yvonne Lipsewers, Henk de Haas, Jaap S. Sinninghe Damsté and Stefan Schouten

   In preparation for *Biogeosciences*.

References

Summary (English)

Samenvatting (Nederlands)

Acknowledgements

Curriculum vitae

CHAPTER 1

INTRODUCTION

INTRODUCTION

CLIMATE CHANGE AND CLIMATE RECONSTRUCTIONS.

It has been extensively documented that the Earth's climate, decade after decade, is undergoing drastic changes (IPCC Core Writing Team, 2007). Greenhouse gas concentrations in the atmosphere and temperatures increase, via a variety of feedback cycles, many of which are not yet fully understood (Denman et al., 2007). These climatic changes will, in different ways, affect all regions and countries on this planet. To predict with precision the changes the Earth's climate will undergo in the coming years, decades and centuries, in order to anticipate and adapt to these changes is thus one of science's biggest challenges (Meehl et al., 2007). While analysis of recorded climate conditions, biogeochemical measurements and modeling of feedback cycles provide useful information, these approaches are limited. Temperature and weather records, for example, do not stretch beyond the Anthropocene, and instrumental records only go back to ca. 1850. The range of conditions in these short periods of time is very small, hence it is difficult to make long-term projections just relying on these values. In order to gain a larger perspective, it is thus very useful to observe changes over longer time scales, at times in which the Earth has been subjected to extreme, but also moderate conditions and at its responses to them, millions of years before our time (Jansen et al., 2007).

The field of science investigating the Earth's climate of the past, paleoclimatology, relies on geological observations using, for example, isotopic compositions of different elements found in rocks and marine sediments, assemblages of fossils of plants and animals, and chemical fossils of microorganisms. These studies have led to some surprising discoveries. One of them was that the transition from the Paleocene and the Eocene, 55 million years ago, was not only characterized by a rapid temperature rise due to an atmospheric CO_2 increase, caused by an injection of ^{13}C-depleted carbon (Kennett and Stott, 1991), but that this was accompanied by a pronounced acidification of the oceans (Zachos et al., 2005). The increase in temperature was much stronger at high latitudes than at low latitudes, in fact, it was so pronounced that it resulted in almost subtropical temperatures at both Poles (Sluijs et al., 2006; Pross et al., 2012). Clearly, paleoclimatology can reveal details of past climate which are highly relevant for climate modeling, which in turn can give valuable predictions of how the Earth's climate will change in the future.

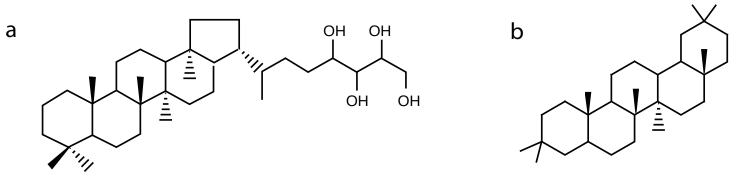

Bacteriohopanetetrol, a hopanoid.

Oleanane, a triterpenoid in Angiosperms.

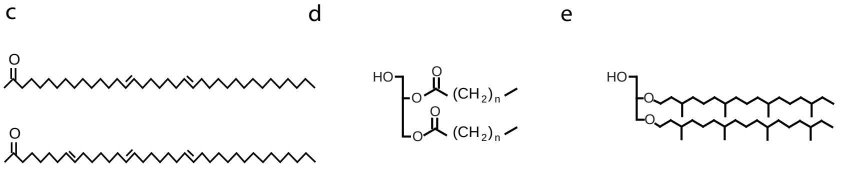

$C_{37:2}$ and $C_{37:3}$ alkenones.

Bacterial diesterlipids.

Archaeal diether lipids.

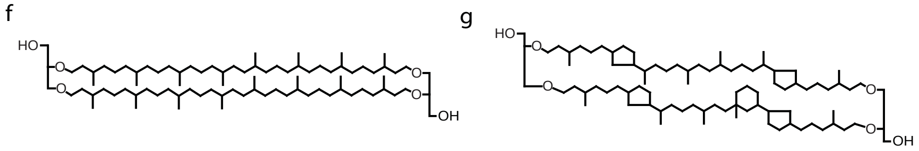

GDGT-0, an archaeal tetraether lipid.

Crenarchaeol, an archaeal tetraether lipid.

Figure 1.1. Biomarker lipids commonly used in molecular paleontology: Bacterial hopanoids (a), triterpenoids (b), alkenones from haptophyte algae (c), bacterial and eukaryotic diester- (d), archaeal dieether- (e) and tetraether lipids (f), with crenarchaeol, the specific tetraether lipid for Thaumarchaeota (g).

BIOMARKER LIPIDS AND ORGANIC PROXIES.

One of the emergent fields within paleoclimatology is the application of biomarker lipids for paleoenvironmental reconstruction. Microorganisms leave traces in the form of recalcitrant biomarker molecules, which can, under favorable conditions, be preserved for up to billions of years, making it possible to find evidence for their existence, distribution, abundance, and even their biochemistry, in the past (Peters et al., 2004 and references cited therein). Biomarkers are compounds which are specific to a group of organisms, can be specific for an environmental condition or a biogeochemical or biochemical process and are chemically stable enough to persist over long – geological - timescales. Many biomarkers fall into the class of the lipids (see examples in Fig. 1.1). These molecules were initially mainly being exploited as indicative for geological periods and processes and evolutionary biology, their research fueled by the added benefit of using them for dating of oil and source rock determination. For example, 2-methylhopanes have been used to constrain the onset of oxygenic photosynthesis (2.5 Gyr; Brocks et al., 1999), and oleanane is used as an indicator for the rise of angiosperms (150 Myr; Moldowan et al., 1994).

Besides their applications as biomarkers, organic microfossils specific for certain paleoenvironmental conditions are now also increasingly used as proxies to quantify past climate conditions. The first organic proxy was developed when a relationship between distribution of long-chain unsaturated alkenones, lipids produced by haptophyte algae, and growth temperature was found, called the U^{K}_{37} index (Brassell et al., 1986; Prahl and Wakeham, 1987). Variations of this index are currently still extensively used to determine past sea surface temperatures, by analyzing alkenone lipids preserved in sediments over millions of years. A second organic temperature proxy was reported in 2002 by Schouten et al. who revealed a correlation of the distribution of different types of archaeal ether lipids in surface sediments with global sea surface temperature. Archaeal lipids and the temperature proxy based upon them, the TEX_{86}, are discussed in more detail below.

ARCHAEAL LIPIDS.

Archaea, long thought of as forming part of the kingdom of bacteria, are in fact biochemically and genetically so fundamentally different from bacteria and eukaryotes, that they now form the third domain of life (Woese and Fox, 1977). While bacterial and eukaryotic membrane lipids consist of fatty acid chains linked to a glycerol moiety (Fig. 1.1d), archaeal lipids are fundamentally different and their lipids consist of isoprenoid chains linked to a glycerol moiety by ether bonds (Fig. 1.1e). In addition

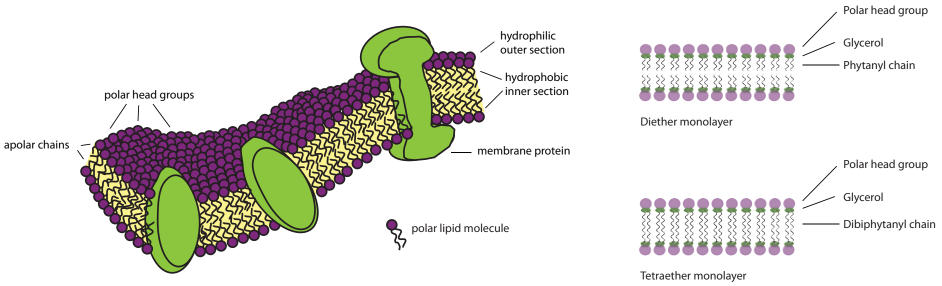
hydrophilic outer section
hydrophobic inner section
polar head groups
apolar chains
membrane protein
polar lipid molecule
Polar head group
Glycerol
Phytanyl chain
Diether monolayer
Polar head group
Glycerol
Dibiphytanyl chain
Tetraether monolayer

a Lipid membrane

b Archaeal GDGT membranes

Figure 1.2. Archaeal lipid membrane bilayers. Figure modified from Madigan et al. (2000).

to diether lipids, consisting of two isoprenoid chains linked to the glycerol backbone, also tetraether lipids, consisting of two glycerols linked together via longer isoprenoid chains, or glycerol dibiphytanyl glycerol tetraether lipids (Fig. 1.1f; GDGTs), have been discovered in Archaea (Langworthy, 1977).

These lipids represent so-called membrane – spanning lipids, as they can, by themselves, form a membrane "bilayer" (Fig. 1.2) by providing both glycerol heads and one long apolar chain. The GDGTs do not possess only acyclic isoprenoid chains, but can also consist of isoprenoid chains containing various ring structures – cyclopentyl and cyclohexyl moieties, which were assumed to have evolved as an adaptation to different growth temperatures, similar to the function of double bonds and branching in esterified fatty acids in eukaryotic membrane lipids (Gliozzi et al., 1983). Many different molecules with ring structures were discovered and shown to be widespread (Schouten et al., 1998; Macalady et al., 2004; Koga and Morii, 2005). Sinninghe Damsté et al. (2002b) characterized the most widespread ring-containing lipid, which possesses one biphytanyl chain with two cyclopentyl and one biphytanyl chain with two cyclopentyl and one cyclohexyl moiety (Fig. 1.1g). This lipid received the name crenarchaeol – after the archaeal phylum it was discovered in, the Crenarchaeota. It has, so far, only been found in a limited number of species, which are all closely related and all possess the same metabolism– aerobic oxidation of ammonia (Könneke et al., 2005; Wuchter et al., 2006a; Eq. 1):

$$NH_3 + 1.5\ O_2 \rightarrow NO_2^- + H_2O + H^+\ (\Delta G^0 = -235\ kJ\ .\ mol^{-1}). \qquad \text{(Eq. 1)}$$

Their carbon metabolism is autotrophic (Hoefs et al., 1997; Wuchter et al., 2003; Könneke et al., 2005; Walker et al., 2010), using bicarbonate via the 3-hydroxypropionate/4-hydroxybutyrate pathway (Berg et al., 2007). Previously, this group was called Marine Group I Crenarchaeota, however, it has recently been re-classified and it is now believed to form a separate phylum, the Thaumarchaeota (Brochier-Armanet et al., 2008; Spang et al., 2010). Crenarchaeol, the biomarker for Thaumarchaeota, is ubiquitously found in present day sediments and soils and also in ancient sediments, stemming from time periods as far back as the Cretaceous (Kuypers et al., 2001) and the Jurassic (Jenkyns et al., 2012).

In live Thaumarchaeota, the GDGTs are present as intact polar lipids (IPL), with polar head groups attached to the glycerol. These head groups comprise sugar- and phosphate moieties (Fig. 1.3a). The most commonly found IPL-GDGTs (Schouten et al., 2008; Koga and Nakano, 2008; Pitcher et al., 2010; Pitcher et al., 2011) contain one sugar moiety (monohexose, MH), two sugar moieties (dihexose, DH) and two sugar and one phosphate group (hexose, phosphohexose, HPH). Degradation of these lipids upon cell death is thought to proceed via hydrolysis of the bond with the polar head groups, leaving only the GDGT-core lipid (CL), followed by complete degradation (Fig. 1.3b). These CL-GDGTs are transported from the upper water column to sediments via fecal pellets and marine snow (Huguet et al., 2006). By empirical observations, it has been shown that variations in the distribution of these GDGTs in surface sediments were related to the sea surface temperature of the overlying water column (Schouten et al., 2002) – a discovery resulting in the development of the sea surface temperature proxy TEX$_{86}$.

The TEX$_{86}$ proxy.

The TEX$_{86}$ is based on a sub-set of the lipids synthesized by Thaumarchaeota, i.e. GDGTs with 1, 2, or 3 cyclopentane moieties, and a regioisomer of crenarchaeol

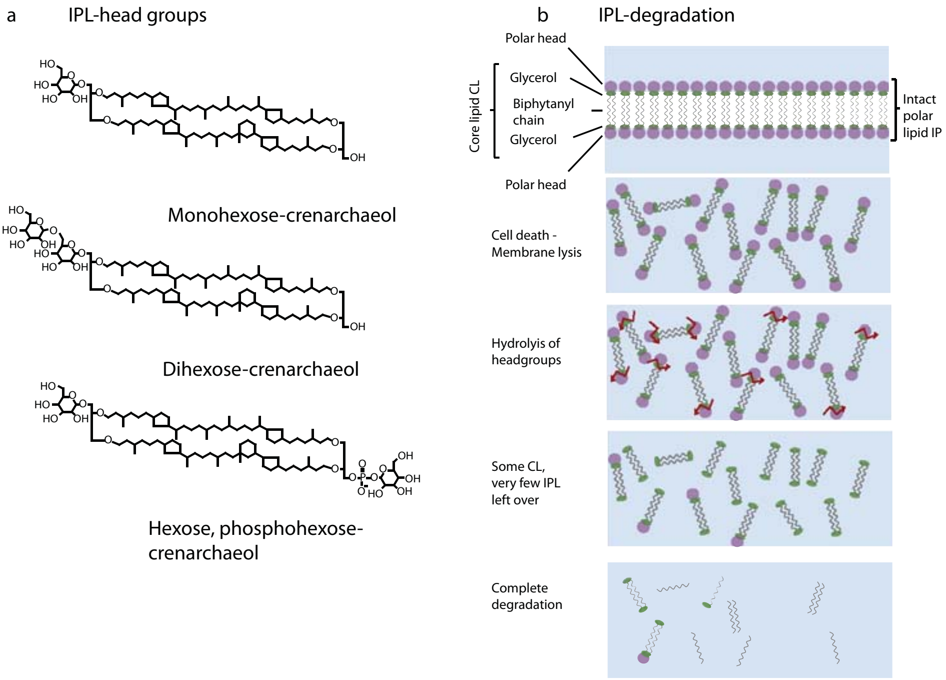
a
IPL-head groups
Monohexose-crenarchaeol
Dihexose-crenarchaeol
Hexose, phosphohexose-crenarchaeol
b
IPL-degradation
Polar head
Core lipid CL
Glycerol
Biphytanyl chain
Glycerol
Polar head
Intact polar lipid IP
Cell death - Membrane lysis
Hydrolyis of headgroups
Some CL, very few IPL left over
Complete degradation

Figure 1.3. IPL-GDGTs most commonly found in Thaumarchaeota and the environment (a) and an illustration of IPL-degradation (b).

(GDGT-1, -2, -3 and Cren'; Fig. 1.4). The regioisomer was shown by chemical degradation to contain the same biphytanyl chains as well as nearly identical chemical shifts in NMR analysis (Schouten et al., 2013) and is thus thought to differ in relative orientation of the glycerol (parallel configuration, Fig. 1.4; Sinninghe Damsté et al., 2002b). The lipids used in the TEX_{86} are not as highly abundant as crenarchaeol and GDGT-0, but similarly widespread (Schouten et al., 2000). The TEX_{86} has been defined as

$$TEX_{86} = \frac{[GDGT-2] + [GDGT-3] + [Cren']}{[GDGT-1] + [GDGT-2] + [GDGT-3] + [Cren']}$$

(Eq. 2; Schouten et al., 2002)

and has been calibrated with globally distributed core-tops by Kim et al. (2008; Fig. 1.4), resulting in

$$T = -10.78 + 56.2 * TEX_{86} \ .$$

(Eq. 3)

The core top data set was further expanded and calibration was refined by using the log of the TEX_{86} ($\text{TEX}_{86}^{\text{H}}$; Kim et al., 2010)

$$T = 38.6 + 68.4 * \log TEX_{86} \ .$$

(Eq. 4)

Experiments using mesocosms confirmed the relationship of TEX_{86} with temperature (Wuchter et al., 2004; Schouten et al., 2007). This correlation was investigated further by analyzing suspended particulate matter in the water column and sediment trap material and shown to be reflective of the surface annual mean sea surface temperature (Wuchter et al., 2005; Wuchter et al., 2006b). The TEX_{86} is now extensively applied for determining paleotemperature, alongside with other proxies (Schouten et al., 2013 and references therein).

Some complications in the application of the TEX_{86} were discovered. One of the problems encountered was the abundance of Thaumarchaeota in terrestrial ecosystems: soils (Leininger et al., 2006), hot springs (Pitcher et al., 2009), and lakes (Schleper et al., 1997). The input of soil organic matter, containing isoprenoid GDGTs used in the TEX_{86} produced in soil and transported by rivers to the ocean, can affect the

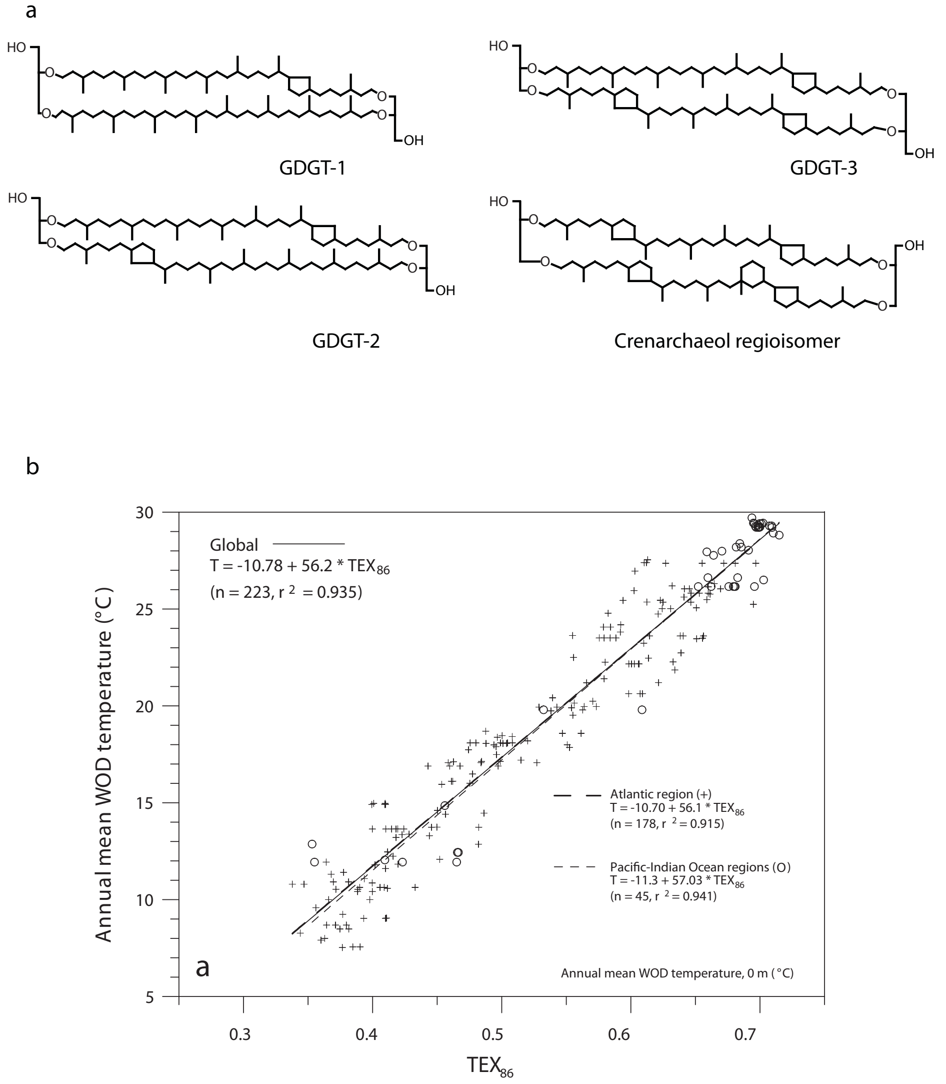

Figure 1.4. Lipids used in the TEX_{86} (a), and the global core top calibration of the TEX_{86}, showing the correlation with sea surface temperature (b adapted from Kim et al., 2008).

TEX_{86} substantially (Weijers et al., 2006). Another potential bias of the TEX_{86} could arise from Thaumarchaeota living deep in the water column. Thaumarchaeota are not restricted to the photic zone as they are presumably chemoautotrophs and thus dependent on inorganic carbon and ammonia, but not on sunlight. Thaumarchaeal cells have been detected by FISH and DNA/RNA analysis also in the meso- and bathypelagic ocean (Herndl et al., 2005; Turich et al., 2007; Reinthaler et al., 2010). Radiocarbon analysis suggested that a substantial proportion of GDGTs encountered at depth is not produced in the surface (Pearson et al., 2001; Ingalls et al., 2006; Shah et al., 2008). However, sedimentary GDGTs are thought to consist to a large degree of GDGTs produced in the photic zone, as they are, due to its active food web, efficiently transported from the upper 200 m to the seafloor by way of inclusion in fecal pellets and marine snow (Wakeham et al., 2003; Huguet et al., 2006). After deposition, GDGTs in the sediment can be affected by two processes which could potentially bias the TEX_{86}: i) Preferential degradation of GDGTs, altering the GDGT distribution in such a way that it leads to changes in the TEX_{86}, and, ii) Production of GDGTs in surface and – potentially – deeply buried sediments by sedimentary Thaumarchaeota (Vetriani et al., 1999; Biddle et al., 2006). These processes are discussed in detail in the following sections.

Degradation and production of GDGTs in sediments.

Preferential preservation and degradation of GDGTs may substantially alter their distribution in the sediment. Sinninghe Damsté et al. (2002a) showed that, in sediments from the Arabian Sea, oxic degradation greatly reduced the concentrations of GDGTs present in sediment. However, when comparing anoxically and oxically deposited sediment in the Arabian Sea, no differences were observed and thus the impact of oxic degradation on the TEX_{86} was estimated to be minimal (Schouten et al., 2004). Kim et al. (2009) showed that the GDGT distribution in anoxic sediments, which were exposed to oxic waters, did not change over one year, while Huguet et al. (2009) found the TEX_{86} to be affected by long-term (>1 kyrs) post-depositional oxidation. They attributed this change to the preferential preservation of soil organic matter, bearing a different TEX_{86} signal, as they also showed that lipids produced by soil bacteria, glycerol di*alkyl* tetraether lipids, were preserved better than the archaeal GDGTs. Thus, it is not yet clear to which extent oxic degradation affects the TEX_{86}.

DNA and RNA analysis have shown that Thaumarchaeota are present and active in marine surface sediments (Vetriani et al., 1999; Stahl and de la Torre, 2012). Thus, GDGTs produced in situ in the sediment may also contribute substantially and this may also lead to an alteration of the pelagic TEX_{86} signal. Thaumarchaeota are aerobic nitrifiers dependent on ammonia, which is typically abundantly present in sediment porewaters, but also on oxygen, which is usually only present down to a certain depth (the oxygen penetration depth). This would limit benthic production to a sediment layer close to the surface, at a depth depending on the type of sediment, which dictates how deep oxygen permeates. However, archaeal IPL-GDGTs, believed to be diagnostic for live archaea, have also been reported in deeply (km) buried anoxic sediments (Biddle et al., 2006; Lipp et al., 2008; Lipp and Hinrichs, 2009; Liu et al., 2011). Based on indirect evidence, e.g. the correlation of these biomarkers with organic carbon content, it was thought that live archaea were using organic carbon at these depths, which would indicate a potential for heterotrophy. Indeed, other studies support the possibility of a heterotrophic metabolism of Thaumarchaeota (Ouverney and Fuhrman, 2000; Herndl et al., 2005; Hallam et al., 2006a; Hallam et al., 2006b; Walker et al., 2010; Tourna et al., 2011). However, they showed the uptake of simple monomeric organic compounds in pelagic waters or enrichment cultures, while benthic archaea would have the ability to degrade the very complex deeply buried, polymeric carbon compounds. Furthermore, using IPL-GDGTs as a proxy for live archaea, and thus in situ sedimentary production, may not be as straightforward as previously believed. Experimental studies conducted by Harvey et al. (1986) showed that archaeal ether lipids are degraded much slower than bacterial ester lipids. While the latter are turned over relatively quickly and can serve as an excellent proxy for live cells, archaeal ether lipid turnover is much slower, and it is questionable how trustworthy IPL-GDGTs as an indicator for live archaeal cells are. Thus, it remains uncertain how well IPL-GDGTs are representative of live archaea in sediments and how in situ production of sedimentary Thaumarchaeota can affect the TEX_{86}.

SCOPE AND FRAMEWORK OF THIS THESIS.

The above discussion showed that in situ production and degradation of GDGTs after deposition in the sediment may affect the application of the TEX_{86} proxy, but to which extent is unclear. This work described in this thesis attempts to investigate the mechanism and extent of in situ production and oxic degradation in sediments, and its impact on the TEX_{86}. To address these issues, IPL- and CL-GDGTs were analyzed in a variety of marine sediments, using different approaches: After establishing the methodology for IPL-analysis, quantification of IPL- and CL-GDGTs and direct IPL-measurements by HPLC/ESI-MS^2 were used to investigate archaeal IPL-degradation (**part I**), while the extent of production of GDGTs in sediments was constrained via stable isotope probing experiments (**part II**). The results were interpreted with respect to the impact of both these processes on TEX_{86} paleothermometry.

Part I. Degradation and preservation of IPL-GDGTs.

In **chapter 2**, several methods for extraction and work-up procedures for IPL-analysis of marine sediments were tested. This showed that the Bligh-Dyer method was superior in extracting IPL-GDGTs of all known types, as it was the only method that also extracted GDGTs with a phosphate head group. Furthermore, results showed that the silica column commonly used for separating IPL- from CL-GDGTs discriminated against the phosphate head group, and distributions of IPL-derived GDGTs measured are thus usually biased towards glycosidic GDGTs.

In **chapter 3**, profiles of CL- and IPL-GDGTs in sediments from the Arabian Sea, deposited under different oxygen concentrations, were analyzed. With depth, the glycosidic IPL-GDGTs were not changing in concentration, contrary to the HPH-GDGTs, where a pronounced decrease is seen, suggesting almost complete degradation within 1-2 kyr. Furthermore, their sedimentary profile bears an imprint of in situ production at the sites and sediment depths where oxygen was present. However, even though this imprint changed the TEX_{86} values of the IPL-GDGTs in the surface sediments, this change was not transferred to the CL-GDGTs. This was probably due to the minor amounts of IPL-GDGTs compared to CL-GDGTs, but also to the higher bioavailability of in situ produced GDGTs, causing a faster turnover. TEX_{86} values of individual GDGTs differed per head group, with the TEX_{86} of HPH-GDGTs being low, MH-GDGTs being higher, and DH-GDGTs having a relatively high TEX_{86}. Total IPL-GDGTs usually had a higher TEX_{86} value than the CL-GDGTs, which was attributed to the preferential degradation of HPH-GDGTs, removing them from the IPL-pool. The TEX_{86} of IPL- and CL-GDGTs decreased with water depth from 900 to 3000 m. In **chapter 4**, the decreasing trend of TEX_{86} with water depth, observed in chapter 3, is discussed in further detail. For this, surface sediment from ten different water depths in the Arabian Sea was analyzed and a linear correlation of CL- and IPL- GDGT concentrations with oxygen exposure times was found, similar to the total organic carbon content. TEX_{86} values were shown to differ at three different locations between head groups in a similar way. The decrease with water depth in TEX_{86} in IPL-derived GDGTs, MH-GDGTs, DH-GDGTs and CL-GDGTs was caused either by specific degradation of certain GDGTs and/or a contribution of GDGTs produced deeper in the water column.

In **CHAPTER 5**, the degradation of IPL-GDGTs over longer timescales (9 Myr) in sediment cores from ODP Leg 201 was investigated. In this sediment, total organic carbon, CL- and IPL-GDGTs followed similar depth trends. Glycosidic GDGTs were present at all depths and changed in the same way as total organic carbon and CL-GDGTs. In contrast, the HPH-GDGTs were degraded fast and decreased to concentrations below detection limit after 7 kyr. This suggests that glycosidic GDGTs are preserved over geological time scales, in contrast to GDGTs with a phosphate head group, and are not good biomarkers for live Archaea.

In **CHAPTER 6**, the effect of post-depositional oxidation on the CL- and IPL-GDGT concentrations and the TEX_{86} in marine sediment was investigated. For this, sediment from turbidite deposits of the Madeira Abyssal Plain was used. MH- and DH-GDGTs were present in the 140 kyr old sediment, while HPH-GDGTs were not detected, in agreement with the results of chapter 5. Upon oxidation, DH-GDGTs were degraded faster than MH-GDGTs. Also in this sediment, DH-GDGTs had a higher TEX_{86} than MH-GDGTs. However, while changes in the distribution of IPL-GDGTs were observed due to preferential degradation of DH-GDGTs, no changes of the TEX_{86} of the CL-GDGTs by the oxidation were detected. This suggests that the amount of IPL-GDGTs present in comparison to CL-GDGTs is negligible.

PART II. STABLE ISOTOPE PROBING EXPERIMENTS INVESTIGATING *IN SITU* PRODUCTION OF ARCHAEAL GDGTS.

In **CHAPTER 7**, the uptake of carbon from phytodetritus by Thaumarchaeota in marine abyssal sediments was examined using stable isotope probing. No incorporation of ^{13}C-label was detected in IPL-derived GDGTs. This was attributed to the type of substrate, as Thaumarchaeota have only been shown to incorporate inorganic carbon into lipids autotrophically. Furthermore, IPL-derived GDGTs have likely a low turnover time, due to low production as well as low degradation rates of archaeal IPL-GDGTs, as shown in Part I.

In **CHAPTER 8**, results from stable isotope probing experiments with sediments from the Iceland Shelf are presented, where different types of ^{13}C-labelled substrates were supplied, i.e. bicarbonate, pyruvate, glucose and amino acids. Like in chapter 7, no incorporation was detected. Since a large variety of substrates were supplied, including those known to be incorporated by Thaumarchaeota, the type of substrate was most likely not the cause. More likely, the lack of detectable uptake can be attributed to the low growth rates of Thaumarchaeota and the high stability of their IPLs.

To summarize, the work described in this thesis has shown that oxic degradation in sediments does not substantially influence the TEX_{86} of CL-GDGTs, i.e. the TEX_{86} measured in paleoclimate studies. However, oxic degradation results in differential degradation of IPL-GDGTs and affects the TEX_{86} of IPL-GDGTs. The archaeal biomarkers MH- and DH-GDGTs are preserved over geological timescales, i.e. millions of years, while HPH-GDGTs are more labile than those, and degraded within kyrs. Compared to the fossil IPL, there was little to no in situ production of GDGTs in surface sediments. The amount of IPL-GDGTs present in the sediment is thus, contrary to conclusions of previous studies, not a reliable proxy for the amount of live archaeal cells. Therefore, the bias on the TEX_{86} by post-depositional, sedimentary processes, i.e. oxic degradation and sedimentary in situ production, was minimal. This knowledge advances the understanding of the TEX_{86} as a proxy, facilitating its application for paleoclimate studies, as well as the use of IPLs as biomarkers for living organisms in sedimentary environments.

CHAPTER 2

COMPARISON OF EXTRACTION AND WORK UP TECHNIQUES FOR ANALYSIS OF CORE AND INTACT POLAR TETRAETHER LIPIDS FROM SEDIMENTARY ENVIRONMENTS

Organic Geochemistry **47** (2012), 34 - 40

COMPARISON OF EXTRACTION AND WORK UP TECHNIQUES FOR ANALYSIS OF CORE AND INTACT POLAR TETRAETHER LIPIDS FROM SEDIMENTARY ENVIRONMENTS

Sabine K. Lengger, Ellen C. Hopmans, Jaap S. Sinninghe Damsté, Stefan Schouten

Department of Marine Organic Biogeochemistry, Royal NIOZ Netherlands Institute for Sea Research, P. O. Box 59, 1790AB Den Burg, Texel, The Netherlands.

ABSTRACT

Glycerol dibiphytanyl glycerol tetraether-based intact polar lipids (IPL-GDGTs) are used as biomarkers for living Archaea and are analyzed utilizing a variety of extraction and quantification techniques. Most IPL-GDGT studies have used a modified Bligh-Dyer extraction method, but it has been suggested that soxhlet extraction may be more efficient for IPL-GDGT extraction from environmental samples and biomass. We investigated the impact of three different extractions (soxhlet, Bligh-Dyer and accelerated solvent extraction, ASE), two IPL quantification methods and two work up techniques (Na_2SO_4 and SiO_2 column) on the amount and distribution of CL- and IPL-derived GDGTs and crenarchaeol-based IPLs in marine sediments from the Arabian Sea and Icelandic shelf and a microbial mat from a Dutch beach. The different extraction procedures gave a similar yield of CL- and IPL-derived GDGTs. Direct analysis of crenarchaeol IPLs showed, however, that, while GDGTs with a monohexose headgroup were not affected by the extraction method, there was a large effect on IPL-GDGTs containing dihexose or hexose, phosphohexose head groups. Quantification of IPL-derived GDGTs by way of either separation over a silica column or by subtraction of CLGDGTs in the total lipid extract before and after hydrolysis gave similar results, but the 'subtraction-method' had a relatively large quantification error. However, the silica column, as well as drying over a Na_2SO_4 column, resulted in a loss of the hexose, phosphohexose IPLs by up to 80%. Based on the results, a modified Bligh-Dyer extraction with as little further treatment as possible is recommended to allow measurement of the full range of IPL-GDGTs in sediments.

1 Introduction

Members of the domain of Archaea occur in many extreme and moderate environments (Schleper, 2007 and references therein). Their cell membranes consist of distinctive ether lipids, amongst which glycerol dibiphytanyl glycerol tetraether (GDGT) lipids are common (Fig. 2.1; de Rosa and Gambacorta, 1988; Sinninghe Damsté et al., 2002b). In the marine environment, the most abundant Archaea are the mesophilic Marine Group I Crenarchaeota (DeLong, 1992; Fuhrman et al., 1992; DeLong et al., 1998; Karner et al., 2001; Schouten et al., 2002), which have been recently proposed to form a separate phylum called Thaumarchaeota, together with other related, ammonia-oxidizing Crenarchaeota (Brochier-Armanet et al., 2008; Spang et al., 2010). These are also the only known producers of crenarchaeol (Sinninghe Damsté et al., 2002b; Schouten et al., 2008; Pitcher et al., 2010), the most abundant GDGT in the marine environment (Schouten et al., 2000). In intact cells, GDGTs occur with polar head groups (intact polar lipids, IPLs; e.g. Fig. 2.1; Koga et al., 1993; Macalady et al., 2004; Koga and Morii, 2005; Schouten et al., 2008; Pitcher et al., 2010), which have been proposed to be rapidly lost after cell death to afford the more stable core lipids (CLs; White et al., 1979; White and Ringelberg, 1998). Hence, analysis of IPL-GDGTs from the environment can, just as for phospholipid-derived fatty acids for bacteria and eukaryotes (cf. White et al., 1979; Boetius and Lochte, 2000), potentially give valuable information about the occurrence of living Archaea (Sturt et al., 2004; Biddle et al., 2006; Pitcher et al., 2011b). However, it has also been suggested that archaeal etherlipids do not degrade as rapidly as bacterial lipids (Harvey et al., 1986; Schouten et al., 2010; Logemann et al., 2011).

Several techniques are available for extracting IPLs and distinguishing them from their fossil counterparts, the CLs. Extraction usually follows a procedure modified from Bligh and Dyer (1959). Following extraction, IPLs can be isolated using separation techniques varying from preparative high performance liquid chromatography (HPLC; Biddle et al., 2006; Schubotz et al., 2009) to SiO_2 column chromatography (Oba et al., 2006; Pitcher et al., 2009b; Liu et al., 2011) or directly analyzed (Lipp et al., 2008; Pitcher et al., 2011b). CL-GDGTs can be quantified using HPLC-atmospheric pressure chemical ionization-mass spectrometry (HPLC-APCI-MS), but IPL-GDGTs with their polar labile head groups have to be analyzed using other techniques such as HPLC-electrospray ionization-tandem mass

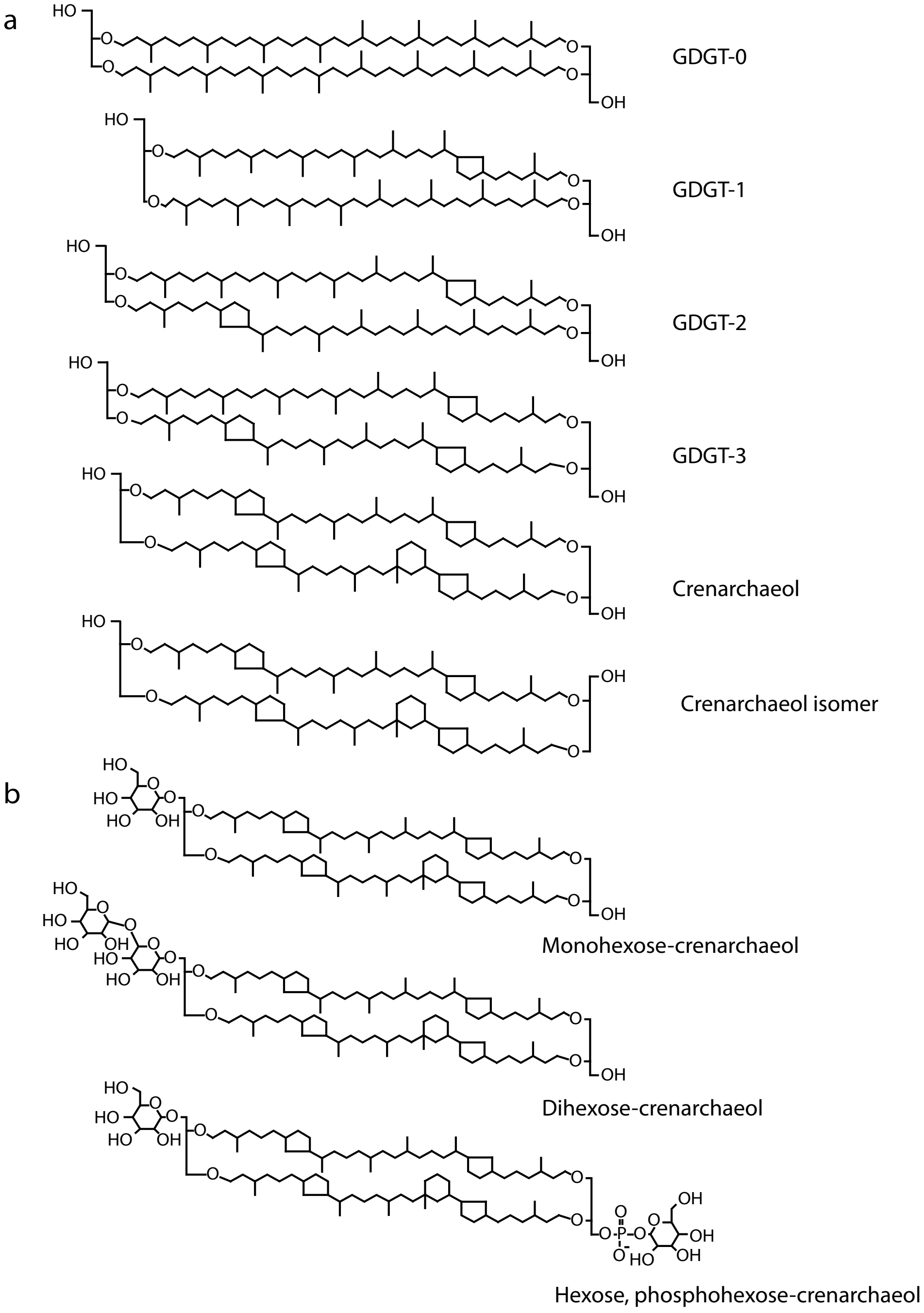
a
GDGT-0
GDGT-1
GDGT-2
GDGT-3
Crenarchaeol
Crenarchaeol isomer
b
Monohexose-crenarchaeol
Dihexose-crenarchaeol
Hexose, phosphohexose-crenarchaeol

Figure 2.1. Structures of CL-GDGTs (a) and IPLs with crenarchaeol as a core lipids (b) analyzed in this study.

spectrometry (HPLC-ESI-MS^2;Sturt et al., 2004). Unfortunately, pure IPL-GDGT standards identical to those found in the natural environment are not commercially available, thereby hindering exact quantification of IPL-GDGTs as ionization efficiency can vary significantly between IPLs (Zink et al., 2003; van Mooy et al., 2009) . Indirect quantification of total IPL-GDGTs is, however, possible after separation from CL-GDGTs and subsequent cleavage of the head groups using acid hydrolysis, which converts them to the quantifiable IPL-derived GDGTs (Pitcher et al., 2009b).

Virtually all studies examining IPL-GDGTs in biomass, sediment, soil and water samples have used a modified Bligh-Dyer technique for extraction. (e.g. Biddle et al., 2006; Schouten et al., 2008; Schubotz et al., 2009; Pitcher et al., 2011b). However, only a few studies have quantitatively examined the effect of extraction and work up on IPL-GDGTs. In fact, Huguet et al. (2010a) have recently suggested that Bligh-Dyer extraction, most commonly used for eukaryotic and bacterial IPLs (White et al., 1996), may be less suitable for extraction of archaeal IPLGDGTs and instead Soxhlet extraction may be preferred. In addition, it was suggested that the concentration of IPL-GDGTs can be determined by determining the concentration of GDGTs in the total lipid extract before and after acid hydrolysis using the so-called ‘subtraction’ method. In this method, the concentration before hydrolysis represents the CL-GDGTs and the concentration after hydrolysis the IPL-derived plus CL-GDGTs. By subtraction of the latter concentration from that of the former, the concentration of IPL-derived GDGTs can be obtained.

To further investigate the efficiency of these extraction techniques, we compared Soxhlet and Bligh-Dyer techniques in quantification of CL- and IPL-derived GDGTs in sediments from the Arabian Sea and Iceland continental shelf, as well as a microbial mat from a Dutch beach. We compared this with accelerated solvent extraction (ASE), a common technique for extract ingCL-GDGTs but not IPL-GDGTs, as it is assumed to destroy part of the IPLs (cf. Huguet et al., 2010a). However, it has been reported that ASE at 100 °C and 20 kPa is capable of quantitatively extracting glycolipids from heterocystous cyanobacteria (Bauersachs et al., 2010), so we re-investigated its potential for extracting archaeal IPLs. IPL quantification was carried out by way of separation over SiO_2, followed by acid hydrolysis, according to Pitcher et al. (2009b), and by direct hydrolysis according to Huguet et al. (2010a). We also directly measured IPL-crenarchaeol using HPLC-ESI-MS^2 in order to compare the extraction efficiency of the methods for different headgroups. Finally, two commonly used work up procedures, i.e. SiO_2 column chromatography and drying over Na_2SO_4 and their effect on IPL distribution were investigated via direct measurement of IPL-crenarchaeol.

2 MATERIAL AND METHODS

2.1 Materials

We used two sediments and one microbial mat sediment. One sample consisted of a large freeze-dried and homogenized composite sample from core top sediments from various water depths (900-3000 m) collected from the Murray Ridge in the Arabian Sea in January 2009. A second sample was a composite sample produced from core tops collected south east and north east off the Iceland shelf in July 2011 at 240-262 m water depth. Finally, a homogenized microbial mat sediment from Green beach at Schiermonnikoog, NL, collected in June 2009 was used. The mat was a mature, as described by Bolhuis and Stal (2011), who analyzed microbial diversity in a similar mat (ST3) and found an archaeal community composed mainly of Halobacteria, but also Marine Group I Crenarchaeota. All samples were frozen immediately after collection.

2.2 Sediment extraction and analysis of GDGTs

Three extraction procedures were used: a modified Bligh-Dyer procedure (Bligh and Dyer, 1959) as described by White and Ringelberg (1998), ASE as described by Huguet et al. (2006) and Soxhlet extraction according to Huguet et al. (2010a). All extractions were performed in triplicate. One blank extraction with 2.0 g diatomaceous earth was used, was performed for each extraction technique. For each experiment 2.0 g of Arabian Sea sediment and Iceland sediment and 3.0 g of the microbial mat were used.

For Bligh-Dyer extraction, samples were extracted x 3 using ultrasonication in dichloromethane (DCM)/MeOH/0.1 M phosphate buffer (PB; 2:1:0.8 v:v) at pH 7.4and the solvent collected after centrifugation. The combined liquid phase was adjusted to a solvent ratio of DCM/MeOH/PB 1:1:0.9 v:v and centrifuged to achieve phase separation and the DCM phase was collected. The extraction was repeated twice with fresh DCM and all DCM phases were combined. For ASE extraction, the samples were extracted after addition of pre-extracted diatomaceous earth in an Accelerated Solvent Extractor 200 (ASE 200, DIONEX, CA, USA) with a mixture of DCM/MeOH 9:1 v:v at 100 °C and 7.6 x 10^6 Pa. For Soxhlet extraction, the samples were placed in pre-extracted thimbles and extracted in Soxhlet extractors in a water bath at 60 °C using 50 ml DCM/MeOH 9:1 (v/v) for 72 h.

From all extracts, the solvent was removed using a rotary evaporator and the extract redissolved in DCM/MeOH 9:1 (v/v), filtered over a 1 cm plug of cotton wool in a Pasteur pipette and dried using a stream of N_2. The extracts were stored at -20 °C until analysis. Each extract was dissolved in DCM/MeOH9:1 (v/v) and divided into aliquots.

One (30%) was fractionated over a SiO_2 column in order to separate IPL-GDGTs from CLGDGTs, following the procedure of Oba et al. (2006) and Pitcher et al. (2009b) with some modification: the CL fraction was eluted with 6 ml hexane/EtOAc 1:2 (v/v) and the IPL fraction with 10 ml MeOH. To each fraction, 0.1 µg of an internal C_{46} glycerol trialkyl glycerol tetraether (GTGT) standard (Huguet et al., 2006) was added. The IPL fraction was hydrolyzed for 3 h under reflux in 2N methanolic HCl to release the IPL-derived GDGTs (Pitcher et al., 2009b). Another aliquot of 30% was analyzed by way of a 'subtraction technique' as described by Huguet et al. (2010). It was divided into two equal parts. Each was spiked with 0.1 µg internal C_{46} GTGT standard. One part was separated on an Al_2O_3 column using 3 ml hexane/DCM 9:1 (v/v) and 3 ml DCM/MeOH 1:1 (v/v) to yield an apolar fraction and the CL-GDGT-containing polar fraction. The other half was directly acid hydrolyzed as described above to give the total 'CL+IPL-derived' GDGTs and then separated over Al_2O_3 as described above, to yield an apolar and a polar fraction, with the latter containing the total (CL+IPL-derived) GDGTs. After analysis, subtraction of these values afforded the concentration difference representing the IPL-derived GDGTs. These two quantification methods were only applied to the Arabian Sea sediment extracts. The third 30% aliquots of the extracts were directly analyzed using HPLC-ESI-MS^2 for crenarchaeol-based IPLs. Also, 30% aliquots of the microbial mat and Iceland shelf sediments were subjected to this direct analysis method.

2.3 Work up for direct IPL analysis

To test the procedures for direct analysis of archaeal IPLs, an additional, large, combined Bligh-Dyer extract of similar, but not identical Arabian Sea core top sediment, was obtained and divided into 9 aliquots. Three were not treated, three were eluted over a Na_2SO_4 column using DCM/MeOH 9:1 (v/v) and three were subjected to

SiO_2 column chromatography to obtain an IPL fraction as described in Section 2.2. A composite Bligh-Dyer extract (several combined core top extracts) of the Iceland Shelf sediment was split into six aliquots, three of which were also subjected to SiO_2 column chromatography, while three were analyzed directly for IPLs. All these fractions were analyzed for crenarchaeol-based IPLs using HPLC-ESI-MS^2.

2.4 HPLC-APCI-MS and HPLC-ESI-MS^2

CL- and IPL-derived GDGTs (Fig. 2.1a) were analyzed using an Agilent 1100 series LC-MSD SL instrument according to Schouten et al. (2007b), using an internal C_{46} GTGT standard as described by Huguet et al. (2006c).

Crenarchaeol-based IPLs were directly analyzed by way of HPLC-ESI-MS^2 modified from Sturt et al. (2004) using a Thermo Quantum Ultra EM triple quadrupole mass spectrometer in selected reaction monitoring (SRM) mode (Pitcher et al., 2011b). Crenarchaeol with a monohexose (MH), dihexose (DH) or hexose, phosphohexose (HPH) head group (Fig. 2.1b) were detected using transitions from *m/z* 1471 to 1292, *m/z* 1634 to 1292, and *m/z* 1713 to 1534, respectively, with an Ar collision gas pressure of 0.8 mTorr. IPLs were quantified as the integrated IPL peak area response g^{-1} of sediment dry wt. All samples were analyzed in duplicate. Long term performance of the mass spectrometer was monitored by injecting an aliquot of a core top extract at regular intervals during analytical sessions. Blanks did not show the presence of any IPL-GDGTs or CL-GDGTs for any extraction method. In order to check for possible ion suppression effects due to matrix extracted from either the diatomaceous earth used in ASE or the thimbles used in Soxhlet extraction, Bligh-Dyer extract of the microbial mat and the Iceland sediment were mixed with ASE and Soxhlet blank extracts and analyzed via HPLC/ESI-MS^2. No ion suppression was observed.

2.5 Data treatment

The results were statistically tested via ANOVA if normally distributed and of equal variance; if not, then ANOVA on ranks, where the data underwent a rank transformation before conducting the ANOVA, was used (Sigmastat/Sigmaplot 11.0; Systat Software Inc., 2008). Standard deviations were calculated for the average of the triplicate experiments. For the subtraction method, the standard deviation was calculated from the two measurements according to error propagation laws as the square root of the sum of their variance. Factor analysis (principal components, PCs) in order to test if all GDGTs were affected similarly by the extraction methods was carried out with Systat 13.0 (Systat Software Inc., 2009).

3 RESULTS AND DISCUSSION

3.1 Efficiency of extraction for CL- and IPL-derived GDGTs

We evaluated differences in the efficiency of methods for the extraction of GDGTs from a composite marine sediment from the Arabian Sea. For the extracts, concentration was determined for CL-GDGTs and IPL-derived GDGTs using the analytical protocols based on chromatographic separation over SiO_2 (Pitcher et al., 2009) and the 'subtraction' method (Huguet et al., 2010). Concentrations of all GDGTs studied (Fig. 2.1a) were highly correlated with each other. A PC analysis showed that the first component explained 99.8% of the overall variation and all loadings exceeded 0.99. This means that all of the variation in GDGT concentration could be explained by the different extraction and quantification methods, he type of GDGT

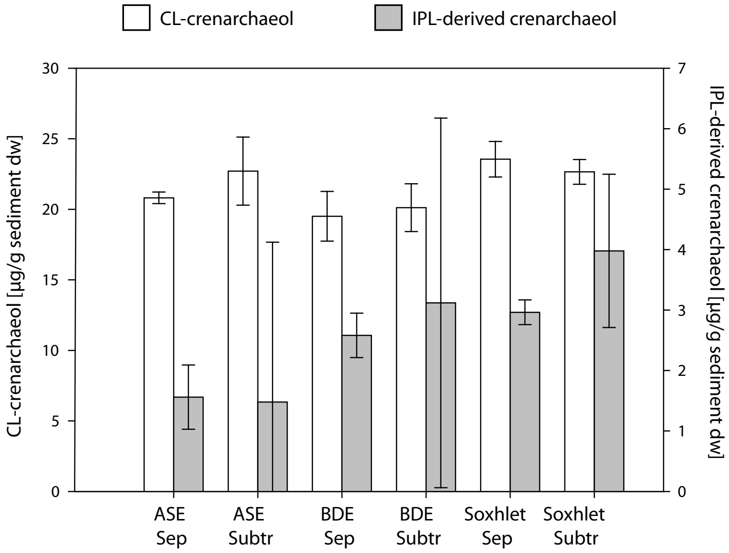

Figure 2.2. Concentrations of GDGT crenarchaeol (µg/g sediment dry weight) as determined from ASE, Bligh-Dyer and Soxhlet extraction, applying two quantification methods of a composite Arabian Sea Bligh-Dyer extract. Labels 'Sep' and 'Subtr' refer to CL and IPL-derived crenarchaeol measured after separation over silica (Pitcher et al., 2009) and to the 'subtraction method'. Data presented are the means of triplicate extractions and error bars indicate ± standard deviation.

having no effect. Since all GDGTs were affected similarly by the extraction and analysis techniques used, we only show the results for crenarchaeol, but conclusions reached also hold for GDGT-0, -1, -2, -3 and crenarchaeol isomer.

Quantification of CL-crenarchaeol (Fig. 2.2; white bars) using the three different extraction and two separation methods revealed similar results, with only Soxhlet extraction yield being slightly, but significantly higher than Bligh-Dyer extraction yield. This indicates that all these extraction and separation techniques are suitable for CL-GDGT analysis.

IPL-derived crenarchaeol concentration (Fig. 2.2; grey bars) showes different patterns vs. the CL-crenarchaeol concentration (Fig. 2.2a). ASE yield was significantly lower than the Bligh-Dyer and Soxhlet yields for the IPL-derived crenarchaeol for the separation method (Fig. 2.2). This is in agreement with observations by Huguet et al. (2010) and indicates that ASE is not an effective method for IPL analysis, most likely due to the high (100 °C) temperature applied, leading to partial destruction of the IPLs, or to the use of diatomaceous earth to which part of the IPLs may have adsorbed. The error of the ‘subtraction-method’ was substantially higher than that of the separation method. In this method, IPL concentration is calculated by subtracting the CL-GDGTs from total (IPL+CL) GDGTs, both of which are in general one order of magnitude higher than the IPL concentration. This leads to a lower significance for the measured values. Thus, even though the CL concentration can be measured relatively reproducibly (with relative standard deviation of 1-11%), the error is relatively much larger for the small IPL concentration derived by subtraction.

3.2 Effect of extraction methods on distributions of IPL-crenarchaeol

Two sediments from the Arabian Sea and the Icelandic shelf, and a microbial mat from Schiermonnikoog were directly analyzed for three crenarchaeol IPLs, i.e. MH-, DH- and HPH-crenarchaeol (Fig. 2.1b; cf. Pitcher et al., 2011b). The extraction yield of DH- and HPH-crenarchaeol was systematically significantly different between methods for the two sediments and the microbial mat (Fig. 2.3).

For all samples, HPH-crenarchaeol was clearly present in highest amount in the Bligh-Dyer extract, but at one to four orders of magnitude lower concentration (microbial mat, Iceland shelf sediment) and not detectable in the ASE extract and two to three orders of magnitude lower in the Soxhlet extract of the Arabian Sea and Iceland sediments and the microbial mat. The highest recovery of HPH-crenarchaeol using Bligh-Dyer extraction is likely due to the higher temperatures at which the ASE and Soxhlet extraction were carried out (100 and 65 °C, respectively), which caused degradation of the HPH-crenarchaeol, in contrast to the room temperature of the Bligh-Dyer extraction. It is also possible that the HPH-crenarchaeol attached irreversibly to the surface of the diatomaceous earth used in ASE or the extraction thimbles used in Soxhlet extraction. Another reason for the superiority of the Bligh-Dyer method might be the use of a phosphate buffer, which increases the polarity of the extraction solvent and allows better dissolution of HPH-crenarchaeol (cf. White and Ringelberg, 1998).

Soxhlet extraction was slightly more efficient in extracting DH-crenarchaeol than Bligh-Dyer and ASE for both the Iceland shelf and the Arabian Sea sediments. The DH-crenarchaeol in microbial mats was below detection limit in microbial mat samples for all extraction methods. It had a yield for the ASE of only 10-20% of those of the Soxhlet and Bligh-Dyer extracts for the Arabian Sea and the Iceland Shelf sediment, while it was not detected at all in the microbial mat samples. This suggests that this IPL is also to some degree affected by high temperature, the diatomaceous earth and/or absence of a phosphate buffer.

The MH-crenarchaeol concentration in the Arabian Sea sediment was surprisingly unaffected by the extraction method as no significant differences were observed between the different treatments. However, it was present in slightly, but significantly, higher amount in the Bligh-Dyer than in the Soxhlet extract (but not the ASE extract) for the Iceland sediments, and both the Soxhlet and the ASE extracts for the microbial mat. It is possible that the MH-crenarchaeol is thermally more stable than the other IPLs or that it was produced by degradation of the other IPLs (e.g. HPH-crenarchaeol and DH-crenarchaeol) with its concentration thereby increasing. However, it is also the least polar IPL and so may be extracted more readily with apolar solvent mixtures.

Thus, although the amount of IPL-derived GDGTs from Soxhlet and Bligh-Dyer extraction of sediments is similar (this study, Fig. 2.2; Huguet et al., 2010), Bligh-Dyer extraction is essential for determining the full suite of IPLGDGT head groups. This is particularly relevant as GDGTs with a phospho head group are predicted to be more labile (Schouten et al., 2010) and so may be a more suitable marker for living Archaea.

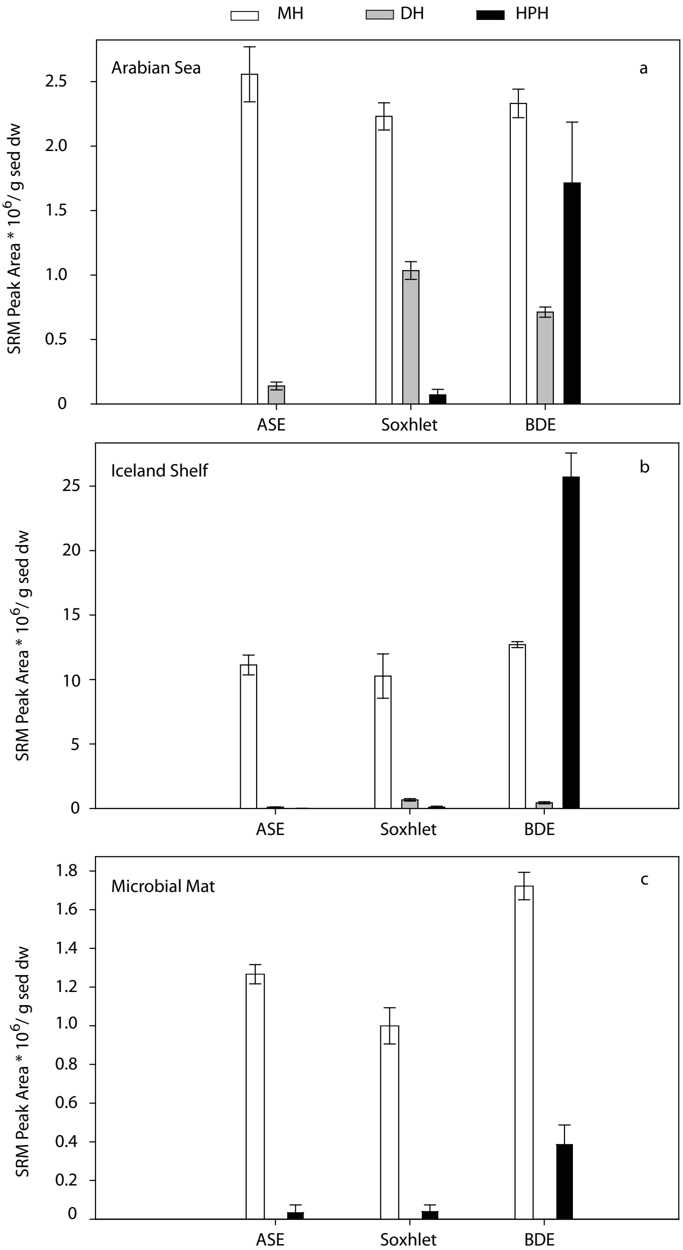

Figure 2.3. IPL crenarchaeol abundance (SRM peak area/ g sediment dry wt) directly analyzed with HPLC/ESI-MS^2 using different extraction methods for (a) Arabian Sea sediment, (b) Icelandic shelf sediment, (c) Schiermonnikoog microbial mat. Data presented are the means of triplicate extractions and duplicate analysis and error bars indicate ± standard deviation (MH, monohexose; DH, dihexose; HPH, hexose, phosphohexose).

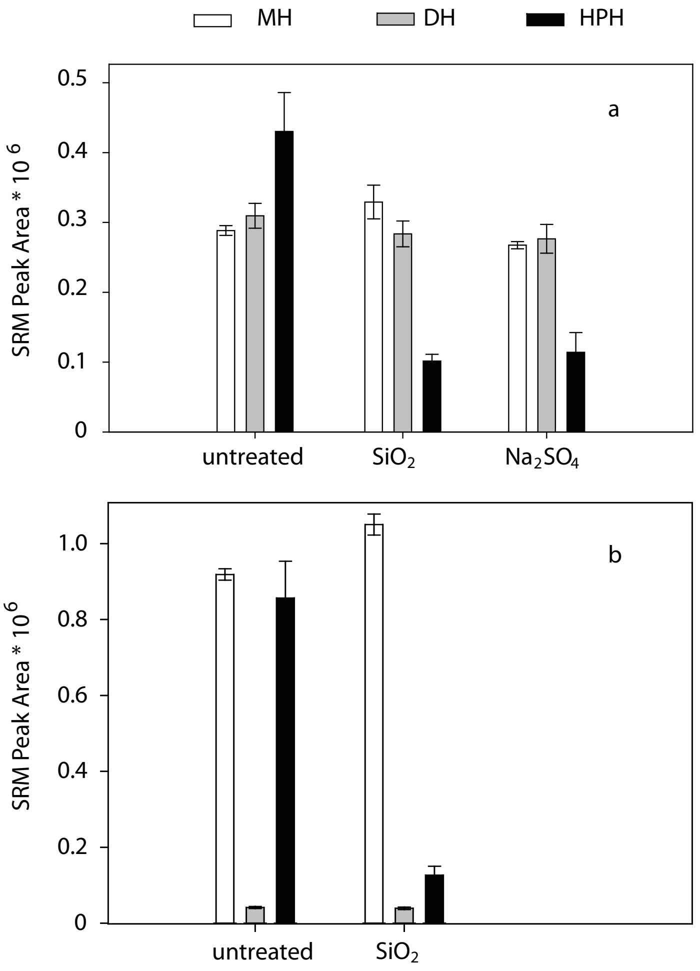

Figure 2.4. IPL crenarchaeol abundance (SRM peak area/aliquot) using different work up procedures with identical aliquots of a large combined Bligh-Dyer extract from (a) an Arabian Sea sediment and (b) an Icelandic shelf sediment (both different from the Bligh-Dyer extracts shown in Fig. 3); SiO_2, IPL fraction of extract eluted from a silica column with MeOH; Na_2SO_4, extract dried over an Na_2SO_4 column. SRM areas represent peak response of identical aliquots injected. Data presented are the means of triplicate extractions and error bars indicate ± standard deviation, with a single analysis for data in (a) and duplicate analysis for data in (b); MH, monohexose; DH, dihexose,; HPH, hexose, phosphohexose.

3.3 Effect of work-up procedures on IPL distribution

Extracts are commonly filtered over Na_2SO_4 to remove traces of water and salt, especially when liquid/liquid extraction from an aqueous phase is involved. This procedure could also affect the distribution of IPLs. Furthermore, separation of IPLs over a SiO_2 column could potentially lead to a bias in quantification of IPL-derived GDGTs if certain head groups adsorb selectively to silica or the glassware used (cf. Pitcher et al., 2009) or are even degraded during elution over silica. Elution of Bligh-Dyer extracts over a Na_2SO_4 or SiO_2 column resulted in no significant changes for DH-crenarchaeol, a slight increase for MH-crenarchaeol and for HPH-crenarchaeol a reduction by ca. 80% vs. the untreated extract for Arabian Sea sediment (Fig. 2.4a). For Iceland shelf sediment, the same was true. HPH-crenarchaeol was significantly reduced (80%) after elution over a SiO_2 column (Fig. 2.4b). Itprobably strongly adsorbs to SiO_2 or Na_2SO_4, or the glassware, or is degraded during elution. The effect is likely much less for DH- and MH-crenarchaeol as they possess the more stable glycosidic bonds and no charged head group. It is possible that some of the HPH-crenarchaeol is degraded to MH-crenarchaeol, as the amount of latter also increased slightly but significantly after elution over the column. However, the MH-crenarchaeol signal could also have been enhanced by the removal of the matrix and a subsequent decrease in ion suppression during the measurement.

These results can be extrapolated to other GDGTs, as the head groups are likely to mainly determine the adsorption properties and chemical stability of IPL-GDGTs. Our results imply that drying should be achieved solely bwitha stream of N_2, without drying agent. Furthermore, indirect IPL-GDGT quantification using SiO_2 column separation will alsp introduce an error as a result of the HPH-GDGTs being lost on the SiO_2 column.

The 'subtraction method' (Huguet et al., 2010a) as discussed above would avoid elution of IPL-GDGTs from a column and instead consist of hydrolyzing the complete extract and determining the IPLs as the difference of the total GDGTs and the CL-GDGTs (Huguet et al. 2010). However, as shown here, the method also introduces greater quantification error than for the SiO_2 separation method (Fig. 2.2). Therefore, both methods have to be used with caution. The use of appropriate standards for direct quantification of IPL-GDGTs in the crude extracts can potentially resolve the dilemma of IPL-GDGT analysis.

4 CONCLUSIONS

ASE, Bligh-Dyer and Soxhlet extraction are all suitable extraction methods for analyzing CL-GDGTs. As shown previously, ASE is not an effective method for extracting IPL-GDGTs. Soxhlet and Bligh-Dyer extraction give similar yields, but the Soxhlet method showed a substantial bias for certain IPL-GDGTs, especially for HPH-GDGTs, which can be recovered mainly by way of Bligh-Dyer extraction. The latter method is therefore recommended for determining the full suite of IPL-GDGTs.

Furthermore, no treatment should be applied to the extract as it will result in substantial loss of at least HPH-GDGTs. Finally, quantification of IPL-GDGTs by subtracting the values before and after acid hydrolysis of the total lipid extract or by separation over a silica column gave similar results. However, problems with quantification errors and a bias due to the adsorption of phospholipids, respectively, suggests that both methods have to be applied with caution.

ACKNOWLEDGEMENTS. The authors thank R. van Bommel for laboratory assistance and L. J. Stal, H. Fan and N. Bale for providing the microbial mat sample, as well as the Master and crew of the R/V Pelagia and the participants of 64PE301 (PASOM) and 64PE341 (Long-chain diols). This is publication number DW-2011-1003 of the Darwin Center for Biogeosciences, which partially funded the project by providing a grant to S.S.

CHAPTER 3

INTACT POLAR AND CORE GLYCEROL DIBIPHYTANYL GLYCEROL TETRAETHER LIPIDS IN THE ARABIAN SEA OXYGEN MINIMUM ZONE: II. SELECTIVE PRESERVATION AND DEGRADATION IN SEDIMENTS AND CONSEQUENCES FOR THE TEX_{86}

Geochimica et Cosmochimica Acta **98** (2012), 244 - 258

INTACT POLAR AND CORE GLYCEROL DIBIPHYTANYL GLYCEROL +TETRAETHER LIPIDS IN THE ARABIAN SEA OXYGEN MINIMUM ZONE: II. SELECTIVE PRESERVATION AND DEGRADATION IN SEDIMENTS AND CONSEQUENCES FOR THE TEX_{86}

Sabine K. Lengger[a], Ellen C. Hopmans[a], Gert-Jan Reichart[b], Klaas G.J. Nierop[b], Jaap S. Sinninghe Damsté[a,b] and Stefan Schouten[a,b]

[a] *NIOZ Royal Netherlands Institute for Sea Research, Department of Marine Organic Biogeochemistry, P.O. Box 59, 1790 AB Den Burg (Texel), The Netherlands.* [b] *Faculty of Geosciences, Department of Earth Sciences-Organic Geochemistry, Utrecht University, P. O. Box 80021, 3508 TA Utrecht, The Netherlands*

ABSTRACT

The TEX_{86} is a proxy based on a ratio of pelagic archaeal glycerol dibiphytanyl glycerol tetraether lipids (GDGTs), and used for estimating past sea water temperatures. Concerns exist that in situ production of GDGTs lipids by sedimentary Archaea may affect its validity. In this study, we investigated the influence of benthic GDGT production on the TEX_{86} by analyzing the concentrations and distributions of GDGTs present as intact polar lipids (IPLs) and as core lipids (CLs) in three sediment cores deposited under contrasting redox conditions across a depth range from 900 to 3000 m below sea level in and below the Arabian Sea oxygen minimum zone (OMZ). Direct analysis of IPLs with crenarchaeol as CL with HPLC/ESI-MS^2 revealed that surface sediments in the OMZ were relatively depleted in the phospholipid hexose, phosphohexose (HPH)-crenarchaeol compared to suspended particulate matter from the water column, suggesting preferential and rapid degradation of this IPL. In sediment cores recovered from deeper, more oxic environments, concentrations of HPH-crenarchaeol peaked at the surface, probably due to in situ production by ammonia-oxidizing Archaea, followed by a rapid decrease with increasing depth. No surface maximum was observed in the sediment core from within the OMZ. In contrast, the glycolipids, monohexose-crenarchaeol and dihexose-crenarchaeol, did not change in concentration with depth in the sediment, indicating that they were relatively well preserved and likely mostly derived from fossil pelagic GDGTs. These results suggest that phospholipids are more sensitive to degradation, while glycolipids might be preserved over longer time scales, in line with previous incubation and modeling studies. Furthermore, in situ produced IPL-GDGTs did not

accumulate as IPLs, and did not influence the CL-TEX_{86}. This suggests that in-situ produced GDGT lipids were more susceptible to degradation than fossil CL and IPL and did not accumulate as CL. In agreement, no significant changes of TEX_{86} with sediment depth in the core lipids were observed. However, consistent differences between IPL-derived and CL-TEX_{86} were found. These could be explained by a different composition of CL-GDGT of the glyco- and phospholipids, in combination with dissimilar degradation rates of phospholipids versus glycolipids. We also observed consistent differences in both IPL-derived and CL-TEX_{86} between the different cores, equivalent to 3°C when converted to temperature, despite the proximity of the core locations. These differences may potentially be due to a larger addition of GDGTs produced in deeper, colder waters to the (sub)surface-derived GDGTs for the deeper core sites.

1 INTRODUCTION

The domain of Archaea consists of four kingdoms, the Eury-, Cren- and Nanoarchaeota as well as the recently, on the basis of genome analysis of enriched Archaea, proposed Thaumarchaeota (Brochier-Armanet et al., 2008; Spang et al., 2010), formerly classified as Group I Crenarchaeota. All Thaumarchaeota known so far are capable of ammonia oxidation (Könneke et al., 2005; de la Torre et al., 2008; Hatzenpichler et al., 2008; Park et al., 2010) and are widespread in non-extreme environments (DeLong, 1992; Fuhrman et al., 1992; DeLong et al., 1998; Schouten et al., 2000). They occur in the ocean (Karner et al., 2001), in soils (Leininger et al., 2006) and lakes (Schleper et al., 1997), and in marine and estuarine surface sediments (Francis et al., 2005; Beman and Francis, 2006; Park et al., 2008). In the present day ocean, these Archaea are found to be among the most abundant microorganisms (Karner et al., 2001; Agogué et al., 2008).

The membrane lipids of the domain Archaea are distinctive as they consist of isopranyl chains linked to a glycerol backbone via ether bonds (Kates et al., 1965; Langworthy et al., 1972; Langworthy et al., 1974). Most of the cultivated Crenarchaeota and Thaumarchaeota produce tetraether lipids consisting of two back-to-back linked diethers (glycerol dibiphytanyl glycerol tetraethers, GDGTs) which can have varying numbers of cyclopentane moieties (Macalady et al., 2004; Koga and Morii, 2005; Schouten et al., 2008; Pitcher et al., 2010). Thaumarchaeota contain in addition a specific GDGT, crenarchaeol, which contains not only cyclopentane moieties but also one cyclohexane moiety (Sinninghe Damsté et al., 2002b). GDGTs are preserved well in the sedimentary record and can thus be used as biomarkers for this group of Archaea (e.g. Kuypers et al., 2001; Pancost et al., 2001; Ingalls et al., 2006; Coolen et al., 2007).

Schouten et al. (2002) found a correlation between sea surface temperature (SST) and the distribution of four specific GDGTs present in sediment core tops (GDGT-1, -2, -3 and -4', Fig. 3.1a) and they expressed this in the TEX_{86} index. This ratio has been calibrated with a global set of core tops (Kim et al., 2008; 2010) and has been frequently used in studies to reconstruct past changes in SST (e.g. Huguet et al., 2006b; Forster et al., 2007; Liu et al., 2009; Bijl et al., 2009). The proxy is based on the assumption that the distribution of pelagic thaumarchaeal membrane lipids changes with temperature, which has been suggested previously for other phyla of Archaea (Gliozzi et al., 1983; Gabriel and Chong, 2000; Cavicchioli, 2006), and that this signal is preserved in sediments. The temperature-dependence of the GDGT distribution was shown in mesocosms of enriched ammonia-oxidizing Archaea (AOA) (Wuchter et al., 2004; Schouten et al., 2007a) as well as suspended particulate matter from marine waters <100 m depth (Wuchter et al., 2005). It has been observed that, even though genetic markers for Thaumarchaeota are present throughout the water column (e.g. Karner et al., 2001; Herndl et al., 2005), surface sediment TEX_{86} values correspond to upper water column temperatures (Kim et al., 2008; 2010). This was explained with the assumption that mainly GDGTs from the upper part of the water column are exported to the sediment by attachment to and sinking with marine snow via organisms which are mainly present in the upper 200 m of the water column (Wakeham et al., 2003; Wuchter et al., 2005; Huguet et al., 2006a).

Using 16S rRNA gene and biomarker analysis, Archaea have also been suggested to be present and active in sediments (Biddle et al., 2006; Lipp et al., 2008). Production of one or more of the GDGTs used for calculation of the TEX_{86} by sedimentary Archaea can thus potentially lead to a significant bias in the past sea surface temperature estimations (Lipp et al., 2008; Lipp and Hinrichs, 2009). The presence of GDGTs of subsurface Archaea was evident from detection of intact polar GDGTs (IPL-GDGTs), i.e. GDGTs with polar headgroups such as glycosidic or phosphate headgroups, the form in which they actually occur in the archaeal cell membrane (Fig. 3.1b, de Rosa and Gambacorta, 1988; Koga and Nakano, 2008). IPL-GDGTs are used as a proxy for living Archaea as the headgroups are thought to be cleaved quickly after cell death through enzymatic hydrolysis yielding core

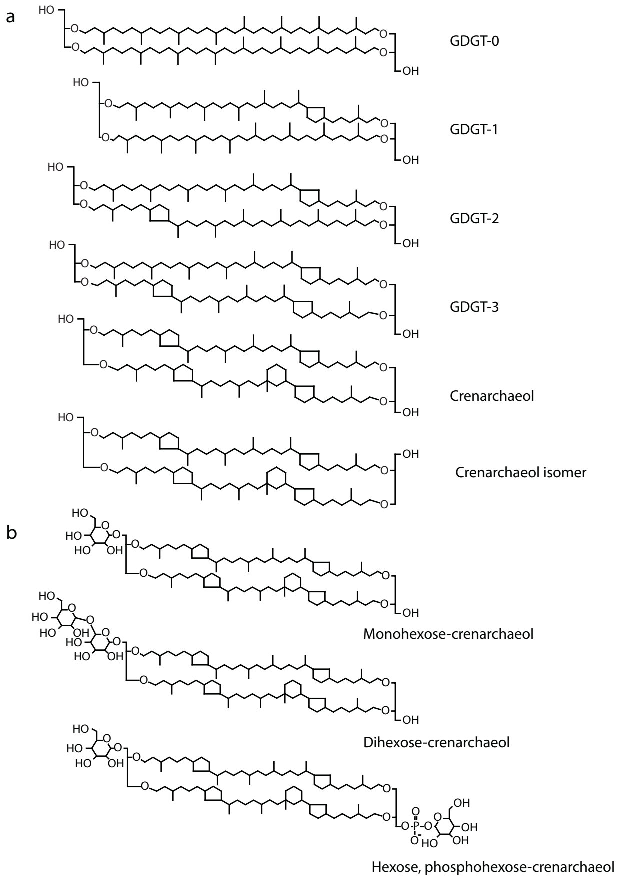
a
GDGT-0
GDGT-1
GDGT-2
GDGT-3
Crenarchaeol
Crenarchaeol isomer
b
Monohexose-crenarchaeol
Dihexose-crenarchaeol
Hexose, phosphohexose-crenarchaeol

Fig. 3.1. Core lipid GDGTs (a) and crenarchaeol-containing IPLs (b) analyzed in the sediment cores.

lipids, CL-GDGTs (Zink et al., 2003; Biddle et al., 2006; Huguet et al., 2010b). The term 'living' in this sense entails all viable, i.e. active as well as dormant, cells which possess an intact membrane (cf. Stevenson, 1978; Lebaron et al., 2001; Luna et al., 2002). IPL-GDGTs found in sediments and reported up to now as indicative of living Archaea are glycolipids with monohexose- and dihexose-GDGTs and GDGTs with an unknown headgroup of m/z 341 (Biddle et al., 2006; Lipp and Hinrichs, 2009; Schubotz et al., 2009). However, IPL-studies of crenarchaeol-producing Thaumarchaeota in enrichments and cultures revealed the presence of glycolipids, but also of phosphate-containing GDGTs, i.e. phosphohexose and hexose, phosphohexose-GDGTs (Schouten et al., 2008; Pitcher et al., 2010; Pitcher et al., 2011c) which, up to now, have not been reported in sediments. Harvey et al. (1986) reported that, in a short-term incubation study, glycosidic ether-lipids were more stable than diacylglycerolphosphoester-lipids and thus degradation rates of glycolipids may be much slower than the degradation rates of phosphate-containing lipids (Harvey et al., 1986). Hence, glycolipid-GDGTs could also be at least partially of fossil pelagic origin (Schouten et al., 2010). It is thus presently not clear whether IPLs present in surface sediments are all in situ produced and if and how archaeal benthic production affects TEX_{86} values of fossil core lipids.

To address this issue, we analyzed sediments from the Arabian Sea which possesses a well-developed oxygen minimum zone (OMZ) with almost no detectable concentrations of molecular oxygen in its core (Wyrtki, 1971; 1973; Olson et al., 1993). Mean O_2 concentration in the core of OMZ has been reported to be as low as 13 µM, with seasonal minima ranging from 0.1-1.0 µM (Paulmier and Ruiz-Pino, 2009). Jensen et al. (2011) found apparent anoxic conditions in the Central and NE-Arabian Sea OMZ between 100 and 800 m depth, deploying a recently described highly sensitive oxygen sensor with a detection limit of 90 nM (Revsbech et al., 2009). The Murray Ridge is a sub-marine high in the Northern Arabian Sea which protrudes into the core of the OMZ (Fig. 3.2). The relief allows sampling of sediments from different water depths in close lateral proximity, and hence containing similar pelagic material, but at contrasting bottom water oxygen concentrations. Here, we analyzed three sediment cores, from within the OMZ, below the OMZ and from the oxygenated bottom waters. Similar to the companion paper on the water column (Schouten et al., 2012), we directly measured crenarchaeol with glyco- and phosphoglyco-headgroups and quantitatively compared CL- and IPL-derived GDGT concentrations and distributions as well as TEX_{86} values. The lipid profiles are discussed with respect to the impact of sedimentary in situ production and preservation potential of archaeal IPLs on the TEX_{86}.

2 MATERIALS AND METHODS

2.1 Sampling

Sediment cores (multi cores) were taken in the Northern Arabian Sea along a transect on the Murray Ridge during the PASOM cruise (64PE301) in January 2009 (Fig. 3.2). The sampling locations, the water depths and oxygen concentrations of the bottom water are summarized in Table 3.1. Three sediment cores were taken at three depths, 900 meters below sea surface (mbss) (station 1, further referred to as P900; within the OMZ), 1300 mbss (station 4 or P1300, just below the OMZ)

Table 3.1. Locations and depths of the sampled surface cores, PASOM original station names in brackets.

Station name	Location	Depth [m]
P900 (Station 1)	22.54823 N 64.03983E	885
P1300 (Station 4)	22.29993N 63.59980E	1306
P3000 (Station 10)	21.92877N 63.15823E	3003

and 3000 mbss (station 10 or P3000, well below the OMZ). The sediment cores of 20 to 36 cm length were sliced on board the *R/V Pelagia* in 0.5 to 4 cm intervals and stored in geochemical bags. They were frozen immediately at -80°C and further transported and stored at -20°C. Prior to analysis, the sediment was freeze-dried and homogenized. Oxygen concentrations of the water column were measured by an SBE 43 dissolved oxygen sensor (Seabird, WA, USA) fitted to the CTD frame and calibrated against Winkler titrations. The limit of detection for these methods was 3 $\mu mol.L^{-1}$. Oxygen penetration depths were measured on board in 0.1 mm resolution using an OX-100 micro sensor (Unisense AS, Aarhus, DK) with a guard cathode as described by Revsbech (1989).

2.2 Total organic carbon content and sedimentation rates

Freeze-dried sediments were analyzed for total organic carbon content (TOC). One aliquot of freeze-dried sediments was acidified in situ with 2N HCl in silver cups to remove carbonates, thereby avoiding the loss of acid-soluble organic carbon. Another aliquot of freeze-dried sediment was acidified over night with 2N HCl, subsequently washed with bidistilled H_2O and freeze-dried. The decalcified sediments were measured on a Flash EA 1112 Series (Thermo Scientific) analyzer coupled via a Conflo II interface to a Finnigan Delta^{plus} mass spectrometer. The organic carbon reported is an average of all (4-8) measurements, excluding outliers identified by a Grubbs Test. Standard deviations of replicate measurements ranged from ± 0.07 to ± 0.7 % TOC with an average of ± 0.4 for P900, ± 0.06 to ± 0.57 % with an average of ± 0.3% for P1300 and ± 0.0004 to ± 0.06% with an average of ± 0.03% for P3000.

For ^{14}C dating, subsamples of parallel cores from the same multicore deployment were used. For each multicore deployment the top 1-2 cm, one subsample from the center of the core (P900: 19-20 cm, P1300: 11-12 cm, P3000: 10-11 cm) and one near the base of the multicore (P900: 39-40 cm, P1300 and 3000: 21-22 cm) was used for dating. The ^{14}C-age determinations were based on the carbonate from the tests of planktonic foraminifera hand-picked from the 150 -595 μm size fraction. All available planktonic foraminiferal species were used due to the limited amount of material available (ranging from 4.5 mg to 28.8 mg). ^{14}C was measured using accelerated mass spectrometry at the Poznan radiocarbon laboratory. ^{14}C-ages were subsequently corrected for reservoir age (400 yr) and calibrated to calendar ages using the Int09 calibration curve (CALIB software package, version 6.0.1). The two deeper samples were used to calculate the linear sedimentation rates, assuming the top sample to represent present day.

2.3 Bligh-Dyer Extraction and IPL-CL separation

Approximately 2 g (P1300 and P3000) and 1 g (P900) aliquots of freeze-dried sediment were extracted with a modified Bligh and Dyer procedure as described by Pitcher et al. (2009b). Briefly, extraction with methanol (MeOH)/dichloromethane (DCM)/phosphate buffer (PB) 50 mM, pH 7.5, in volume ratios 2:1:0.8 was carried out three times by ultrasonication and the solvent was collected after centrifugation. The combined liquid phases were adjusted to a solvent ratio of MeOH/DCM/PB of 1:1:0.9 (v/v) which led to phase separation between the DCM and the MeOH/PB. The DCM phase was collected and the MeOH/PB mixture was extracted twice more with DCM. The combined DCM phases were reduced with a rotary evaporator,

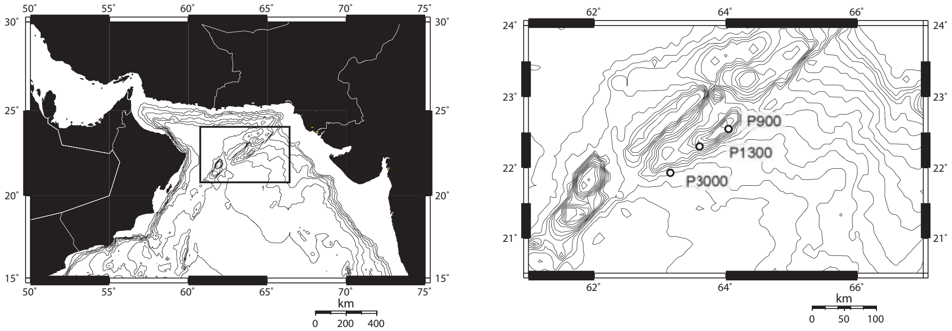

Figure 3.2. Map of the Arabian Sea (left) and of the Murray Ridge (right). Stations sampled during the PASOM cruise are marked with a circle. Station P3000 is equivalent to the station investigated in the companion publication (Schouten et al. 2012a).

re-dissolved in DCM/MeOH 9:1 (v/v), filtered over cotton wool and subsequently dried under a stream of N_2. The extract was stored at -20°C.

One aliquot of extract was directly analyzed by HPLC/ESI-MS^2 for intact polar lipids (IPL), while another aliquot was fractionated over a silica column in order to separate the IPL from the core lipids (CL) following the procedure of Oba et al. (2006) and Pitcher et al. (2009b). Fractionation was achieved over a column with 0.8 g silica gel (60 mesh) activated at 130°C overnight. Core lipids were eluted using 6 mL hexane/ethyl acetate 1:1 (v/v) and intact polar lipids using 10 mL MeOH. The core lipid fractions were dried and 0.1 µg C_{46}-GDGT internal standard (Huguet et al., 2006c) was added. To the intact polar lipid fractions 0.1 µg internal standard was added and an aliquot of 3 mL was transferred to a vial, dried and stored frozen for quantification of core lipids which eluted in the intact polar lipid fraction ("carry over"). These were typically <2% of the GDGTs present in CL fraction or 10% of GDGTs present in the IPL fraction. The remaining IPL fraction was dried and hydrolyzed for 3 h under reflux in 5% methanolic HCl to release CL-GDGTs. Bidistilled H_2O was added and the pH was adjusted to 4-5 with methanolic 1M KOH, then the MeOH/H_2O ratio was adjusted to 1:1 (v/v). The core lipids were extracted from the aqueous phase 3 times with DCM. The DCM phases were combined, the DCM was removed with a rotary evaporator, and the residue was re-dissolved in DCM and dried over Na_2SO_4. This yielded the IPL-derived CL fraction.

2.4 HPLC/APCI-MS and HPLC/ESI-MS^2

Analysis of CL-GDGTs and IPL-derived GDGTs by HPLC/APCI-MS and calculation of TEX_{86} was carried out as described in the companion paper (Schouten et al., 2012). The average relative standard deviation for quantification of GDGTs, calculated from triplicate extractions of 1 (P1300) or 3 (P900, P3000) sediment samples, was 6 % (CL) and 10 % (IPL-derived) for P900, 11 % (CL) and 16 % (IPL-derived) for P1300 and 13 % (CL) and 21 % (IPL-derived) for P3000. Reproducibility for TEX_{86} values were typically < 0.01, corresponding to errors of < 0.5 °C. Temperatures were calculated according to the TEX^H_{86} calibration (which is the log of TEX_{86}) according to Kim et al. (2010).

Intact polar lipids, i.e. monohexose (MH)-crenarchaeol, dihexose (DH)-crenarchaeol and hexose, phosphohexose (HPH)-crenarchaeol, were directly analyzed by HPLC/ESI-MS^2 using a specific selected reaction monitoring method (SRM; Pitcher et al., 2011b). No absolute quantification was possible due to a lack of standards. Therefore, response areas (in arbitrary units, au) per g sediment are reported. Due to variation in MS performance over longer time periods, measurements are comparable down core as they were analyzed in batch runs, but not between cores which were measured at different times. An IPL fraction of *Candidatus* Nitrososphaera gargensis (Pitcher et al., 2010) was injected typically after 8 sample runs to monitor performance of the ESI-MS^2 during batch runs. Standard deviations from triplicate extractions of sediment at 22 cm depth at P1300 were 8 % area/g sediment dw for the monohexose-crenarchaeol and 20% area/g sediment dw for the dihexose-crenarchaeol.

2.5 Semi-preparative HPLC

For the isolation of particular IPL-GDGTs, repetitive preparative HPLC was used as described previously in Schouten et al. (2008). Bligh Dyer extracts of ca. 4 g of sediment from 0-2 cm depth ("top") and of 4 g of sediment from 20-24 cm depth ("bottom") from P1300 were separated on an Agilent (San Jose, CA, USA) 1100 series LC with an Inertsil diol column (250 by 10 mm; 5 µm particles; Alltech Associates Inc., Deerfield, IL) at a flow rate of 3 mL/min and identical conditions as for intact polar lipids (see above and Pitcher et al., 2011b). Fractions of 3 mL were collected and subsequently measured with Flow Injection Analysis using ESI-MS^2 in SRM mode at the same conditions as the analytical SRM, monitoring the same transitions. Injection solvent was a mixture of 60% A and 40 % B with A being hexane/isopropanol/formic acid/14.8M aqueous NH_3 (79:20:0.12:0.04, vol/vol/vol/vol) and B being isopropanol/water/formic acid/14.8 M aqueous NH_3 (88:10:0.12:0.04, vol/vol/vol/vol). In the top sediment, three fractions, comprising monohexose-GDGTs, dihexose-GDGTs and hexose, phosphohexose-GDGTs respectively, were collected. The dihexose-GDGTs likely contained a minor amount of co-eluting GDGTs with a hexose and an unknown headgroup of *m/z* 180 as observed in *Candidatus* Nitrosopumilus maritimus SCM1 (Schouten et al., 2008). From the bottom sediment sample, the monohexose- and dihexose-crenarchaeol fractions were collected while hexose, phosphohexose-crenarchaeol was not detected. The fractions containing the IPL-GDGTs were acid-hydrolyzed and the CL-GDGT distributions were quantified using HPLC/APCI-MS and the C_{46}-GDGT internal standard method as described above.

3 RESULTS

3.1 Oxygen concentrations, total organic carbon content (TOC) and sedimentation rates

Sediment cores were taken at three stations: P900 was in the oxygen minimum zone (OMZ) at 885 mbss; P1300 was just below the OMZ at 1306 mbss, while P3000 was located at the foot of the Murray Ridge in oxygenated bottom waters at 3003 mbss (Fig. 3.2). The oxygen concentration of the bottom water of P900 was below detection limit (<3 µmol.L^{-1}), and of P1300 and P3000 at 14 and 83 µmol.L^{-1}, respectively. Oxygen penetration depths measured on-board with microelectrodes were less than 0.125 mm at P900, 3 mm at P1300 and 18 mm at P3000.

The sediment core at P900 was composed of very dark olive-brown mud, uniform over the whole depth. In the cores at P1300 and P3000, a change in texture and col-

Table 3.2. Radiocarbon dating results. Medium ^{14}C-age (minimum – maximum) in yr of foraminiferal test carbonate picked from respective depth intervals. Mix depth – mixing or bioturbation depth in cm below sea floor [cmbsf], sed rates – sedimentation rates. Reservoir age used was 400 yrs.

Station	Interval [cmbsf]	^{14}C-age [yr]	Mix depth [cmbsf]	Sed rates [cm . kyr^{-1}]
P900				
	1-2	88 (18-145)		
	19-20	1207 (1118-1282)	-	8.5
	39-40	2941 (2792-3078)		
P1300				
	1-2	2233 (2152-2280)		
	11-12	2920 (2839-3042)	8.5	3.8
	21-22	5524 (5465-5622)		
P3000				
	1-2	1735 (1611-1825)		
	10-11	1463 (1375-1541)	14.5	8.3
	21-22	2376 (2310-2491)		

or was observed. The core from P1300 had a distinct 1 cm red-brown layer on top, while that of P3000 was brown colored down to 7 cm depth, and then changed to grey with a clayish texture. The organic carbon content varied substantially between the three stations (Fig. 3.3). At P900, TOC ranged from 5 to 8 % (organic carbon . g sed dw^{-1}), while it was 1.3 to 3 % at P1300 and ≤1 % at P3000. The profiles at P900 and P1300 showed little variation downcore (Fig. 3.3) but an increase in organic carbon content from 0.6 to 1% between 9 and 16 cm depth was observed at P3000.

^{14}C-ages determined from planktonic foraminiferal shells (Table 3.2) showed an age offset between the ^{14}C-age of the top sample and the reservoir age, due to ongoing bioturbation. Bioturbation depth could be estimated by multiplying the age of the top sediment (corrected for the reservoir age of 400 yrs) with the sedimentation rate (Table 3.2). Average linear sedimentation rates were 8.5, 3.8 and 8.3 cm/kyr for P900, P1300 and P3000, respectively, and mixing depths were 8.5 and 13-14 cm for P1300 and P3000. Sedimentation rates differed considerably between sites, which is probably due to the local topography. Values are, however, similar to what has been reported earlier for the same area: 13.3 cm/kyr at 970 m water depth and 4.3 cm/kyr at 1511 m water depth (van der Weijden et al., 1999). Bioturbation depths were also comparable to values reported earlier for the northernmost Arabian Sea (ibid.) and increased with increasing bottom water oxygenation. Pore water profiles, ^{210}Pb dating and Ti/Ca ratios of sediments from the same locations showed that sedimentation was relatively continuous with no evidence for winnowing or gravity flows (Kraal et al., 2012).

3.2 Abundance and distribution of CL and IPL-derived GDGTs

The concentrations of CL-GDGTs and the IPL-derived GDGTs were determined for crenarchaeol, GDGT-0, and the sum of GDGTs -1, -2, -3 and -4' which are used for determination of the TEX$_{86}$ (Fig. 3.4). Total IPL- and CL-GDGT-concentrations in the core from P900 ranged from 4 to 8 µg.g sed dw^{-1} for IPL-derived GDGTs and 60 to 110 for CL-GDGTs. These concentrations were one order of magnitude higher than in P1300 (1 to 2 and 10 to 17 µg.g sed dw^{-1}) and two orders of magnitude higher than in P3000 (0.3 to 1.7 and 1 to 7 µg.g sed dw^{-1}). IPL-derived GDGTs were always less abundant than CL-GDGTs and amounted to 5-15% of CL-GDGTs at P900, 5-15% at P1300 and 10% at P3000 for crenarchaeol and the sum of GDGT-1, -2, -3 and -4'. However, IPL-derived GDGT-0 showed a peak in concentration in the surface sediment of P3000 (Fig. 3.5c) and the highest percentage of IPL-derived/

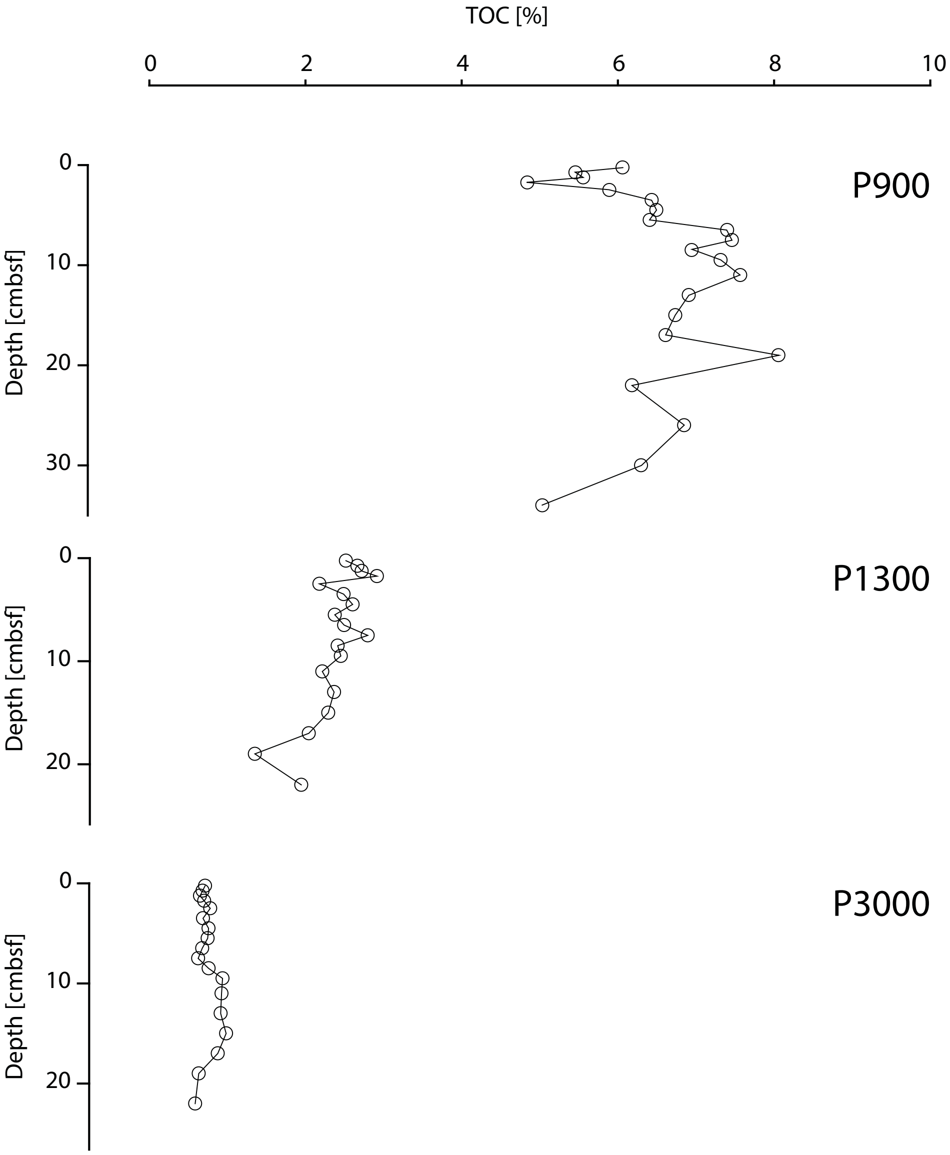

Figure 3.3. Total organic carbon content (TOC) in % of organic carbon per g dry weight of the three analyzed cores vs. depth in cm below sea floor.

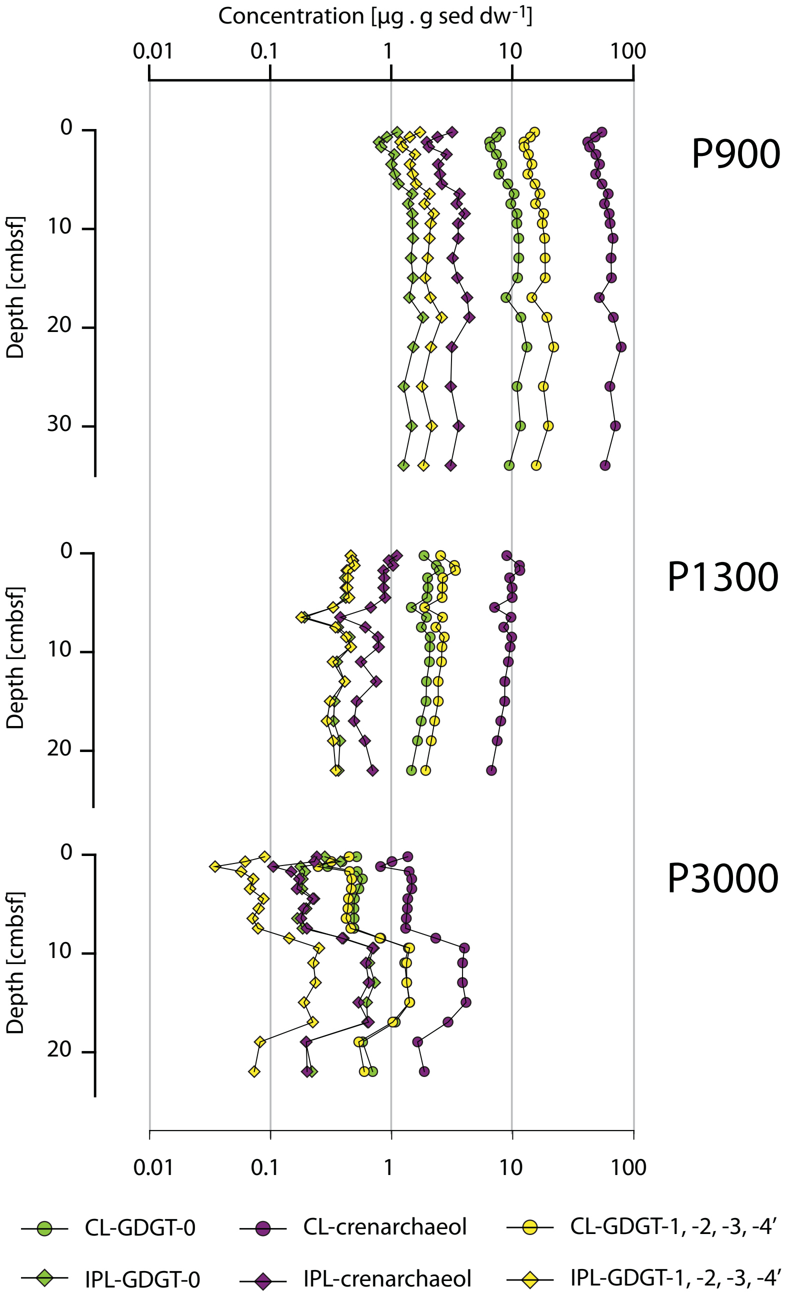

Figure 3.4. Concentrations per g dry weight sediment and accumulation rates of crenarchaeol, GDGT-0 and the sum of GDGTs-1, -2, -3 and -4′ for (a) P900, (b) P1300 and (c) P3000. Note the logarithmic scales of the x-axis.

CL-concentrations in all three cores, particularly in the core from P3000, with almost 50% in the top horizon, and 25-35% in lower horizons of the core. Otherwise, there was relatively little variation in CL- and IPL-derived GDGT concentrations with depth at P900 and P1300. A three-fold increase in concentration was observed at P3000 (Fig. 3.4), where a transient strong increase in CL-GDGTs concentrations between 8 and 18 cm and an overall increase with depth were apparent (Fig. 3.4c).

TEX_{86} values calculated from the CL-GDGTs varied no more than 0.03 (corresponding to 1°C; Kim et al., 2010) with depth within the cores (Fig. 3.5). At P900 (Fig. 3.5a), they ranged from 0.79 to 0.76 and at P1300 from 0.77 to 0.73, while the TEX_{86} values at P3000 did not change significantly with depth (0.71±0.01). The TEX_{86} of IPL-derived GDGTs at P900 ranged from 0.77 to 0.80, and from 0.75-0.78 at P1300. At P3000, there was a distinct minimum in the surface sediment with low IPL-derived TEX_{86} values (down to 0.65), coinciding with the maximum in IPL-derived GDGT-0 concentration. The TEX_{86} of IPL-derived GDGTs was generally 0.01 to 0.04 higher than the TEX_{86} of the core lipids, except in the surface sediments at P900 and P1300, where they were identical.

TEX_{86} values differed significantly between stations: The CL-GDGTs in the top layer of sediment had a TEX_{86} of 0.79 at P900, 0.76 at P1300 and 0.70 at P3000. Similar differences were also observed in the TEX_{86} values of the IPL-derived GDGTs (0.78, 0.76 and 0.72, respectively). The average TEX_{86} values over the whole cores of the CL-GDGTs were 0.77±0.01 at P900, 0.74±0.01 at P1300 and 0.71±0.01 at P3000 and for the IPL-derived GDGTs 0.78 ±0.02, 0.76±0.01 and 0.71±0.02.

3.3 Direct analysis of IPLs with a crenarchaeol core

The sediments were also analyzed directly for a number of IPL species containing crenarchaeol as the core lipid (Fig. 3.1). The three most abundant IPLs detected by this method were monohexose (MH)-crenarchaeol, dihexose (DH)-crenarchaeol and hexose, phosphohexose (HPH)-crenarchaeol. Crenarchaeol with a hexose and a 180 Da (unknown) headgroup (equivalent to the IPL with the m/z 341 headgroup found by Sturt et al., 2004, and Lipp et al., 2008) was also present, but near detection limit in all cores and is therefore not shown in Fig. 3.6. The assay was developed for IPLs with crenarchaeol as a core lipid (Pitcher et al., 2011b) and therefore GDGT-0, -1, -2 and -3 with IPL moieties were not measured, but we assume that the distribution of the crenarchaeol-IPL will provide insights on the general dynam-

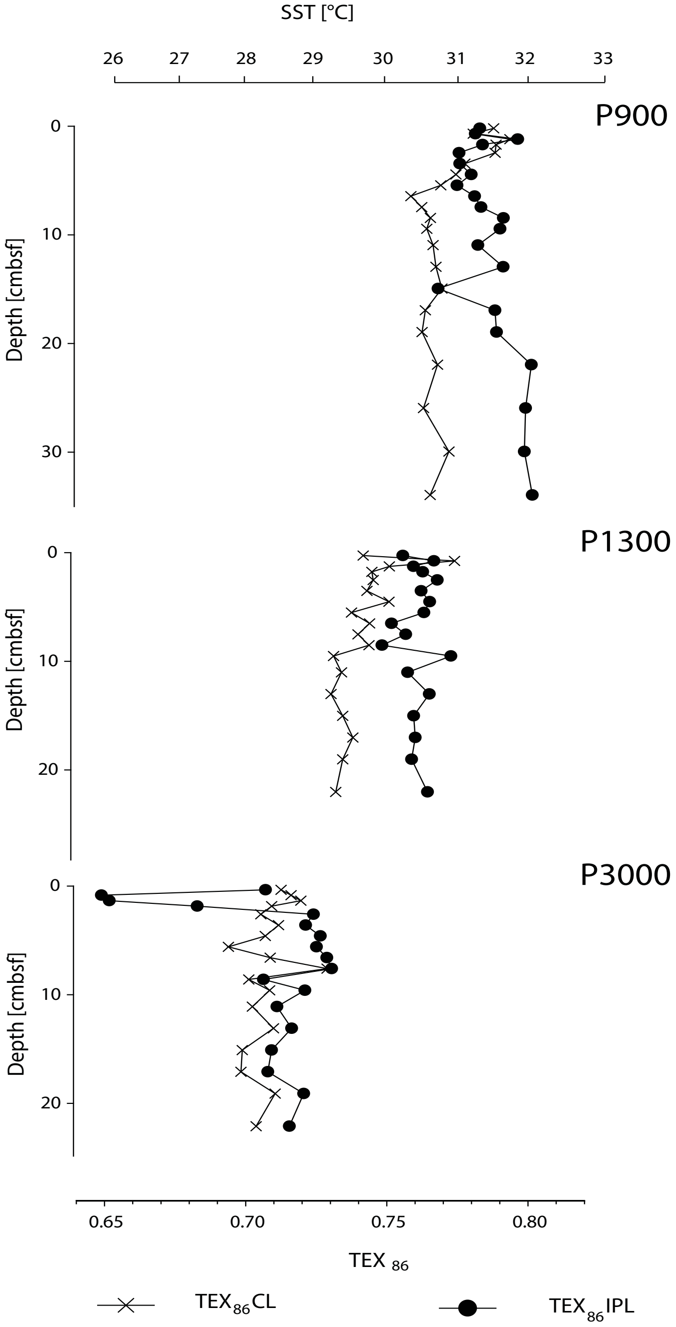

Figure 3.5. TEX_{86} values with depth for (a) P900 (b) P1300 and (c) P3000 well below the OMZ. The standard deviation is 0.01 units of TEX_{86}. The corresponding SST was calculated according to the global core top calibration (Kim et al., 2010) and is shown in the upper axis.

ics of IPL-GDGTs in the three different sediment cores.

The depth profiles of the glycolipids MH- and DH-crenarchaeol differed from those of HPH-crenarchaeol (Fig. 3.6). In the cores from P900 and P1300, the glycolipids showed no particular trends with depth and remained relatively constant. At P3000, the glycolipid concentrations increased at the same depth interval where increases in TOC and IPL-derived and CL-GDGTs were measured. The HPH-crenarchaeol profiles at the different stations showed a strikingly different pattern compared to the glycolipids. While the HPH-crenarchaeol concentrations measured at P900 did not show significant trends with depth except for the deepest sediments (Fig. 3.6a), at P1300, just below the OMZ, its abundance decreased within 3 cm by more than one order of magnitude and then remained low and relatively variable (Fig. 3.6b). HPH-crenarchaeol at P3000 showed a similar but even more pronounced decrease by two orders of magnitude from 1.25 to 5 cm (Fig. 3.6c). At this station, an increase in the HPH concentration was noted in the same interval where increases in TOC and IPL-derived and CL-GDGTs were observed (cf. Fig. 3.3c and Fig. 3.6c).

3.4 Distribution of GDGTs in IPLs with different headgroups

In order to determine the distributional variation in CL-composition of the different intact polar lipid species, the IPL-GDGTs were isolated by semi-preparative HPLC from 0- 2 cm and from 20-24 cm depth layers of the sediment core at P1300 and subsequently acid hydrolyzed and analyzed for GDGT distributions. While from the sediment at 0-2 cm depth, fractions containing MH-, DH- and HPH-GDGTs were obtained, at 20-24 cm depth, only MH- and DH-GDGTs were present in high enough quantities (Fig. 3.7a).

For both sediments, it was found that the DH-GDGTs (combined with GDGTs having the hexose + unknown 180 Da headgroup), contained relatively more-GDGT-2, -3 and 4’ and less GDGT-1 as a core lipid than the MH-GDGTs and, in case of the top sediment, the HPH-GDGTs. This resulted in large differences in TEX_{86} values between the various types of IPL-GDGTs, i.e. 0.88 for the DH-GDGTs, 0.65 for the MH-GDGTs and 0.55 for the HPH-GDGTs (Fig. 3.7b).

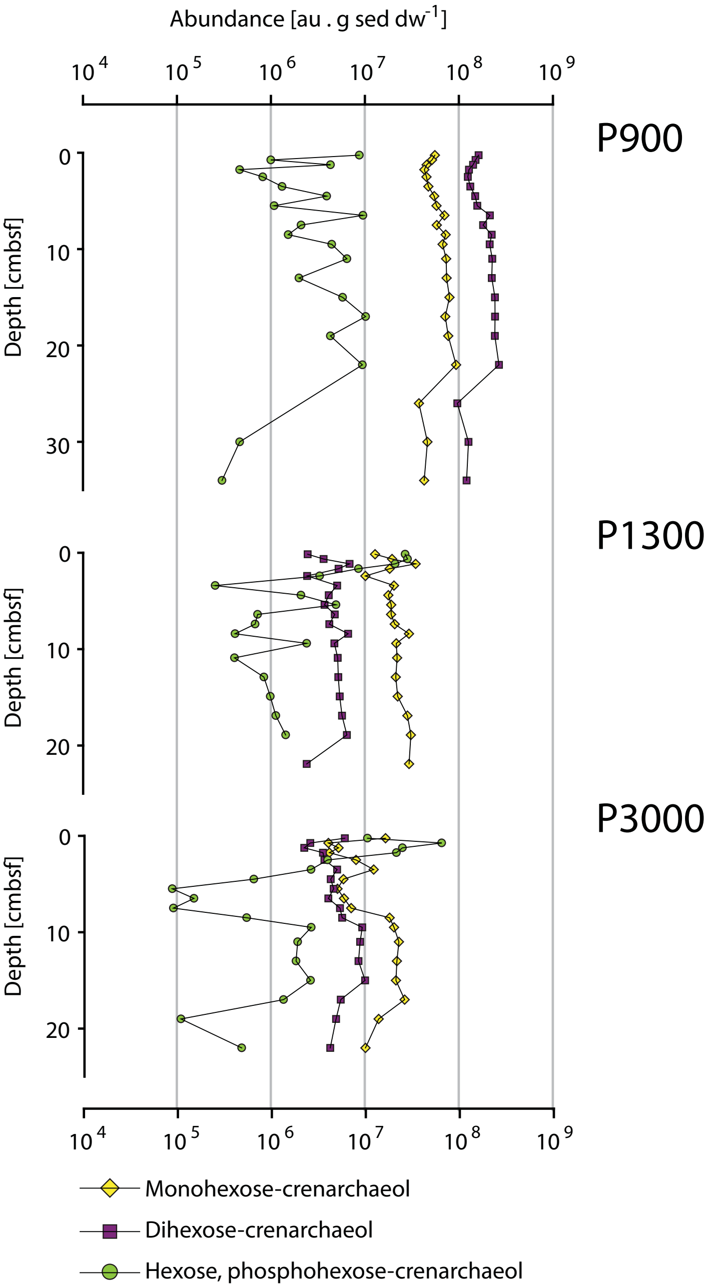

Figure 3.6. Direct measurement of intact polar lipids monohexose-crenarchaeol, dihexose-crenarchaeol and hexose, phosphohexose-crenarchaeol by HPLC/ESI-MS^2. Note the logarithmic scales of the X-axis.

4 DISCUSSION

4.1 Sedimentary production and preservation of GDGTs

IPL-GDGTs in the sediments can have two sources: water-column derived GDGTs (i.e. either from the water column directly above the sediment or laterally transported GDGTs), and GDGTs produced in situ by sedimentary Archaea (cf. Lipp and Hinrichs, 2009; Liu et al., 2011). Ammonia-oxidizing Archaea, whose IPLs consist mainly of GDGTs with MH-, DH- and HPH- as well as an unknown head-group (Sinninghe Damsté et al., 2002b; Schouten et al., 2008; Pitcher et al., 2010; 2011c), are ubiquitous and active in marine surface sediments (Francis et al., 2005; Caffrey et al., 2007; Park et al., 2008; Park et al., 2010). Since archaeal ammonia-oxidation proceeds aerobically (Könneke et al., 2005; Hatzenpichler et al., 2008; Erguder et al., 2009; Park et al., 2010) and also in environments with low oxygen concentrations ranging from <3 μM to 0.2 mM, we expected in situ production of crenarchaeol-IPLs in (sub-) surface layers where low amounts of oxygen were still present, i.e. P1300 and P3000, and negligible production at P900, where oxygen hardly penetrated into the sediments. Indeed, pronounced (sub-) surface maxima of HPH-crenarchaeol, likely the most suitable tracer for living AOA (see Schouten et al., 2012), are observed in the cores from P1300 and P3000, where oxygen penetrated the sediments (Fig. 3.6), suggesting production by benthic aerobic AOA. This maximum is not observed in the sediment core at station P900, where oxygen hardly penetrates into the sediment. Indeed, it is remarkable that the HPH-crenarchaeol constituted on average 50 % of the SRM area measured in SPM of the >0.7 μm size fraction (Fig. 3.8, cf. Schouten et al., 2012), while in the sediment underlying this water profile (station P900), the relative contribution of HPH-crenarchaeol to the total peak area is relatively low (ca. 4 %) both at the surface and at 20-24 cm depth (Fig. 3.8). Collectively, this indicates negligible benthic production of HPH-crenarchaeol at station P900, in contrast to stations P1300 and P3000.

Sedimentary degradation of HPH-crenarchaeol seems to proceed in the first few cm (1 - 2 kyrs), and then ceases, suggesting two pools of HPH-crenarchaeol: a readily degradable pool, which is rapidly broken down (<1-2 kyr), probably derived from in situ sedimentary production and therefore accessible for degradation, and a slowly degrading pool, likely fossil pelagic IPLs attached to the mineral matrix of particles and protected from degradation. The second, more resistant pool of HPH-crenarchaeol likely stems from the water column where IPL-GDGTs are found in >0.7

µm size SPM (Schouten et al., 2012), where they are probably being protected from degradation by adsorption to particles and into mesopores (Mayer, 1994; Hedges and Keil, 1995; Mayer et al., 2004). The rapid decrease of the HPH-crenarchaeol below the surface sediment production peak at stations P1300 and P3000 and the relatively low amounts of HPH crenarchaeol at station P900, are in accordance with the rapid degradation kinetics for phosphoester-lipids found by Harvey et al. (1986). Furthermore, the resemblance of the HPH-crenarchaeol concentration profile to the TOC profile below 7 cm depth at station P3000 suggests that increased preservation, indicated by the higher TOC values, results in high amounts of HPH-crenarchaeol, again indicating its probable origin from the water column.

In contrast, MH- and DH-crenarchaeol profiles did not show any significant peaks in the surface sediment, which could either mean their production was occurring – to the same degree – at all depths, including anoxic zones, or that they are degraded so slowly that the majority of them is fossil and derived from the water column where they are abundantly present (Schouten et al., 2012). Recent studies in the Arabian Sea water column support the latter hypothesis: only the HPH-crenarchaeol concentration profile matched the archaeal amoA gene transcript abundance (Pitcher et al., 2011b), whereas MH- and, to a lesser degree, DH-crenarchaeol concentrations showed disparate profiles (Schouten et al., 2012). The MH- and DH-crenarchaeol in sediments showed no decrease at all with depth, confirming the slow degradation rates, i.e. >10 kyrs, the timeframe covered by our cores, as theoretically predicted (Schouten et al., 2010). The strong resemblances of MH- and DH-profiles to those of TOC are indicating their pelagic provenance. Small amounts of MH- and DH-crenarchaeol are likely also produced in the surface sediment, but, other than with HPH-crenarchaeol, these in situ produced MH- and DH-crenarchaeol amounts must be relatively minor compared to the fossil amounts of preserved pelagic MH- and DH-crenarchaeol. Our results thus suggest that (i) glycolipids are mainly derived from the water column. (ii) HPH-crenarchaeol is relatively rapidly degraded and (iii) benthic AOA are actively producing IPL-crenarchaeol in the (sub-)surface of the sediment underneath the OMZ, probably occupying a low oxygen niche (cf. Abell et al., 2011; Chen et al., 2008; Pitcher et al., 2011b). Interestingly, while the HPH-crenarchaeol shows subsurface maxima indicating in situ production, the ratio of IPL-derived vs. CL-crenarchaeol does not increase as perhaps would be expected (Fig. 3.4). The amount of IPL-derived crenarchaeol, which represents the sum of all IPLs with crenarchaeol as a core lipid, is thus seemingly unaffected by the changes in

HPH-crenarchaeol concentration. The reason for this could be an analytical bias, as the SiO_2 column used to isolate IPL-derived GDGTs selectively retains or degrades phospho-GDGTs but not glyco-GDGTs (Lengger et al., 2012a). Thus, an increase in abundance in the phospho-GDGTs would not be readily visible in the IPL-derived GDGT fraction. Alternatively, the IPL-GDGTs are mainly composed of glycolipid GDGTs with low amounts of phospholipid GDGT and thus the total concentration in IPL-derived GDGTs is mainly determined by the amount of glycolipid GDGTs.

A notable exception to the general trend is the high abundance of IPL-derived GDGT-0 in the in the surface sediment of P3000 core (located in oxic bottom waters), possibly from benthic Archaea other than Thaumarchaeota, i.e. Eury- or Crenarchaeota. Importantly, however, the amount of CL-GDGT-0 is not simultaneously increasing; suggesting that also the in situ produced IPL-GDGT-0 is not affecting the CL-pool to a significant degree. IPL-GDGTs that are produced in situ are probably more vulnerable to microbial degradation as they may not be strongly absorbed to the sedimentary matrix and are therefore more readily degraded. Similarly, Liu et al. (2011) observed no transfers between the CL- and IPL-pool of GDGTs, except

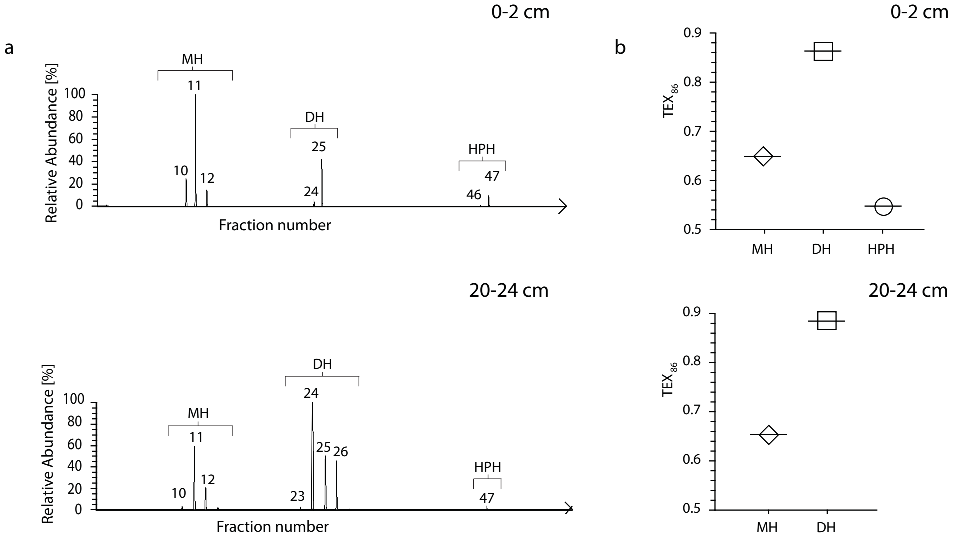

Figure 3.7. (a) Relative total ion current (TIC) of the fractions obtained by semi-preparative HPLC of sediment from P1300, 0-2 and 20-24 core depth. Measured by flow injection analysis and SRM of the 1-minute fractions. Types of main IPL contained are indicated. (b) TEX_{86} values of the different IPL species. MH– monohexose-GDGTs, DH- dihexose-GDGTs, HPH- hexose, phosphohexose-GDGTs from the top 2 cm and 20 cm depth.

in sulfate-methane transition zones. Indeed, changes in CL distributions reflecting input of sedimentary methane-oxidizing Euryarchaeota have been observed in other sulfate-methane transition zones (e.g. Pancost et al., 2001; Weijers et al., 2011). These zones likely contain highly active archaeal communities which are productive over prolonged time periods, in an anoxic environment and thus slower degradation kinetics. Hence, at sites with high archaeal abundance and activity over prolonged time periods, the GDGTs produced in situ may eventually affect the composition of the fossil pool of pelagic GDGTs, while at other sites, this does not seem to be the case. The higher concentrations of IPL-derived GDGTs measured in the core from P3000 at 9-16 cm depth, however, are most likely not due to in situ production. The increase is, unlike the peak in the surface sediments, accompanied by a similar increase in organic carbon and CL-GDGT concentrations, with no change in CL-distribution and hence most likely due to higher accumulation rates or potentially bioturbation activity.

The organic carbon content as well as the amounts of GDGTs preserved in the sediment varied strongly with the oxygen concentrations of the bottom water (cf. Sinninghe Damsté et al., 2002a). The organic carbon content of sediment recovered from the OMZ (P900) was 2 to 3 times higher than in sediments recovered from below the OMZ. CL- as well as IPL-derived GDGT concentrations were 1-2 orders of magnitude higher at P900 than at P1300 and P3000. IPL-derived GDGTs amounted to 5-20% of total GDGTs, with percentages of IPL-derived GDGTs increasing from P900 to P3000. The strong increase of both IPL-derived and CL-GDGT abundance with TOC is in agreement with the behavior of other biomarkers, as revealed previously in studies addressing oxic degradation of biomarkers (e.g. Prahl et al., 1997; Hoefs et al., 2002; Sinninghe Damsté et al., 2002a) and suggests that preservation of IPL-GDGTs is also strongly dependent on oxygen exposure times.

4.2 Implications for the TEX_{86} paleothermometer

The TEX_{86} of the IPL-GDGTs did not differ in general from the respective CL-TEX_{86} by more than 0.03 units (corresponding to ca. 1°C, within the calibration error of 2°C, Kim et al., 2010) within the three core locations (Fig. 3.5). Nevertheless, the TEX_{86} of IPL-derived GDGTs was consistently higher than that of the CL-GDGTs, which has been observed previously in other settings (Schubotz et al., 2009; Lipp and Hinrichs, 2009). In particular, Liu et al. (2011) reported a consistently higher TEX_{86} of IPL-derived GDGTs than of CL-GDGTs for a large variety (in depth as well as age) of marine sediments and a large range of TEX_{86} values. Their observations on longer timescales (>100 kyrs) agree well with our short-timescale observations (<10 kyrs). The TEX_{86} values of the individual IPL-GDGTs, obtained by preparative HPLC, provide an explanation for this phenomenon. These show that HPH-GDGTs have a substantially lower TEX_{86}-value than that of IPL-derived GDGTs, whereas MH-GDGTs have a similar TEX_{86} and DH-GDGTs a comparatively high TEX_{86}. These different TEX_{86} values of the different IPLs are likely already biosynthetically determined in Thaumarchaeota, since Schouten et al. (2008) and Pitcher et al. (2011c) reported that GDGT-1 is mainly associated with the HPH-IPLs while GDGT-2, -3 and -4 are mainly associated with the DH-headgroup in (enrichment) cultures of Thaumarchaeota. A more rapid lysis of the HPH-GDGTs, as observed in this study and that of Schouten et al. (2012), will preferentially remove GDGT-1 from the pool of IPL-GDGTs and bring it into the pool of CL-GDGTs. This process would result in increasing TEX_{86} values of the IPL-pool, which then mainly consists of MH- and DH-GDGTs, and a reduction of the TEX_{86} value of CL-GDGTs. Indeed, studies reporting high TEX_{86} values of IPL-derived GDGTs relative to CL-GDGTs also report high abundance of DH-GDGTs (Lipp and Hinrichs, 2009; Schubotz et al., 2009), consistent with this explanation. Furthermore, discrimination against the labile and "sticky" HPH-lipids during extraction and work-up (Pitcher et al., 2009b; 2011c; Lengger et al., 2012a) could also cause a higher TEX_{86} of the GDGTs in the IPL fraction.

Our results also explain the observations of Liu et al. (2011) that, in eight different settings, TEX_{86} of IPL-derived GDGTs was strongly correlated with the TEX_{86} values of CL- GDGTs (R^2=0.68) even if in situ temperatures differed largely from SST. These authors suggested that both pools were connected because benthic Archaea would recycle the biphytanyl-chains contained in fossil core lipids when producing IPL-GDGTs as a means to decrease energy requirements. This hypothesis, however, does not explain the slightly higher TEX_{86} of the IPL-derived GDGTs compared to the CL-GDGTs, as an exchange of biphytanyl chains between both pools would ultimately lead to convergent TEX_{86} values. Furthermore, as shown in the companion paper (Schouten et al., 2012), the same offset between TEX_{86} values of CL- and IPL-derived GDGTs was already observed in the water column where Thaumarchaeota are presumably actively synthesizing membrane lipids themselves. Thus, it is likely that a large part of the IPL-GDGTs in sediments is derived from fossil pelagic GDGTs and is not produced in situ. The similar observations by Liu et al. indicate

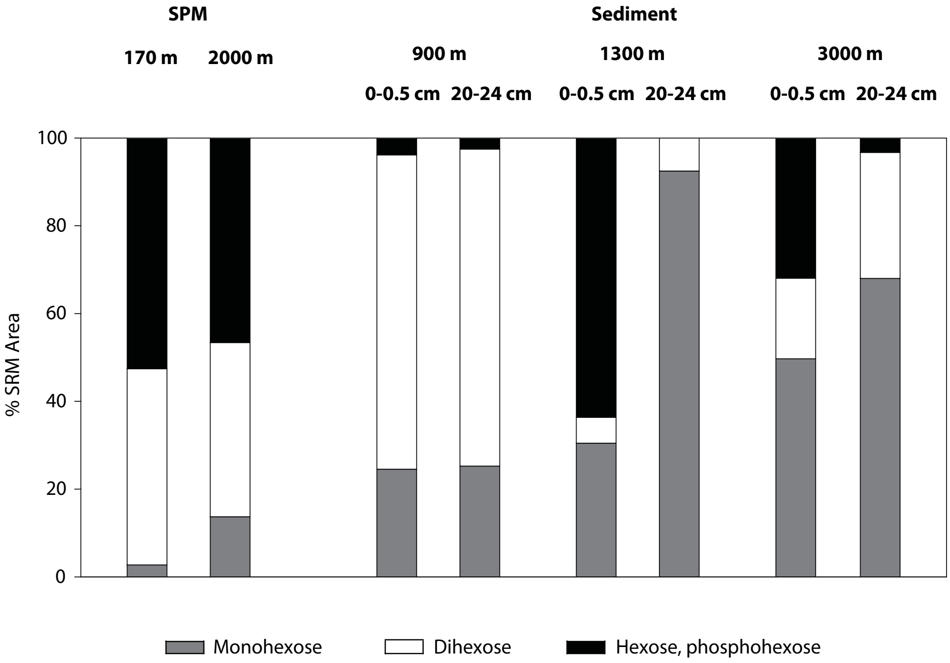

Figure 3.8. % of SRM peak area of monohexose-, dihexose and hexose, phosphohexose-crenarchaeol in SPM at 170 m and 2000 m water column depth (Schouten et al., 2012) and from the top 0.5 cm and 20-24 cm sediment depth at P900, P1300 and P3000.

that this is a general observation that can be applied to other marine settings.

Only at station P3000 at 0-2 cm depth, in situ production was high enough to change the TEX_{86} of the IPL-derived GDGTs, but the TEX_{86} signal of the CL-GDGTs does not reflect this change. This indicates that, as discussed above, in situ produced IPL-GDGTs are likely degraded quickly and do not accumulate as core lipids, probably due to a lack of matrix protection leading to rapid microbial degradation of the IPLs (Mayer, 1994; Huguet et al., 2008).

While we could not detect a strong effect on the TEX_{86} by benthic in situ production of GDGTs, a consistent decrease in TEX_{86} was observed in sediments, but also, as shown in the companion paper (Schouten et al., 2012), in suspended particulate matter (SPM) with increasing water depth at which the sediment cores were retrieved from. For the core lipids, TEX_{86} decreased from 0.79 for sediments and 0.78 for SPM in the OMZ (900 m) to 0.71 for the sediments and 0.66 for the water column SPM in the oxic bottom waters (2000 and 3000 m, respectively, Fig. 3.9). These TEX_{86} values correspond to 31.5 – 28.0°C using the Kim et al (2010)

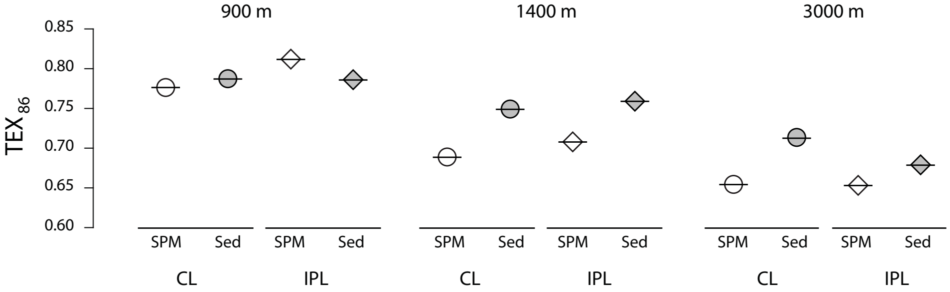

Figure 9. TEX_{86} values of SPM in the Arabian Sea water column (WC; from Schouten et al., 2012) and of surface sediments on the Murray Ridge. Water depths were 900 m, 1400 m (1350 m for SPM) and 3000 m (2000 m for SPM). CL- core lipids, IPL – intact polar lipids.

calibration, while the mean annual sea surface temperature was 26.4°C (Wuchter et al., 2006a). Similar decreases from 0.81 to 0.65 (water column SPM) and 0.79 to 0.68 (surface sediment) were observed for the IPLs. Interestingly, the TEX_{86} values of CL-GDGTs in sediment traps from the Arabian Sea also decrease from 450 m depth downwards (Wuchter et al., 2006). The apparent decreasing trend in sedimentary TEX_{86} values with increasing water depth could be due to several reasons: (i) preferential degradation of certain CL-GDGTs; (ii) sedimentary in situ production; (iii) contribution from Archaea in the deeper water column. The preferential diagenesis of certain core lipids can be discarded as a hypothesis, as the difference in TEX_{86} also occurs with IPL-derived GDGTs in the water column as well as in sediments. Regarding the second hypothesis, as discussed above, sedimentary in situ production is unlikely to be significantly affecting TEX_{86} values in surface sediments. Thus, the most likely explanation may be the incorporation of a signal from the lower, colder, part of the water column. This would be consistent with Pearson et al. (2001) and Shah et al. (2008) who found ^{14}C-depleted GDGTs in Santa Monica Basin sediments, inferring provenance from deeper water horizons. Furthermore, Ingalls et al. (2006) found evidence for deep water production based on ^{14}C-depleted values of GDGTs in the water column in the Pacific Ocean. The incorporation of a GDGT signal from deeper waters raises the question how well the TEX_{86} is reflecting surface water conditions. Indeed, several studies have shown that TEX_{86} is frequently not reflecting surface but subsurface (0-200 m) conditions (cf. Huguet et al., 2007; Lopes dos Santos et al., 2010). Kim et al. (2008) has shown that the correlation of TEX_{86} with 0-200m temperatures is similarly high as with SST. This correlation, however, strongly decreases with depth, suggesting there is no substantial deep water component . While there is a significant shift in TEX_{86} value corresponding to ca. 3 °C, the shift is relatively small considering that the potential GDGT pool is increasing from 0-900 m to 0-3000 m, i.e. tripling in size. This suggests that although there may be an addition of deep water GDGTs, this amount may be relatively small compared to that of the upper part (0-200 m) of the water column.

In summary, the TEX_{86} is likely not strongly affected by benthic in situ production in normal marine settings. However, the differential degradation of IPL-GDGTs we observed could potentially have an impact on TEX_{86} calibration studies. Methods used for TEX_{86} calibrations and paleotemperature assessment are based on the analysis of CL-GDGTs. Faster degradation of the HPH-GDGTs and the more slowly progressing transfer of the MH- and DH-GDGTs to the CL-pool could potentially lead to lower TEX_{86} values of CL in surface sediments than in deeper sediments. Calibration studies have so far relied on CL-GDGTs in surface sediments, while paleoclimate studies measure TEX_{86} values in deeper, older horizons, where potentially also some MH- and DH-GDGTs have been transformed to CL-GDGTs, thereby slightly increasing TEX_{86} values. However, since IPL-derived GDGTs are relatively minor compared to CL-GDGTs (< 10 %) this process likely leads to only slight overestimations of past SST.

5 CONCLUSION

Our study of sediments from the Arabian Sea deposited under contrasting oxygen conditions suggests that IPL-derived GDGTs, in particularly glycolipids, stemming from the water column are likely preserved in sediments and that their degradation is dependent on oxygen exposure time. Phospholipid-GDGTs are produced in oxic surface layers of sediment, probably by benthic AOA, but rapidly degrade within less than 1 or 2 kyrs, while the amount of glycolipid-GDGTs hardly changes. Additional evidence from concentrations of IPL-derived and CL-GDGTs and their TEX_{86} values shows that in situ production in the surface sediment does not substantially influence the TEX_{86} of the CL because it is either too small in amount compared to the fossil GDGTs or it is completely degraded quickly and not transferred into the CL-pool. Differences between TEX_{86} values of IPL-derived GDGTs and CL-GDGTs are likely due to differences between TEX_{86} values of phospholipids and glycolipids and their dissimilar degradation rates. The average TEX_{86} for IPL-derived as well as CL decreased with increasing water depth, possibly due to the incorporation of a lower water column signal.

Acknowledgements. We would like to thank the Master and the crew of the R/V Pelagia as well as the technicians and scientists participating in cruise 64PE301 for assistance during sampling. We also thank J. Ossebaar and S. Crayford for support with the LC/MS and TOC measurements, respectively. K. Koho kindly provided the data for the oxygen penetration depths. The PASOM cruise was funded by the Netherlands Organization for Scientific Research, NWO, by providing grant 817.01.015 to G. J. R. This is publication number DW-2011-1009 of the Darwin Center for Biogeosciences, which partially funded a studentship (S.K.L.) by providing a grant to S.S.

CHAPTER 4

IMPACT OF OXYGEN EXPOSURE TIME AND DEEP WATER COLUMN PRODUCTION ON GDGT ABUNDANCE AND DISTRIBUTION IN SURFACE SEDIMENTS IN THE ARABIAN SEA: IMPLICATIONS FOR THE TEX_{86} PALEOTHERMOMETER

In preparation for *Geochimica et Cosmochimica Acta*

IMPACT OF OXYGEN EXPOSURE TIME AND DEEP WATER COLUMN PRODUCTION ON GDGT ABUNDANCE AND DISTRIBUTION IN SURFACE SEDIMENTS IN THE ARABIAN SEA: IMPLICATIONS FOR THE TEX$_{86}$ PALEOTHERMOMETER

Sabine K. Lengger, Ellen C. Hopmans, Jaap S. Sinninghe Damsté and Stefan Schouten

Department of Marine Organic Biogeochemistry, Royal NIOZ Netherlands Institute for Sea Research, P. O. Box 59, 1790AB Den Burg, Texel, The Netherlands.

ABSTRACT

The TEX$_{86}$ is a widely used paleotemperature proxy based on isoprenoid glycerol dibiphytanyl glycerol tetraethers (GDGTs) produced by Thaumarchaeota. Archaeal membranes are composed of GDGTs with polar head groups (IPL-GDGTs), most of which are degraded completely or transformed into more recalcitrant core lipid (CL)-GDGTs upon cell lysis. However, some of the IPL-GDGTs, i.e. mainly those containing glycosidic head groups, can be preserved, although the extent of preservation under different conditions has not yet been fully defined. Here, we examined the impact of oxic degradation on the distributions of core lipid (CL)- and intact polar lipid (IPL)-GDGTs in surface sediments from a sea mount (Murray Ridge), whose summit protrudes into the oxygen minimum zone of the Arabian Sea, deposited at a range of depths and exposited to different oxygen bottom water concentrations(<3 to 83 µmol . L^{-1}). Concentrations of organic carbon, IPL- and CL-GDGTs decreased linearly with increasing oxygen exposure time (OET), suggesting that this is an important controlling factor in determining the concentrations of GDGTs in marine sediments. IPL-GDGT-0 was the only exception and increased with water depth, indicating that this GDGT was produced in situ in the surface sediment. Concentrations of crenarchaeol with glycosidic headgroups decreased with increasing OET, while crenarchaeol with a hexose, phosphohexose head (HPH) group, in contrast, showed an increase with increasing OET, indicating that the concentration of HPH crenarchaeol was primarily determined by in situ production in surficial sediments. TEX$_{86}$ values of both IPL-derived GDGTs and CL-GDGTs decreased by ~0.08 units with increasing water depth, in spite of the sea surface temperatures being identical at all settings. In situ production in sediments could be excluded as

the main cause, as well as differential oxic degradation of IPL-GDGTs. Instead, the main cause for the observed change in TEX_{86} values may be the incorporation of GDGTs produced in the deeper water column (at water depths > 200 m) into the surface sediments. However, the effect of this potential deep water contribution on TEX_{86} values is relatively small (translating into reconstructed temperature changes of <3°C), considering the large depth interval (900 to 3000 m), but it may have to be accounted for in TEX_{86} calibration and paleotemperature studies of deep water sedimentary records.

1 Introduction

The TEX_{86} is a paleotemperature proxy developed over the last decade. Schouten et al. (2002) discovered a relationship of ring distributions of common archaeal membrane lipids, isoprenoid glycerol dibiphytanyl glycerol tetraethers (GDGTs; Fig. 4.1a), with sea surface temperature and quantified this, using a ratio of four different GDGTs, called the TEX_{86}. These compounds have been shown to be mainly produced by Thaumarchaeota in the marine environment (Sinninghe Damsté et al., 2002b; Sinninghe Damsté et al., 2002c). They are present in the cell membranes of live cells as intact polar lipids (IPLs; Fig. 4.1b), with polar head groups such as hexose- and phosphate-groups (Schouten et al., 2008; Pitcher et al., 2010; Pitcher et al., 2011c). These IPL-GDGTs were generally assumed to be associated only with living and active cells (Biddle et al., 2006; Lipp et al., 2008; Lipp and Hinrichs, 2009; Schubotz et al., 2009). There is, however, an increasing amount of evidence that IPL-GDGTs, and especially those with glycosidic headgroups, can be preserved over geological timescales, especially under anoxic conditions (Harvey et al., 1986; Schouten et al., 2010; Liu et al., 2011; Logemann et al., 2011; Lin et al., 2012; Lengger et al., 2012b; Lengger et al., 2013, chapter 6, this volume).

For the TEX_{86}, a global calibration was developed based on marine surface sediments (Kim et al., 2008) and recently, two calibrations for two GDGT ratios were proposed – one for tropical/subtropical and one for polar oceans, the TEX^{H}_{86} and the TEX^{L}_{86} (Kim et al., 2010), respectively. The TEX_{86} is now widely used to reconstruct paleotemperatures of the sea surface using ancient marine sediments (e.g. Liu et al., 2009; Bijl et al., 2009). However, even though the TEX_{86} is strongly related to sea surface temperature, an equally strong relation with temperatures from 0-200 m water depth is observed (Kim et al., 2008; Kim et al., 2012b). Indeed, it was shown in several areas that the TEX_{86} temperatures reflect subsurface temperatures (Ingalls et al., 2006;

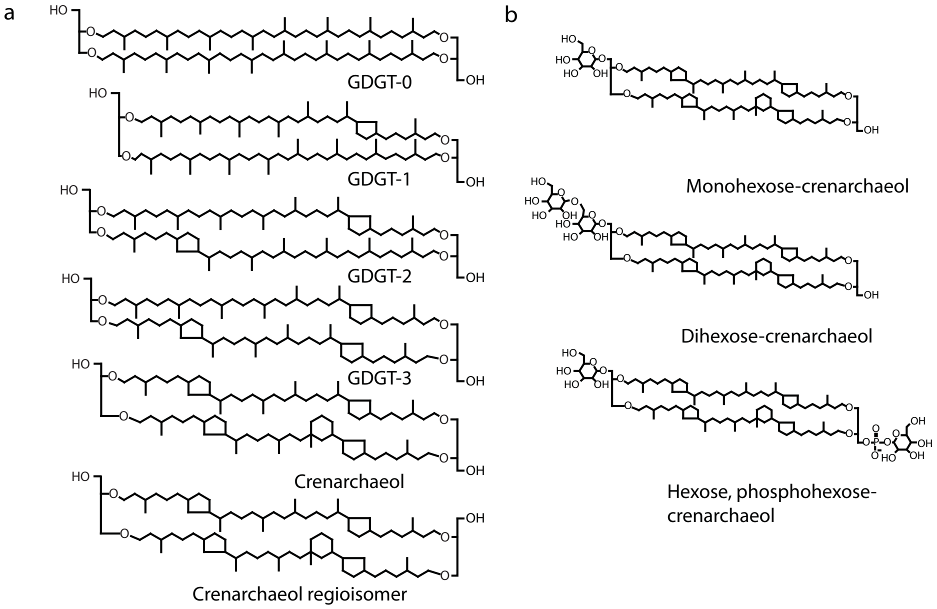

Figure 4.1. Structures of CL-GDGTs (a) and IPL-GDGTs isolated by semi-preparative HPLC (b).

Huguet et al., 2007; Lopes dos Santos et al., 2010; Nakanishi et al., 2012; Kim et al., 2012b). Molecular ecological studies have shown that Thaumarchaeota are not only present in the upper 200 m of the marine water column but also deeper in the water column, although their cell numbers generally decrease with depth (e.g. Karner et al., 2001; Herndl et al., 2005; Agogué et al., 2008; Reinthaler et al., 2010). The reason why most of the GDGTs present in marine surface sediments may still derive from the upper 0-200 m could be the preferential packaging of these GDGTs into fecal pellets and marine snow. This process mainly takes place in the photic zone and just below, as this is, due to high abundance of phytoplankton, the preferred habitat for zooplankton and possesses thus the most active food web (Wakeham et al., 2003; Wuchter et al., 2005; Huguet et al., 2006a). Below the photic zone, the grazing organisms have to rely on sinking particles and chemoautotrophic production of prokaryotic biomass. Thus, the food web activity, and presumably fecal pellet packaging, is much reduced (Burd et al., 2010). However, the TEX$_{86}$ values of material collected in sediment traps suggest that there may be a contribution of archaea from the deeper water column, i.e. >200m (Wuchter et al., 2006a; Turich et al., 2007). Indeed, radiocarbon analysis of sedimentary GDGTs suggested a contribution of deep water-dwelling archaea (>200 m) to the sedimentary GDGTs, estimating it to be as high as 100% (Pearson et al., 2001), 83% (Ingalls et al., 2006) and 74 to 100% (Shah et al., 2008). Nonetheless, the TEX_{86} from surface sediments collected from all over the world shows a robust correlation with sea surface temperatures (Kim et al., 2008; Kim et al., 2010). Thus, it remains unknown to what extent sedimentary GDGTs derive from deeper water-dwelling archaea. This makes it hard to constrain the potential bias of deeper water production on TEX_{86} paleothermometry.

Additionally, some bias of the TEX_{86} could arise from preferential degradation of specific GDGTs as a result of exposure to oxygen. Oxic degradation has been shown to cause a decrease in TEX_{86} in re-oxidized turbidite sediments as preferential degradation of marine over soil-derived isoprenoid GDGTs revealed a terrestrial signal (Huguet et al., 2009). Short-term degradation by exposure of anoxically deposited sediments to an oxic water column, however, showed no significant impact on the TEX_{86} (Kim et al., 2009). Schouten et al. (2004), who compared the TEX_{86} of oxically and anoxically deposited sediments, also found no differences between them. The studies by Huguet et al. (2009) and Kim et al. (2009), however, showed the impact of short term (1 year) or very long term (>10 kyr) degradation, and Schouten et al. (2004) compared the TEX_{86} of sediment deposited at different times and different environmental conditions. The sole impact of oxic degradation on intermediate time scales is not clear.

To address the issues of oxic degradation as well as the depth origin of sedimentary GDGTs we investigated surface sediments from the Murray Ridge in the Northern Arabian Sea. The Murray Ridge is a steep ridge which impinges the vast oxygen minimum zone (OMZ) that the Arabian Sea possesses. It thus allows the sampling of surface sediments that principally receive the same particle flux from the base of the photic zone, but at a wide range of water depths (900 – 3000 m) and bottom water oxygen concentrations (<3 to 83 μmol . L^{-1}). An earlier limited study of three surface sediments at 900, 1300 and 3000 m water depth showed that concentrations of CL- and IPL-derived GDGTs as well as IPL-crenarchaeol species were decreasing with increasing water depth and thus bottom water oxygen concentrations, but also that the TEX_{86} values of GDGTs (CL- and IPL-derived) were decreasing in the same way (Lengger et al., 2012b). It was speculated that part of the GDGTs in the sediment originated not only from the surface waters but also, in part, from the deeper waters. An alternative explanation offered was the differential degradation of IPL-GDGTs, as they were shown to have different TEX_{86} values dependent on the nature of the head group. Here we substantially extended our previous study by analyzing IPL- and CL-GDGT concentrations and distributions in ten surface sediments (0-0.5 cm) from the Murray Ridge, collected at regular intervals between 900 to 3000 m water depths. In addition, IPL-GDGTs from surface sediment (0-2 cm) and deeper sediment (20-24 cm) from cores recovered from the water depths 900, 1300 and 3000 m were separated according to head groups and their GDGT-distribution was investigated. The results were used to determine the impact of oxygen exposure time on sedimentary IPL- and CL-GDGTs and to investigate the contribution of deep water Thaumarchaeota to the GDGT-pool and the impact on the TEX_{86} in surface sediments.

2 MATERIALS AND METHODS

2.1 Sampling

Surface sediments were taken from multicores in the Northern Arabian Sea along a transect of the Murray Ridge during the PASOM cruise (64PE301) in January 2009 (Fig. 4.2, Table 1). The sediment cores, of 20 to 36 cm length, were sliced on board the *R/V Pelagia* in 0.5 to 4 cm intervals and stored in geochemical bags, frozen immediately at -80°C and further transported and stored at -20°C. Prior to analysis, the sediment was freeze-dried and homogenized. Surface sediment (0-0.5 cmbsf) was used for all measurements, except for the semi-preparatory HPLC, where a mixture of the top 0-2 cm and 20-24 cmbsf were used. Oxygen concentrations of the water column were measured by an SBE 43 dissolved oxygen sensor (Seabird, WA, USA) fitted to the CTD frame and calibrated against Winkler titrations. The limit

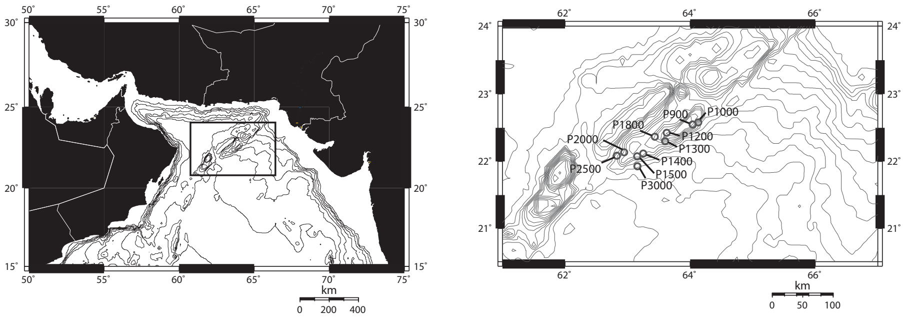

Figure 4.2. Map of the Murray Ridge in the North Arabian Sea with sampling stations indicated. Underwater topography is shown as 100 m contour lines.

of detection for these methods was 3 µmol . L^{-1}. Oxygen penetration depths were measured on board in 0.1 mm resolution using an OX-100 micro sensor (Unisense AS, Aarhus, DK) with a guard cathode as described by Revsbech (1989). The Murray Ridge sediment cores have been described previously by Kraal et al. (2012), who reported pore water profiles and the inorganic geochemistry of the depositional settings, and Koho et al. (2012), who reported evidence for the dependence of organic carbon concentrations and organic matter quality on oxygen, macrofaunal activity and microbial biomass.

2.2 Organic carbon concentrations, sedimentation rates and oxygen exposure times

Freeze-dried sediments were analyzed for organic carbon concentrations (C_{org}). The freeze-dried sediment was acidified over night with 2N HCl, subsequently washed with bidistilled H_2O and the water was removed by freeze-drying. The decalcified sediments were measured on a Flash EA 1112 Series (Thermo Scientific) analyzer coupled via a Conflo II interface to a Finnigan Delta^{plus} mass spectrometer. Standard deviations from three measurements ranged from 0.01 to 0.2 % total organic carbon (TOC).

As described by Lengger et al. (2012b) for the cores at P900, P1300 and P3000, and Koho et al. (2012) for all cores, determination of the sedimentation rates was carried out by ^{14}C dating. The average oxygen exposure times of the top 0.5 cm were calculated according to Hartnett et al. (1998), using the oxygen penetration depth and the sediment accumulation rates. As in some of the cores, oxygen penetrated rather deeply, but we only used the upper 0.5 cm of the core for TOC, CL- and IPL-GDGT determination, we divided by the 0.5 cm instead of the oxygen penetration depth.

2.3 Sediment extraction and separations

Aliquots (1-2 g) of freeze-dried surface sediment (0-0.5 cm sediment depth) were extracted with a modified Bligh and Dyer procedure as described previously in Lengger et al. (2012b). Briefly, extraction with methanol (MeOH)/dichloromethane (DCM)/phosphate buffer (PB) 50 mM, pH 7.5, in volume ratios 2:1:0.8 was carried out three times by ultrasonication and the solvent was collected after centrifugation. The combined liquid phases were adjusted to a solvent ratio of MeOH/DCM/PB of

1:1:0.9 (v/v) which led to phase separation between the DCM and the MeOH/PB. The DCM phase was collected and the MeOH/PB mixture was extracted twice more with DCM. The combined DCM phases were reduced with a rotary evaporator, re-dissolved in DCM/MeOH 9:1 (v/v), filtered over cotton wool and subsequently dried under a stream of N_2. The extract was stored at -20°C.

An aliquot was fractionated over a silica column in order to separate the IPL from the core lipids (CL) following the procedure of Oba et al. (2006) and Pitcher et al. (2009b). Briefly, fractionation was achieved over a silica column using 6 column volumes hexane/ethyl acetate 1:1 (v/v; CL-GDGTs) and 10 column volumes MeOH (IPL-GDGTs). Quantification was achieved by adding 0.1 µg C_{46}-GDGT internal standard (Huguet et al., 2006c) to the fractions. An aliquot of the IPL-GDGT fraction was transferred to a vial, dried and stored frozen for quantification of core lipids which eluted in the intact polar lipid fraction ("carry over"). These were typically <2% of the GDGTs present in CL fraction or 10% of GDGTs present in the IPL fraction and thus negligible. The remaining IPL-fraction was subjected to hydrolysis to release CL-GDGTs (=IPL-derived GDGTs).

In order to compare TEX_{86} values of the surface sediments with those of surface sediments in other studies, we analyzed the TEX_{86} values of the surface sediments using standard extraction and separation methods used for calibration of the TEX_{86} index (Kim et al., 2008; Kim et al., 2010). Aliquots of a few hundred mg of freeze-dried surface sediment were extracted after addition of pre-extracted diatomaceous earth in an Accelerated Solvent Extractor 200 (ASE 200, DIONEX, CA, USA) with a mixture of DCM/MeOH 9:1 v:v at 100 °C and $7.6 \cdot 10^6$ Pa. The polar GDGTs were separated from the apolar fraction by open column chromatography (Al_2O_3, three column volumes hexane/DCM 9:1 for the apolar and 4 column volumes DCM/MeOH 1:1 for the polar fraction).

2.4 Semi-preparative HPLC

For the isolation of particular IPL-GDGTs, repetitive semi-preparative HPLC was used as described previously (Lengger et al., 2012b) for sediments from stations P900, P1300 and P3000. Bligh Dyer extracts of ca. 4 g of sediment from 0-2 cm depth ("top") and of 4 g of sediment from 20-24 cm depth ("bottom") from P1300 were separated, and fractions of 3 mL were collected and subsequently analyzed with Flow Injection Analysis using ESI-MS^2 in SRM mode, monitoring intact polar lipids, i.e. monohexose (MH)-crenarchaeol, dihexose (DH)-crenarchaeol and hexose, phosphohexose (HPH)-crenarchaeol (Pitcher et al., 2011b). Six fractions, the ones containing monohexose-GDGTs, dihexose-GDGTs and hexose, phosphohexose-GDGTs, and the combined eluted fractions between those, were collected and 0.1 µg C_{46}-GDGT internal standard was added to each of them. The dihexose-GDGTs likely contained a minor amount of co-eluting hydroxyl-GDGTs (Liu et al., 2012), as observed in *Candidatus* Nitrosopumilus maritimus SCM1 and previously described as "unknown + 180" (Schouten et al., 2008). All fractions were acid-hydrolyzed and the specific IPL-derived GDGT distributions were quantified using HPLC/APCI-MS and the C_{46}-GDGT internal standard method as described above.

2.5 HPLC/APCI-MS

Analysis of CL-GDGTs and IPL-derived GDGTs by HPLC/APCI-MS and calculation of TEX_{86} was carried out as described previously (Schouten et al., 2012). Reproducibility for TEX_{86} values is typically < 0.02, corresponding to errors of < 1 °C. Temperatures were calculated according to the calibrations according to Kim et al. (2010) for TEX^{H}_{86}.

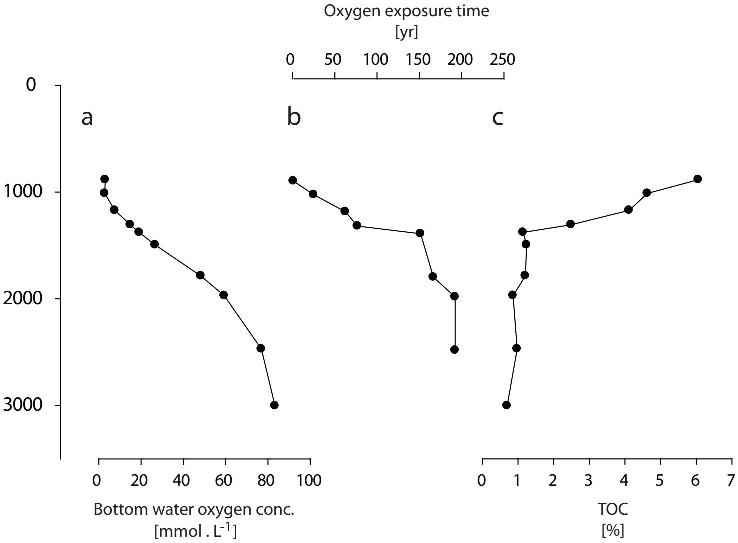

Figure 3.3. Bottom water oxygen concentrations (a), oxygen exposure time (as calculated from sedimentation rates and oxygen penetration depths; b) and organic carbon content (c) of the surface (0-2 cm) sediments of the Murray Ridge plotted vs. water depth.

Table 4.1. Organic carbon content (C_{org}), bottom water oxygen concentration (BWO), oxygen penetration depth (OPD) and sedimentation rates as well as oxygen exposure times (OET) of surface (0-0.5 cm) sediments deposit

Station	Water depth [m]	[C_{org}] [mg . g sed dw^{-1}]	BWO [µmol . L^{-1}]	OPD [mm]	Sed. rate [mm . kyr^{-1}]	OET [yr]
P900	885	60.6	3.0	0.1	134[a]	1
P1000	1013	46.3	2.8	1.0	40[b]	25
P1200	1172	41.2	7.6	1.4	22[b]	63
P1300	1306	24.9	15.0	2.9	38[a]	77
P1400	1379	11.4	19.2	5.8	33[b]	152
P1500	1495	12.4	26.6	7.1	n.d.[c]	n.d.[c]
P1800	1786	12.1	48.2	6.2	30[b]	167
P2000	1970	8.6	59.3	5.8	26[b]	192
P2500	2470	9.8	76.9	9.8	26[b]	192
P3000	3003	7.0	83.3	19.0	83[a,d]	60

[a] Lengger et al., 2012
[b] Koho et al., 2012
[c] Values could not be determined.
[d] This value is likely overestimated due to of lateral transport.

3 RESULTS

3.1 Sedimentation rate, organic carbon concentration and oxygen exposure time

Sedimentation rates for the ten cores ranged from 26 to 134 mm . kyr^{-1}, and generally decreased with water depth (Table 1). No sedimentation rate could be obtained for P1500 due to a constant age throughout the core (Koho et al., 2012). Furthermore, sedimentation rate for station P3000 was unusually high (83 mm . kyr^{-1}), which can be explained by lateral transport probably affecting the sediment at this station, causing the surface sediment to appear older. Therefore, the sedimentation rates of these two stations were not used in this study. Organic carbon concentrations (C_{org}) decreased steadily with depth from 6 to 1%, while bottom water oxygen concentrations increased with depth (from 3 µmol . L^{-1} to 83 µmol . L^{-1} ; Fig. 4.3; Table 1). Oxygen penetration depths (OPD) increased from 0.125 mm at P900 to 18 mm at P3000 (Table 1), resulting in an increase of the average oxygen exposure time (OET) of the 0 - 0.5 cm sediment slice with water depth, initially strongly from 1 yr to 152 yr between stations P900 and P1400, and subsequently more slowly from 152 to 192 yr between stations P1400 and P2500 (Fig. 4.3b, Table 1).

3.2 Concentrations and TEX_{86} values of GDGTs

CL- and IPL-GDGTs concentrations in the surface (0-0.5 cm) sediments generally decreased with increasing water depth (Fig. 4.4). CL-GDGT concentrations were 7.7 and 55 µg . g sed dw^{-1} for GDGT-0 and crenarchaeol, respectively, in the shallowest sediment and 0.25 and 0.67 µg . g sed dw^{-1}, respectively, in the surface sediment from the greatest depth (Fig. 4.4a). The isoprenoid GDGTs used in the TEX_{86} palaeothermometer (i.e. GDGT-1, -2, -3 and the crenarchaeol regioisomer; i-GDGTs) had summed concentrations of 15 µg . g sed dw^{-1} at the shallowest station, decreasing to values of 0.22 µg . g sed dw^{1} at the deepest station (Fig. 4.4a). IPL-derived GDGTs were present in much lower concentrations compared to CL-GDGTs; i.e. 0.14 – 1.1 µg . g sed dw^{-1} for GDGT-0, 0.1 – 3.1 µg . g sed dw^{-1} for crenarchaeol, and 0.04 – 1.7 µg . g sed dw^{-1} for the sum of the other i-GDGTs, with declining concentrations with increasing water depth (Fig. 4.4b). This corresponded to 10 to 20% of total CL-GDGTs for all except for GDGT-0, which showed IPL/total CL ratios of > 30% at water depths > 1000 m (Fig. 4.4c).

The TEX_{86} values for the CL-GDGT fraction decreased with increasing water depth from 0.78 at Station P900 to 0.72 at Station P3000 (Fig. 4.5). IPL-derived GDGTs showed a similar trend, with TEX_{86} values of 0.78-0.80 decreasing to 0.72. In order to compare these results to paleotemperature studies, which typically do not use Bligh Dyer extractions and IPL/CL separations as used here, we also performed ASE extraction, followed by a separation and analysis of the obtained extract. The TEX_{86} values obtained from analysis of the polar fraction obtained (Fig. 4.6) are comparable to the TEX_{86} values measured on the CL-fraction within the range of the analytical error (0.02 units).

3.3 Individual IPL-GDGTs in Arabian Sea surface sediments

As there is evidence that degradation behavior of IPL-GDGTs differs dependent on their head group composition (Harvey et al., 1986; Lengger et al., 2012b; Lengger et al., 2013, chapter 6, this volume), we separated IPL-GDGTs from three stations according to their head group composition using semi-preparatory HPLC. This al-

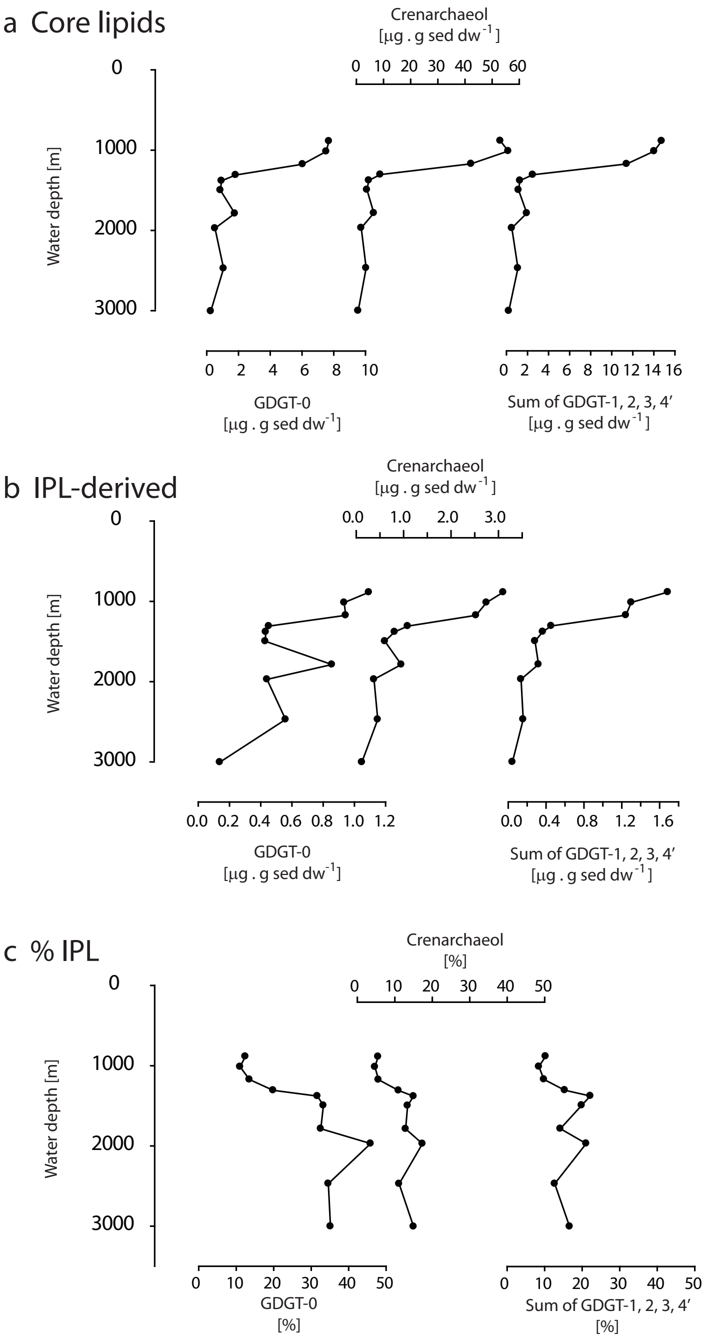

Figure 4.4. Graphs of core lipid-GDGT concentrations (a), IPL-derived GDGT concentrations (b) and %IPL of total GDGTs (c) in surface (0-0.5 cm) sediments plotted versus water depth of the sampling station.

lowed investigation of differences in degradation behavior and how this influences the TEX_{86}. For quantification of all IPL-GDGTs with different headgroups, preparatory HPLC was the most accurate available method. The fractions containing the IPL-GDGTs (MH-, DH- and HPH-derived GDGTs) were subsequently hydrolyzed and the obtained core lipids were quantified. This procedure was used with sediments of the top 0-2 cm and from 20-24 cm sediment depth for three different water depths (900, 1300 and 3000 m) (Fig. 4.6 left panels). Preliminary results of sediment from P1300, 0-2 and 20-24 cm, have already been described earlier (Lengger et al., 2012b), i.e. the TEX_{86} values of the released GDGTs. In this study, IPL-GDGTs were also quantified.

The isolation of individual IPLs showed that IPL-GDGT concentrations were highest in the surface sediment from shallow water depth compared to those from greater water depth (Fig. 4.6, left panels), consistent with the IPL-GDGT concentration profiles (Fig. 4.4b). MH-derived GDGTs dominated, but DH-derived GDGTs were present in high proportions as well (Fig 6, left panels). HPH-derived GDGTs

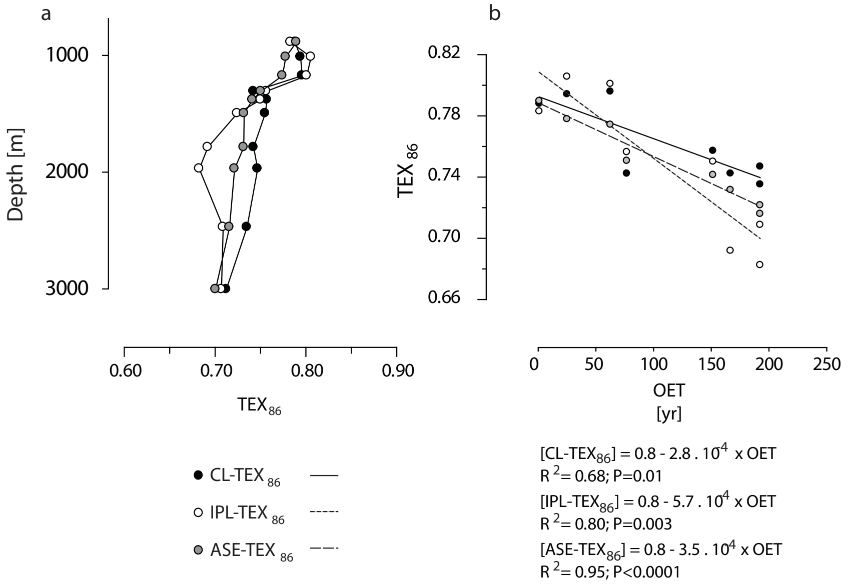

Figure 4.5. TEX_{86} values of the CL-GDGT and IPL- GDGT fractions and GDGTs extracted by the technique usually used in paleotemperature studies, ASE, plotted vs. depth (a) and correlation of the TEX_{86} values with OET (b). Values were those of surface sediment, i.e. the top 0.5 cm of the sediment.

were present in increasingly higher absolute abundance with increasing water depth with HPH-derived GDGTs at station P3000 representing the most abundant form of IPL-GDGTs. The deeper sediments (20-24 cm) showed similar MH- and DH-derived concentrations as in the surface sediments but a much lower concentration of HPH-derived GDGTs was evident, especially for station P3000 (Fig. 4.6, left panels). The distribution of core lipid GDGTs showed substantial differences for the different collected IPL fractions; i.e. DH contained a much higher fractional abundance of GDGT-1, -2, -3, and the crenarchaeol isomer than MH and HPH (right panels in Fig. 4.6). Some smaller differences were observed when these GDGT distributions per specific IPL group were compared for the surface and deeper (20-24 cm) sediments (right panels in Fig. 4.6).

These differences were also reflected in the TEX_{86} values of the different IPL fractions (Fig. 4.7). DH-derived GDGTs always showed the highest, and MH-derived GDGTs intermediate TEX_{86} values, i.e. 0.80 - 0.90 for the DH-derived GDGTs and 0.60 - 0.72 for the DH-derived GDGTs (Fig. 7). These values decreased for both MH- and DH-derived GDGTs with water depth but not with depth in the sediment. For HPH-derived GDGTs, TEX_{86} values in the surface (0-2 cm) sediments of stations P1300 and P3000 only could be reliably determined as concentrations were too low in the other sediments. Distributions are shown in Fig. 4.6, but it is obvious that they mainly consist of GDGT-0 and crenarchaeol, and the minor i-GDGTs are not present in high amounts. HPH-derived GDGTs showed the lowest TEX_{86} values, i.e. 0.37 - 0.42, much lower than those of the MH and DH IPLs (Fig. 4.7). Weighted-average TEX_{86} values (Total; Fig. 4.7) were calculated from the absolute abundances of the MH-, DH- and HPH-IPL and their GDGT composition. These are similar to those of the IPL-GDGT fractions (IPL-GDGTs; Fig. 4.7), confirming that the three major IPLs isolated are quantitatively representative of the total IPL-GDGT pool.

4 Discussion

4.1 Impact of oxic degradation and in situ sedimentary production on GDGT concentrations

Organic carbon concentrations in the surface sediments (0-0.5 cm) are decreasing with increasing water depth, coincident with increasing bottom water oxygen concentrations (BWO), increasing oxygen penetration depths (OPD), decreasing sedi-

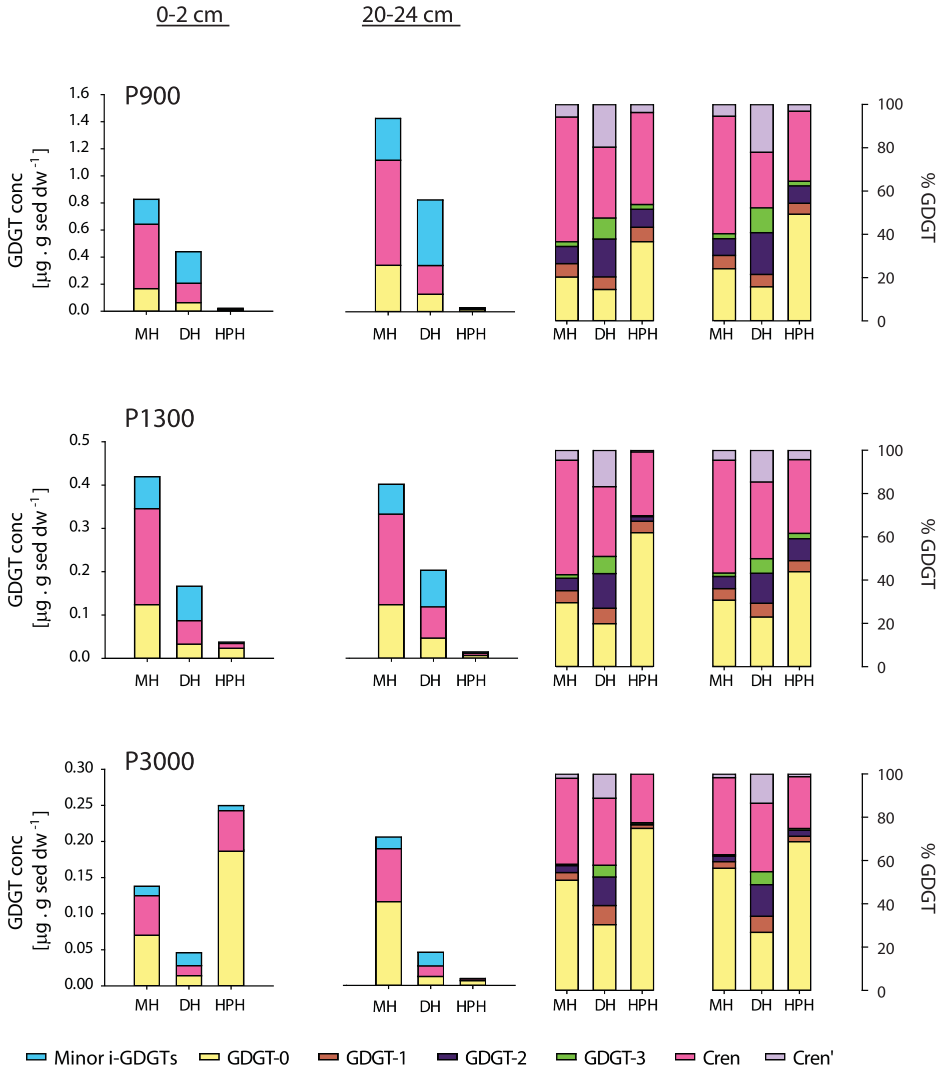

Figure 4.6. Amounts of different GDGTs (GDGT-0, crenarchaeol, and other isoprenoid GDGTs) in the IPLs (i.e. MH, DH and HPH) isolated by semi-preparative HPLC in the surface (0-2 cm) and deeper (20-24 cm) of stations P900, P1300, and P3000 (Left panels). GDGT distributions of the different isolated IPLs are shown in the right panels.

mentation rates and thus longer oxygen exposure times (OET) (Fig. 4.3; Table 1). Strikingly, there is a strong linear correlation between C_{org} and OET (R^2 0.93; Fig. 4.8a). This confirms the assumption that longer OETs cause lower organic carbon contents, in agreement with previous observations: Hartnett et al. (1998) found a linear correlation between the organic carbon burial efficiency and log OET in a range of marine sediments, suggesting that the organic carbon contents in these sediments are mainly determined by this parameter. Hedges et al. (1999) compared OET and other factors of many sedimentary regimes and concluded that it was not OET alone, but that OET was a proxy for other preservational factors as well. Interestingly, Sinninghe Damsté et al. (2002a) reported a significant impact of OET on the extent of preservation of biomarkers and organic carbon in Arabian Sea sediments, also from the Murray Ridge. Burdige (2007) summarized these observations and concluded that OET, in combination with factors that are correlated with it (i.e. benthic macrofaunal processes, physical reworking and redox oscillations), is the determining factor for organic carbon preservation.

Similarly to C_{org}, CL-GDGT concentrations were also strongly linearly negatively correlated to OET (R^2 0.82-0.83), with crenarchaeol showing the most pronounced decrease with OET (Fig. 4.8b). Remarkably, IPL-derived crenarchaeol and other isoprenoid GDGTs (sum of -1, -2, -3 and the crenarchaeol regioisomer) showed a high correlation (R^2 0.87-0.88) with OET too, but less so IPL-derived GDGT0 (R^2 0.49). As GDGT-0 is produced by many archaea (Koga and Nakano, 2008), not

Table 4.2. Degradation constants, i.e. slopes relative to initial concentrations for C_{org}, core lipid (CL)- and intact polar lipid (IPL)-derived GDGTs.

		C_0	**k**	**k/C_0**	**R^2**	**P**
		[μg . g sed dw^{-1}]	**[yr^{-1}]**	**[μg . g sed dw . yr^{-1}]**		
	C_{org}	5.4 ± 0.4	0.025 ± 0.003	0.46	0.93	0.0001
CL	Crenarchaeol	53 ± 7	0.28 ± 0.005	0.54	0.82	0.0020
	GDGT-0	7.4 ± 0.9	0.037 ± 0.007	0.50	0.80	0.0016
	Minor i-GDGTs	14 ± 2	0.075 ± 0.014	0.53	0.80	0.0016
IPL	Crenarchaeol	3.0 ± 0.3	0.014 ± 0.002	0.45	0.86	0.0005
	GDGT-0	0.98 ± 0.13	0.0025 ± 0.0010	0.25	0.49	0.0538
	Minor i-GDGTs	1.5 ± 0.2	0.0074 ± 0.0011	0.49	0.85	0.0006

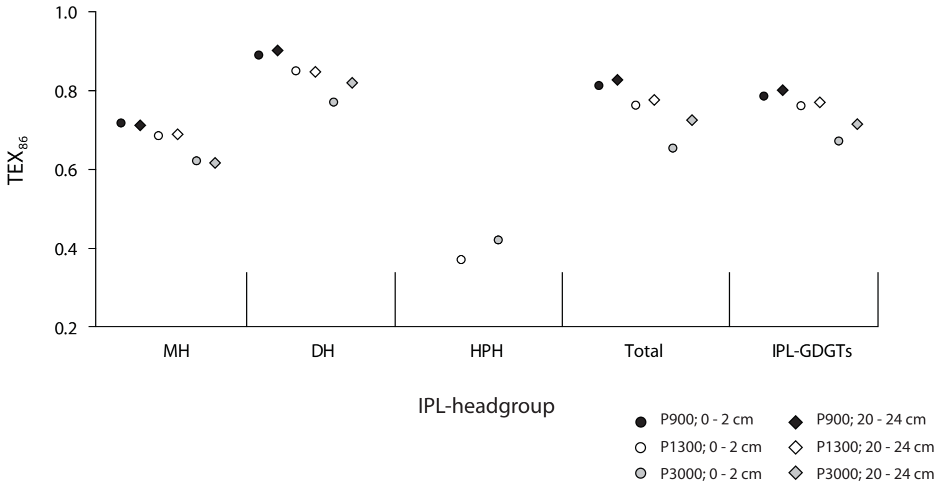

Figure 4.7. TEX_{86} values of IPL-fractions (MH-, DH- and HPH-GDGTs) at the three stations and two sediment depths, and the combined TEX_{86} values of those fractions isolated by semi-preparative HPLC ("total"). For comparison, the TEX_{86} values at these stations measured by separating IPL-GDGTs using silica column chromatography are shown ("IPL-derived").

only Thaumarchaeota, it is possible that it is produced in situ in the surface sediment. Lengger et al. (2012b), who analyzed sediment cores of 24-32 cm length at stations P900, P1300 and P3000 in high (0.5 – 4 cm) resolution, also found high abundance of GDGT-0 in the surface sediments with oxygenated pore waters (P1300, P3000). The concentrations of IPL-derived GDGT-0 were particularly high for P3000, at 0.5 - 1.5 cm sediment depth. However, interestingly, this high relative abundance was not present further downcore. Lengger et al. (2012b) thus concluded that the in situ-produced IPL-derived GDGT-0 was degraded quickly, as it was probably more bioavailable than the matrix-embedded material transported from the sea surface. The significant correlation of the other IPL-GDGTs with OET is strong evidence for oxic degradation being the predominant control on IPL-GDGT concentrations. Comparison of the slopes of this correlation, when normalized on initial concentrations, showed that it is similar for all IPL-derived GDGTs, CL-GDGTs and C_{org}, i.e. 0.45-0.54 units (Table 2), except for IPL-derived GDGT-0. This suggests that the concentrations of all these GDGTs (except for GDGT-0) are primarily controlled by preservation.

Semi-preparative HPLC provided quantitative information about the proportions of

GDGTs derived from IPL-GDGTs with different head groups, i.e. MH-, DH- and HPH-derived GDGTs (Fig. 4.6). This showed that MH- and DH-derived GDGTs decreased by an order of magnitude with water depth between stations P900 and P3000. Contrastingly, when the surface sediment (0-2 cmbsf) and the deep sediment (20-24 cmbsf) were compared, no substantial changes in concentration were observed. HPH-derived GDGTs showed a different pattern, i.e. with increasing water depth, the concentrations actually increased in the surface sediment. In the deep sediment, however, concentrations were always lower than those of the surface sediments. From the preparative HPLC results, it can also be seen that the HPH-derived GDGTs are mainly responsible for the increase in GDGT-0 in the IPL-GDGT fraction compared to the CL-GDGT fraction. These results strongly support the idea that, as suggested previously (Schouten et al., 2010; Logemann et al., 2011; Lengger et al., 2012b), in these sediments, the MH- and DH-GDGTs are predominantly fossil. They are most likely stemming from the water column and are not in situ produced in the sediment, as their concentrations decrease with increasing OET, and do not decrease with sediment depth or over time (down to 24 cmbsf). HPH-GDGTs are, in contrast to the glycolipids, not preserved to a large extent, and their presence is also substantially influenced by sedimentary in situ production of Thaumarchaeota, most probably involved in nitrification. Indeed, in the sediments from deeper water depths, the organic carbon content is also much lower, resulting primarily from oxic degradation in the surface sediments (Fig. 4.8a). During this process, ammonium will be generated from organic nitrogen and this, together with the increased oxygen concentration, may provide a niche for benthic Thaumarchaeota in these sediments. The fact that HPH-derived GDGT concentrations are near detection limit in the sediments from 20-24 cm depth compared to surface sediments is strong evidence for the rapid degradation of this lipid over a few kyrs, as suggested earlier (cf. Lengger et al., 2012b).

4.2 **Decrease of TEX_{86} with water depth: causes and implications**

An important observation in our study is the decrease of TEX_{86} in surface sediments with increasing water depth in CL- and IPL-derived GDGTs, the MH-GDGTs and DH-GDGTs as well as in the GDGTs extracted by ASE extraction (Fig. 4.5). There are three possible explanations for this decrease with water depth:

(i) An increasing contribution of in situ production of GDGTs in surface sediments with water depth by benthic Thaumarchaeota, and potentially other

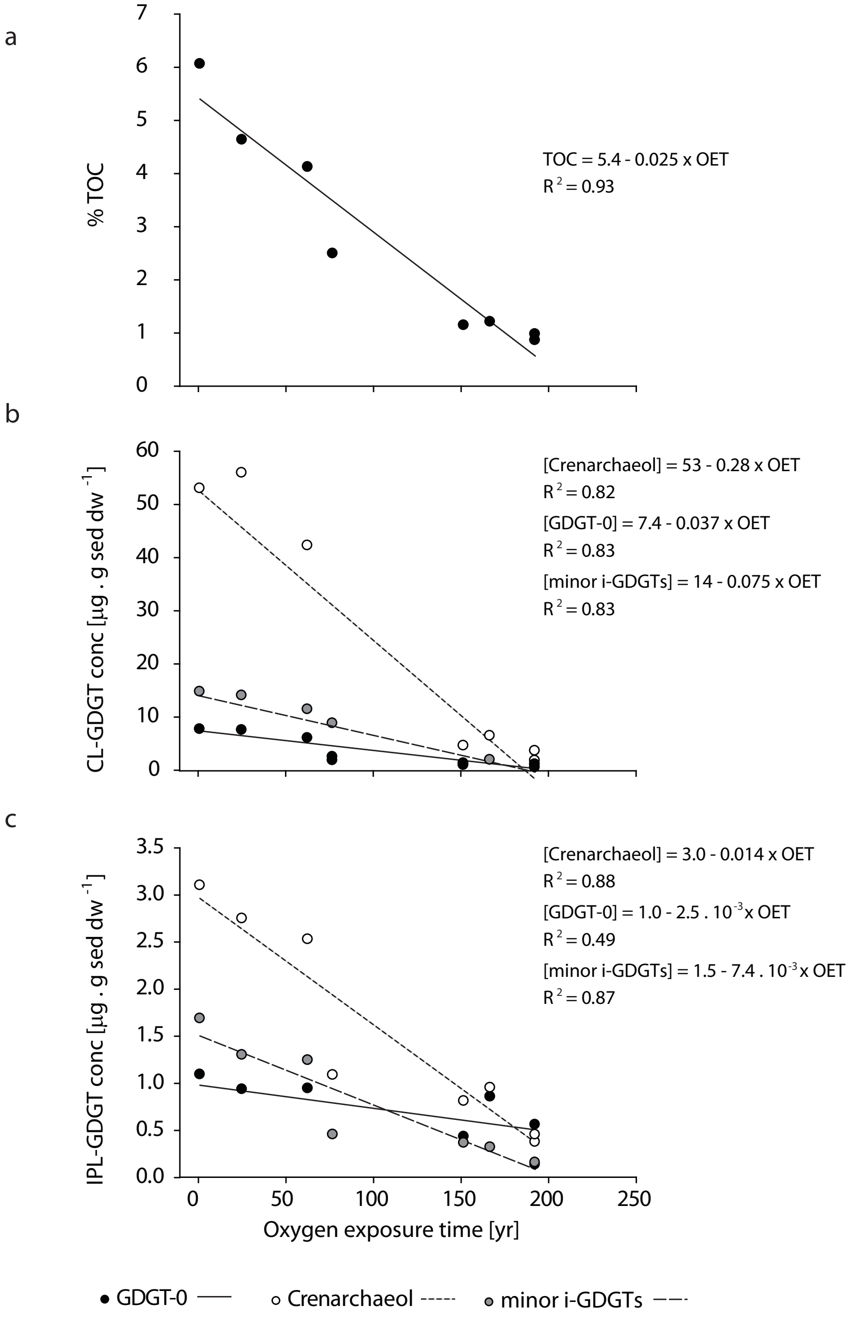

Figure 4.8. Correlations of C_{org} (a), CL-GDGT concentrations (b) and IPL-derived GDGT concentrations (c) with oxygen exposure time.

archaea, which are dependent on oxygen and thus produce GDGTs to a higher degree in sediments with a higher bottom water oxygen concentra tion;

(ii) Increasing degradation of CL- and IPL-GDGTs in surface sediments with increasing water depth due to the increase in OET, resulting in alterations in GDGT distributions.

(iii) An increasing contribution of GDGTs produced by archaea in the deeper water column in sediments deposited at greater depth. GDGTs produced by deeper water dwelling archaea may have a lower TEX_{86} (Schouten et al., 2012) and, thus, this may cause the decrease in TEX_{86}.

Regarding explanation (i), this would require that sedimentary Thaumarchaeota are increasingly present and active in the sediments with increasing water depth and that the GDGTs produced by the benthic archaeal population have a different GDGT distribution, i.e. with a lower TEX_{86} value, than that of the descending particles in the water column. This seems a plausible explanation for these changes since Thaumarchaeota are known for oxidizing ammonia aerobically, and, accordingly, the abundance of HPH-GDGTs is higher at P3000 than at P1300 and P900 (Fig. 4.6). Lengger et al. (2012b), who investigated depth trends in the sediments, also observed anomalous GDGTdistributions and TEX_{86} values as low as 0.65 in the IPL-GDGTs in sediments at 0.5-2 cm depth of core P3000, which was attributed to in situ production, as the distributional changes were occurring starting from 0.5 cm sediment depth. However, these drastic deviations disappeared with increasing depth in the sediment and TEX_{86} values returned to the surface values. Furthermore, such “anomalies” in TEX_{86} values were not observed in the CL-GDGT distribution of these surface sediments, thus indicating that in situ production in the sediment is unlikely to be the cause for the decrease in TEX_{86}. Evidence from settling particles further corroborates this conclusion: Wuchter et al. (2006a) analyzed fluxes and TEX_{86} values of CL-GDGTs in sediment traps from the Arabian Sea at different water depths (500, 1500 and 3000 m). They noted that the CL-GDGT fluxes and TEX_{86} values in the deepest trap did not show any seasonal trend, as was observed in the 500 m trap, and that the flux-weighted TEX_{86} value in the deepest trap was lower (ca. 0.02) than in the shallowest trap. This suggests that the observed trend of decreasing TEX_{86} value with increasing water depth is already a characteristic of the settling particles and thus likely created in the water column.

To examine option (ii), we correlated TEX_{86} values and OET and found a strong linear relationship (R^2 values 0.68 – 0.95; Fig. 4.5b). It is thus possible that progressing oxic degradation of GDGTs is, partially, causing the decrease in TEX_{86} with increasing water depth. However, this cannot be the only explanation since it would not explain the observation of Wuchter et al. (2006a) that TEX_{86} values in the settling particles decrease with increasing water depth. The short timescales over which settling occurs are likely too short to cause substantial changes in the TEX_{86} by degradation in the water column: Kim et al. (2009) investigated short timescales (1 year) and showed that oxygen exposure of sedimentary GDGTs, did not have an effect on TEX_{86} values. Furthermore, the change in TEX_{86} with depth is visible even in individual IPLs, i.e. the MH- and DH-GDGTs (Fig. 4.6). This would imply that degradation rates of IPL-GDGTs are determined by core lipid composition rather than headgroup, which seems unlikely. Instead, we have to also invoke option (iii), i.e. that GDGTs from the deeper water column (with a lower TEX_{86} value) are increasingly contributing to the settling flux of GDGTs received by the surface sediments in sediments deposited at greater water depth, which would cause a decrease of the TEX_{86}. This would explain why Wuchter et al. (2006a) noted a decrease in TEX_{86} value in the sediment trap at 3000 m compared to that at 500 m, suggesting addition of GDGTs with a lower TEX_{86} in deeper waters. Furthermore, TEX_{86} values of water column SPM samples between 900-2000 m in the Arabian Sea were also decreasing with water depth from 0.78 at 900 m to 0.66 at 2000 m for CL and from 0.81 to 0.65 for IPL-derived GDGTs (Schouten et al., 2012), although this may be only providing a snapshot and the SPM analyzed probably consisted of a mixture of sinking and suspended particles. The incorporation of GDGTs from deeper waters into settling particles has been suggested previously based on radiocarbon values and GDGT distributions (Ingalls et al., 2006; Huguet et al., 2007; Turich et al., 2007). This would mean that GDGTs that are being produced by free or particle-associated Thaumarchaeota in deeper waters are, in part, also exported to the sediment. Thus, the decrease in TEX_{86} in the surface sediments with increasing depth of deposition may be due to selective degradation of GDGTs, in combination with the addition of GDGTs produced in the deeper water column. Despite the contribution of deeper water column production, it should be noted, however, that the differences in TEX_{86} values over the 900-3000 m depth interval (Fig. 4.5) correspond to changes in reconstructed temperature of < 3 °C, which is relatively small, but potentially a significant difference in paleoenvironmental studies. It may also have an effect on calibration studies, as our data suggests that sediments from deeper waters will have lower TEX_{86} values compared to those in shallow waters, despite similar surface water temperatures.

5 CONCLUSIONS

Analysis of core top sediments in the Arabian Sea revealed that IPL-derived and CL-GDGT concentrations are negatively correlated to OET, which indicates that their concentrations are dependent on preservation of fossil pelagic sources rather than in situ sedimentary production. Specific IPLs such as MH- and DH-GDGTs isolated via semi-preparative HPLC, also showed this pattern. Only IPL-derived GDGT-0, as well as HPH-derived GDGTs, did not show this dependence, likely due to a contribution of in situ production in the sediment. Nevertheless, the in situ produced GDGTs were degraded quickly in the sediment, as concentrations of HPH-derived GDGTs at 20-24 cm sediment depth were near detection limit. TEX_{86} values of CL- and IPL-derived GDGTs decreased consistently with water depth. This trend is probably not due to in situ production in the sediment, or oxic degradation of IPL-GDGTs. Instead, it may be due to a combination of the degradation of GDGTs produced in the OMZ and a contribution of GDGTs produced in the water column at depths below 900 m. Even though the bias is relatively small regarding the reconstructed temperature (< 3°C over 2100 m water depth), this effect might have to be accounted for in calibration studies as well as paleoclimate studies.

CHAPTER 5

FOSSILIZATION AND DEGRADATION OF ARCHAEAL INTACT POLAR TETRAETHER LIPIDS IN DEEPLY-BURIED MARINE SEDIMENTS (PERU MARGIN)

In preparation for *Geobiology*

FOSSILIZATION AND DEGRADATION OF ARCHAEAL INTACT POLAR TETRAETHER LIPIDS IN DEEPLY-BURIED MARINE SEDIMENTS (PERU MARGIN)

Sabine K. Lengger , Ellen C. Hopmans, Jaap S. Sinninghe Damsté
and Stefan Schouten

NIOZ Royal Netherlands Institute for Sea Research, Department of Marine Organic Biogeochemistry, P.O. Box 59, 1790 AB Den Burg (Texel), The Netherlands

ABSTRACT

Glycerol dibiphytanyl glycerol tetraether (GDGT) lipids are part of the outer cellular membranes of Thaumarchaeota, a kingdom within the Archaea composed of aerobic ammonia oxidizers, and are used in the paleotemperature proxy TEX_{86}. GDGTs are present in live cells with polar head groups attached, as so-called intact polar lipids or IPL-GDGTs. Their transformation to core lipids (CL) by cleavage of the head group was assumed to proceed rapidly after cell death but it has been suggested that some of these IPL-GDGTs can, just like the CL-GDGTs, be preserved over geological timescales. We examined IPL-GDGTs in deeply buried (0.2-186 mbsf) sediments from the Peru Margin up to 9 Myr old. Direct measurements of the most abundant IPL-GDGT, IPL-crenarchaeol, specific for Thaumarchaeota, revealed depth profiles which differed per head group. Shallow sediments (<1 mbsf) contained IPL-crenarchaeol with glycosidic- and phosphate headgroups, as also observed in thaumarchaeal cultures, marine suspended particulate matter and marine surface sediments. However, hexose, phosphohexose-crenarchaeol is not detected anymore below 6 mbsf (or ca. 7 kyr), suggesting a high lability. In contrast, IPL-crenarchaeol with glycosidic head groups is preserved over time scales of Myr. This agrees with previously published analyses of deeply buried (>1 m) marine sediments, which only reported glycosidic and no phosphate-containing IPL-GDGTs. The TEX_{86} values of the CL-GDGTs did not markedly change with depth, and the TEX_{86} of IPL-derived GDGTs decreased only when the proportions of monohexose- to dihexose-GDGTs changed, likely due to the enhanced preservation of the monohexose GDGTs. Our results support the hypothesis that in situ GDGT production and differential IPL degradation in sediments is not substantially affecting TEX_{86} paleotemperature estimations based on CL-GDGTs. Our data also indicate that likely only a small amount

of IPL-GDGTs present in deeply buried sediments are part of cell membranes of active Archaea, and that the amount of archaeal biomass in the deep biosphere based on these IPLs may have been substantially overestimated.

1 INTRODUCTION

Archaea form the third domain of life as discovered by Woese and Fox (1977). One of the characteristics that distinguishes them from bacteria and eukaryotes is their membrane lipid composition, which consist of isoprenoid chains linked to glycerol moieties via ether bonds, as opposed to bacteria and eukaryotes whose membrane lipids generally consist of fatty acids linked to a glycerol via ester bonds. Many archaea produce glycerol dibiphytanyl glycerol tetraether lipids (GDGTs; Koga and Nakano, 2008). These include acyclic biphytanes, such as GDGT-0 (Fig. 5.1), but also GDGTs with cyclopentane moieties. The cyclohexane-containing crenarchaeol and the crenarchaeol regio-isomer (Fig. 5.1) are produced exclusively by Thaumarchaeota (Sinninghe Damsté et al., 2002b; Sinninghe Damsté et al., 2012). In live cells, GDGTs are present as intact polar lipids (IPL), i.e. with polar head groups such as hexose- or/and phosphate groups (Fig. 5.1b; e.g. Koga and Morii, 2005 and references therein). These IPLs are, upon cell death, supposedly transformed, by cleavage of the head group, into core lipids (CLs)GDGTs which are more recalcitrant and preserved over geological time scales of millions of years (Schouten et al., 2013 and references cited therein). The relative amounts of these CL-GDGTs are used in the temperature proxy TEX_{86} (Fig. 5.1; Schouten et al., 2002). In (enrichment) cultures of Thaumarchaeota, IPL-GDGTs mainly occur as monohexose (MH)-, dihexose (DH)-, phospho- and hexose, phosphohexose (HPH)-GDGTs (Schouten et al., 2008; Pitcher et al., 2010; Pitcher et al., 2011c; Sinninghe Damsté et al., 2012). These IPLs are also observed in suspended particulate matter in the water column (Schubotz et al., 2009; Pitcher et al., 2011b; Schouten et al., 2012) and in marine surface sediments (Schubotz et al., 2009; Lengger et al., 2012b).

As IPLs are, especially in sediments, better quantifiable than RNA and DNA, and are potentially less biased towards certain microbial groups, they are used as biomarkers for live microbes in studies of deeply buried sediments, the so-called “deep biosphere” (Biddle et al., 2006; Lipp et al., 2008; Lipp and Hinrichs, 2009). These studies have shown, in general, that archaeal IPLs dominate over bacterial IPLs (the latter representing generally <10% of total IPLs) in marine sediments at depths >1 mbsf. However, the IPL-GDGTs reported in these sediments consisted only of gly-

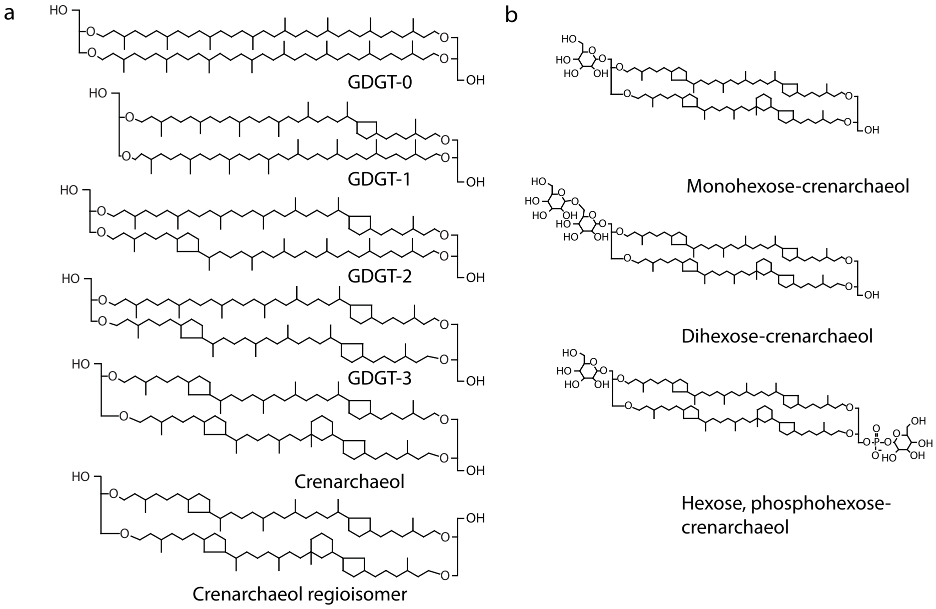

Figure 5.1. Structures of core lipid (a) and intact polar lipid (b) GDGTs.

colipids, and several studies indicate that these are less suitable for use as biomarkers for live archaea. Experiments conducted by Harvey et al. (1986) have shown that archaeal ether lipids with a glycosidic head group are not degraded as rapidly as eukaryotic phosphoester lipids. Schouten et al. (2012) showed that water column profiles of crenarchaeol with a MH-head group in the Arabian Sea were not showing any resemblance to thaumarchaeal DNA or RNA profiles, suggesting they do not reflect live archaea. Lengger et al. (2012b) demonstrated that MH- and dihexose (DH)-crenarchaeol barely degraded over several kyr in Arabian Sea sediments when compared to HPH- crenarchaeol. Logemann et al. (2011) conducted degradation experiments over 100 days, in which IPL-GDGTs, including those with a phosphate head group, did not degrade at all. Finally, even within glycosidic GDGTs different degradation rates are observed, i.e., MH-crenarchaeol was reduced an order of magnitude less by post-depositional oxidation than DH-crenarchaeol (Lengger et al., 2013, chapter 6, this volume). This relatively recalcitrant nature of glycolipids does not only hold true for archaeal glycolipids, but extends to other types of lipids as well. For example, Bauersachs et al. (2010) have shown that glycolipids from heterocystous cyanobacteria were present in Eocene sediments. It is thus questionable how much of the IPL-GDGTs buried in deep marine sediments is part of live archaeal cells, and how much is fossil.

Although the above studies show slow degradation of glycosidic GDGTs over days, years and kyrs, less is known about phospholipid-GDGTs, which abound in all cultured Thaumarchaeota to date (Schouten et al., 2008; Pitcher et al., 2010; Pitcher et al., 2011c; Sinninghe Damsté et al., 2012). Lipp and Hinrichs (2009) did not report phospholipid-GDGTs in the sediments they analyzed. However, Schouten et al. (2010) predicted that the, supposedly more labile, IPLs containing a phosphate head group (e.g. hexose, phosphohexose (HPH)-GDGTs) would disappear rapidly with sediment age/depth compared to strictly glycosidic IPLGDGTs, explaining why only glycosidic GDGTs are detected in deeply buried marine sediment. Indeed, Lengger et al. (2012b) showed that the concentration of HPH-crenarchaeol decreased rapidly in surface sediments, although it was still detected in sediments of several kyrs old. However, to the best of our knowledge, no study has yet investigated the behavior of phospho-GDGTs, including HPH-crenarchaeol, over much longer time scales, i.e. millions of years, in order to test the hypothesis of Schouten et al. (2010).

To this end, we re-investigated deeply buried marine sediments from site 1229 of ODP leg 201 (Peru Margin), which have previously been used by Lipp and Hinrichs (2009), amongst other sediments, to determine concentrations of CL- and IPL-derived GDGT as well as individual IPL-crenarchaeol species, including those with an HPH-head group, over a large depth (186 mbsf) and time (9 Myr) interval. The results are interpreted to reflect preferential degradation of certain IPL-species originally present in the surface sediments. We also discuss the consequence of these findings for TEX_{86} palaeothermometry.

2 Materials and methods

2.1 Site description

The sediments were recovered during ODP Leg 201 from the Peru Margin at site 1229, a leg specifically designed for microbial investigations (D'Hondt et al., 2003). The samples investigated were from holes A, D and C at depths from 0 to 186 m (Table 1). The samples were directly frozen after recovery and stored at -20°C. The ages of the sediments were estimated based on reported sedimentation rates of 32.3 cm . kyr^{-1} for the top 0-20 cm, 98.1 cm . kyr^{-1} for 21-230 cmbsf and 5.1 cm . kyr^{-1} for 231 to 270 cmbsf, which is interpreted as the base of the Holocene (D'Hondt et al., 2003). Below, an average sedimentation rate of 2.1 cm . kyr^{-1} was calculated using the Pleistocene/Pliocene transition as stratigraphic marker (2,588 kyrs), lo-

Table 5.1. Sample details, absolute depths, sedimentation rates, age and organic carbon content at station 1229 (Leg 201). Sedimentation rates used taken from Skilbeck and Fink (2006) and Lomstein et al. (2012), who used data from D'Hondt et al. (2003).

Hole	Core	Section	Interval [cm]	Sampling depth [mbsf]	Sed. Rate [cm . kyr $^{-1}$]	Age [Myr]	C_{org} [%]
D	1	1	20-25	0.2	32	0.00064	5.9
D	1	1	82-92	0.8	98	0.00084	7.1
D	1	4	120-125	6.0	2.1	0.28	4.8
A	2	2	10-15	6.5	2.1	0.31	2.8
A	2	2	137-147	7.8	2.1	0.37	3.2
A	2	5	50-60	11.4	2.1	0.54	1.8
A	4	2	10-15	25.5	2.1	1.2	6.8
A	4	5	69-79	30.6	2.1	1.4	6.9
A	5	5	10-15	39.5	2.1	1.9	2.4
D	6	1	130-135	41.1	2.1	1.9	3.9
A	6	2	99-109	42.4	2.1	2.0	2.3
D	7	4	89-94	54.7	2.1	2.6	1.2
C	8	2	0-7	60.4	2.1	2.8	0.9
A	8	5	50-60	65.4	2.1	3.1	1.0
A	10	2	55-65	81.5	2.1	3.8	3.9
D	12	2	79-89	85.6	2.1	4.0	3.0
D	12	3	74-79	87.1	2.1	4.1	4.0
D	13	2	20-25	89.0	2.1	4.2	1.2
A	12	3	65-75	102.1	2.1	4.8	3.0
A	18	2	70-80	157.6	2.1	7.4	0.9
A	22	1	70-75	185.6	2.1	8.8	0.2

cated at 56.5 mbsf (Skilbeck and Fink, 2006). Freeze-dried sediments were analyzed for organic carbon concentrations (C_{org}). The freeze-dried sediment was acidified overnight with 2N HCl, subsequently washed with bidistilled H_2O and the water was removed by freeze-drying. The decalcified sediments were measured on a Flash EA 1112 Series (Thermo Scientific) analyzer coupled via a Conflo II interface to a Finnigan Delta^{plus} mass spectrometer. Standard deviations from three measurements ranged from 0.01 to 0.2 % TOC.

2.2 Sediment extraction and IPL-CL-GDGT separation

Aliquots (1-2 g) of freeze-dried sediment were extracted with a modified Bligh and Dyer procedure as described previously in Lengger et al. (2012a). The extracts were stored at -20°C.

One aliquot of extract was directly analyzed by HPLC/ESI-MS^2 for intact polar lipids (IPL) containing crenarchaeol, while another aliquot was fractionated over a silica column in order to separate the IPL from the core lipids (CL) following the procedure of Oba et al. (2006) and Pitcher et al. (2009b). Fractionation was achieved over a column with 0.8 g silica gel (60 mesh) activated at 130°C overnight. Core lipids were eluted using 6 column volumes hexane/ethyl acetate 1:1 (v/v) and intact polar lipids using 10 column volumes MeOH. The core lipid fractions were dried and 0.1 µg C_{46}-GDGT internal standard (Huguet et al., 2006c) was added. To the intact polar lipid fractions 0.1 µg internal standard was added and an aliquot of 3 mL was transferred to a vial, dried and stored frozen for quantification of core lipids which eluted in the intact polar lipid fraction ("carry over"). These were typically <2% of the GDGTs present in CL fraction or 10% of GDGTs present in the IPL fraction, and thus negligible. The remaining IPL fraction was dried and hydrolyzed to release CL-GDGTs acc. to Pitcher et al. (2009b). This yielded the so called IPL-derived GDGTs.

2.3 HPLC/APCI-MS and HPLC/ESI-MS^2 analysis

Analysis of CL-GDGTs and IPL-derived GDGTs by HPLC/APCI-MS and calculation of TEX_{86} was carried out as described previously (Schouten et al., 2012). Reproducibility for TEX_{86} values is typically < 0.02, corresponding to errors of < 1 °C. Temperatures were calculated using the calibrations according to Kim et al. (2010) for TEX^H_{86}.

Intact polar lipids with a crenarchaeol core, i.e. monohexose (MH)-crenarchaeol, dihexose (DH)-crenarchaeol and hexose, phosphohexose (HPH)-crenarchaeol, were directly analyzed by HPLC/ESI-MS^2 using a specific selected reaction monitoring method (SRM; Pitcher et al., 2011b). No absolute quantification was possible due to a lack of standards. Therefore, response areas per g sediment are reported. Performance of the ESI-MS^2 was monitored by repeat injections of an extract of Arabian Sea sediment (Lengger et al., 2012b), typically after each 8 sample runs. Duplicate injections yielded relative standard deviations of the areas on average 2%.

3 RESULTS

Organic carbon concentrations ranged from 0.2 to 6.9 %, with a tendency to decrease with depth, but with large scatter (Table 1). This was also observed for concentrations of CL-GDGT-0, which ranged from 0.1 to 21 μg . g sed dw^{-1}, of CL-crenarchaeol, ranging from 0.2 to 35 μg . g sed dw^{-1}, and of the minor isoprenoid GDGTs (minor i-GDGTs, the sum of GDGT-1, -2, -3 and crenarchaeol regio-isomer, which are used in the TEX$_{86}$), ranging from 0.04 to 6 μg . g sed dw^{-1} (Fig. 5.2a). When concentrations were normalized on TOC, no depth trend is observed and concentrations ranged between <0.1 and 0.5 μg . g C$_{org}$$^{-1}$ for the minor i-GDGTs, 0.2 and 1.3 for GDGT-0 and <0.1 and 2.1 for crenarchaeol. CL-GDGT-0 slightly increased proportionally with depth (from 27 to 41 %), and crenarchaeol decreased in proportion (from 61 to 47 %) (Fig. 5.2a; right panel).

IPL-derived GDGT concentrations, i.e. GDGTs released in the IPL-fraction after hydrolytic cleavage of head groups, were consistently lower than the CL-concentrations. Their concentrations also showed a tendency to decrease with depth, but again with large scatter (Fig. 5.2b). Concentrations ranged from 0.05 to 3.2 μg . g sed dw^{-1} for GDGT-0, 0.03 to 2.2 μg . g sed dw^{-1} for crenarchaeol, and 0.01 to 2.8 μg . g sed dw^{-1} for the IPL-derived minor i-GDGTs. When concentrations were normalized on TOC, no particular depth trend is observed, and concentrations ranged from <0.01 to 0.012 for the minor i-GDGTs and crenarchaeol, and from 0.01 to 0.2 for GDGT-0 (Fig. 5.2b). The proportion of GDGT-0 in the IPL-GDGTs was higher than in the CL-GDGTs (38 %), and increased with depth to 52 %, while the minor i-GDGTs decreased from 26 to 14 % and crenarchaeol from 36 to 33% %) (Fig. 5.2b; right panel).

The MH- and DH-crenarchaeol directly measured by HPLC-ESI-MS^2, showed

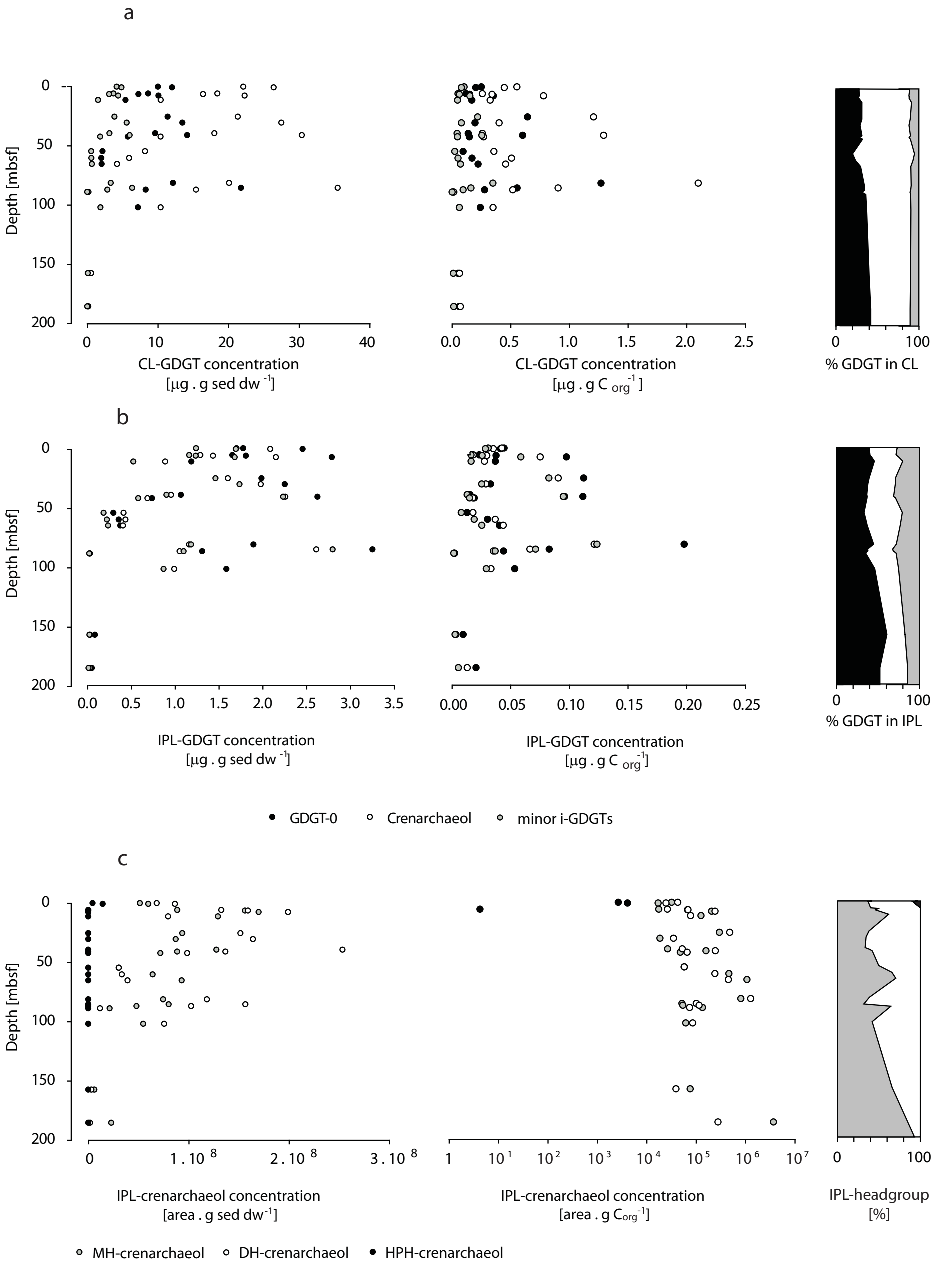

Figure 5.2. Concentrations vs. depth (mbsf) in μg . g sed dw^{-1} and μg . g C$_{org}$$^{-1}$ as well as distributions (in % of total) of (a) CL-GDGTs, (b) IPL-derived GDGTs and (c) the relative abundance of the total of the three different headgroups.

a general decrease in concentration with depth, from 10^8 down to almost 10^6 area . g sed dw^1 for both IPL-crenarchaeol species, though again with large scatter (Fig. 5.2c). In contrast, the concentration of HPH-crenarchaeol showed a strongly deviating profile: It decreased rapidly with depth and was not detected anymore below 6 mbsf. When normalized on TOC, the depth trends disappeared for both MH- and DH-crenarchaeol, ranging between 10^4 and 10^7 area . g C_{org}^{-1}, but not for HPH-crenarchaeol, which decreased from 10^3 area . g C_{org}^{-1} to below the detection limit (Fig. 5.2c). The proportion of DH crenarchaeol compared to MH-crenarchaeol decreased with depth (Fig. 5.2a; right panel).

Finally, the TEX_{86} of the CL-GDGTs ranged from 0.51 to 0.62 with no specific depth trend, while that of IPL-derived GDGTs were slightly higher and ranged from 0.62 to 0.74 with a sharp decline below 102 mbsf (Fig. 5.3a).

4 Discussion

4.1 Degradation of IPL-GDGTs

Our results show that both CL- and IPL-derived GDGT-concentrations as well as TOC were decreasing with depth, although with large scatter. The large scatter is most probably due to the variations in depositional environment, due to the large timescales investigated (Myr). The Peru Margin productivity is controlled by a coastal upwelling regime and possesses a pronounced oxygen minium zone (OMZ). The productivity, OMZ intensity and sedimentation rate has varied over time (cf. Powell et al., 1990; Gutiérrez et al., 2011), leading to changes in organic matter fluxes, oxygen concentrations, oxygen exposure time and, consequently, organic carbon preservation efficiency (cf. Hedges and Keil, 1995; Hartnett et al., 1998; Sinninghe Damsté et al., 2002a). These different degrees of oxygen exposure time (OET) can potentially have a large effect on both TOC as well as on the concentration of biomarker lipids. Indeed, upon normalization on TOC, no trend is observed and it was apparent that the concentrations per g sed dw were mainly defined by the amounts of organic carbon preserved in the original depositional environment (Figs. 2a-b). The similar behavior of IPL-GDGTs as that of TOC and CL-GDGTs hints at a fossil input, as preservation of TOC and biomarkers are both favored by the same environmental conditions.

Direct measurements of IPL-crenarchaeol with different head groups allowed us to investigate the prediction of Schouten et al. (2010) on the different degradation behavior of phospholipids versus glycolipids. At depths > 6 mbsf only glycosidic crenarchaeol was detected, in particular the MH and DH-crenarchaeol, which is in agreement with the results obtained by Lipp and Hinrichs (2009). However, at shallow depths, we also detected HPH-crenarchaeol, a phospholipid which shows a rapid decrease with depth and is undetectable below 6 mbsf, i.e. within <7 kyrs. This confirms the prediction of Schouten et al. (2010) that HPH-GDGTs are degraded faster than IPLs with glycosidic head groups. An alternative explanation is that HPH-crenarchaeol is simply not produced by the Thaumarchaeota living at depths below. This, however, is unlikely, as all cultured Thaumarchaeota have been shown to produce HPH-crenarchaeol in substantial amounts (Schouten et al., 2008; Pitcher et al., 2010; Jung et al., 2011; Pitcher et al., 2011c; Sinninghe Damsté et al., 2012). Furthermore, crenarchaeol has, until now, only been found in Thaumarchaeota performing the aerobic oxidation of ammonia and not in anaerobic archaea. Aerobic Thaumarchaeota are therefore unlikely to inhabit the anoxic, deeper sediments and be the source of IPL-crenarchaeol. A further argument against IPL-crenarchaeol, and other IPL-GDGTs being largely produced in the sediment, is that this would likely alter the distribution of GDGTs in the sediment, especially at depths where a strong archaeal contribution would be expected, i.e. in the sulfate-methane transition zones (SMTZ). However, the GDGT distribution hardly changes at depth in the IPL-fraction (Fig. 5.2b), rendering it highly unlikely all the IPL-GDGTs are produced in the sediment. The decrease in HPH-crenarchaeol is thus more likely due to its fast degradation. The depth profile of HPH-crenarchaeol is in strong contrast to that of the glycosidic crenarchaeol-IPLs, which show a behavior similar to that of TOC and CL-GDGTs. One observation is that MH-crenarchaeol concentrations are increasing compared to DH-crenarchaeol, possibly due to a better preservation of the MH-crenarchaeol. The deeper sediments are also those containing the lowest amounts of organic carbon and were likely deposited in times of low OMZ intensity and thus subjected to longer OET. It has been shown that DH-crenarchaeol is more labile under oxic conditions than MH-crenarchaeol (Lengger et al., 2013, chapter 6, this volume), and this could be the reason for its decrease in proportion. However, another possibility is a change in pelagic Thaumarchaeota communities producing relatively more MH-crenarchaeol.

Our findings have implications for the use of IPL-GDGTs as biomarkers for live Archaea, especially for the use of glycosidic IPL-GDGTs in deeply buried sediments.

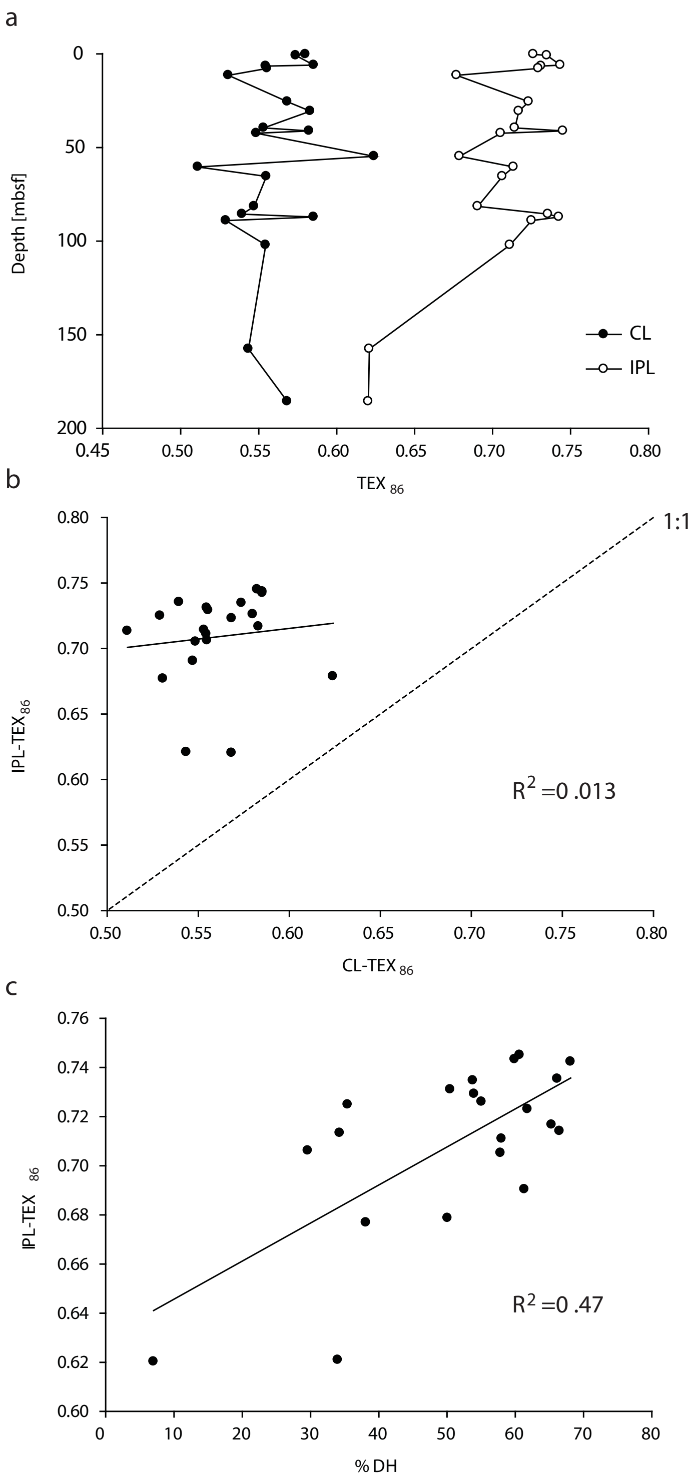

Figure 5.3. CL- and IPL-derived TEX$_{86}$ values plotted against depth in mbsf (a), and correlation of IPL-derived TEX$_{86}$ with CL-TEX$_{86}$ (b), with IPL-TEX$_{86}$ = 0.618 + 0.162 . CL-TEX$_{86}$ (R^2 = 0.013; P = 0.6177). (c) IPL-derived TEX$_{86}$ as a function of % DH-crenarchaeol. IPL TEX$_{86}$ = 0.63 + 0.155 x % DH (R^2 = 0.47; P = 0.006).

According to our results, a large amount of these glycosidic IPLs is most probably fossil in nature and is not representative of the actual amount of live and active archaeal cells. Rather, it is advisable to focus on IPLs with more labile headgroups such as phospholipids as markers for living archaea and bacteria.

4.2 Impact of IPL-GDGT degradation on TEX_{86}

IPL-GDGTs in sediments are not only of importance because of their implications for microbial ecology but also because of their application as a paleotemperature proxy. It has previously been shown that, over short time scales, the TEX_{86} is not being affected by sedimentary processes on short time scales (<10 yrs) (Lengger et al., 2012b; Lengger et al., 2013, chapter 6, this volume). However, this has not been investigated yet over larger timescales. The TEX_{86} of the CL-GDGTs varied from 0.51 to 0.62 (Fig. 5.3a), likely reflecting the substantial changes in sea surface temperature (Schouten et al., 2002) that happened on this long time scale which includes glacial-interglacial cycles. IPL-derived GDGTs have TEX_{86} values higher than the CL-GDGTs and ranged from 0.62 to 0.74 (Fig. 5.3a). This is similar to what was observed previously in deeply buried sediments analyzed by Liu et al. (2011), including those of the Peru Margin, and by Lengger et al. (2012b) in Arabian Sea surface sediments. Liu et al. (2011) found a correlation between TEX_{86} values obtained from IPL-derived GDGTs and CL-GDGTs, respectively. However, we did not find such a correlation (R^2=0.013; P=0.62; Fig. 5.3b). The reason for this might be the range of TEX_{86} values, which was relatively limited in our case (0.1 units compared to 0.4 units in the data presented by Liu et al., 2011), causing scatter to mask the correlation. The higher TEX_{86} values of IPL-GDGTs may be due to the fact that core lipids are not distributed evenly over the IPLs (Schouten et al., 2008; Schubotz et al., 2009; Pitcher et al., 2010; Sinninghe Damsté et al., 2012; Lengger et al., 2012b) showed that the higher TEX_{86} of IPL-GDGTs versus CL-GDGTs is due to preferential degradation of HPH-GDGTs, which generally have lower TEX_{86} values, leaving mainly GDGTs with higher TEX_{86} values, such as DH-GDGTs, in the IPL-fraction. This is probably also the case here, as only glycosidic GDGTs remain preserved in the sediment, as shown here by the IPL-crenarchaeol depth profiles, but also by others who found only glycosidic GDGTs at depth (Lipp et al., 2008; Lipp and Hinrichs, 2009; Liu et al., 2011). Indeed, a trend to lower TEX_{86} values from 0.2 to 6.5 m depth is accompanied by the disappearance of the HPH-crenarchaeol. However, the change is relatively small, which is possibly due to the HPH-GDGTs being present in little amounts compared to the MH- and DH-GDGTs even in the shallow sediment at 0.2 mbsf. A rapid decline of the HPH-crenarchaeol abundance in the surface sediments (0-24 cmbsf) of the Arabian Sea was also noted (Lengger et al., 2012b).

A strong decrease in TEX_{86} from 0.71 to 0.62 was observed for the IPL-derived GDGTs but not for the CL-GDGTs between 102 and 158 mbsf (Fig. 5.3a). In this interval, the DH-crenarchaeol concentrations were decreasing faster than the MH-crenarchaeol concentrations (Fig. 5.2c; Table 5.2). In fact, the proportion of DH-crenarchaeol to summed IPL-crenarchaeol changed between these sediments from 58 to 31% and then decreased further to 7% in the deepest sediment (186 mbsf; Fig. 5.2c). It is likely that this degradation pattern is more dependent on the head group than on the core lipid (cf. Lengger et al., 2013, chapter 6, this volume), and thus this proportional change in MH versus DH-head group was likely occurring in all IPL-GDGTs. DH-GDGTs have a higher TEX_{86} value than MH-GDGTs in all settings and organisms where this has been investigated (Schouten et al., 2008; Schubotz et al., 2009; Pitcher et al., 2010; Pitcher et al., 2011c; Sinninghe Damsté et al., 2012; Schouten et al., 2012; Lengger et al., 2012b; Lengger et al., 2013, chapter 6, this volume). Thus, it may well be that the change in TEX_{86} was due to the proportional change in DH-GDGTs versus MH-GDGTs. Indeed, a significant correlation (IPL TEX_{86} = 0.63 + 0.155 x % DH; R^2 = 0.47; P=0.006) was observed between TEX_{86} of IPL-GDGT and the % DH crenarchaeol (Fig. 5.3c). It is thus likely that the IPL-derived TEX_{86} value depends, apart from the original pelagic signature, also on the relative degradation rates of types of IPL present. Schouten et al. (2012) found a similar correlation in suspended particulate matter in the Arabian Sea water column, although with a much more gradual slope (IPL-TEX_{86} = 0.628 + 0.0035 x %DH; R^2=0.40). A similar phenomenon was observed in the post-depositional oxidation of marine sediment from the Madeira Abyssal Plain, i.e. the TEX_{86} value changed with a changing proportion of DH-crenarchaeol (Lengger et al., 2013, chapter 6, this volume). As stated above, though, the CL-GDGT TEX_{86} does not seem to be impacted by this effect, agreeing with previous observations. It is thus likely that the IPL-derived TEX_{86} value depends, in addition to the original signature, also on the relative degradation rates of types of IPL present.

Interestingly, at ODP Site 1229 there are reports of sulfate-methane reduction zones (D‘Hondt et al., 2003) in the sedimentary column from 40 to 60 mbsf and from 70-100 mbsf . However, no major distributional changes of the GDGTs that could be related to a contribution of active methane oxidizing archaea could be observed in these zones, in contrast to results obtained by Liu et al. (2011) at a range of ODP sites, including site 1229, who did observe a distributional change in some horizons of the SMTZs. Indeed, GDGT-0, produced by Thaumarchaeota, but also by methane oxidizing archaea (which do not produce crenarchaeol) present in SMTZs, is increasing proportionally over depth in CL-GDGTs. However, these depths are seemingly unrelated to SMTZs. Methanotrophic archaea in the sediment we investigated thus either did not produce enough GDGTs in order to significantly change the TEX_{86}, or the SMTZ bears only an imprint on a small depth interval with most intense AOM (cf. Weijers et al., 2011). In any case, this did not affect the GDGT distributions in sediments underlying the SMTZ, similar to what was observed by Weijers et al. (2011).

5 CONCLUSIONS

The analysis of deeply buried sediments retrieved from the Peru Margin showed that HPH-crenarchaeol was rapidly degraded in contrast to other IPL-crenarchaeol species, indicating its labile nature compared to glycosidic crenarchaeol-IPL-GDGTs, and was reduced to amounts below detection limits within less than 7 kyr. This higher degradability makes it a suitable biomarker for living organisms in contrast to glycosidic IPL-GDGTs. TEX_{86} values of CL-GDGTs did not show any obvious depth / age trends, however, IPL-derived GDGTs showed a strong decrease of TEX_{86} in the deepest/oldest sediments coinciding with low TOC values. In agreement with previous studies, this could be due to the faster degradation of DH-crenarchaeol compared to the MH-crenarchaeol. Indeed, DH-crenarchaeol percentages showed a correlation with IPL-derived TEX_{86}. Differential degradation, however, in spite of affecting IPL-derived TEX_{86} values, does not have an impact on CL-TEX_{86}.

ACKNOWLEDGEMENTS. We thank D. Rush and A. Mets for analytical assistance. This research used samples from the Ocean Drilling Program (ODP).The ODP was sponsored by the U.S. National Science Foundation and participating countries under management of Joint Oceanographic Institutions (JOI) Inc. S. K. L. was partly funded by a studentship granted to S. S. by the Darwin Institute for Biogeosciences. This is a publication of the Darwin Institute for Biogeosciences.

CHAPTER 6

DIFFERENTIAL DEGRADATION OF INTACT POLAR AND CORE GLYCEROL DIALKYL GLYCEROL TETRAETHER LIPIDS UPON POST-DEPOSITIONAL OXIDATION

Submitted to *Organic Geochemistry*

DIFFERENTIAL DEGRADATION OF INTACT POLAR AND CORE GLYCEROL DIALKYL GLYCEROL TETRAETHER LIPIDS UPON POST-DEPOSITIONAL OXIDATION

Sabine K. Lengger[a*#], Mariska Kraaij[a], Marianne Baas[a], Rik Tjallingii[b], Jan-Berend Stuut[b,c], Ellen C. Hopmans[a], Jaap S. Sinninghe Damsté[a] and Stefan Schouten[a]

[a] Department of Marine Organic Biogeochemistry, Royal NIOZ Netherlands Institute for Sea Research, P. O. Box 59, 1790AB Den Burg, Texel, The Netherlands. [b] Department of Marine Geology, Royal NIOZ Netherlands Institute for Sea Research, Texel, The Netherlands. [c]MARUM-Center for Marine Environmental Sciences, Bremen University, Bremen, Germany

ABSTRACT

Archaeal and bacterial glycerol dialkyl glycerol tetraether lipids (GDGTs) are used in various proxies, such as the TEX_{86} and the BIT index. In live cells, GDGTs contain polar head groups (intact polar lipids -IPL). IPL-GDGTs have also been detected in ancient marine sediments and it is not clear if they are fossil or part of live cells. In order to determine the extent of degradation of IPL-GDGTs over geological time scales, we analyzed turbidite deposits, which had been partly re-oxidized for several kyr after deposition on the Madeira Abyssal Plain. Analysis of core lipid (CL)- and IPL-derived GDGTs showed a reduction in concentration by two orders of magnitude upon post-depositional oxidation, and of IPL-GDGTs with a mono- or dihexose head group by 23 orders of magnitude. The BIT index for CL- and IPL-derived GDGTs increased substantially upon oxidation from 0.1 to up to 0.5. Together with changing MBT/CBT values this indicates a preferential preservation of branched GDGTs over isoprenoid GDGTs combined with in situ production of branched GDGTs in the sediment. The TEX_{86} of IPL-derived GDGTs decreased by 0.07 units upon oxidation, while that of CL-GDGTs showed no significant changes. Isolation of IPLs revealed that the TEX_{86} value of monohexose-GDGTs was 0.55, while the TEX_{86} of dihexose-GDGTs was substantially higher, 0.70. Thus, the decrease of the TEX_{86} of IPL-derived GDGTs was in agreement with the preferential preservation of monohexose-GDGTs. Due to the low amounts of IPL-GDGTs compared to CL-GDGTs, the impact of IPL-degradation on CL-based TEX_{86} paleotemperature estimations is negligible.

1 INTRODUCTION

The TEX_{86} (TetraEther indeX of tetraethers consisting of 86 carbon atoms) and the BIT (Branched and Isoprenoid Tetraether) index are proxies based on archaeal and bacterial glycerol dialkyl glycerol tetraether lipids (GDGTs). The BIT index is based on the relative amounts of the abundant, mainly marine, isoprenoid GDGT crenarchaeol (Fig. 6.6.1a) and branched GDGTs (br-GDGTs), which are mainly produced in terrestrial environments (Fig. 6.1b). Thus, the BIT index is used to quantify the relative amounts of soil contribution to the organic matter contained in marine sediments (Hopmans et al., 2004). Proxies based on br-GDGTs are the CBT index, based on the relative amount of cyclopentane moieties of br-GDGTs, which is correlated to pH, and the MBT/CBT proxy, based on the degree of methylation of br-GDGTs, which is correlated with mean annual air temperatures (MAT; Weijers et al., 2007; Peterse et al., 2012). Lipids used for the TEX_{86} are isoprenoid GDGTs (or i-GDGTs) containing different amounts of cyclopentane or cyclohexane moieties (Fig. 6.1a), which are produced in marine environments by marine Thaumarchaeota, formerly classified as Marine Group I Crenarchaeota (Brochier-Armanet et al., 2008; Spang et al., 2010). The TEX_{86} of marine suspended matter and surface sediments has shown to be strongly related to sea surface temperature (Schouten et al., 2002; Wuchter et al., 2005; Wuchter et al., 2006a). The TEX_{86} ratio has been calibrated globally in order to enable a quantification of past sea surface temperatures (Kim et al., 2008; Kim et al., 2010).

Isoprenoid GDGTs occur in living archaeal cells with polar head groups, such as hexoses and phosphate groups, bound to the sn-3 hydroxyl group of the glycerol via ester- or glycosidic bonds (Fig. 6.1c; e.g. Koga and Morii, 2005; Schouten et al., 2008; Albers and Meyer, 2011). Upon death of the cells, most of these intact polar lipids (IPL) are transformed into core lipids (CL) by hydrolysis of the polar head groups (White et al., 197 9). This rapid loss of functional groups makes them suitable markers for living cells, in contrast to the core lipids, which can be preserved even over geological timescales for millions of years (e.g. Kuypers et al., 2001; Jenkyns et al., 2012).

Surprisingly, though, when shallow to deeply buried marine sediments (0.7 to 121 mbsf) were probed for IPL-GDGTs, they were found to be present in considerable amounts of 10 – 10 000 ng . mL^{-1} (Lipp et al., 2008). It has been assumed that most of those IPL-GDGTs are indicative for living cells (Biddle et al., 2006; Lipp et al., 2008; Lipp and Hinrichs, 2009). However, it has also been suggested that the degradation rates of certain IPL-GDGTs might be lower than for bacterial phospholipids, which could result in preservation of IPL-GDGTs over geological times (Harvey et al., 1986; Schouten et al., 2010; Logemann et al., 2011; Lengger et al., 2012b). Harvey et al. (1986) investigated the degradation of eukaryotic phospho- and archaeal glycolipids, and found no degradation of the glycolipids over 100 days, in contrast to the phospholipids, which were derived from yeast. The reason for this may to be the nature of the head groups, as phosphate can be a scarce resource and worth regenerating by lysis. Furthermore, the phosphoester bond is chemically less stable than the glycosidic bond. Most of the IPL-GDGTs found in deeply buried sediments are comprised of glycolipids rather than phospholipids, and it is thus possible that these lipids are simply preserved more efficiently. Indeed, Lengger et al. (2012b), reported the degradation of hexose, phosphohexose (HPH)-crenarchaeol (for structures see Fig. 6.1c) to proceed within 1-2 kyrs, but found no evidence for substantial degradation of monohexose (MH)- and dihexose (DH)-crenarchaeol over these time scales. Furthermore, Schouten et al. (2012) showed that, in the Arabian Sea water

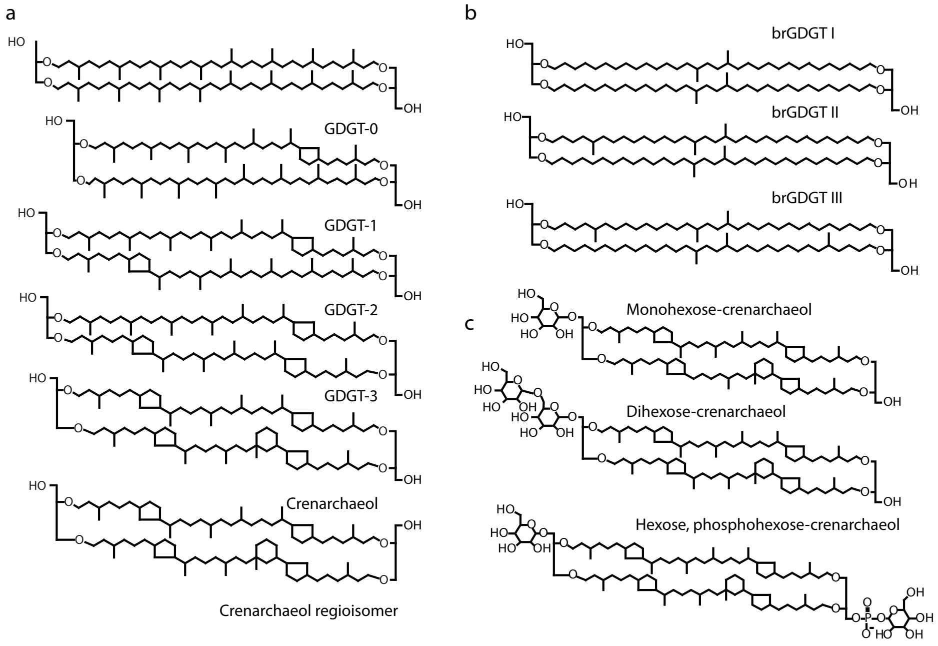
a
GDGT-0
GDGT-1
GDGT-2
GDGT-3
Crenarchaeol
Crenarchaeol regioisomer
b
brGDGT I
brGDGT II
brGDGT III
c
Monohexose-crenarchaeol
Dihexose-crenarchaeol
Hexose, phosphohexose-crenarchaeol

Figure 6.1. Structures of GDGTs. Isoprenoid CL-GDGTs (a), branched CL-GDGTs (b) and measured IPL-crenarchaeol species (c).

column, HPH-crenarchaeol and DH-crenarchaeol abundances were correlated with the abundance of genetic markers for Thaumarchaeota, in contrast to the MH-crenarchaeol abundance, which showed no correlation with thaumarchaeal rRNA copy numbers. Finally, degradation experiments conducted by Logemann et al. (2011) showed that archaeal IPL-GDGTs were hardly degraded in sediments over 100 days, and the decay proceeded significantly slower than the degradation of bacterial and eukaryotic ester lipids, which decayed within weeks. However, these degradation rates were independent from the head group and were low for both phospho- and glyco-etherlipids. Thus, it is not clear how degradation rates of IPL-GDGTs differ from each other especially over time scales of thousands of years.

While studies on the degradation of IPL-GDGTs have hardly been undertaken, degradation of CL-GDGTs has been investigated in more detail, with the focus on comparing anoxic and oxic depositional settings. Sinninghe Damsté et al. (2002a) found differences in concentrations of GDGTs, when anoxically and oxically deposited sediments were compared in cores from a sea mount in the Arabian Sea, while Schouten et al. (2004) examined the GDGT-distribution in the same sediments and found no effect of the depositional environment on TEX_{86} values. Kim et al. (2009) also found no impact on the TEX_{86} when anoxically deposited, organic-rich sediments were exposed to oxygenated waters for one year. However, a study that used 140 kyr old sediment from Madeira Abyssal Plain (MAP) turbidite deposits, found a substantial effect of a post-depositional oxidation event that lasted for 10 kyrs on the GDGT distributions (Huguet et al., 2008; Huguet et al., 2009). The sedimentary sequence on the MAP is characterized by massive distal turbidite deposits (Buckley and Cranston, 1988). They are comprised of organic-rich sediment deposited in a low oxygen zone on the shelf, which is completely mixed during transport within the turbiditic current and, following deposition in the deeper, oxygenated part of the ocean, oxidized by a slowly downward moving oxidation front (De Lange, 1992). Oxidation results in a decrease of the biomarker lipid concentrations by up to two orders of magnitude (Cowie et al., 1995; Prahl et al., 1997; Cowie et al., 1998; Hoefs et al., 2002). Indeed, Huguet et al. (2008) found a substantial decrease in all GDGT concentrations across oxidation fronts, but also observed the preferential degradation of isoprenoid over branched GDGTs. This resulted in a substantial increase of the BIT index across these fronts. Huguet et al. (2008) attributed the enhanced preservation of branched GDGTs to the difference in matrix protection or to the lower initial reactivity (as described by Middelburg, 1989) of soil organic matter, which had been transported over longer distances before deposition. Both increases and decreases of the TEX_{86} were detected upon oxidation of the CL-GDGTs (Huguet et al., 2009), which was attributed to enhanced preservation of terrestrial isoprenoid GDGTs, of variable composition. For IPL-GDGTs, however, the effect of post-depositional oxidation has not been examined yet.

Here, we investigate the long-term (10 kyrs for the f-turbidite; Buckley and Cranston, 1988) effects of post-depositional oxic degradation on the distribution of IPL-GDGTs and compared them to the effects on CL-GDGTs. We analyzed CL-and IPL-GDGT concentrations, and TEX_{86}, BIT, and MBT/CBT index values in both the oxidized and unoxidized part of a freshly cored MAP f-turbidite deposit. The results were used to examine the differential degradation of IPL-GDGTs and their effect on the GDGT based indices.

2 MATERIALS AND METHODS

2.1 Sampling

The core (MAP-1) was taken during cruise JCR209 onboard the R/V James Clark Ross in September 2007 using a piston corer. Sampling location was the Madeira Abyssal Plain (MAP), in the Eastern North Atlantic, at coordinates 31°26.8'N 024°48.8'W in proximity to well-studied turbidite deposits (De Lange, 1992; Cowie et al., 1995; Prahl et al., 1997; Cowie et al., 1998; Hoefs et al., 2002; Huguet et al., 2008; Huguet et al., 2009). The f-turbidite is a > 140 kyrs old, approximately 4 m-thick, organic-matter rich turbidite at ca. 10-12 mbsf, with 40-50 cm of oxidized sediment on top of the unoxidized turbidite, equivalent to ca. 10 kyrs of oxidation (Buckley and Cranston, 1988). It was labeled "f" (Weaver and Kuijpers, 1983; Weaver et al., 1989) for being one turbidite deposit in a series of turbidite deposits of varying organic content. Based on these previous studies, the f-turbidite was expected at ~10 m core depth at our coring location. The recovered, ca. 12 m long, piston core was cut in half and inspected visually for differences in sediment color and type. The sections most likely containing the f-turbidite were sub-sampled in 2-20 cm resolution from 9 to 12 m core depth on board of the ship. Samples were stored in geochemical bags and kept frozen at 20°C until analysis.

2.2 Particle size analysis

Twenty nine samples from 9 to 12 m core depth were analyzed for particle-size distributions, after isolation of the terrigenous fraction (cf. McGregor et al. 2009). For removal of the organic carbon and $CaCO_3$, approximately 500 mg sediment was boiled in 10 mL 35% H_2O_2 until the reaction ceased and excess H_2O_2 disintegrated into H_2O and O_2, then in 10 mL of 10% HCl for 1 min in order to remove the $CaCO_3$ and diluted ten times twice with H_2O to neutral pH. Immediately prior to particle-size analysis, the organic matter- and carbonate-free sediment was boiled with 300 mg of the soluble salt sodium pyrophosphate ($Na_4P_2O_7.10H_2O$) to ensure disaggregation of all particles. The particle size of the non-soluble fraction was consequently analyzed in degassed H_2O using a Beckmann-Coulter Laser Particle Sizer LS230 which measures particle size from 0.04 – 2000 µm and describes them with 116 size classes.

2.3 Total organic carbon content

Freeze-dried and homogenized sediments were analyzed for total organic carbon content (TOC). An aliquot of freeze-dried sediment was decalcified (overnight, 2N HCl) and subsequently washed with bidistilled H_2O. H_2O was removed by freeze-drying. The TOC of the sediments was measured on a Flash EA 1112 Series (Thermo Scientific) analyzer coupled via a Conflo II interface to a Finnigan Delta^{plus} mass spectrometer. The TOC reported is the average of duplicate measurements, with standard deviations ≤ 0.2% of TOC.

2.4 XRF scanning

The inorganic geochemical composition of the samples was analyzed using a Avaatech XRF core scanner (Tjallingii et al., 2007). The XRF Core Scanner uses energy-dispersive fluorescence radiation to measure the chemical composition of the sediment as element intensities in counts s^{-1} in a non-destructive way. Loosely packed sediment samples were prepared for XRF scanning by pressing about 4 g freeze dried powder into a sample cup without additional binder and were covered with SPEX-Certi Ultralene® foil. XRF measurements were conducted at 10 and 30 kV using a count time of 10 s, which covers the elements Aluminum (Al) through to Zircon (Zr). The 30 kV run was performed in combination with a Pd-thin filter to suppress the background bremsstrahlung that originates from the primary X-ray source and increases with the applied source current. The element intensities of 13 elements (Al, Ca, Cl, Fe, K, Mn, S, Si, Ti, Br, Rb, Sr, Zr) were transformed into centered-log ratios (CLR), which are represented by the logarithm of the raw data after normalization by the geometric mean (Aitchison, 1981). This transformation avoids misinterpretations resulting from the constant-sum constraint that is embedded in compositional data sets, and allowing application of multivariate statistics in a meaningful way (Weltje and Tjallingii, 2008). Statistical analysis was carried out by application of principal component analyses (PCA) and K-means clustering of the CLR correlation matrix using the open source software PAST.

2.5 Lipid extraction and IPL/CL separation

Lipids were extracted with a modified Bligh-Dyer extraction method as described in Lengger et al. (2012a). One aliquot of the extract was used directly for analysis of IPL-GDGTs via HPLC/ESI-MS^2, and another one was used for separation of IPL-GDGTs from CL-GDGTs over an SiO_2 column according to Pitcher et al. (2009b). To both the IPL and the CL fraction, 0.1 µg of internal GDGT standard C_{46} was added (cf. Huguet et al., 2006c). The IPL fraction was hydrolyzed under reflux in 5% methanolic HCl to yield the IPL-derived GDGTs, which were extracted 3 times from the aqueous phase with DCM (cf. Pitcher et al., 2009b). CL- and IPL-derived GDGT concentrations were subsequently analyzed via HPLC/APCI-MS and areas were normalized to the internal standard. The standard was corrected for the difference in relative response to crenarchaeol using a C_{46}/crenarchaeol 1:1 (wt:wt) mixture.

2.6 HPLC/APCI-MS and HPLC/ESI-MS^2

CL- and IPL-derived GDGTs were analyzed by HPLC/APCI-MS as described previously (Schouten et al., 2007). TEX_{86} values and the corresponding sea-surface temperatures were calculated according to the TEX^H_{86} calibration of Kim et al. (2010) and typically show standard deviations below 0.02 TEX_{86}. CBT and MBT values, and temperatures derived from it, were determined according to the method described by Weijers et al. (2007). HPLC/ESI-MS^2 in selected reaction monitoring (SRM) mode as described by Pitcher et al. (2011b) was used to analyze selected IPL-GDGTs. IPL-GDGTs monitored were monohexose (MH)-crenarchaeol, dihexose (DH)-crenarchaeol, hexose, phosphohexose (HPH)-crenarchaeol. HPH-crenarchaeol was detected in levels just above the detection limit and was therefore not quantified. Signal stability was monitored using a lipid extract of *Candidatus* Nitrososphaera gargensis (Pitcher et al., 2010) that was injected every 8 runs. Quantification of IPL levels was done using results from the preparative HPLC. In order to determine concentrations in ng per gram sediment dry weight (ng . g sed dw^{-1}), the average MS response peak area measured in the unoxidized sediment (1111.5 cmbsf, 1136.5 cmbsf, 1147.5 cmbsf, 1161.5 cmbsf) was divided by the actual concentrations measured by semi-preparative HPLC of crenarchaeol, which yielded a correction factor (8.0 . 10^{-5} ng . area^{-1} for MH-crenarchaeol and 1.3 . 10^{-5} ng . area^{-1} for DH-crenarchaeol), allowing us to determine the concentrations from the SRM areas measured. All concentrations given are per g sediment dry weight (g sed dw).

2.7 Semi-preparative HPLC

In order to isolate IPL-GDGTs, semi-preparative HPLC was used as described by Schouten et al. (2008) and Lengger et al. (2012b). A mix of Bligh Dyer extract of four samples (1111.5 cmbsf, 1136.5 cmbsf, 1147.5 cmbsf, 1161.5 cmbsf) of 0.7 g sediment each, of the unoxidized f-turbidite, was separated on an Agilent (San Jose, CA, USA) 1100 series LC with an Inertsil diol column (250 by 10 mm; 5 μm particles; Alltech Associates Inc., Deerfield, IL) at a flow rate of 3 mL . min^{-1} and identical mobile phase and gradient as for intact polar lipid LC/MS^2 analysis (see above and Pitcher et al., 2011b). Fractions of 3 mL were collected and subsequently measured with Flow Injection Analysis using ESI-MS^2 in SRM mode at the same conditions as the analytical SRM, monitoring the same transitions. Injection solvent was a mixture of 60% A and 40% B with A being hexane/isopropanol/formic acid/14.8M aqueous NH_3 (79:20:0.12:0.04, vol/vol/vol/vol) and B being isopropanol/water/formic acid/14.8 M aqueous NH_3 (88:10:0.12:0.04, vol/vol/vol/vol). The fractions containing the MH-GDGTs were combined, as well as the DH-GDGTs. No other IPL-GDGTs were present in detectable amounts. Fractions were acid-hydrolyzed and the MH- and DH-derived GDGTs were analyzed via HPLC/APCI-MS as described above.

3 RESULTS AND DISCUSSION

3.1 Sedimentology and location of the f-turbidite

The total organic carbon (TOC) content in the sampled core section from 1162 up to 905 cmbsf was high: on average 2.6 ± 0.08% (Fig. 6.2b). TOC content decreased sharply above 1111.5 cmbsf, revealing the oxidation front, and stayed low (0.3%) up to 1024.5 cmbsf (oxidized turbidite, covered by hemipelagic sediments), above which the TOC content increased again to 1.1 – 1.8%. This pattern in TOC indicates that the sampled section contained two turbidites which, based on their depth in the core, were likely the unoxidized and oxidized f- and the unoxidized e-turbidite, respectively (cf. Weaver and Kuijpers, 1983; Buckley and Cranston, 1988; Weaver et al., 1989).

The stratigraphy of core MAP-1 was established using grain-size as well as XRF analyses. Particle-size analysis showed uniform mean modal sizes (MMS) of 5.8 µm up to 1070.5 cmbsf, followed by a decrease to 3.3-4.0 µm between 1070.5 and 1044.5 cmbsf, and a substantial increase to 16-20 µm between 1034.5 and 1019.5 cmbsf (Fig. 6.2b). At 999.5 cmbsf and above, MMS were uniformly 4.4 µm. Statistical interpretation of the XRF data was obtained by application of principal-component analyses (PCA) and K-means clustering of the CLR correlation matrix (Fig. 6.2a). The bi-plot of the PCA analysis shows that PC1 and PC2 explain 79% of the total variance and reveal the reciprocal correlation of the individual elements (Fig. 6.2a). Ratios of elements were selected based on the anti-correlation indicated by the bi-plot (Ca/Si, Ti/Al and Br/Ti, Fig. 6.2a) and were plotted versus depth (Fig. 6.2b). The PCA scores of the data are distributed in mainly four clusters that correspond to the different stratigraphic units of core MAP-1 (Fig. 6.2b). This revealed that all samples of cluster 1 are characterized by relatively low Ti/Al ratios, high Ca/Si and Br/Ti ratios, as well as a relatively high TOC content. Contrary, samples of cluster 4 are characterized by high Ti/Al ratios and low Ca/Si and Br/Ti ratios. All ratios are relatively low for the samples of cluster 3, whereas the ratios of cluster 2 fit in between the values of cluster 1 and 3 suggesting that the samples of cluster 2 represent a mixture of clusters 1 and 3.

The base of the e-turbidite was clearly identified by the abrupt increase of the MMS between 999.5 and 1044.5 (Fig. 6.2b). Turbidites are characterized by a coarse-grained base that is overlain by a fining- upward sequence, which follows the sequence of depositional changes during and after these events (Bouma, 1962). This is visible in Fig. 6.2b for the e-turbidite, where there are four samples with a grain size above 15 µm MMS. The three deepest samples of the base of the e-turbidite have the highest Ti/Al ratio (cluster 4) suggesting relatively high amounts of heavier Ti-bearing minerals and relatively low amounts of Al-bearing clay minerals. Above the base of the e-turbidite, fine-grained, organic-matter rich sediments representing the unoxidized e-turbidite are present (cluster 1; below 1115 cmbsf). Below the base of the e-turbidite we expected, in accordance with the observations of Buckley and

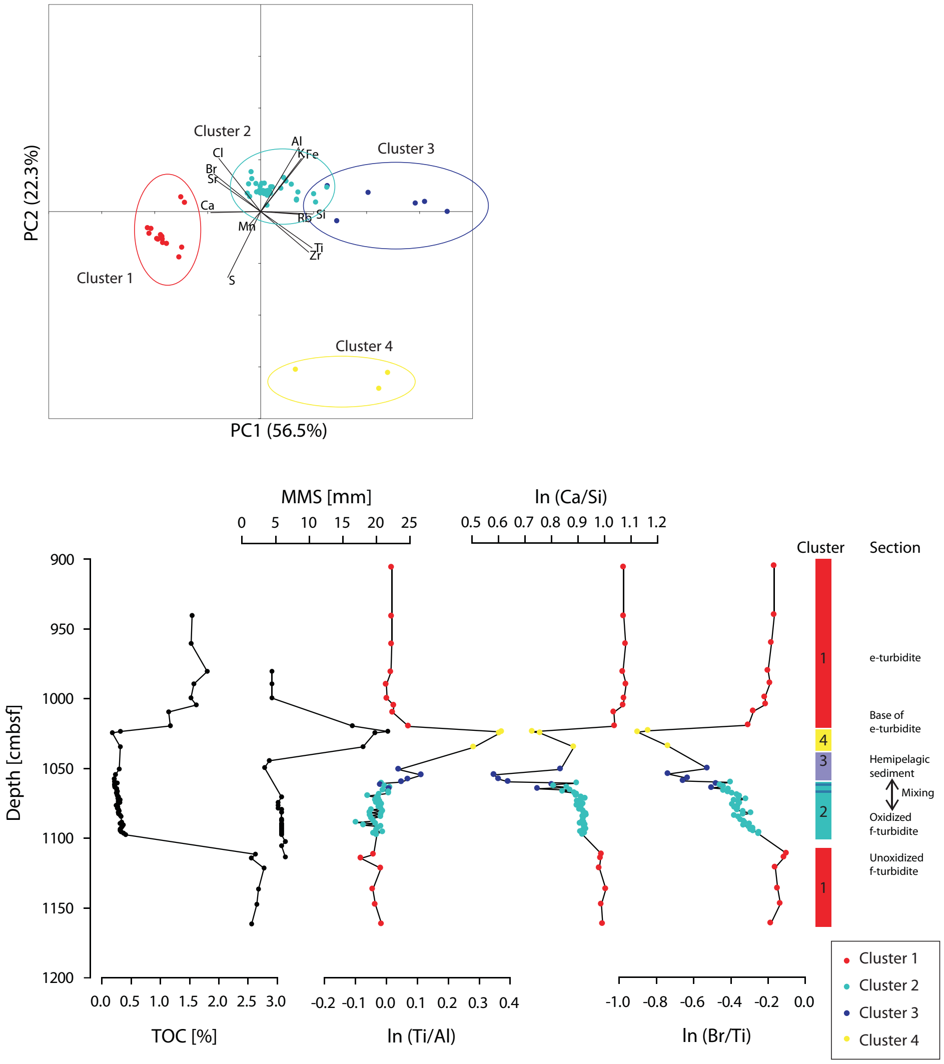

Figure 6.2. Results of the principal component and clustering analysis of the XRF cores scanning data. (a) Bi-plot of PC1, PC2, and the individual chemical elements. (b) Depth profiles of TOC, mean modal grain size (MMS) and ln(Ca/Si), ln (Ti/Al) and ln(Br/Ti).

Cranston (1988), a mixture of hemipelagic sediment and the oxidized part of the f-turbidite that can be up to several decimeters thick. The sediment of cluster 3 is situated between the oxidized f- and the base of the overlaying e-turbidite, and has a low TOC content that is characteristic for hemipelagic sediments. The gradual changes from oxidized f-turbidite (cluster 2) to hemipelagic sediment (cluster 3) reflected by the Ca/Si, Ti/Al and Br/Ti ratio profiles between 1044.5 and 1076.5 cmbsf (Fig. 6.2b) suggest mixing of turbidite and hemipelagic sediments by bioturbation.

Thus, to investigate the impact of post-depositional oxidation, we analyzed IPL- and CL-GDGTs in sediments from 1162 to 1076 cmbsf depth, representing the unoxidized and oxidized f-turbidite without the interference of hemipelagic sedimentation. Based on the TOC profile the boundary between the oxidized and unoxidized part of the f-turbidite was set at ca. 1105 cmbsf.

3.2 Oxic degradation of branched GDGTs – CL and IPL

Branched GDGTs were present in low concentrations relative to isoprenoid GDGTs, as commonly observed in open marine sediments (Schouten et al., 2013 and references cited therein). In the oxidized part of the turbidite deposit, these concentrations decreased by two orders of magnitude, i.e. from 90 to 4, and 30 to 1 ng . g sed dw^{-1} for the CL and IPL fraction, respectively (Figs. 3a b; Table 6.1). These changes occurred gradually over the oxidation front (Figs. 3a and b). Based on the concentrations, we can calculate preservation efficiencies of individual GDGTs, i.e. the concentration of a GDGT in the oxidized part of the turbidite (average of 1076.5 to 1095.5 cmbsf) as a percentage of the average concentration in the un-oxidized part (average of 1111.5 to 1161.5 cmbsf; cf. Sinninghe Damsté et al., 2002a; Hoefs et al., 2002). Preservation efficiencies were 4% for CL and 3% for IPL-derived br-GDGTs, which was less than reported by Huguet et al. (2008), who found 8% of the CL-GDGTs preserved in the sediment which had been subjected longest to oxic conditions. For comparison, the preservation efficiency of TOC was 10% (20% in the f-turbidite of Huguet et al., 2008). This suggests that the oxidized interval analyzed by Huguet et al. was subjected less to oxic conditions, although the interval of oxidized sediment examined here was of the same thickness (20 cm + 10 cm transition). Both IPL-derived and CL-br-GDGTs were seemingly preserved to a significant extent in this f-turbidite. This is remarkable since IPLs are generally considered to be labile components that transform rapidly into CL upon cell lysis.

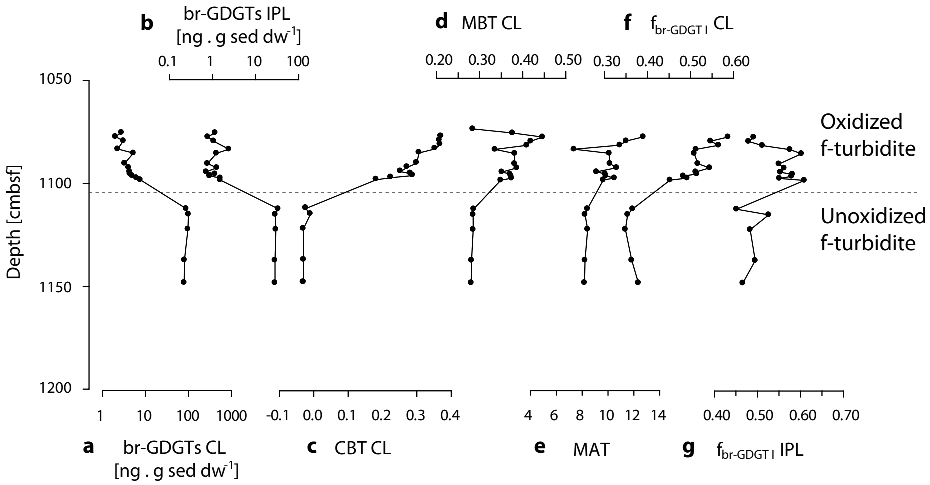

Figure 6.3. CL- and IPL-derived br-GDGT concentrations (a, b, note the log scale), CBT-values (c), MBT-values of the CL-GDGTs (d), MAT calculated for the CL-GDGTs from MBT/CBT (e), and $f_{br-GDGT-I}$ of the CL- (f) and IPL-derived br-GDGTs (g).

In general, branched GDGTs are assumed to derive from terrestrial sources, mainly soil organic matter (e.g. Hopmans et al., 2004; Weijers et al., 2009; Peterse et al., 2011; Smith et al., 2012). However, br-GDGTs have been shown to be in situ-produced in small amounts in marine sediments as well (Peterse et al., 2009). Indeed, their presence in the IPL-derived fraction could indicate that they are, in part, produced in situ. For the turbidite deposits, this could mean that the br-GDGTs were either produced in situ in the original shelf sediments or that they were produced after deposition of the turbidites on the abyssal plain. In order to obtain clues about their origins, we determined the MBT and CBT values of the CL-GDGTs. Unfortunately; this was not possible for the IPL-fraction due to their low abundance and limited amount of material. Interestingly, the CBT of CL-br GDGTs in the unoxidized section was relatively low (0.01-0.03; Fig. 6.3c), corresponding to a relatively high pH of 8.8, using the Weijers et al. (2007) calibration. Such a distribution has been interpreted as characteristic for br GDGTs that are produced in situ in marine sediments (Peterse et al., 2009) since the pH of soil is typically much lower and such a high pH would fit with the pH of pore waters of shallow marine sediments. The MBT values in the unoxidized turbidite were 0.28-0.29 (Fig. 6.3d), and the mean annual air temperature (MAT) calculated from the MBT/CBT using the Weijers et al. (2007) calibration was relatively low, i.e. 8.2 – 8.4°C (Fig. 6.3e). This would also be consistent with a dominant origin of these br-CL-GDGTs from in situ-production in the sediment, most probably at the continental shelf, before the sediment was transported to the abyssal plain by the turbidite. In the oxidized turbidite deposits, the br-GDGT distribution gradually changed to yield a higher CBT value (0.3, corresponding to pH 7.9) and a higher MBT (0.35-0.45), resulting in higher calculated MATs (9-13°C). In combination with the observed substantial decrease in the concentration of the br-GDGTs (Figs. 3ab), this suggests that the CBT and MBT values changed due to preferential degradation of a group of br-GDGTs with a different provenance. In addition to br-GDGTs produced in situ on the shelf, br-GDGTs derived of continental soil, brought into the marine environment by fluvial transport, could also be present in the sediment. These terrestrial GDGTs would likely be characterized by a higher CBT and MBT, reflecting a lower pH and a higher MAT, as they would be derived from subtropical northwestern African soils. Therefore, the compositional changes in the CL-br-GDGTs could be explained by selective preservation of terrestrial over marine br-GDGTs. Such an enhanced preservation could be due to a better protection by the inorganic soil matrix they are embedded in (Keil et al., 1994). Terrestrial organic matter, having endured long-distance transport, has been exposed to oxic degradation over a longer time than the marine material and the remaining compounds are thus relatively well protected from degradation. This was defined as a lower "initial reactivity" of the terrestrial organic matter by Middelburg (1989).

Intriguingly, the IPL-derived br-GDGTs were preserved to an almost similar degree as the CL (Table 6.1). This seems irreconcilable with the idea that IPL-GDGTs are more labile than CL-GDGTs and would suggest a similar higher degree of preservation of IPL-derived GDGTs compared to CL-GDGTs. To investigate the provenance of these GDGTs, we determined their distribution as well. However, as concentrations of many of the GDGTs were too low to accurately determine MBT and CBT values, we used the fractional abundance of the dominant GDGTs, i.e. br-GDGT I, II and III. The fraction of br-GDGT I, $f_{\text{br-GDGT I}}$ (i.e., the concentration of br-GDGT I divided by the sum of br-GDGT I, II and III; for structures see Fig. 6.3b), was used as an indicator for distributional changes. The $f_{\text{br-GDGT I}}$ of the IPL-derived GDGTs increased from 0.40 to 0.55, which is a substantial change, though less than observed for the CL-GDGTs (Fig. 6.3e). This is consistent with a shift to a predominantly terrestrial provenance of IPL- br-GDGTs in the oxidized turbidite deposit, i.e. a higher fractional abundance of br-GDGT I corresponds with higher

MAT values (Weijers et al., 2007) consistent with northwest African air temperatures. The less-pronounced increase compared to the CL-br-GDGT is likely due to production of IPL-br-GDGTs during exposure of the turbidite sediment to oxygenated conditions, which would have a "marine" distribution, thus causing a less strong increase in $f_{\mathrm{brGDGT\ I}}$.

3.3 Oxic degradation of isoprenoid GDGTs – CL and IPL

In the unoxidized section of the f-turbidite, isoprenoid CL-GDGT concentrations were between 4-6 µg . g $^{-1}$ for the most abundant GDGTs, i.e. GDGT-0 and crenarchaeol, with lower amounts for the minor isoprenoid GDGTs (i-GDGTs), used for determination of the TEX_{86}, i.e. summed concentrations were 1.5-1.7 µg . g $^{-1}$ (Fig. 6.4a; Table 6.1). IPL-derived GDGTs had much lower concentrations, from 0.1-0.2 µg. g sed dw^{-1} for GDGT-0 and crenarchaeol and 0.5 and 1.0 ng . g sed dw^{-1} for the minor i-GDGTs (Fig. 6.4b; Table 6.1). In the oxidized part, these concentrations decreased by two orders of magnitude, i.e. to 13 ng . g sed dw^{-1} for the CL-GDGT-0 and crenarchaeol, and 4 ng . g sed dw^{-1} for the sum of the minor i-GDGTs (Fig. 6.4). IPL-derived GDGTs were reduced in the oxidized section by at least two orders of magnitude as well. Concentrations in the oxidized part were 2.5 and 0.7 ng. g sed dw^{-1} for crenarchaeol and GDGT-0, and 0.5 and 1.0 ng . g sed dw^{-1} for the minor i-GDGTs. These changes initially occurred abruptly and then more gradually over the first 10 cm of the oxidation front (Fig. 6.4).

The preservation efficiencies for isoprenoid CL-GDGTs were 0.25-0.31% and 0.41 to 1.8% for IPL-derived isoprenoid GDGTs, substantially lower than for TOC and branched GDGTs (Table 6.1). These results are similar to what was reported previously by Huguet et al. (2008) for the f-turbidite, i.e. the branched CL-GDGTs were preserved more efficiently than the isoprenoid CL-GDGTs (0.2% for crenarchaeol versus 7% for br-GDGTs in Huguet et al., 2008). This is likely due to the much larger contribution of terrestrially sources to branched GDGTs compared to i-GDGTs. Surprisingly, preservation efficiencies were slightly higher for IPL-derived isoprenoid GDGTs than for CL-GDGTs, though still substantially lower than those of TOC (Table 6.1). Most likely, the same explanation as for branched GDGTs can be applied here, i.e. in situ-production of a small amount of IPL-GDGTs in the oxidized sediment by sedimentary Thaumarchaeota. These likely function by aerobic oxidation of ammonia (Könneke et al., 2005; Wuchter et al., 2006b; de la Torre et al., 2008; Walker et al., 2010; Tourna et al., 2011) and thus, when oxygen was supplied

Table 6.1. Average concentrations in the oxidized and the unoxidized part of the turbidite and preservation efficiencies (concentrations in the oxidized section divided by concentrations in the unoxidized section) for the CL- and IPL-derived GDGTs. Concentrations are in ng per g sediment dry weight.

	Br-GDGTs	**GDGT-0**	**Crenarchaeol**	**Minor i-GDGTs**
CL				
Unoxidized	87.3 ± 9.0	4360 ± 230	5540 ± 320	1621 ± 90
Oxidized	3.83 ± 1.1	13.5 ± 3.3	13.7 ± 4.0	4.13 ± 1.2
IPL-derived				
Unoxidized	29.6 ± 2.0	188 ± 18	175 ± 16	116 ± 8.3
Oxidized	0.97 ± 0.7	2.5 ± 1.2	0.67 ± 0.7	0.47 ± 0.2
%IPL-derived of total				
Unoxidized	25	4.1	3.1	6.7
Oxidized	20	16	4.7	10
Preservation efficiency (%)				
CL	4.4	0.31	0.25	0.25
IPL	3.3	1.3	0.38	0.41

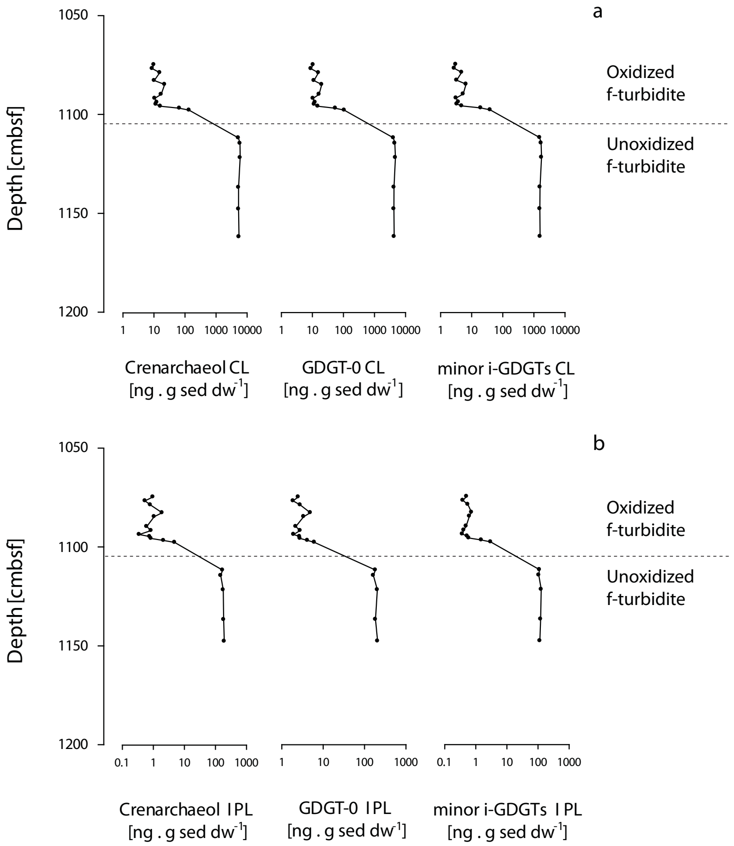

Figure 6.4. Concentrations of CL- and IPL-derived lipids (in ng . g sed dw^{-1}) of crenarchaeol, GDGT-0, and the sum of the minor i-GDGTs (GDGT-1, -2, -3 and crenarchaeol region-isomer). Note the log scale.

to the sediments, and ammonium is formed from the oxidation of organic matter, these Thaumarchaeota could have thrived and produced IPL-GDGTs.

To examine the oxic degradation and potential production of individual isoprenoid IPL-GDGTs, we performed direct analysis of IPL-crenarchaeol. Analysis of the unoxidized sediment showed the presence of two main intact polar lipid species, MH- and DH-crenarchaeol, while no HPH-crenarchaeol was detected. This distribution is different from the distribution found in cultures, where HPH-crenarchaeol is always present (Schouten et al., 2008; Pitcher et al., 2010; Pitcher et al., 2011c; Sinninghe Damsté et al., 2012) but is similar to that of IPLs found in deeper marine sediments (Biddle et al., 2006). The absence of HPH-crenarchaeol is probably due to the higher lability of this IPL-GDGT, as shown previously for the Arabian Sea, where degradation in surface sediments occurred within a few cm (Lengger et al., 2012b). This was also predicted by theoretical modeling (Schouten et al., 2012). As direct quantification is not possible via SRM due to the lack of authentic standards,

Table 6.2. Concentrations in the unoxidized part of the turbidite of MH- and DH-GDGTs and their sums, isolated by preparative HPLC, and the average of IPL-derived GDGTs isolated by silica column. Concentrations are reported in ng per g sediment dry weight.

	GDGT-0	GDGT-1	GDGT-2	GDGT-3	Cren	Cren'	Total	TEX_{86}
MH	113	9.7	7.2	1.6	80.9	3.4	216	0.55
DH	18.9	10.7	15.0	3.6	10.0	6.0	64.4	0.70
Sum	132	20.5	22.2	5.2	91.0	9.3	280	0.64
IPL-derived	188	41.0	45.3	10.6	175	19.1	479	0.64

we used semi-preparative HPLC of a composite sample of the unoxidized sediment to isolate the MH- and DH-GDGT fractions, which were subsequently hydrolyzed and quantified via the derived GDGTs quantified, through comparison to an internal standard. These results were then used for indirect quantification of the other turbidite samples (see section 2, Material and Methods). The MH- and DH-crenarchaeol concentration in the unoxidized sediments showed little variation (ca. 80 ng . g sed dw^{-1} for MH-crenarchaeol and ca. 10 ng . g sed dw^{-1} for DH-crenarchaeol) but were substantially lower in the oxidized sediment (on average 1.0 and 0.01 ng . g sed dw^{-1} for the MH- and DH-crenarchaeol; Table 6.2; Fig. 6.5).

The preservation efficiency of MH-crenarchaeol (1.3%) was substantially higher than that of DH-crenarchaeol (0.1%) and was also higher than that of CL- and IPL-derived crenarchaeol. Contrastingly, the DH-crenarchaeol exhibited lower preservation efficiency than CL-crenarchaeol, suggesting it is more labile, as would be expected for an IPL. The reasons for the high preservation efficiency of MH-crenarchaeol could be a higher chemical stability of the MH-crenarchaeol than that of DH- and CL-crenarchaeol. However, this seems unlikely as functionalized compounds should be more readily degradable than CL-GDGTs. It is also possible that the MH-crenarchaeol is partially derived from DH-crenarchaeol, when only one hexose-group is cleaved off, resulting in a MH-crenarchaeol. Another possibility is that MH-crenarchaeol is produced in situ by sedimentary archaea in the oxygenated sediments,

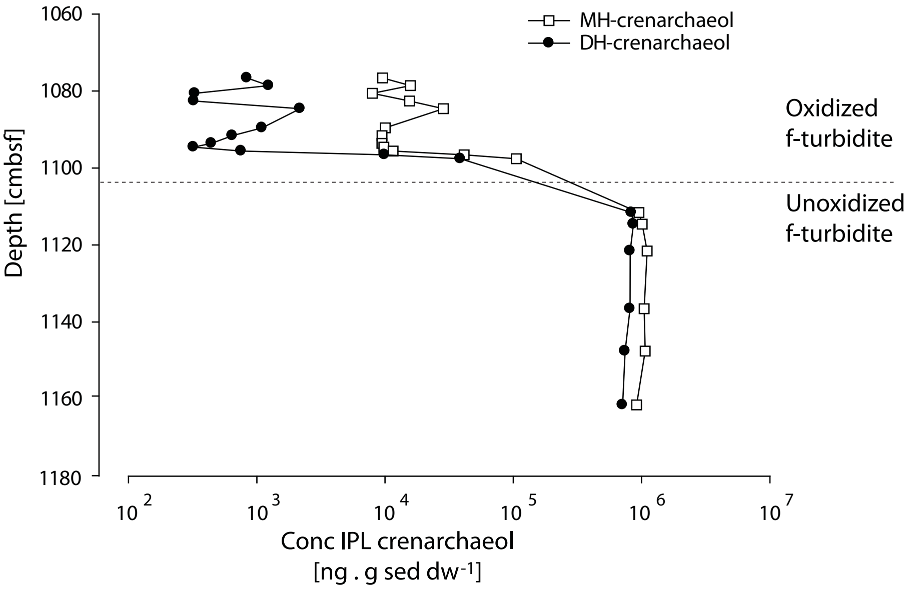

Figure 6.5. Concentrations (in ng . g sed dw^{-1}) of monohexose-(MH-) and dihexose-(DH-) crenarchaeol. Note the log scale.

and in particular Thaumarchaeota, which thrive in oxic marine surface sediments (Francis et al., 2005; Roussel et al., 2009; Wang et al., 2010; Cao et al., 2011; Moeseneder et al., 2012). This relatively small in situ production of MH-crenarchaeol in the oxidized part of the sediment, would lead to a smaller than expected decrease in the amount of MH-crenarchaeol, but would also require that these Thaumarchaeota would only produce MH-crenarchaeol and no DH-crenarchaeol. This seems unlikely as sedimentary and soil Thaumarchaeota are synthesizing GDGTs with MH-, DH- and HPH-head groups in enrichment cultures (Pitcher et al., 2011c; Sinninghe Damsté et al., 2012) and in surface sediments (Lengger et al., 2012b). Most likely, part of the MH-crenarchaeol, and to a minor extent DH-crenarchaeol, stems from terrestrial sources, which results in enhanced preservation as discussed above for the branched GDGTs. If so, soil Thaumarchaeota would produce more MH- compared to DH-crenarchaeol, in contrast with results reported from enrichment cultures (Sinninghe Damsté et al., 2012) as well as the presence of MH-, DH- and HPH-crenarchaeol in riverine SPM in the Amazon (Zell et al., 2013). Nevertheless, up to now there has been no quantitative, detailed survey of IPL-GDGTs in terrestrial organic matter or riverine SPM and thus it is difficult to evaluate this hypothesis. As for the br-GDGTs, a combination of a small amount of in situ production of IPL-GDGTs,

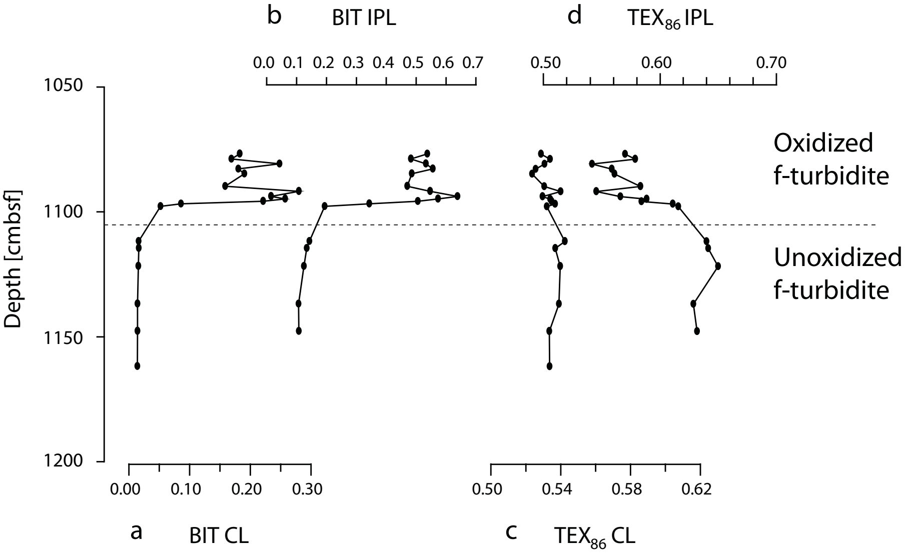

Figure 6.6. CL- and IPL-derived BIT and TEX_{86} values of the f-turbidite across the oxidation front.

and the preferential degradation of marine over terrestrial organic matter, can be regarded as the causes for the apparent enhanced preservation of MH-crenarchaeol.

3.4 Effect of post-depositional oxidation on the MBT/CBT, BIT index and TEX_{86} proxies

As stated above, the MBT/CBT proxy is affected by the oxidation and values are changing for the CL-GDGTs to, presumably, more terrestrial values. The MBT/CBT of IPL-derived GDGTs could not be determined due to limited material; however, we did show that oxidation causes a substantial change in distribution of the branched GDGTs I, II and III (Fig. 6.3g). The BIT-index increased strongly with increasing level of oxidation, from on average of 0.01 for the CL in the unoxidized section to 0.2 in the oxidized section and from 0.1 in the unoxidized sediment to as high as 0.5 for the IPL-derived GDGTs in the oxidized part (Fig. 6.6ab). The results for the core lipids agree with those of Huguet et al. (2008). Over the oxidation front, a gradual increase of BIT-index is observed, associated by the decrease in concentration, indicating that the increase in BIT-index is only occurring upon substantial degradation. Intriguingly, this effect is stronger for the IPL-derived BIT (increase by 0.6 units) than for the CL-BIT (increase by 0.3 units). The higher BIT-index for IPL-derived GDGTs could be due to either enhanced preservation of br-GDGTs over crenarchaeol, or in situ production of br-GDGTs in the oxidized part of the turbidite, as discussed above.

The TEX_{86} values of the CL-GDGTs showed hardly any changes across the oxidation front, despite the large drop in concentrations of CL-isoprenoid GDGTs (Fig. 6.6c), and were always lower than the TEX_{86} of the IPL-GDGTs (0.53; Fig. 6.6d). This partially agrees with the results obtained by Huguet et al. (2009), who observed an increase in TEX_{86} in the f-turbidite upon oxidation, but not for all other turbidite deposits. In contrast to the CL, the TEX_{86} of the IPL-derived fraction strongly decreased by ca. 0.07 across the oxidation front from 0.64 to 0.57. One reason why the TEX_{86} of IPL-derived GDGTs changed could be the observed preferential degradation of the DH-GDGTs compared to the MH-GDGTs as discussed above (Fig. 6.5). It has previously been shown that the ring distribution and, thus, TEX_{86} of IPLs varies with head group in thaumarchaeal cultures and marine sediments (Sinninghe Damsté et al., 2012; Lengger et al., 2012b). In order to examine the impact differential degradation could have on the TEX_{86}, MH- and DH-GDGT fractions were isolated by semi-preparative HPLC from a combined sample of the unoxidized f-turbidite. This resulted in a TEX_{86} value of 0.55 for the MH-GDGTs, and a TEX_{86}

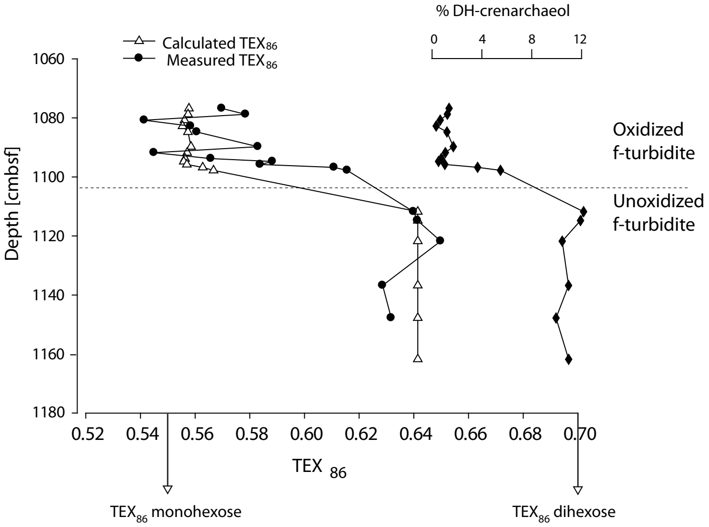

Figure 6.7. TEX_{86} values calculated from the relative proportions of MH- and DH-GDGTs compared to the measured TEX_{86} values of IPL-derived GDGTs, acc. to Eq. 1; and the proportion of DH-crenarchaeol of total (MH+DH) IPL-derived crenarchaeol.

value of 0.70 for the DH-GDGTs (Table 6.2), with a weighted averageTEX_{86} value of 0.64. This is consistent with results from thaumarchaeal cultures, which show that MH- and HPH-GDGTs have a higher contribution of GDGT-1, while DH-GDGTs consist mainly of GDGT-2, -3 and -4 (Schouten et al., 2008; Pitcher et al., 2011c; Sinninghe Damsté et al., 2012). Considering the substantial differences in TEX_{86} values of MH- and DH-GDGTs (0.15), the proportional decrease of DH-GDGTs compared to MH-GDGTs in the oxidized part of the turbidite (Fig. 6.5; Fig. 6.6), should result in a shift of TEX_{86}. To test this hypothesis, we calculated the theoretical TEX_{86} values based on the concentrations of MH-derived and DH-derived GDGTs measured by prep-HPLC for the unoxidized turbidite ($GDGT_{MH}$ and $GDGT_{DH}$, respectively) and the proportion of MH- versus the sum of MH- and DH-crenarchaeol, f_{MH} as determined by SRM measurements:

$$TEX_{86,theor} = \frac{(GDGT-2_{MH}+GDGT-3_{MH}+Cren'_{MH})*f_{MH}+(GDGT-2_{DH}+GDGT-3_{DH}+Cren'_{DH})*(1-f_{MH})}{(GDGT-1_{MH}+GDGT-2_{MH}+GDGT-3_{MH}+Cren'_{MH})*f_{MH}+(GDGT-1_{DH}+GDGT-2_{DH}+GDGT-3_{DH}+Cren'_{DH})*(1-f_{MH})}$$

(Eq. 1)

Using Eq. 1, a decrease of the TEX_{86} from 0.64 to 0.56-0.57 upon oxidation is predicted due to the changing proportion of MH-GDGTs compared to DH-GDGTs (Fig. 6.7), which is similar to the measured IPL-derived TEX_{86} values (Fig. 6.5; Table 6.2). Thus, the change in IPL-derived TEX_{86} can be explained by the apparent relatively larger preservation of MH-GDGTs, compared to DH-GDGTs.

Apparently, the degradation and in situ production of IPL-GDGTs has no influence on the TEX_{86} of CL-GDGTs. It is possible that IPL-GDGTs are degraded completely and do not accumulate as CL-GDGTs. However, the amounts of isoprenoid IPL-derived GDGTs are small compared to the respective CL-GDGTs (36% in the unoxidized sediment, Table 6.1). It is thus likely that the IPL-GDGTs are present in too small amounts to significantly influence the CL-TEX_{86}, which is the value ultimately used for paleotemperature estimations.

4 CONCLUSIONS

Both CL- and IPL-GDGTs were strongly degraded upon post-depositional oxidation of the organic-rich f-turbidite from the Madeira Abyssal Plain. Degradation patterns revealed that terrestrial GDGTs were better preserved while marine GDGTs seemed to be relatively more labile, resulting in changes in the BIT index upon oxidation, in line with previous studies. Surprisingly, IPL-GDGTs were equally well or better preserved upon oxidation than CL-GDGTs. Also the directly measured IPL MH-crenarchaeol was preserved better than the CL-crenarchaeol. Since MH-GDGTs showed lower TEX_{86} values than DH-GDGTs, this preferential preservation resulted in changes in TEX_{86} of the IPL-derived GDGTs. However, the TEX_{86} of CL-GDGTs, ultimately used in paleotemperature estimations, was not affected by post-depositional oxidation, most likely due to the small amounts of IPL-GDGTs compared to CL-GDGTs (<10%). Contrastingly, there were large changes occurring upon oxidation in the BIT values, and also changes in the MBT/CBT, suggesting that care has to be taken with the interpretation of proxies containing br-GDGTs, when they are present in low amounts and have been exposed to post-depositional oxidation. Furthermore, our results show that progressing degradation can cause changes in abundance and distribution of IPL-GDGTs in sediments, and can thus not be interpreted as due to in situ-production in the absence of other evidence.

ACKNOWLEDGEMENTS. The authors would like to thank the participants in the JCR209 and the Master and crew of the R/V James Clark Ross. Thanked for analytical assistance are R. Gieles, J. Ossebaar and F. Temmesfeld. S.K.L. was funded partially by a grant from the Darwin Center for Biogeosciences to S.S. This is a publication of the Darwin Center for Biogeosciences.

CHAPTER 7

NO DIRECT ROLE OF ARCHAEA IN DEEP SEA BENTHIC ORGANIC CARBON PROCESSING

Submitted to *PLoS ONE*

NO DIRECT ROLE OF ARCHAEA IN DEEP SEA BENTHIC ORGANIC CARBON PROCESSING

Sabine K. Lengger[a], Markus M. Moeseneder[b,#], Lara Pozzato[c], Barry Thornton[d], Ursula Witte[b], Leon Moodley[c], Jack J. Middelburg[c,e], Jaap S. Sinninghe Damsté[a,e] and Stefan Schouten[a,e]

[a] Marine Organic Biogeochemistry, Royal NIOZ Netherlands Institute for Sea Research, P. O. Box 59, 1790AB Den Burg, Texel, The Netherlands. [b] Institute of Biological and Environmental Sciences, Oceanlab, University of Aberdeen, Newburgh, UK. [c] Ecosystem Studies, Royal NIOZ Netherlands Institute for Sea Research, Yerseke, The Netherlands. [d] The James Hutton Institute, Craigiebuckler, Aberdeen, United Kingdom. [e] Faculty of Geosciences, Utrecht University, Utrecht, The Netherlands. [#]Present address: Ocean Biogeochemistry and Ecosystems Research Group, National Oceanography Centre, University of Southampton, Southampton, UK.

ABSTRACT

While the widespread archaea of the phylum Thaumarchaeota have been shown to mediate the oxidation of ammonia in marine environment, their involvement in organic carbon processing in marine sediments has not been extensively investigated yet. In this study, we conducted experiments by administering ^{13}C-labelled *Thalassiosira* diatom organic matter to marine sediments. Shipboard incubations with sediments from outside and within the oxygen minimum zone of the Arabian Sea and in situ incubations at an abyssal setting in the NE Pacific were performed. We measured the ^{13}C incorporation into intact polar lipid crenarchaeol, a specific membrane lipid of Thaumarchaeota, and into other archaeal glycerol dibiphytanyl glycerol tetraether lipids (GDGTs), which in these settings are probably also mainly stemming from Thaumarchaeota. No incorporation of ^{13}C-label could be detected in the isoprenoid chains of any of the GDGT lipids, in contrast to bacterial phospholipid fatty acids, which were shown to be substantially enriched in ^{13}C post-incubation. This likely suggests that Thaumarchaeota play a minor direct role in benthic organic carbon processing, as the phytodetritus was not being taken up at all, in contrast to bacteria, meio- and macrofauna. Alternatively, the lack of labeling might be due to a much lower turnover rate of archaeal membrane lipids than that of bacterial membrane lipids, whereby high background concentrations mask any ^{13}C label uptake into the

GDGTs.

1 INTRODUCTION

Archaea have traditionally been regarded as extremophiles, preferring saline, acidic or high temperature conditions. However, over the last decades, members of the domain have been discovered to be present and abundant in the global oceans (DeLong, 1992; Fuhrman et al., 1992). Since then, archaea have been found in many moderate and cold marine environments (Cavicchioli, 2006). They are not only dominating the marine picoplankton (e.g. Karner et al., 2001; Church et al., 2009), but various members of the kingdoms of the Eury- and the Crenarchaeota have also been found to thrive in marine sediments (Vetriani et al., 1999).

In sediments with high methane fluxes, most of the archaea present are involved in anaerobic oxidation of methane (Boetius et al., 2000; Pancost et al., 2001; Wakeham et al., 2003; Dang et al., 2010). However, other sediments are dominated by other phylotypes: Wang et al. (2005) found Marine Group I (MG-I) Crenarchaeota to be the dominant group in deep-sea surface sediments from the West Pacific, along with a new group of Euryarchaeota. Francis et al. (2005) found MG-I Crenarchaeota to be ubiquitous not only in the water column, but also in surface sediments. This group has recently been reclassified and shown to form a separate kingdom, the Thaumarchaeota (Brochier-Armanet et al., 2008; Spang et al., 2010). In addition to Thaumarchaeota, archaea pertaining to other clusters, such as Marine Benthic Group or Miscellaneous Group (MCG) Crenarchaeota, have been detected in marine sediments (Jiang et al., 2007; Wang et al., 2010; Cao et al., 2011; Köchling et al., 2011). MCG have also recently been found to be widespread in marine sediments, constituting 12-100% of archaea, mainly present in sediments that show low respiration rates (Kubo et al., 2012). In spite of their universal presence though, archaeal biomass is much lower than the bacterial biomass in marine surface sediments (1 - 4 orders of magnitude; Wang et al., 2005).

One of the characteristics of the archaeal domain are their membrane lipids, which consist of ether-bound isoprenoid chains linked to a glycerol (Kates et al., 1965). Many archaea also produce glycerol dibiphytanyl glycerol tetraether lipids (GDGTs; Langworthy et al., 1972), two biphytanyl chains linked to two glycerol units, which sometimes contain cyclic moieties (de Rosa and Gambacorta, 1988; Fig. 7.1a). GDGT-0, which contains no rings (Fig. 7.1a), is present in many different archaeal

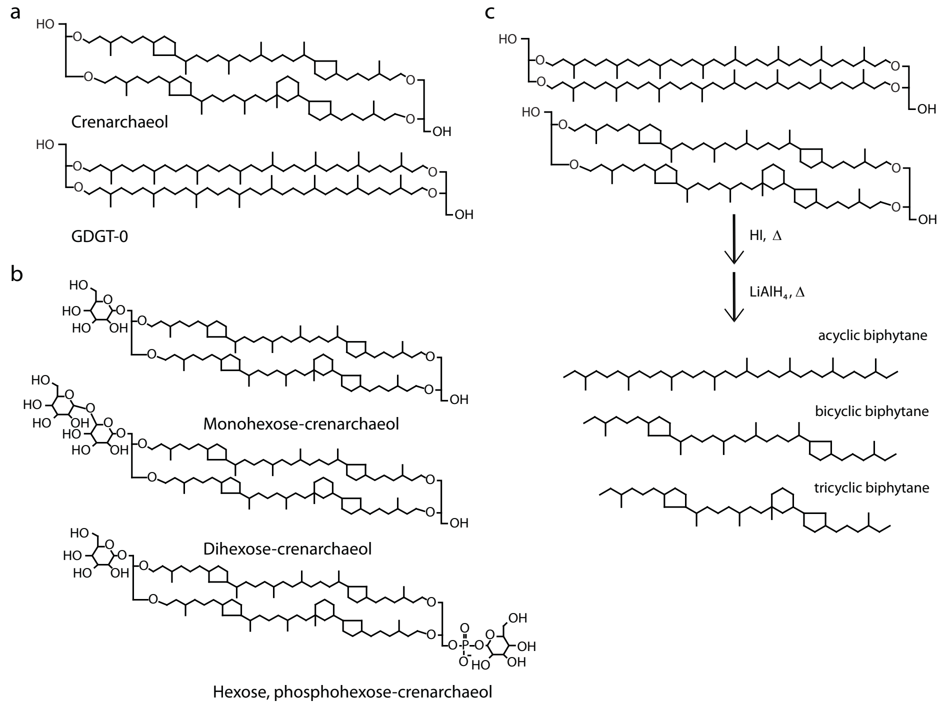
a
Crenarchaeol
GDGT-0
b
Monohexose-crenarchaeol
Dihexose-crenarchaeol
Hexose, phosphohexose-crenarchaeol
c
HI, Δ
LiAlH$_4$, Δ
acyclic biphytane
bicyclic biphytane
tricyclic biphytane

Figure 7.1. Structures of crenarchaeol and GDGT-0 (a), IPL-crenarchaeol species (b) and biphytanyl chains released from crenarchaeol and GDGT-0 by chemical degradation (c).

species and hence considered a more general archaeal biomarker (Schouten et al., 2013 and references cited therein). In contrast, crenarchaeol, a GDGT containing in total 4 cyclopentyl and 1 cyclohexyl moieties, is considered to be specific to Thaumarchaeota (Sinninghe Damsté et al., 2002b; Pitcher et al., 2010; Hatzenpichler, 2012). GDGT-0 and crenarchaeol are by far the most abundant archaeal GDGT lipids in marine sediments (Kim et al., 2010). In living archaea, these lipids occur as intact polar lipids (IPL), i.e. containing polar headgroups (Fig. 7.1b; e.g. Koga and Morii, 2005; Schouten et al., 2008) attached to the glycerol moieties, e.g. hexose- and/or phosphate-groups. In Thaumarchaeota, GDGTs mainly occur as monohexose-, dihexose-, phospho- and hexose, phosphohexose-GDGTs (Schouten et al., 2008; Pitcher et al., 2010; Tourna et al., 2011; Pitcher et al., 2011c; Sinninghe Damsté et al., 2012).

Recent research on enrichment cultures and environmental studies have shown that Thaumarchaeota are autotrophic and gain energy from the aerobic oxidation of ammonia (Wuchter et al., 2003; Könneke et al., 2005; Wuchter et al., 2006b; de la Torre et al., 2008; Hatzenpichler et al., 2008; Park et al., 2010; Tourna et al., 2011). However, Thaumarchaeota also show a potential for heterotrophy, as evident from genomic analyses, which showed that *Cenarchaeum symbiosum*, a sponge symbiont (Preston et al., 1996), and *Nitrosopumilus maritimus*, isolated from an aquarium (Könneke et al., 2005), possessed not only genes for cellular import of simple organic molecules, but also metabolic genes generally associated with heterotrophy (Hallam et al., 2006b; Walker et al., 2010). Enrichment culture studies indeed showed that, if pyruvate was supplied, it was incorporated into cells of the Thaumarchaeote *Nitrososphaera viennensis* and even spurred growth (Tourna et al., 2011). Furthermore, environmental studies suggest potential heterotrophy: Ouverney and Fuhrman (2000) and Herndl et al. (2005) showed the uptake of ^{14}C-labelled amino acids in thaumarchaeal cells present in the water column. Circumstantial evidence for the potential for mixotrophy of Thaumarchaeota was presented by Ingalls et al. (2006) by comparison of the natural abundance ^{14}C-isotopic composition of archaeal lipids with that of dissolved inorganic and organic carbon of the water column. Mußmann et al. (2011) found that cell numbers of Thaumarchaeota in a wastewater treatment plant were 2-3 orders of magnitude higher than possible to sustain purely by autotrophic ammonia oxidation, together with only a weak label incorporation from ^{13}C-bicarbonate, suggesting a heterotrophic metabolism. Alonso-Sáez et al. (2012) detected genes for urea-degradation in the thaumarchaeal metagenome isolated from polar waters, while Baker et al. (2012) found expression of thaumarchaeal genes involved in the utilization of urea, together with genes involved in ammonia oxidation, in hydrothermal vent plumes in the Guaymas Basin. These results suggest a potential for uptake of at least simple organic compounds by pelagic Thaumarchaeota.

Even though Thaumarchaeota in the water column have been researched thoroughly, fewer studies have been carried out on their sedimentary counterparts. Park et al. (Park et al., 2008) and Roussel et al. (2009) showed that Thaumarchaeota were present and active in abyssal sediments, as suggested by results from 16S rDNA and rRNA analyses, and were capable of ammonia oxidation, as evidenced by the co-occurrence of archaeal *amo*A genes with the 16SrRNA. Biddle et al. (2006) and Lipp et al. (2008) inferred that, in subsurface (>1 mbsf) anoxic sediments, archaea could be heterotrophs, based on the correlation of organic carbon concentrations with archaeal IPLs (Lipp and Hinrichs, 2009). However, it is also possible that this correlation is due to the preservation of IPL-GDGTs, because of a general relationship of biomarker lipid concentrations with organic carbon (Sinninghe Damsté et al., 2002a). This preservation was thought to be due to the low rate of degradation of IPL-GDGTs compared to regular bacterial phospholipids (Harvey et al., 1986; Logemann et al., 2011).

An in situ labeling experiment with deep-sea surface sediments targeted at archaea was conducted by Takano et al. (2010), who performed 450 days of incubation with ^{13}C-glucose. The authors could not detect any ^{13}C-incorporation into the biphytane chains, but found the glycerol moiety of archaeal GDGTs to be enriched in ^{13}C, by up to more than 2000 ‰ (Takano et al., 2010). This remarkable result was explained by the recycling of biphytanyl chains from fossil GDGTs, while the glycerol moiety was thought to be newly synthesized via a pathway that incorporated carbon of the supplied ^{13}C-enriched glucose. In a laboratory experiment, Lin et al. (2012) provided ^{13}C-enriched organic matter from the algae *Spirulina platensis* to sediment slurries from oligotrophic deep subsurface settings and incubated this anaerobically for >400 days. Some incorporation was reported but the evidence is ambiguous: the tricyclic biphytane derived from crenarchaeol was enriched by ~2 ‰, while the δ^{13}C of the bicyclic biphytane, the second isoprenoid chain in crenarchaeol, actually became depleted in ^{13}C by 2 ‰. Thus, it is not clear if, and in what way, archaea are involved in organic matter processing at the benthic interface of the ocean floor. In contrast, bacterial and metazoan contributions have been extensively researched in many different settings and shown to play an important role in uptake of phytodetritus reaching deep sea sediments (cf. Moodley et al., 2002; Witte et al., 2003; Moodley et al., 2005).

To examine the role of archaea in benthic carbon processing in deep sea sediments, we performed ^{13}C in situ and shipboard incubation studies of a phytodetritus pulse administered to the surface of deep sea sediments and examined the uptake of the label into archaeal lipid biomarkers. One labeling experiment was carried out in the Arabian Sea using shipboard incubations with ^{13}C-labelled phytodetritus derived from the diatom *Thalassiosira pseudonana*. Sediments in the Arabian Sea are characterized by high organic carbon contents, but low organic matter quality and a lack of sedimentary processes such as sulfate reduction (Cowie and Levin, 2009; Law et al., 2009). The second experiment was carried out in situ with abyssal sediments of the Northeast Pacific (Moeseneder et al., 2012) and involved administering a ^{13}C-labelled pulse of *Thalassiosira weissflogii* phytodetritus to sediment cores (Enge et al., 2011). Concentrations of IPL-crenarchaeol and ^{13}C-enrichments of GDGT-0 and in crenarchaeol were determined. The results are discussed in view of the role of archaea in benthic organic carbon processing.

2 MATERIALS AND METHODS

2.1 In-situ and shipboard incubations

The incubations of sediment cores from the Murray Ridge in the NE Arabian Sea were carried out during the PASOM cruise in January 2009, on board of the R/V Pelagia, with sediment cores taken outside and within the extensive Arabian Sea oxygen minimum zone (OMZ) (i.e. at 889 m water depth, within the OMZ, and at 1786 m water depth, outside the OMZ,) as described in detail by Pozzato et al. (2013). Material used for incubation was from the diatom *Thalassiosira pseudonana*, cultivated in a 30% ^{13}C enriched f/2 medium, which had been washed to remove any remaining ^{13}C-bicarbonate (see Pozzato et al., 2013, and Moodley et al., 2002, for further details). Centrifuged pellets were frozen, freeze-dried, lysed with MilliQ Water and separated into particulate organic matter (POM) and dissolved organic matter (DOM) by centrifugation. For incubations, the DOM was dissolved in 0.2 µm natural seawater and supplied to the top 4 cm of the sediment by injection at regularly spaced horizontal intervals by means of a syringe mounted on an extension rod. POM was delivered freeze-dried to the surface of the cores and evenly distributed. Cores from within the OMZ were incubated suboxically (~6 µM O_2) and include the control core (Ctr) incubated alongside the experimental cores without any labelled phytodetritus, and cores to which ^{13}C-labelled algal material was added as POM and DOM, the amount added was 100 mg C.m^{-2} for the cores from outside the OMZ and 400 mgC.m^{-2} for the cores from inside the OMZ. Cores from outside the OMZ analyzed included a control core, and cores incubated oxically (125 µM O_2), similar to the natural conditions, with ^{13}C-POM and DOM, and suboxically (8 µM O_2) with ^{13}C-POM. Suboxic incubation was achieved by sealing the cores on the bottom and the top with O-ring lids. For the oxic incubations, premixed air was bubbled through the overlying water of the sealed cores, and emerging gases were led through CO_2 traps for respiration measurements. Oxygen was measured after incubation. The cores were incubated for 7 days in the dark, frozen at -20°C and subsampled. The 0-2 cm slice was freeze-dried and used for extraction of archaeal lipids. Reports from one core per incubation condition are reported.

Sediment cores from Station M (34° 50’ N, 123° 00’ W) at 3953 m water depth in the Northeast (NE) Pacific were obtained during the PULSE 53 cruise on board of the R/V Western Flyer in September 2007, and incubated in situ on the seafloor. To this end, freeze dried biomass from labeled *Thalassiosira weissflogii* containing 53.5 atom% ^{13}C (grown with 99% ^{13}C-bicarbonate in f/2 medium, harvested and washed) was released in situ onto cores pushed into sediment by the ROV Tiburon at 3953 m water depth (see Enge et al., 2011 for details). Control cores did not receive the phytodetritus pulse. After a 4 day incubation time, the push cores were retrieved and immediately sliced on board into the subsamples 0-1, 1-2, 2-3, 3-5 and 10-15 cm core depth, transported frozen, freeze-dried and homogenized. In total, three control and three incubated cores were available. Two control and incubated cores were analyzed for IPL-crenarchaeol (only top 3 cm), one control and one incubated core for label incorporation into biphytanes from IPL-GDGTs (all 5 subsamples), and three control and incubated cores were analyzed for label incorporation into the phospholipid-derived fatty acids (PLFA).

2.2 Lipid extraction and separation

The freeze-dried subsamples of the cores were ground and extracted by a modified Bligh-Dyer extraction method (Pitcher et al., 2009b). Briefly, they were extracted ultrasonically three times in a mixture of methanol/dichloromethane (DCM)/phosphate buffer (2:1:0.8, v:v:v), centrifuged and the solvent phases were combined. The solvent ratio was then adjusted to 1:1:0.9, v:v:v, which caused the DCM to separate. Liquid extraction was repeated two more times, the DCM fractions were combined, the solvent was evaporated and bigger particles were filtered out over cotton wool. An aliquot of the extracts was stored for later analysis of IPL analysis via high performance liquid chromatography coupled to electron spray ionization mass spectrometry (HPLC/ESI-MS), and another aliquot was separated into CL and IPL-GDGTs by silica column separation with hexane/ethyl acetate (1:2, v:v) for the CL-fraction and MeOH to elute the IPL-fraction.

The IPL fraction was then subjected to ether cleavage in order to release biphytanyl chains from GDGTs (Fig. 7.1c), following procedures described by Schouten et al. (1998). To this end, the IPL fraction was refluxed in 57% HI for 1 h to cleave the ether bonds and produce alkyliodides and subsequently extracted 3 times with hexane. The hexane phase was washed with 5% NaS_2O_7 and twice with water. The alkyliodides were purified over Al_2O_3 with hexane/DCM 9:1, reduced with $LiAlH_4$

in 1,4-dioxane for 1 h under reflux, the remaining $LiAlH_4$ was reacted with ethyl acetate, bidistilled H_2O was added and the biphytanes were extracted with DCM from the dioxane/H_2O mixture. Additional purification was done by elution over an Al_2O_3 column using hexane.

One aliquot of the Bligh Dyer extract of the sediments of Station M was used for isotopic analysis of phospholipid-derived fatty acids (PLFA), following procedures modified from Guckert et al. (1985). The aliquots were separated over a silica column with DCM, acetone and methanol, with the methanol-fraction containing the PLFA. PLFA fractions were saponified in methanolic KOH (2 N) and, after adjusting to pH 5, the resulting fatty acids were extracted with DCM and methylated with BF_3-MeOH before measurements by gas chromatography – isotope ratio mass spectrometry (GC-irMS).

2.3 Analysis

Aliquots of the extracts were analyzed for IPL-GDGTs via HPLC/ESI-MS^n in selective reaction monitoring-mode (SRM) according to Pitcher et al. (2011b). Compounds monitored and reported here are monohexose (MH)-, dihexose (DH)- and hexose, phosphohexose (HPH)-crenarchaeol. Absolute quantification was not possible and hence the response peak area per g sediment dry weight (g sed dw) is reported. Standard deviations for these measurements are typically 2 – 20%.

GC-MS was used to identify the biphytanes formed upon ether cleavage of GDGTs and PLFAs using a TRACE GC with a DSQ mass spectrometer. The gas chromatograph was equipped with a fused silica capillary column (25 m, 0.32 mm internal diameter) coated with CP Sil-5 (film thickness 0.12 µm). The carrier gas was helium. The compound specific carbon isotopic composition of the biphytanes was measured with an Agilent 6800 GC, using the same GC column conditions, coupled to a ThermoFisher Delta V isotope ratio monitoring mass spectrometer. The isotopic values were calculated by integrating the mass 44, 45 and 46 ion currents of the peaks and that of CO_2-spikes produced by admitting CO_2 with a known ^{13}C-content into the mass spectrometer at regular intervals. The performance of the instrument was checked by daily injections of a standard mixture of a C_{20} and a C_{24} perdeuterated n-alkane. Values reported were determined by one (Arabian Sea, too little material for duplicate injections) or two (NE Pacific) analyses. When two analyses were carried out, the results were averaged in order to obtain average and standard deviations. Material from the Arabian Sea, outside the OMZ and incubated suboxically with POM showed a too low signal for δ^{13}C determination. The stable carbon isotope compositions are reported in the delta notation against the V-PDB standard.

In addition, selected PLFAs present in the extracts of the sediments of station M were measured for their stable carbon isotopic composition at the James Hutton Institute, Aberdeen, UK, using a GC Trace Ultra attached via a GC combustion III interface to a Delta V Advantage irm-MS. Gas chromatography was achieved by on-column injection onto a DB5 50m x 0.20mm x 0.33µm column. Values for the fatty acids were corrected for the added carbon by BF_3-MeOH methylation (δ^{13}C of -30.0 ± 0.2 ‰VPDB).

3 RESULTS

3.1 Arabian Sea

Direct analysis using HPLC-ESI-MS^2 of crenarchaeol IPLs showed differences in distribution of the head groups between the stations inside and outside of the OMZ. MH-crenarchaeol and DH-crenarchaeol concentrations in the sediment (upper 2 cm) collected in the OMZ were much higher than in the cores from outside the OMZ, while HPH-crenarchaeol concentrations were one order of magnitude lower (Fig. 7.2a,b), consistent with earlier findings of Lengger et al. (2012b). Concentrations of crenarchaeol IPLs were not elevated after incubation with diatom-derived POM and DOM. At the station outside the OMZ, the surface (0-2 cm) sediments contained similar amounts in the control core as in the oxically incubated cores. The core from this station incubated under suboxic conditions, however, showed an order of magnitude lower abundance of HPH-crenarchaeol. MH- and DH-crenarchaeol showed no difference in concentrations between the cores (Fig. 7.2a). For the core from the station within the OMZ, the only observed differences in the IPL crenarchaeol concentrations between the incubated and the control cores were the slightly lower values for the core suboxically incubated with POM (Fig. 7.2b). This suggests that the addition of the phytodetritus did not cause growth of Thaumarchaeota.

The δ^{13}C-values of the bicyclic and tricyclic biphytane, both mainly derived from crenarchaeol, show values of -20 ‰ for the control core at the station outside the OMZ and slightly more depleted values, -21 ‰, for the incubated cores, independent of the type of organic matter used for incubation (Fig. 7.2c). This difference in

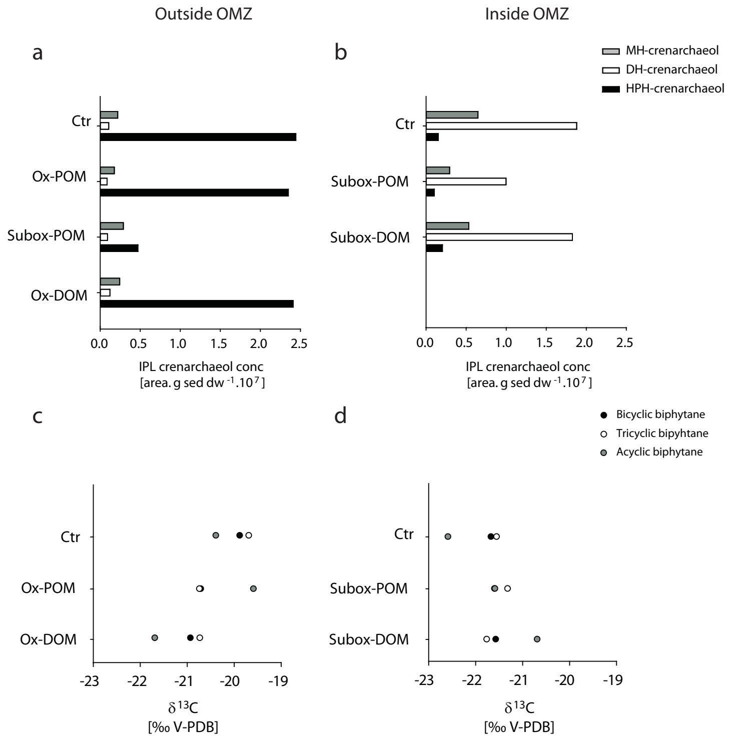

Figure 7.2. IPL-crenarchaeol concentrations in surface (0-2 cm) sediments from the Arabian Sea; (a) outside the OMZ, (b) inside the OMZ for the control cores (Ctr), and the cores incubated under oxic (ox) conditions with POM or DOM, and under suboxic (subox) conditions with POM and DOM. In the lowermost panels (c and d), the stable carbon isotopic composition of the acyclic, bicyclic and tricyclic biphytanes are shown for the cores from outside (c, no data for Suboxic-POM) and within the OMZ (d). Values are from single cores, single analysis.

δ^{13}C-values is typically within the error margin of our irm-GC/MS measurements of biphytanes (ca. 0.5‰). The acyclic biphytane, predominantly derived from GDGT-0, had a similar δ^{13}C value of -20 ‰ and only in the oxically incubated core with DOM, a slightly more depleted value, -22 ‰ (Fig. 7.2c). In the sediment from within the OMZ, bicyclic and tricyclic biphytanes from the control core showed values of -22 ‰, similar to the biphytanes from the incubated cores, with values between -21 and -22 ‰ (Fig. 7.2d). The acyclic biphytane had a δ^{13}C of -23 ‰ in the control core, and was slightly enriched in ^{13}C in the incubation cores, with -22 ‰ in the core incubated with POM and -21 ‰ in the core incubated with DOM (Fig. 7.2d). Thus, the differences between control cores and incubation cores ($\Delta\delta^{13}C_{inc-ctr}$) were

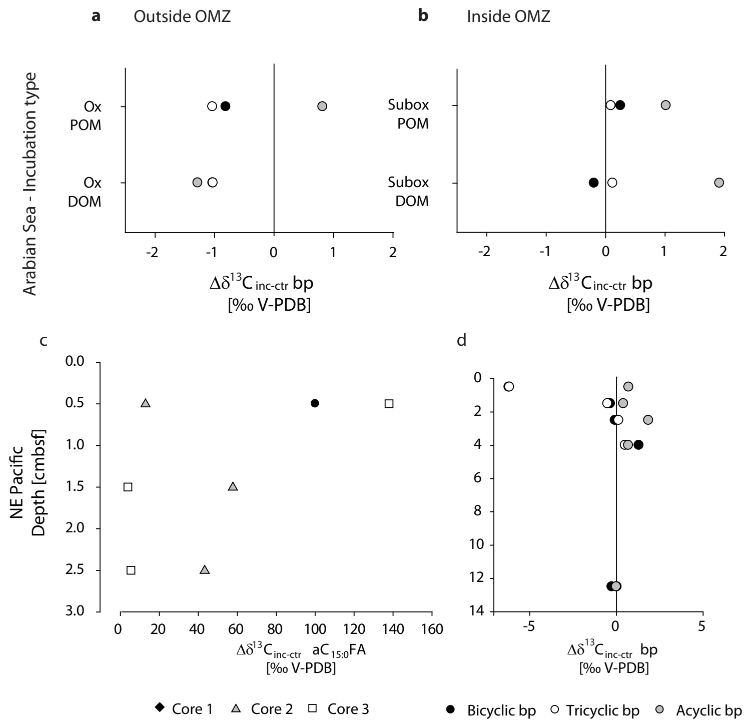

Figure 7.3. The differences in isotopic values between the incubation and the control cores ($\Delta\delta^{13}C_{inc\text{-}ctr}$) for cores from the Arabian Sea, outside (a) and inside the OMZ (b). Below, the difference in isotopic values between the incubation and the control cores ($\Delta\delta^{13}C_{inc\text{-}ctr}$) of the core from the NE Pacific, of the bacterial *anteiso* $C_{15:0}$ fatty acid (c) and the biphytanyl chains (d). Notice the difference in scales. Values for biphytanyl chains are shown for one incubation core for the top 3 cm, for the fatty acid for three incubation cores, for the top 3 cm (top 1 cm for Core 1).

always <2 ‰ (Fig. 7.3ab). In contrast bacterial PLFAs were substantially enriched in ^{13}C with $\Delta\delta^{13}C_{inc\text{-}ctr}$ values ranging from by +80 to +100 ‰ in the cores from within the OMZ and +8 to +20 ‰ in the cores from outside the OMZ for POM incubations (Pozzato et al., 2013).

3.2 Northeast Pacific abyssal sediments

IPL-crenarchaeol concentrations from the Station M in the North East Pacific are averaged results from two cores incubated as controls and averaged values from two cores incubated with labeled phytodetritus, analyzed for the upper 3 cm at several depth intervals). Direct analysis of crenarchaeol IPLs in these cores showed that the

MH-crenarchaeol and the DH-crenarchaeol concentrations were constant with sediment depth (Fig. 7.4a,b). The HPH-crenarchaeol concentration, however, decreased with sediment depth by an order of magnitude in the control cores. Such a rapid decline in HPH-crenarchaeol concentration with sediment depth has been previously reported for Arabian Sea sediments (Lengger et al., 2012b). Some differences were apparent in crenarchaeol IPL concentrations when comparing control and incubated cores (cf. Figs. 4a and b), with slightly higher concentrations of HPH-crenarchaeol in the deeper sediments of the incubated than in the control cores. However, variation between cores was too large to allow any conclusions. In any case, there was no evidence that the addition of phytodetritus resulted in substantial growth of benthic Thaumarchaeota.

The $\delta^{13}C$ values of the acyclic, bicyclic and tricyclic biphytanes released from GDGTs were measured in sediment slices down to 15 cm depth and varied between -18 to -20 ‰ with depth in both the control and the incubation core (Fig. 7.4c and d). The only value outside of this range was in the top slice of the incubated core, which showed slightly more depleted values for the bicyclic and the tricyclic biphytane, -25 ‰. The acyclic biphytane in this segment of the core, however, had a $\delta^{13}C$ of -18 ‰ comparable to values in the other cores. Thus, the difference in the $\delta^{13}C$ of biphytanes between incubation and control cores were all < 2 ‰, indicating a limited enrichment in ^{13}C and even more depleted $\delta^{13}C$ values in one sample (the top slice $\Delta\delta^{13}C_{inc\text{-}ctr}$ values for the bicyclic and tricyclic biphytanes was -6 ‰; Fig. 7.3d). In contrast, bacterial PLFA such as the *anteiso* $C_{15:0}$ fatty acid in the upper 3 cm, had substantially enriched $\delta^{13}C$ values, with $\Delta\delta^{13}C_{inc\text{-}ctr}$ ranging from +10 to +140 ‰ (Fig. 7.3c). This was seen for most of the sediment PLFAs (Moeseneder et al., unpublished results).

4 DISCUSSION

4.1 Sources of GDGTs

Our lipid analyses show unambiguously the presence of crenarchaeol IPLs in the marine sediments studied. HPH-crenarchaeol was present in all cores. It is the preferred biomarker for living Thaumarchaeota, as it is relatively labile (Lengger et al., 2012b) and its concentration compares well with thaumarchaeal 16S rRNA copy numbers, as reported by Pitcher et al. (2011b). However, it has also been shown that archaeal phospholipids are preserved well over timescales of at least 100 days (Logemann et al., 2011). A substantially higher abundance of HPH-crenarchaeol relative to the crenarchaeol glycolipids was found in the surface sediments from outside the OMZ, and also in the surface sediments from the NE Pacific, compared to the sediments from within the OMZ (Fig. 7.2a,b), similar to what was observed previously (Lengger et al., 2012b). This was attributed to the fact that Thaumarchaeota, as aerobic ammonia oxidizers, are dependent on oxygen and that they are thus more active and abundant in the surface sediments underlying oxic bottom waters. This indicates that HPH-crenarchaeol is likely derived from living Thaumarchaeota in the oxygenated surface sediments from the NE Pacific and from outside the OMZ in the Arabian Sea, while the relatively low amounts present in the surface sediments from within the OMZ of the Arabian Sea likely reflect remains of lipids produced in the overlying oxic surface waters and preserved under the favorable low oxygen conditions of the OMZ, i.e. lack of oxidation and biodegradation. Alternatively, it is possible that thaumarchaeal communities differ depending on the oxygen concentrations, and that Thaumarchaeota present at much reduced oxygen levels (within the OMZ) produce relatively more DH-crenarchaeol. However, this is less likely, as it has not been observed in cultured sedimentary Thaumarchaeota (Schouten et al., 2008; Pitcher et al. 2011a; Sinninghe Damsté et al., 2012). Interestingly, the suboxic incubation of the sediment core retrieved from outside of the OMZ also showed low abundances of HPH-crenarchaeol, but no increase in abundance of the DH-crenarchaeol. It is thus likely that the HPH-crenarchaeol is not being produced under low oxygen conditions, but is rapidly degraded under low oxygen conditions. All the other cores that were incubated at conditions similar to their natural conditions (Pozzato et al., 2013) showed no differences to the control cores.

The control cores from the NE Pacific showed a strong decrease with depth of the HPH-crenarchaeol concentrations, while the MH- and DH-crenarchaeol concentrations did not change (Fig. 7.4a and b). This compares well with the results of Lengger et al. (2012b) for sediment cores from the Arabian Sea taken outside the OMZ, where it was found that HPH-crenarchaeol was more labile and concentrations decreased quickly with depth, while the concentrations of the glycolipids MH- and DH-crenarchaeol were not changing over depth. This is consistent with the idea that most of the MH- and the DH-crenarchaeol is fossil and stems from the water column, while most of the HPH-crenarchaeol in the NE Pacific was produced by active benthic Thaumarchaeota, and quickly degraded upon burial (Schouten et al., 2010; Lengger et al., 2012b). If so, our results indicate that thaumarchaeal cell numbers rapidly decrease with sediment depth in NE Pacific sediments. However, there are no indications as to why this abundance is decreasing: oxygen profiles measured at Station M in the NE Pacific show that oxygen is penetrating into the upper 3 cm (Reimers, 1987) and the zone of aerobic ammonia oxidation based on pore water profiles was identified as 0-4 cmbsf (up to 4 μmol . kg^{-1} NH_4^+), below which [NH_4^+] increased to 10 μmol . kg^{-1} (Reimers et al., 1992). Also molecular biology results for

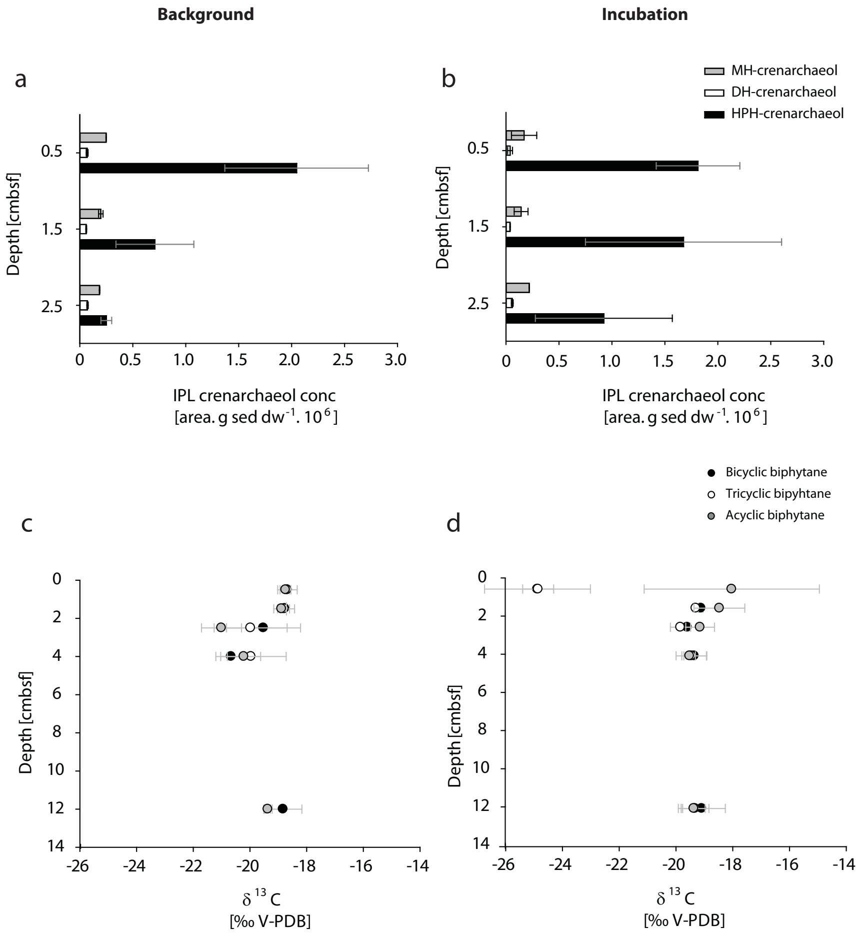

Figure 7.4. Averages of IPL-crenarchaeol concentrations and standard deviations of the two control cores (a) and the two incubated cores (b) plotted with sediment depth at station M in the NE Pacific. The stable carbon isotopic composition of acyclic, bi- and tricylic biphytanes is shown as the average plotted with the standard deviation of, typically, two measurements, for the control core (c) and the incubation cores (d).

these cores do not show a corresponding decrease of rRNA or rDNA with depth (Moeseneder et al., 2012).

The crenarchaeol natural abundance ^{13}C values in the Arabian Sea and NE Pacific sediments, as determined from the bi- and tricyclic biphytane values, were similar to those reported for other deep sea marine sediments and thaumarchaeal biomass, i.e. from -18 to -25 ‰ (Hoefs et al., 1997; Könneke et al., 2012; Schouten et al., 2013 and references cited therein). All cultured Thaumarchaeota up to now are aerobic ammonium oxidizers, growing chemolithoautotrophically by oxidizing NH_3 to NO_2^- and fixing HCO_3^- via the 3-hydroxypropionate/4-hydroxybutyrate pathway (Berg et al., 2007; Walker et al., 2010). Fractionation factors for bulk biomass and biphytanes from DIC were reported for *N. maritimus*, a Thaumarchaeote, to be ca. 20 ‰ (Könneke et al., 2012). The δ^{13}C values of the biphytanes are thus consistent with the interpretation that crenarchaeol is likely derived of chemoautotrophic Thaumarchaeota. Since ^{13}C-DIC values usually do not differ by more than a few ‰ between the surface waters and the deep ocean as well as pore waters of surface sediments (slightly more depleted), and fractionation factors are not precisely known, it is not possible to make statements about the provenance of the biphytanes just by their δ^{13}C values. δ^{13}C values are agreeing with the values usually found for biphytanes (cf. Hoefs et al. 1997), which are similar to the bulk organic carbon values encountered in marine sedimentary environments, but slightly less depleted, as they are using the 3-hydroxypropionate/4-hydroxybutyrate pathway, in contrast to phytoplankton. This was also shown previously by Kuypers et al. (2001), who found values for biphytanes which were more enriched in ^{13}C than today in the Cretaceous, consistent with the global shift in δ^{13}C of DIC, while algal biomarkers were less enriched due to the higher CO_2 concentrations.

Since GDGT-0 can be produced by many different archaea (e.g. Koga and Nakano, 2008; Schouten et al., 2013), it is unclear what its sources are in the Arabian Sea and abyssal NE Pacific sediments. However, the natural abundance δ^{13}C value of GDGT-0 (acyclic biphytane) is similar to that of crenarchaeol (bi- and tricyclic biphytane) (Figs. 2c,d and 4c,d), which agrees with data from cultures that shows that thaumarchaeal biphytanes are characterized by identical δ^{13}C biphytane values (Könneke et al., 2012; Sinninghe Damsté et al., 2012). Other archaea commonly present in marine sediments are involved with methanotrophic or methanogenic processes and would show a severe depletion in δ^{13}C (Pancost et al., 2001; Blumenberg et al., 2004). This suggests that the biphytanes analyzed here, acyclic, bicyclic, and tricyclic, are all derived from Thaumarchaeota.

4.2 Uptake of ^{13}C label in archaeal and bacterial lipids.

The results for all labeling experiments, independent of oxygen concentrations, type of carbon supply (POM vs. DOM), location and core depth, show that Thaumarchaeota did not incorporate a detectable amount of the diatom carbon. The $\delta^{13}C$ values for the bicylic and tricyclic biphytanes of the incubated cores were not significantly enriched in ^{13}C with maximum $\Delta\delta^{13}C_{inc-ctr}$ value of only +2 ‰. Similarly, the acyclic biphytane, mainly derived from GDGT-0, produced by Thaumarchaeota, but possibly also by other archaea, showed no substantially enriched values in the incubated cores compared to the control cores. Thus, apparently the Thaumarchaeota did not take up the supplied labeled OM, at least not in detectable amounts and on the time scale of the experiments (4-7 days). These results contrast those obtained for bacteria specific PLFAs. In the NE Pacific sediments, the $\Delta\delta^{13}C_{inc-ctr}$ for $aC_{15:0}$, ranged from+10 to + 140 ‰. Furthermore, ^{13}C-uptake was also noted for benthic foraminifera in these sediments (Enge et al. 2011), of which some were enriched in ^{13}C up to more than 1000 ‰.

In the Arabian Sea, in the same sediment cores, bacterial PLFAs were enriched by + 80 to + 100 ‰ in ^{13}C in the cores from within the OMZ and +8 to +20 ‰ in the cores from outside the OMZ (Pozzato et al., 2013). Furthermore, these authors also reported a substantial enrichment in ^{13}C of +5 to+720 ‰ of several meio- and macrofaunal specimen for the Arabian Sea incubations (Pozzato et al., 2013). This lack of incorporation of ^{13}C into biphytanes is in agreement with the observation that no increase in concentrations of IPL-crenarchaeol, in particular HPH-crenarchaeol, was noted between incubated and control cores, suggesting no increase in thaumarchaeal biomass, consistent with the 16s rDNA results of Moeseneder et al. (2012).

There could be several explanations for the lack of ^{13}C label incorporation into Thaumarchaeota. Most likely, the lack of label incorporation is due to chemoautotrophy being the preferred metabolism of Thaumarchaeota, i.e. the sedimentary Thaumarchaeota are active, but are not incorporating the phytodetrital organic carbon. Further evidence that the benthic community as a whole remained active during the experimental treatments is the clear evidence of tracer processing by all other major benthic compartments (see discussion above). Thaumarchaeota, have, up to now, only been shown to incorporate inorganic carbon (Wuchter et al., 2003; Sinninghe Damsté et al., 2012), and pyruvate (Tourna et al., 2011) and other simple organic compounds (Ouverney and Fuhrman, 2000; Herndl et al., 2005; Takano et al., 2010) and possibly are not adapted to take up the more complex OM. Strikingly, not only the complex, polymeric carbon of the POM, but also the DOM-experiments did not result in labeling, even though the organic carbon in this form is broken down into supposedly easily processed, soluble compounds.

Alternatively, they are capable of mixotrophic growth, but the incorporation of the $\delta^{13}C$ could not be detected due to low labeling of tracer OM. If Thaumarchaeota do use some of the added carbon, but are growing too slowly, they will not incorporate ^{13}C in detectable amounts within the 4-7 days incubation period. If incubation times would have been longer, however, it would not be possible to determine whether the archaea are incorporating the ^{13}C directly from the organic matter, as the label would have been distributed over the different pools of organic and inorganic carbon. If the low amount of labeling is due to low growth rates, then thaumarchaeal growth rates must be very low. Incorporation into lipids would require an incorporation of only ~0.003 atm % ^{13}C for detection (i.e. a $\delta^{13}C$-shift of 3 ‰, which can unambiguously be interpreted as labeling with errors of ± 1 ‰, as common for irm-GC-MS). If repair and exchange, i.e. recycling, of lipids is not considered, and the Thaumarchaeota are in the exponential growth phase, the minimal growth rate needed to detect this incorporation can be calculated (cf. alkenone lipids for eustigmatophyte algae; Popp et al., 2006) based on the isotope dilution theory of Laws (1984) :

$$\mu = -\frac{1}{t} \cdot \mathrm{h}\left(1 - \frac{P*}{A*}\right) \tag{Eq. 1}$$

where μ represents the growth rate, t the incubation time, $P*$ the atom%-excess of the product, in our case the biphytane, and $A*$ the atom%-excess of the substrate added. In our case, the added labeled carbon (53% in the NE Pacific, but only 11-20 % in Arabian Sea incubations) equals A^*, and the product excess P^* would correspond to our minimum incorporation of 0.003 atom% . Since the incubation time t was 7 d for the Arabian Sea cores (less for the NE Pacific incubations, 4 d), the minimum growth rate for detection would then be as low as ~1.42-3.90 . 10^{-5} d^{-1}, corresponding to a generation time of ~48-134 yrs. If a steady state and just replacement of lipids is assumed, the necessary turnover time of the sedimentary lipid pool

t_{to} for detection (causing a 3‰ shift) can be calculated with the incubation time t_{inc} according to a linear model shown in equations 2a,b,c.

$$t_{to} = \frac{A^* \cdot t_{inc}}{P^*} \qquad \text{(Eq. 2a)}$$

$$t_{to} = \frac{conc}{prod.rate} \qquad \text{(Eq. 2b)}$$

$$prod.rate = \frac{conc \cdot P^*}{A^* \cdot t_{inc}} \qquad \text{(Eq. 2c)}$$

The minimum turnover time, i.e. the time needed for replacement of the lipids present in sediments, is thus 70-194 years. Lin et al. (2012) conducted labeling experiments over 340 days but only analyzed the dihexose-GDGTs, which, due to their higher resilience to degradation (Lengger et al., 2012b) are perhaps less suitable for stable isotope probing experiments. They hypothesized even that turnover times of 1700 up to 20500 years were possible. Such a slow metabolism is in agreement with postulations by Valentine (2007) that archaea are particularly adapted to and thriving in low energy conditions, and are thus not stimulated by sudden high organic matter inputs. Their role in benthic carbon processing is thus likely low compared to the more active bacteria, meio- and macrofauna (Moodley et al., 2005).

Finally, it also possible that the undetectable labeling in IPL-crenarchaeol is due to a large contribution of fossil IPL-crenarchaeol present in sediments, and thus the cell numbers are much lower than would be expected from the amount of IPL-GDGTs, but lipid production rates are actually high. Experimental and environmental data (Harvey et al., 1986; Lengger et al., 2012b) and theory (Schouten et al., 2010) have suggested that MH- and DH-crenarchaeol can be preserved better than HPH-crenarchaeol, and it has been shown that even phosphate-containing ether lipids can be preserved over at least 100 days (Logemann et al., 2011). Furthermore, silica column separation has been found to discriminate against the HPH-crenarchaeol (only 20% recovery), leading to an enrichment of MH- and DH-GDGTs in the isotopically measured IPL-fraction (Lengger et al., 2012b). This may substantially lower the sensitivity for label detection. A fossil contribution could also be the reason for the low to non-detectable ^{13}C incorporation into DH-GDGTs reported by Lin et al. (2012). Furthermore, the lack of ^{13}C incorporation into biphytanes in the >400 day long in situ labeling experiments conducted by Takano et al. (2010), may be explained by the fact that they were analyzing core lipid-GDGTs, for which the fossil contribution is expected to be even higher than for IPL-GDGTs.

The high label incorporation into bacterial PLFA observed during both experiments (Arabian Sea: Pozzato et al., 2013; NE Pacific: this study) reflects the comparatively much higher involvement of bacteria in processing of phytodetrital organic matter. Additionally, it may also confirm that bacterial PLFA are better biomarkers for living organisms due to their much higher turnover rates, when compared to archaeal ether lipids as discussed above.

5 Conclusions

Labeling experiments with sediments receiving a pulse of ^{13}C-enriched diatom OM in two different oceanic settings showed that there was no enrichment in ^{13}C in biphytanyl chains stemming from archaeal GDGTs. This was in strong contrast to the bacteria specific fatty acids, and biomass of meio- and macrofauna, which were highly enriched in ^{13}C. Also, no changes of IPL-crenarchaeol concentrations were observed between the experiment and the control cores. Our results suggest that the role of benthic archaea in the direct processing organic matter reaching sediments is minor, and possible uptake of carbon derived from phytodetritus proceeds either slowly or, more likely, not at all. Another reason for not detecting the ^{13}C label in archaeal lipids could be a high fossil contribution to the analyzed intact polar lipid fractions masking any ^{13}C uptake. The much larger stability of intact polar tetraether lipids compared to bacterial ester lipids, could thus make them a less sensitive tool to determine the carbon uptake of active Thaumarchaeota.

Acknowledgements. The authors would like to thank the crew and captain of the R/V Pelagia and the R/V Western Flyer and the participants in the PASOM and PULSE 53 cruise. S.K.L. and L.P. were funded by a grant to S. S. and J.M. from the Darwin Center for Biogeosciences.

CHAPTER 8

LACK OF ^{13}C-LABEL INCORPORATION SUGGESTS LOW TURNOVER RATES OF THAUMARCHAEAL INTACT POLAR TETRAETHER LIPIDS IN SEDIMENTS FROM THE ICELAND SHELF

In preparation for *Biogeosciences*

LACK OF ^{13}C-LABEL INCORPORATION SUGGESTS LOW TURNOVER RATES OF THAUMARCHAEAL INTACT POLAR TETRAETHER LIPIDS IN SEDIMENTS FROM THE ICELAND SHELF

Sabine K. Lengger[a], Yvonne A. Lipsewers[a], Henk de Haas[b], Jaap S. Sinninghe Damsté[a] and Stefan Schouten[a]

[a] *Department of Marine Organic Biogeochemistry, Royal NIOZ Netherlands Institute for Sea Research, P. O. Box 59, 1790 AB Den Burg, Texel, The Netherlands.* [b] *Department of Marine Geology, Royal NIOZ Netherlands Institute for Sea Research, Texel, The Netherlands.*

ABSTRACT

Thaumarchaeota are amongst the most abundant microorganisms in aquatic environments, however, their metabolism in marine sediments is still debated. Labeling studies in marine sediments have previously been undertaken, but focused on complex organic carbon substrates which Thaumarchaeota have not yet been shown to take up. In this study, by supplying different ^{13}C-labeled substrates which have previously been shown to be incorporated into archaeal cells in water incubations and/or enrichment cultures, we investigated the activity of Thaumarchaeota in sediments. For this, we determined the incorporation of ^{13}C-label from bicarbonate, pyruvate, glucose and amino acids, into thaumarchaeal intact polar lipid-glycerol dibiphytanyl glycerol tetraethers (IPL-GDGTs) during 4-6 day incubations of marine sediment cores from three different sites at the Iceland Shelf. Thaumarchaeal intact polar lipids were detected at all stations and concentrations remained constant or decreased slightly, upon incubation. No ^{13}C incorporation in any IPL-GDGT was observed at stations 2 (clay-rich sediment) and 3 (organic-rich sediment). In contrast, a large uptake of ^{13}C label (up to + 80‰) was found in bacterial/eukaryotic IPL-derived fatty acids for station 3. In IPL-GDGTs recovered from the sandy sediments at station 1, however, some (1-4‰) enrichment in δ^{13}C was detected from incubations with bicarbonate and pyruvate. The low incorporation rates suggest a low activity of Thaumarchaeota in marine sediments and/or a low turnover rate of thaumarchaeal IPL-GDGTs due to their low degradation rates. Cell numbers and activity of sedimentary Thaumarchaeota based on IPL-GDGT measurements may thus have previously been overestimated.

1 INTRODUCTION

Thaumarchaea are ubiquitous microorganisms (Hatzenpichler, 2012 and references cited therein) which have recently been discovered to form a kingdom, consisting of one phylum, the Thaumarchaeota (Brochier-Armanet et al., 2008; Spang et al., 2010). They were initially discovered as the Marine Group I Crenarchaeota in the coastal and open ocean (DeLong, 1992; Karner et al., 2001) where they are abundantly present in the epipelagic zone (e.g. Francis et al., 2005; Beman et al., 2008) but also in deep water (Fuhrman and Davis, 1997; Herndl et al., 2005; Agogué et al., 2008) where they can be as abundant as the total bacterial population. Thaumarchaeota have also been detected in marine sediments (Hershberger et al., 1996; Francis et al., 2005).

The metabolism of Thaumarchaeota has long been unclear due to a lack of enrichment cultures. Hoefs et al. (1997) suggested, based on ^{13}C-enrichment of thaumarchaeal lipids compared to algal biomarkers, the possibility of autotrophic assimilation of dissolved inorganic carbon (DIC), using a different pathway than via Rubisco, or, alternatively, the heterotrophic uptake of small organic molecules. Indeed, ^{13}C-labeling studies with bicarbonate showed the incorporation of ^{13}C-labelled DIC into thaumarchaeal membrane lipids and thus their autotrophic metabolism (Wuchter et al., 2003). Unambiguous proof of the growth of Thaumarchaeota on inorganic carbon came with the first enrichment culture of a Thaumarchaeote, *Nitrosopumilus maritimus*, which was growing chemolithoautotrophically on bicarbonate, and gaining energy by the oxidation of ammonia to nitrite (Könneke et al., 2005). It was suggested that 3-hydroxypropionate/4-hydroxybutyrate pathway was used by these microorganisms (Berg et al., 2007), which was supported by genetic analyses of *C. symbiosum* (Hallam et al., 2006b) and *N. maritimus* (Walker et al., 2010). However, in these two species, also genes involved in heterotrophic metabolisms were detected, which implies their potential for mixotrophy. Furthermore, the uptake of pyruvate into cell material in cultures of a Thaumarchaeote enriched from soil, *Nitrososphaera viennensis*, was demonstrated (Tourna et al., 2011).

Indeed, there is some environmental evidence for a mixotrophic metabolism of Thaumarchaeota. Ouverney et al. (2000) as well as Herndl et al. (2005) showed, via MICRO-CARD-FISH using ^{3}H-labeled amino acids, that thaumarchaeal cells present in sea water take up amino acids. There is also circumstantial evidence for mixotrophy of Thaumarchaeota, such as the radiocarbon values of archaeal lipids in

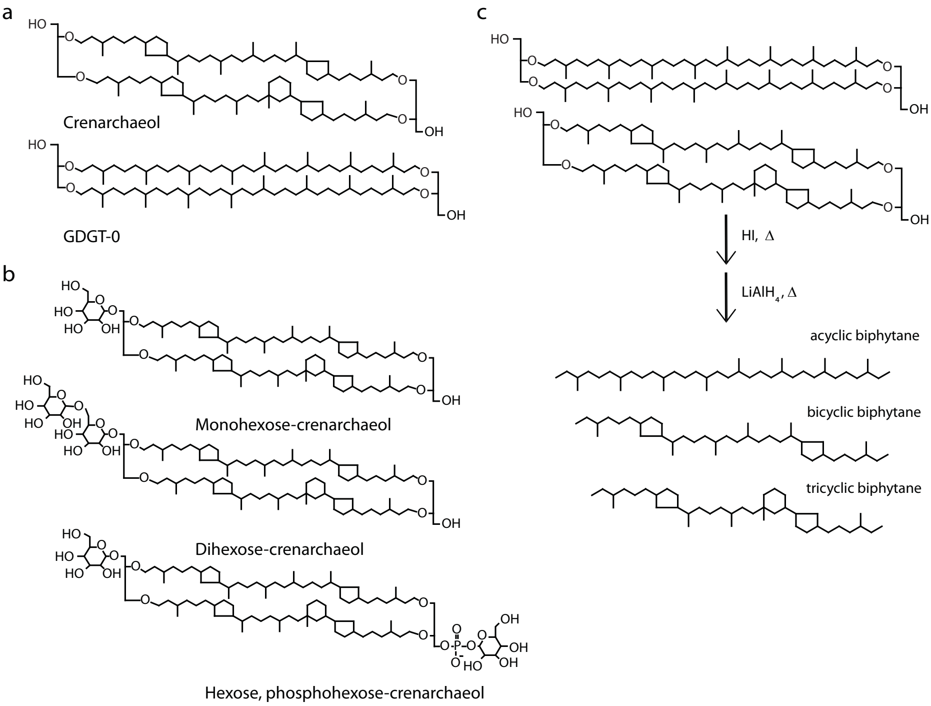
a
Crenarchaeol
GDGT-0
b
Monohexose-crenarchaeol
Dihexose-crenarchaeol
Hexose, phosphohexose-crenarchaeol
c
HI, Δ
LiAlH4, Δ
acyclic biphytane
bicyclic biphytane
tricyclic biphytane

Figure 8.1. Structures of crenarchaeol and GDGT-0 (a), IPL-crenarchaeol species (b) and biphytanyl chains released from crenarchaeol and GDGT-0 by chemical degradation (c).

the deep ocean (Ingalls et al., 2006), thaumarchaeal activity (as quantified by uptake of substrate measured by MAR-FISH) being correlated to the presence of urea (Alonso-Sáez et al., 2012) and the possession of genes for urea transporters (Baker et al., 2012). Mußmann et al. (2011) found thaumarchaeal cell numbers in waste reactors that were too high to be supported by the rates of ammonia oxidation, and a lack of incorporation of ^{13}C-labelled DIC into thaumarchaeal lipids during growth, also suggesting heterotrophy of Thaumarchaeota. Circumstantial evidence, based on the correlation of organic carbon concentration with archaeal biomarker lipids, suggests that Archaea in deep subsurface marine sediments (<1 m) use organic carbon (Biddle et al., 2006; Lipp et al., 2008; Lipp and Hinrichs, 2009), however, this empirical correlation could also be due to preservation factors affecting biomarkers and total organic carbon in a similar way (Hedges et al., 1999; Schouten et al., 2010).

Cell membranes of Thaumarchaeota consist of glycerol dibiphytanyl glycerol tetraether lipids (GDGT) in the form of intact polar lipids (IPL; Schouten et al., 2008; Pitcher et al., 2011c; Sinninghe Damsté et al., 2012; Fig. 8.1 a). They possess GDGTs which are also present in other Archaea (Koga and Nakano, 2008), such as GDGT-0, -1, -2 and -3 (Fig. 8.1b), but also a specific lipid named crenarchaeol (Sinninghe Damsté et al., 2002b). Stable isotope probing (SIP) experiments targeting the biphytanyl chains contained in crenarchaeol (Fig. 8.1c), have been undertaken in order to determine the uptake of different substrates. This revealed the incorporation of ^{13}C from bicarbonate into crenarchaeol (Wuchter et al., 2003). Pitcher et al. (2011a) showed that this uptake was dependent on ammonia oxidation in North Sea water, as addition of inhibitors for ammonia oxidation, nitrapyrine (N-serve) or chlorate, resulted in a decreased incorporation of ^{13}C-labelled DIC. Other SIP experiments carried out with organic substrates were less successful: Lin et al. (2012) achieved only a 2 ‰ enrichment in one of the biphytanyl chains of crenarchaeol, but 2 ‰ depletion in the other biphytanyl chain when adding ^{13}C -labeled phytodetrital organic carbon to sediment slurries. Lengger et al. (2013; chapter 7, this volume) found no incorporation of ^{13}C in crenarchaeol when analyzing sediment from the Arabian Sea and the North East Pacific incubated in situ with ^{13}C-labeled phytodetritus. Takano et al. (2010) also did not find incorporation of ^{13}C in the biphytanyl chains in an incubation experiment with ^{13}C –labeled glucose in sediment from Sagami Bay, Japan, but remarkably did find labeling of the glycerol moieties of the GDGT molecules. Thus, not much evidence for substantial incorporation of carbon from organic substrates into thaumarchaeal lipids is observed in SIP experiments performed with sediments. It is possible that the types of substrate used in these studies were not suitable, i.e. not readily taken up by the Thaumarchaeota, and that other organic compounds would result in higher incorporation. Interestingly, none of the previously conducted labeling studies in sediments used ^{13}C-labelled DIC. Bicarbonate had previously unambiguously been shown to be incorporated by pelagic Thaumarchaeota (Wuchter et al., 2003) and by Thaumarchaoeta enriched from sediments (Park et al., 2010) and soils (Jung et al., 2011; Kim et al., 2012a).

To shed further light on the metabolism of sedimentary Thaumarchaeota, we performed labeling experiments using ^{13}C-labeled substrates, i.e. bicarbonate, pyruvate, amino acids and glucose in sediment cores from the Iceland shelf. The results are discussed with respect to the uptake of substrates as well as the turnover rates of thaumarchaeal GDGTs.

2 MATERIALS AND METHODS

2.1 Sampling stations

Sediment cores were sampled at three stations, located on the Iceland Shelf, during the 'Long Chain Diols' cruise on the R/V Pelagia in July 2011 (Fig. 8.2). Station 1 (63°21'N 16°38'W), South of Iceland, was at 240 m water depth and consisted of dark, sandy sediment. Station 2 (66°18'N 13°58'W) is located North-East of Iceland, at 261 m water depth, and the sediment was sandy-clayish. Sediment at Station 3 (67°13'N 19°07'W), North of Iceland, at 503 m water depth, and further offshore than the other two stations, consisted of dark, soft, black mud. From each station, multicores were retrieved in polycarbonate core tubes. Ten cores from each station were retrieved in tubes of 10 cm diameter with drilled holes downwards, spaced 1 cm apart, and used for incubation. Cores sampled with tubes of 5 cm diameter were used for oxygen microprofiling, pore-water extraction, and four cores from each station were sliced and stored for density and total organic carbon (TOC) analysis.

2.2 Core characterization

For each station, control cores were sliced into 1 cm thick layers from 0 – 10 cm core depth. The water content of each sediment was determined by weighing prior to and after freeze-drying. Total organic carbon was determined from freeze-dried sediments following overnight acidification with 2N HCl, subsequent washes with bidistilled H_2O and water removal by freeze-drying. The decalcified sediments were measured on a Flash EA 1112 Series (Thermo Scientific, Waltham, MA) analyzer coupled via a Conflo II interface to a Finnigan Delta^{plus} mass spectrometer. Standard deviations from three measurements ranged from 0.0 to 0.6 % TOC.

Two cores (5 cm diameter) from each cast were used for oxygen microprofiling with an OX-100 Unisense oxygen microelectrode (Unisense, Aarhus, DK; Revsbech, 1989). A two-point calibration was carried out with bottom water from the same station bubbled with air at 4°C for at least 5 min (100% saturation) and a solution of 0.1 M sodium ascorbate in 0.1 N NaOH in Milli-Q Water (0% saturation) and the electric current measured in pA was converted to $mg \cdot l^{-1}$ O_2. The sensor was moved with a micromanipulator one mm at a time.

Pore water was extracted on board from slices of several cores by centrifugation. Five mL from each depth was preserved air-free with added $HgCl_2$ for analysis of the $\delta^{13}C$

of the dissolved inorganic carbon (DIC) at 4°C, and 3 mL were preserved at -20°C for analysis of phosphate, ammonia, nitrite and nitrate.

Dissolved inorganic phosphate, ammonia, nitrite and nitrate were measured on a Traacs 800 Autoanalyzer (Seal Analytical, Fareham, UK). Ortho-phosphate was measured using potassium antimonyltartrate as a catalyst and ascorbic acid as a reducing reagent which resulted in formation of a blue (880 nm) molybdenum phosphate-complex at pH 0.9-1.1 (Murphy and Riley, 1962). Ammonia was measured via formation of the indo-phenol blue-complex (630 nm) with phenol and sodium hypochlorite at pH 10.5 in citrate (Helder and de Vries, 1979). Dissolved inorganic nitrite concentrations were measured after diazotation of nitrite with sulphanilamide and N-(1-naphtyl)-ethylene diammonium dichloride to form a reddish-purple dye measured at 540 nm. Nitrate was first reduced in a copperized Cd-coil using imidazole as a buffer, measured as nitrite and concentrations were calculated by subtraction of nitrite (Grasshoff et al., 1983).

$\delta^{13}C$ of DIC was measured in pore water from all stations, and bottom water samples from the experiments, on a Thermo GasBench II coupled to a Thermo Delta Plus and is reported in the delta notation against theVienna Pee-Dee Belemnite (V-PDB) standard. To this end, 0.5 mL of each sample was? injected into gastight exetainers, containing 0.1 mL of 80% H_3PO_4, that had been flushed for 15 min each with He. Performance was monitored by analysis of an in-house laboratory standard of Na_2CO_3 with a $\delta^{13}C$ of -0.57 ‰ after every 12 measurements and an in-house laboratory standard of $CaCO_3$, with a $\delta^{13}C$ value of -24.2 ‰ at the start and the end of every series. Measured values of these standards were usually not deviating by more than 0.5 ‰ from the calibrated (on NBS-19) values.

2.3 Incubation conditions

Ten cores from each station were used for incubations (Table 8.2). For this, splitable polycarbonate core tubes with 10 cm diameter were prepared by drilling two rows of 1 mm holes spaced at distances of 1 cm. The two rows were 90° contorted; holes were filled with silicon and covered with plastic non-permeable tape (see setup in Fig. 8.3). The cores were, after recovery from the multicorer, transferred as quickly as possible to a temperature-controlled room kept at 4°C, and the bottom water was sampled with a sterile pipette for determination of pH, $\delta^{13}C$ of DIC and nutrients as described above. Four whole cores at each station were incubated with ^{13}C-labelled

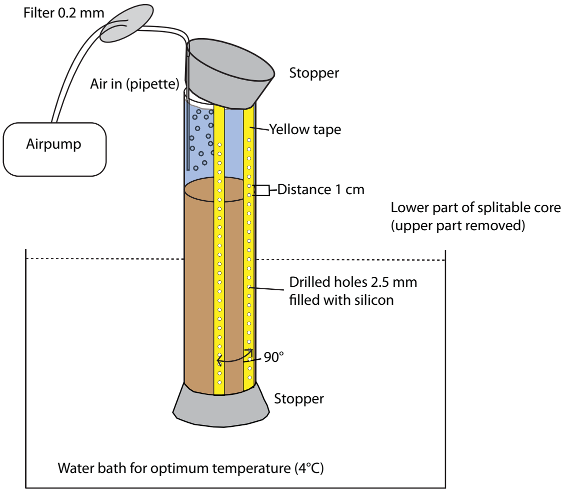
Filter 0.2 mm
Air in (pipette)
Airpump
Stopper
Yellow tape
Distance 1 cm
Lower part of splitable core (upper part removed)
Drilled holes 2.5 mm filled with silicon
90°
Stopper
Water bath for optimum temperature (4°C)

Figure 8.3. Scheme of the incubation set-up of the cores.

substrates, i.e. bicarbonate, pyruvate, amino acids and glucose, and one whole core ('background') was injected with MilliQ water only. Four more cores were incubated with solutions containing one of the substrates and a nitrification inhibitor, and one ('background + inhibitor') with MilliQ water and the nitrification inhibitor. The incubation solutions were injected into the seven injection ports from the surface downwards, i.e. the first 8 cm were supplied with the labeled substrate. Injection solutions contained 99% ^{13}C-labelled substrates as supplied by Cambridge Isotope Laboratories (Andover, MA, USA). The substrates were dissolved in MilliQ-H_2O in concentrations of 3.7 mg · mL^{-1} for $NaHCO_3^-$ (Bic), 1.01 mg · mL^{-1} for Glucose (Glu), 0.89 mg · mL^{-1} for a mix of 16 algal amino acids (AA; 98% labeled) and 1.24 mg · mL^{-1} of sodium pyruvate (Pyr). 200 µL were delivered to each slice by injection through the two 90° contorted injection ports, which corresponded to a total addition of 1.6 g ^{13}C · m^{-3} sediment for the bicarbonate, and 1.2 g ^{13}C · m^{-3} for the organic compounds. The nitrification inhibitor was Nitrapyrine (N-Serve, Pestanal) at 11.5 µg · mL^{-1}, which is known to inhibit archaeal ammonia oxidation (Park et al., 2010; Pitcher et al., 2011a). As Nitrapyrine cannot be dissolved in pure water, 5% of EtOH was added and the solutions were kept at 30°C to prevent precipitation of the Nitrapyrine. Nitrapyrine-free incubation solutions were kept at the same conditions.

After injection, the cores were stored in the dark at 4°C in a water bath - boxes with core holders filled with water for 62 h (38 h for Station 3), after which the bottom water was sampled for ^{13}DIC and N- and P-nutrients as described above and re-injected with a fresh solution of the substrates in water, with or without nitrapyrine added. During the incubation time, the cores were covered lightly with a rubber stopper, so that the escape of air was possible, and aerated through a sterile plastic pipette, with air pumped by an aquarium pump and filtered through a 0.2 µm filter for sterilization purposes. After 144 h (96 h for Station 3), bottom water samples for ^{13}DIC (dissolved inorganic carbon) and N- and P-nutrients were taken again, and oxygen microprofiles were measured as described above on all cores (except for Station 2, where cores were too short and thus surfaces too low in the core tubes, to allow measurements in more than three cores). Subsequently, the upper 10 cm of the sediment were sliced in 1 cm resolution and each slice mixed thoroughly, split in half and both parts were frozen at -80°C immediately. The incubations at station 3 were shorter due to time constraints.

2.4 Lipid extraction, separation and measurements

The freeze-dried sediments of 0-1 cm, 1-2 cm and 7-8 cm depth intervals of the incubation and background cores were ground and extracted by a modified Bligh-Dyer extraction method (Pitcher et al., 2009b). Briefly, they were extracted ultrasonically three times in a mixture of methanol/dichloromethane (DCM)/phosphate buffer (2:1:0.8, v:v:v), centrifuged and the solvent phases were combined. The solvent ratio was then adjusted to 1:1:0.9, v:v:v, which caused the DCM to separate. Liquid extraction was repeated two more times, the DCM fractions were combined, the solvent was evaporated and bigger particles were removed over cotton wool. An aliquot of the extracts was stored for high performance liquid chromatography /electron spray ionization tandem mass spectrometry (HPLC/ESI-MS^2) analysis, and another aliquot was separated into core lipid (CL)- and intact polar lipid (IPL)-GDGTs by silica column separation with hexane/ethyl acetate (1:2, v:v) for the CL-fraction and MeOH to elute the IPL-fraction. 0.1 mg C_{46} internal standard (Huguet et al., 2006c) were added to the CL-fractions. The IPL-fraction was split in three aliquots: 5% were used to determine the carry-over of CL-GDGTs into the IPL-fraction and measured directly via HPLC-APCI-MS, 60 % were kept for ether cleavage in order to determine the ^{13}C incorporation into the biphytanes (see below), and 35 % were subjected to acid hydrolysis under reflux for 2 h with 5% HCl in MeOH, followed by addition of water and extraction (3×) of the aqueous phase at an adjusted pH of 4-5 with DCM. This yielded the IPL-derived GDGTs which were measured via HPLC/APCI-MS. The C_{46} internal standard was used to quantify the IPL-derived

GDGTs and the carry over, but was added after the aliquot for ^{13}C analysis was taken in order to prevent any possible interference of alkyl chains released from the internal standard molecule.

2.5 $\delta^{13}C$ analysis of biphytanes

Aliquots (60%) of the IPL-fractions were subjected to chemical treatment in order to cleave GDGTs, releasing the biphytanyl chains (Fig. 8.1c) according to Schouten et al. (1998). For this, the IPL fraction was refluxed in 57% HI for 1 h to break the ether bonds and produce alkyliodides and subsequently extracted three times with hexane. The hexane phase was washed with 5% NaS_2O_7 and twice with water. The alkyliodides were cleaned over Al_2O_3 with hexane/DCM (9:1, v:v), hydrogenated with H_2/PtO_2 in hexane for 1 h (Kaneko et al., 2011) and eluted over Na_2O_3 with DCM. As the H_2/PtO_2 hydrogenation-procedure has never been tested for stable carbon isotope analysis, we used four CL-fractions of extracts from Station 1 and Station 2, split them in half and hydrogenated one half with the conventional $LiAlH_4$ reduction method described by Schouten et al. (1998), the other half with the method described here and by Kaneko et al. (2011). The conventional method consisted of $LiAlH_4$ in 1,4-dioxane for 1 h under reflux, then the remaining $LiAlH_4$ was reacted with ethyl acetate, bidistilled H_2O was added and the biphytanes were extracted with DCM from the dioxane/H_2O mixture. Additional purification was done by elution over an Al_2O_3 column using hexane. The results showed that the $\delta^{13}C$ values of the biphytanes were not significantly different when H_2/PtO_2 treatment and $LiAlH_4$ hydrogenation were compared (Table 8.1). However, when amounts were compared, it was obvious that hydrogenation with H_2/PtO_2 resulted in higher yields. This is probably due to the fact that the H_2/PtO_2 treatment requires fewer workup procedures after hydrogenation (only one drying step) than the $LiAlH_4$ treatment, which requires two column separations in addition to a drying step.

2.6 $\delta^{13}C$ of phospholipid-derived fatty acids

In order to demonstrate that the incubation experiments did result in label uptake by the sedimentary microbial community, we determined the uptake of ^{13}C-label by bacteria and eukaryotes by isotopic analysis of polar lipid-derived fatty acids (PLFA). For this, one third of the extract of the 0-1 cm sediment slice from Station 3, from the cores incubated with bicarbonate, glucose, amino acids and the background core (all without nitrapyrine), were used and analyzed for PLFA according to Guckert et al. (1985). Briefly, the aliquots were separated over a silica column with DCM, acetone and methanol, respectively, with the methanol-fraction containing the PLFA. PLFA fractions were saponified in methanolic KOH (2 N) and, after adjusting to pH 5, the resulting fatty acids were extracted with DCM and methylated with BF_3-MeOH (with a $\delta^{13}C$ of -25.4 ± 0.2 ‰V-PDB) before measurements by gas chromatography – isotope ratio mass spectrometry (GC-irMS). The $\delta^{13}C$ values for the fatty acids were corrected for the added carbon.

2.7 HPLC-APCI-MS and HPLC-ESI-MS^2

The CL-fractions, hydrolyzed IPL- fractions and the IPL-fractions themselves (to determine the carry-over of CL into the IPL fraction) were analyzed by HPLC-APCI-MS as described previously (Schouten et al., 2007). HPLC/ESI-MS^2 in selected reaction monitoring (SRM) mode, as described by Pitcher et al. (2011b), was used to analyze selected IPL-GDGTs. IPL-GDGTs monitored were monohexose (MH)-crenarchaeol, dihexose (DH)-crenarchaeol and hexose, phosphohexose (HPH)-crenarchaeol. Performance was monitored using a lipid extract of sediment known to contain the monitored GDGTs that was injected every 8 runs. Response areas per mL sediment (mL sed) are reported, as absolute quantification was not possible due to a lack of standards. The values reported are the averages of duplicate injections and their standard deviations.

2.8 GC-MS and GC-irMS

GC-MS was used to identify the biphytanes and phospholipid-derived fatty acid methyl esters (FAME) using a TRACE GC with a DSQ-MS. The gas chromatograph was equipped with a fused silica capillary column (25 m, 0.32 mm internal diameter) coated with CP Sil-5 (film thickness 0.12 µm). The carrier gas was helium. The compound specific isotope composition of the biphytanes and fatty acids was measured with an Agilent 6800 GC, using the same GC column conditions, coupled to a ThermoFisher Delta V isotope ratio monitoring mass spectrometer. The isotopic values were calculated by integrating the mass 44, 45 and 46 ion currents of the peaks and that of CO_2-spikes produced by admitting CO_2 with a known ^{13}C-content into the mass spectrometer at regular intervals. The performance of the instrument was checked by daily injections of a standard mixture of a C_{20} and a C_{24} perdeuterated n-alkane. Two replicate analyses (one in the case of the fatty acids) were carried out and the results were averaged in order to obtain the average and standard deviations.

Table 8.1. $\delta^{13}C$ values of the acyclic, bicyclic, and tricyclic biphytanes obtained via H_2/PtO_2 and $LiAlH_4$ reduction of alkyliodides formed via HI ether cleavage.

	$\delta^{13}C$ (‰)					
	acyclic		bicyclic		tricyclic	
Sample	H_2/PtO_2	$LiAlH_4$	H_2/PtO_2	$LiAlH_4$	H_2/PtO_2	$LiAlH_4$
Station 1 0-1 cm	-20.3 ± 0.4	-20.2 ± 0.0	-19.7 ± 0.7	-20.0 ± 0.6	-19.5 ± 1.1	-21.2 ± 0.8
Station 1 1-2 cm	-19.9 ± 0.6	-22.0 ± 0.2	-18.4 ± 0.2	-20.2 ± 1.6	-19.0 ± 0.2	-19.8 ± 0.6
Station 2 0-1 cm	-22.7 ± 0.7	-22.0 ± 0.4	-24.2 ± 1.0	-22.4 ± 0.3	-22.6 ± 1.6	-22.0 ± 0.4
Station 2 1-2 cm	-24.0 ± 1.0	-25.6 ± 0.2	-22.3 ± 1.4	-25.6 ± 0.8	-22.6 ± 0.2	-25.0 ± 0.6

	Total amount / µg					
	acyclic		bicyclic		tricyclic	
Sample	H_2/PtO_2	$LiAlH_4$	H_2/PtO_2	$LiAlH_4$	H_2/PtO_2	$LiAlH_4$
Station 1 0-1 cm	0.79	0.28	0.27	0.16	0.31	0.18
Station 1 1-2 cm	0.42	0.16	0.14	0.07	0.15	0.08
Station 2 0-1 cm	0.45	0.34	0.17	0.16	0.23	0.23
Station 2 1-2 cm	0.13	0.05	0.04	0.0	0.06	0.0

The stable carbon isotope compositions are reported in the delta notation against the V-PDB standard. Some values of the biphytanes could not be determined due to low concentrations, mainly in the background cores at station 2. For calculations of incorporation thus, the background values from station 1 were used.

3 RESULTS

3.1 Sediment characteristics

The sediments at stations 1-3 consisted of sand, sandy clay, and dark and soft mud, respectively. Oxygen penetration depth was on average 17 mm at station 1, while oxygen penetrated slightly less deep at station 2 (13 mm on average) and station 3 (15.5 mm on average; Fig. 8.4). At station 1, organic carbon contents were low with

0.6 % at 0-1 cm depth and 0.3 % at 1-2 cm and 6-7 cm depth. Organic carbon contents were higher at station 2 and amounted to 1.4-1.7% and were highest at station 3 (2.0-2.5%). The pH of the bottom water hardly differed between stations and was typically marine, i.e. 8.2 at station 1, 8.0 at station 2, and 7.9 at station 3.

Pore water concentrations of nutrients, as shown in Fig. 8.4, showed similar trends with depth at the three stations. Inorganic phosphate concentrations were 1 µmol · l^{-1} in the bottom water and generally increased with depth up to 7-14 µmol · l^{-1} Ammonia concentrations increased as well with sediment depth, from 0.19 to 1.3 µmol · l^{-1} in bottom water to 44-70 µmol · l^{-1} at depth. Nitrite concentrations were an order of magnitude higher in the pore water (0.32-0.62 µmol · l^{-1}) than in the bottom water (0.055 µmol · l^{-1}), and increased with sediment depth. Nitrate concentrations were high in the bottom water, 14 µmol · l^{-1}, and generally decreased quickly with depth in the sediment to values between 0.6 and 3 µmol · l^{-1} . The $\delta^{13}C$ of the DIC showed also similar profiles at the three stations. It decreased from 1 ‰ in the bottom water to -3 ‰ in the pore water. At station 2, $\delta^{13}C$ of the DIC could only be measured in the bottom water and the four uppermost pore water samples, but, in these samples, showed the same decrease with depth as observed at Station 1, from -1.3 ‰ to -2.9 ‰.

3.2 GDGT-abundance

GDGT-concentrations averaged over all cores from the incubations (10 per station) are shown with standard deviation in order to give an impression of the range of concentrations found (Fig. 8.5). GDGT-0 and crenarchaeol were present as a core lipid in concentrations of 0.4 to 0.8 µg · mL sed^{1}, and 0.08 to 0.12 µg · mL sed^{1} for the minor isoprenoid GDGTs (i-GDGTs; GDGT-1, -2 and -3). Concentrations were similar at all stations and did not show substantial changes with sediment depth. IPL-derived GDGTs were present in lower concentrations and amounted to 0.09 to 0.3 (GDGT-0), 0.07 to 0.18 (crenarchaeol) µg · mL sed^{-1}. Concentrations were generally lower at station 1 compared to stations 2 and 3.

Direct analysis of individual IPL-crenarchaeol showed that the head groups mainly consisted of monohexose (MH)- and hexose, phosphohexose (HPH)- headgroups, with only a small contribution of dihexose (DH)- head groups (Fig. 8.5c). The proportion of HPH- to the total peak area of IPL-crenarchaeol was ca. 80 - 90% in the surface sediments (0-1 and 1-2 cm) of all stations. At station 1 and 2, this decreased

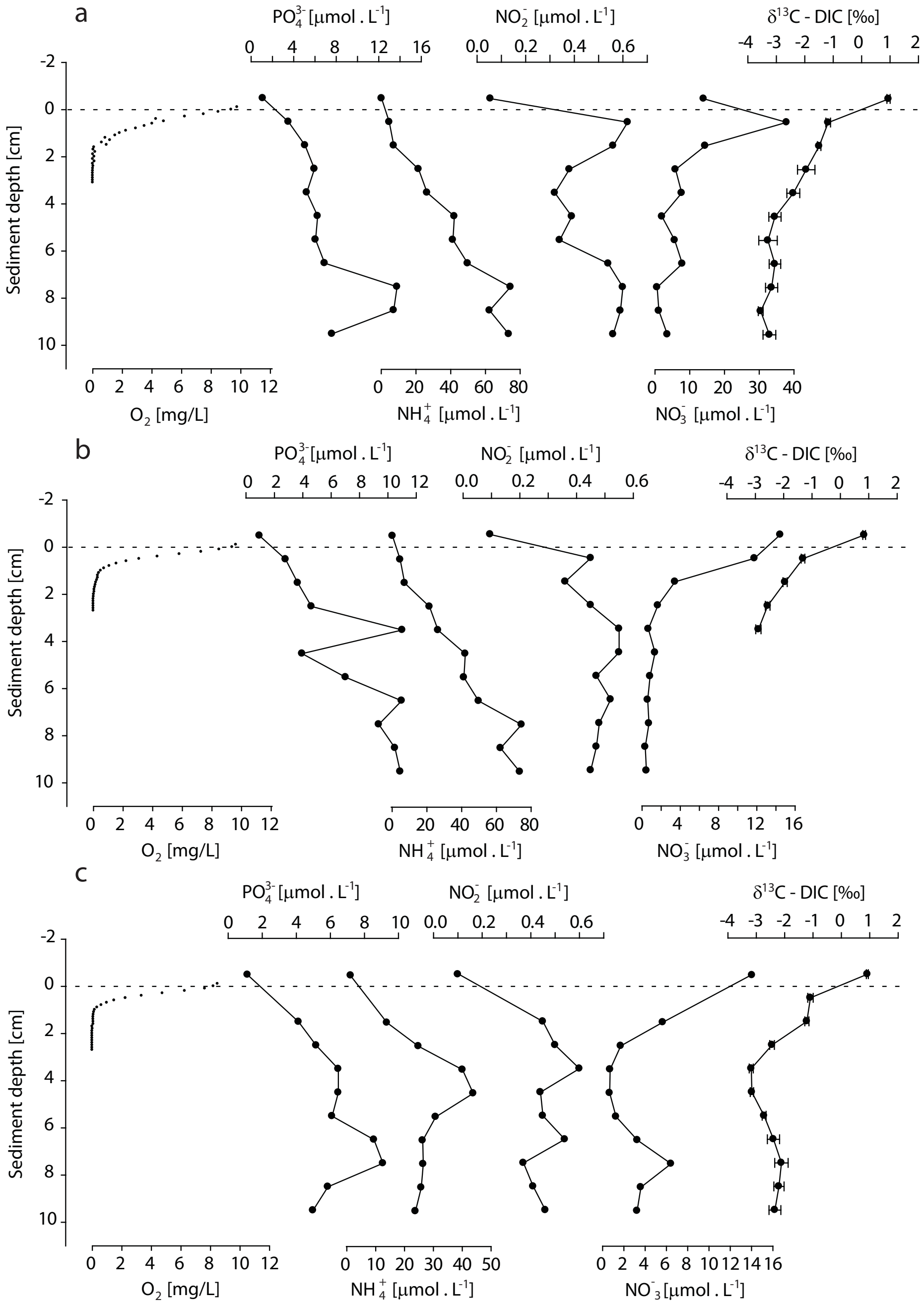

Figure 8.4. Oxygen microprofiles and pore water results vs. depth at station 1 (a), 2 (b) and 3 (c).

to 10 – 25 % in the deepest sediment slice analyzed, 6-7 cm. At station 3, HPH-crenarchaeol dominated at all sediment depths (Fig. 8.4).

3.3 Incubation experiments

Incubations experiments were started directly after core recovery and initial sampling by injection of solutions, which contained ^{13}C-bicarbonate, pyruvate, glucose , amino acids or just water (incubated for comparison and further called the “background core”) over the first 7 cm of the cores. The cores were incubated at *in situ* temperatures (4°C) for 6 days (4 days for station 3) and subsequently sliced and stored for analysis of ^{13}C-enrichment in lipids. Oxygen penetration depths were measured and bottom water was sampled at the start of the experiment, after 48 hours (36 for Station 3) and at the end of the incubations. At all stations, nutrient concentrations of the bottom water did not change over the 6 days (5 days for station 3) of incubation, except for nitrate, which generally showed a decrease (Table 8.2). The bottom water pH remained mostly constant, except at station 1, where it changed during from 8.2 to 8.0 in all incubations, similar to the other sediment cores and perhaps indicating that the initial value of 8.2 might have been due to an error in the measurement. The δ^{13}C of the DIC in the bottom water substantially increased in the cores where ^{13}C-labeled compounds and bicarbonate was added, but not in the background cores (Table 8.2). In cores from station 2, oxygen penetration depths decreased to 6-9 mm in all incubation experiments except for the core incubated with pyruvate and inhibitor, as well as in cores from station 3, where a decrease in oxygen penetration depth to 8-10 mm was observed (Table 8.2). In all cores from the three stations, no major differences in IPL-crenarchaeol concentrations upon incubation could be detected (Fig. 8.6-8).

The δ^{13}C-values of the biphytanes released from the IPL-GDGTs of the background cores were ranging from -17 to -24 ‰ at all stations (Table 8.3), which is within the natural variation observed for biphytanes sourced by Thaumarchaeota in marine sediments (Hoefs et al., 1997; Könneke et al., 2012; Schouten et al., 2013). No substantial ^{13}C enrichment of biphytanes was observed in nearly all of the incubation experiments (Fig. 8.9). The only exception was the tricyclic biphytane in some of the incubations at station 1 (with ^{13}C-labelled substrates bicarbonate, bicarbonate and inhibitor, and pyruvate and inhibitor at nearly all depths) and one incubation (with pyruvate and inhibitor at 6-7 cm depth) at station 2 with enrichments ranging from 2 to 4 ‰. However, due to the large standard deviations in the δ^{13}C values of the BG

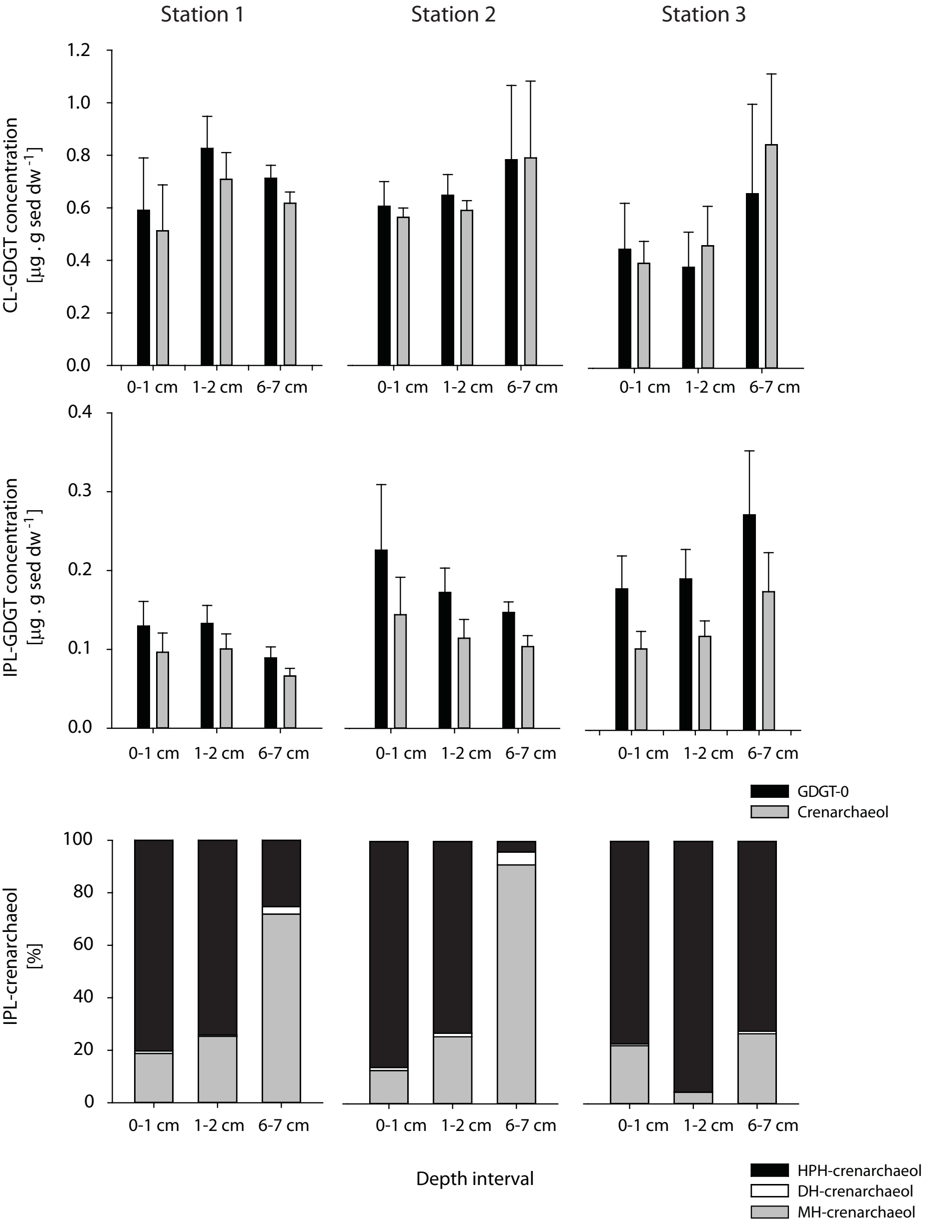

Figure 8.5. GDGT-0 and crenarchaeol concentrations (averages), for CL-GDGTs (a) and IPL-derived GDGTs (b) at all three stations and core depths. Proportions of head groups of IPL-crenarchaeol at all three stations (c)..

Table 8.2. The bottom water NO_3^- concentrations and δ^{13}DIC changes over the incubation time ($\Delta_{t\text{-}t0}$), as well as oxygen penetration depths measured after the incubations. In brackets, the average values of oxygen penetration depth for the cores before incubation. BG … background, Bic … bicarbonate, Pyr … pyruvate, +Inh … nitrification inhibitor nitrapyrine added.

Station	Incubation	NO_3^- [µmol · l^{-1}]			$\Delta\delta^{13}DIC_{t\text{-}t0}$ [‰]		O_2 pen. depth [mm]
		t=0h	t=62 h	t=144h	t=62 h	t=144h	t=144h
							(before: 17)
1	BG	17.9	19.1	4.1	0.6	2.8	11
	Bic	15.9	16.2	8.2	66.5	156.2	16
	Pyr	18.1	19.2	5.9	109.1	457.0	16
	BG+Inh	15.5	16.3	13.9	-0.5	2.6	20
	Bic+Inh	11.5	12.0	3.8	135.3	275.5	20
	Pyr+Inh	25.4	25.6	14.3	72.7	671.1	16
							(before: 13)
2	BG	12.14	11.37	0.09	-0.5	2.9	9
	Bic	5.55	4.05	0.07	336.5	606.0	6
	Pyr	13.77	12.48	0.12	366.6	1570.7	6
	BG+Inh	10.72	10.45	0.19	0.1	3.5	5
	Bic+Inh	7.22	6.79	0.09	255.4	570.1	6
	Pyr+Inh	5.01	3.17	0.06	511.3	1136.4	16
							(before: 16)
3	BG	13.84	0.00	0.13	1.5	-2.3	n.d.*
	Bic	13.83	12.60	0.08	558.2	814.3	n.d.*
	Pyr	6.45	4.23	0.12	1108.9	1496.3	n.d.*
	Glu	14.14	12.03	0.11	90.4	194.2	n.d.*
	AA	15.34	13.55	0.15	82.7	201.9	n.d.*
	BG+Inh	16.06	13.39	0.11	0.3	4.9	8
	Bic+Inh	15.23	14.05	0.18	244.8	520.3	n.d.*
	Pyr+Inh	8.92	6.68	0.10	682.7	1644.5	8
	Glu+Inh	5.86	4.77	0.03	110.8	301.2	10
	AA+Inh	14.36	13.41	0.09	62.2	368.2	n.d.*

* n.d. - could not be determined

cores, only the enrichment of 2-5 ‰ in the 1-2 cm slices of station 1 is statistically significant at a 95% confidence level (t(2)= 6.6 – 9.0, P=0.05).

To determine whether the added ^{13}C-labelled substrate was incorporated into sedimentary microbial biomass at all, phospholipid-derived fatty acids, stemming from bacteria or eukaryotes, were analyzed from the surface sediments of the bicarbonate, amino acids and glucose incubation experiments. δ^{13}C values of the most common fatty acids, $C_{16:0}$ and $C_{18:0}$ were enriched in ^{13}C by up to 80 ‰ in the amino acid and glucose incubation experiments compared to the background (Table 8.4). The cores incubated with ^{13}C-labeled bicarbonate showed no ^{13}C-enriched fatty acids.

4 DISCUSSION

4.1 Biomarkers indicative for live sedimentary Thaumarchaeota

The only biomarker lipids up to now which are probably indicative for live Thaumarchaeota are crenarchaeol IPLs (Pitcher et al., 2011b). Of these, the ones with a glycosidic head group likely contain a substantial fossil component, while the hexose, phosphohexose (HPH)-crenarchaeol is more labile and its concentration corresponds well to DNA-based thaumarchaeal abundance (Pitcher 2011a and 2011b; Schouten et al., 2012; Lengger et al., 2012b). The presence and dominance of HPH-crenarchaeol in the sediments strongly suggests that live Thaumarchaeota were present in sediments at all the stations (Fig. 8.5). This was expected for the surface sediment, as oxygen and ammonium were present (Martens-Habbena et al., 2009; Erguder et al., 2009; Hatzenpichler, 2012). The ammonium concentration profiles, with concentrations decreasing upwards, agree with aerobic ammonia oxidation proceeding in the oxygenated parts, using the ammonium diffusing from below. However, HPH-crenarchaeol was present down to 7 cm depth, below the oxygen penetration depth, which could indicate that either live Thaumarchaeota were present at depth, using a metabolic process different from aerobic ammonia oxidation, or that this HPH-crenarchaeol is not stemming from live Thaumarchaeota at depth and was partly preserved. In any case, it is not yet known what exactly the preferred environment for Thaumarchaeota is, as they have been found to be active in low and high ammonia and low and high oxygen environments (Martens-Habbena et al., 2009; Erguder et al., 2009; Hatzenpichler, 2012).

Table 8.3. Background (BG) values of $\delta^{13}C$ of the biphytanes measured in the sediment, i.e. $\delta^{13}C$ of the biphytanes that were incubated just with water, but under the same conditions. These values were used for determination of the $\Delta\delta^{13}C$: BG values were subtracted from the $\delta^{13}C$ of the corresponding value measured from the cores incubated with label (Fig. 8.9). Numbers indicate the depth interval the sample was coming from, + : nitrification inhibitor nitrapyrine added for incubation, - : no inhibitor added. Values at station 2 could not be determined due to low concentrations.

			Station 1			**Station 2**			**Station 3**	
			$\delta^{13}C$			**$\delta^{13}C$**			**$\delta^{13}C$**	
			[‰]			**[‰]**			**[‰]**	
Inh.	**Sed. depth [cm]**	**acyclic BP**	**bicyclic BP**	**tricyclic BP**	**acyclic BP**	**bicyclic BP**	**tricyclic BP**	**acyclic BP**	**bicyclic BP**	**tricyclic BP**
-	**0-1**	-22.0 ± 0.1	-20.5 ± 1.1	-19.9 ± 0.3	n.d.[*]	n.d.[*]	n.d.[*]	-20.4 ± 0.2	-20.2 ± 1.2	-19.8 ± 0.8
	1-2	-21.4 ± 0.5	-20.7 ± 0.1	-20.2 ± 0.0	n.d.[*]	n.d.[*]	n.d.[*]	-19.6 ± 1.2	-18.3 ± 1.4	-17.7 ± 1.9
	6-7	-21.4 ± 0.2	-22.4 ± 1.9	-21.5 ± 2.3	n.d.[*]	n.d.[*]	n.d.[*]	-20.6 ± 0.4	-20.1 ± 0.4	-19.2 ± 0.6
+	**0-1**	n.d.[*]	n.d.[*]	n.d.[*]	n.d.[*]	n.d.[*]	n.d.[*]	-19.3 ± 0.6	-19.7 ± 0.6	-19.4 ± 0.3
	1-2	-22.0 ± 0	-21.2 ± 0.4	-21.3 ± 0	-22.9 ± 0.9	-21.4 ± 1.4	-20.3 ± 0.9	-19.4 ± 0.1	-19.9 ± 0.4	-19.2 ± 0.2
	6-7	-22.4 ± 0	-20.0 ± 0.6	-22.2 ± 0	-22.0 ± 0.0	-21.0 ± 0.4	-20.0 ± 0.4	-22.4 ± 0.0	-21.4 ± 0.4	-20.7 ± 0.1

[*] n.d. – could not be determined.

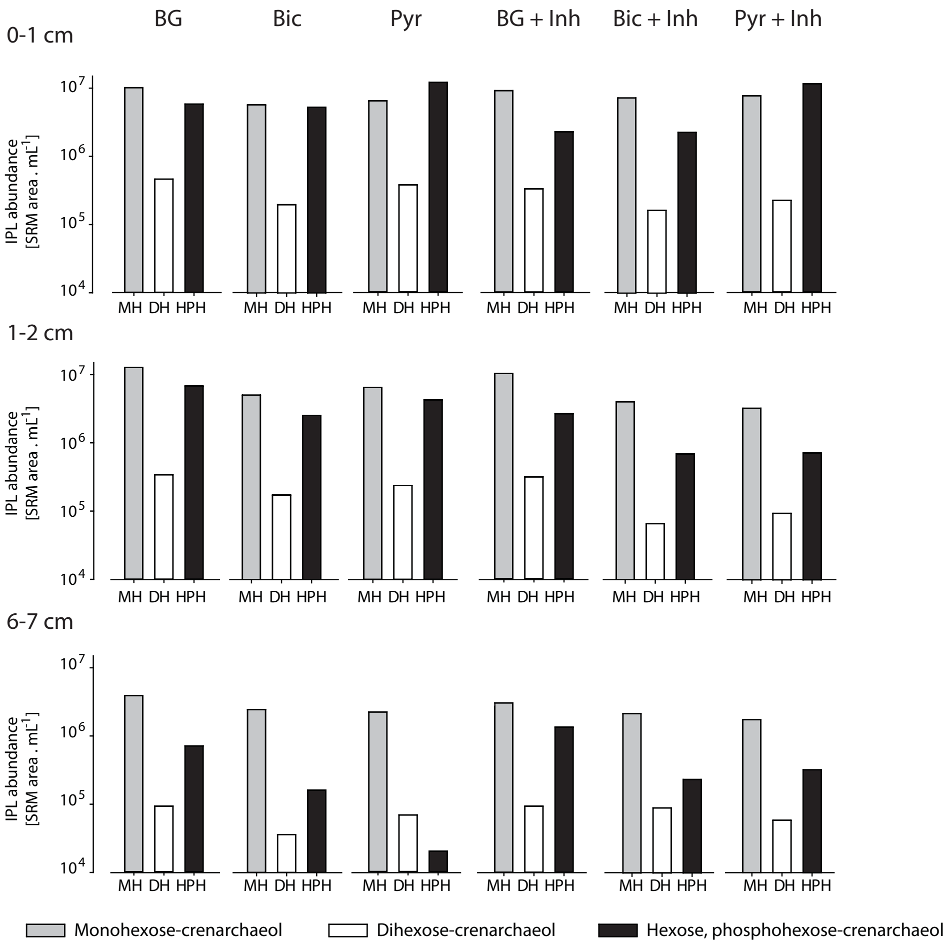

Figure 8.6. IPL-crenarchaeol profiles of the incubated cores for Station 1 - background (BG), bicarbonate (Bic) and pyruvate (Pyr) without (left plot) and with nitrification inhibitor (right plot). Top graphs shows the values from 0-1 cm depth, graphs in the middle the profiles from 1-2 cm depth and at the bottom the profiles from 6-7 cm depth.

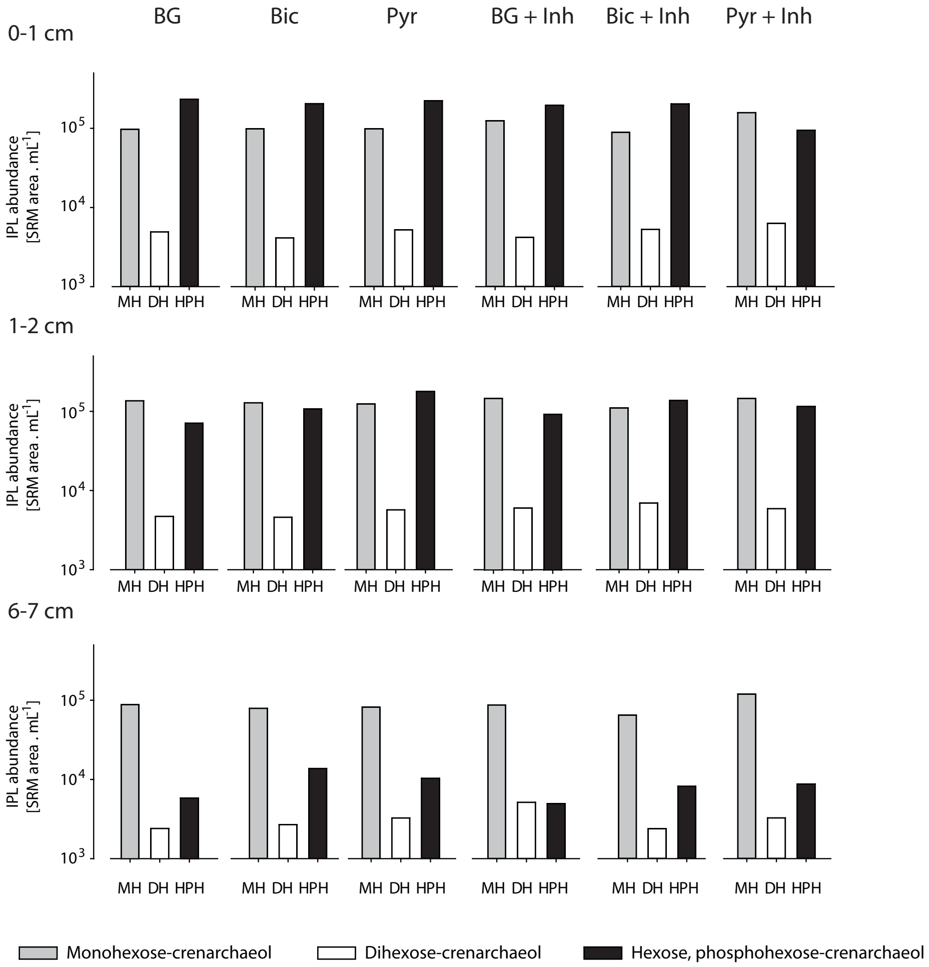

Figure 8.7. IPL-crenarchaeol profiles of the incubated cores for Station 2 - background (BG), bicarbonate (Bic) and pyruvate (Pyr) without (left plot) and with nitrification inhibitor (right plot). Top graphs shows the values from 0-1 cm depth, graphs in the middle the profiles from 1-2 cm depth and at the bottom the profiles from 6-7 cm depth at station 2.

Figure 8.8. IPL-crenarchaeol profiles of the incubated cores for Station 3 - background (BG), bicarbonate (Bic), pyruvate (Pyr), glucose (Glu) and amino acids (AA) without (left plot) and with nitrification inhibitor (right plot). Top graphs shows the values from 0-1 cm depth, graphs in the middle the profiles from 1-2 cm depth and at the bottom the profiles from 6-7 cm depth at station 3.

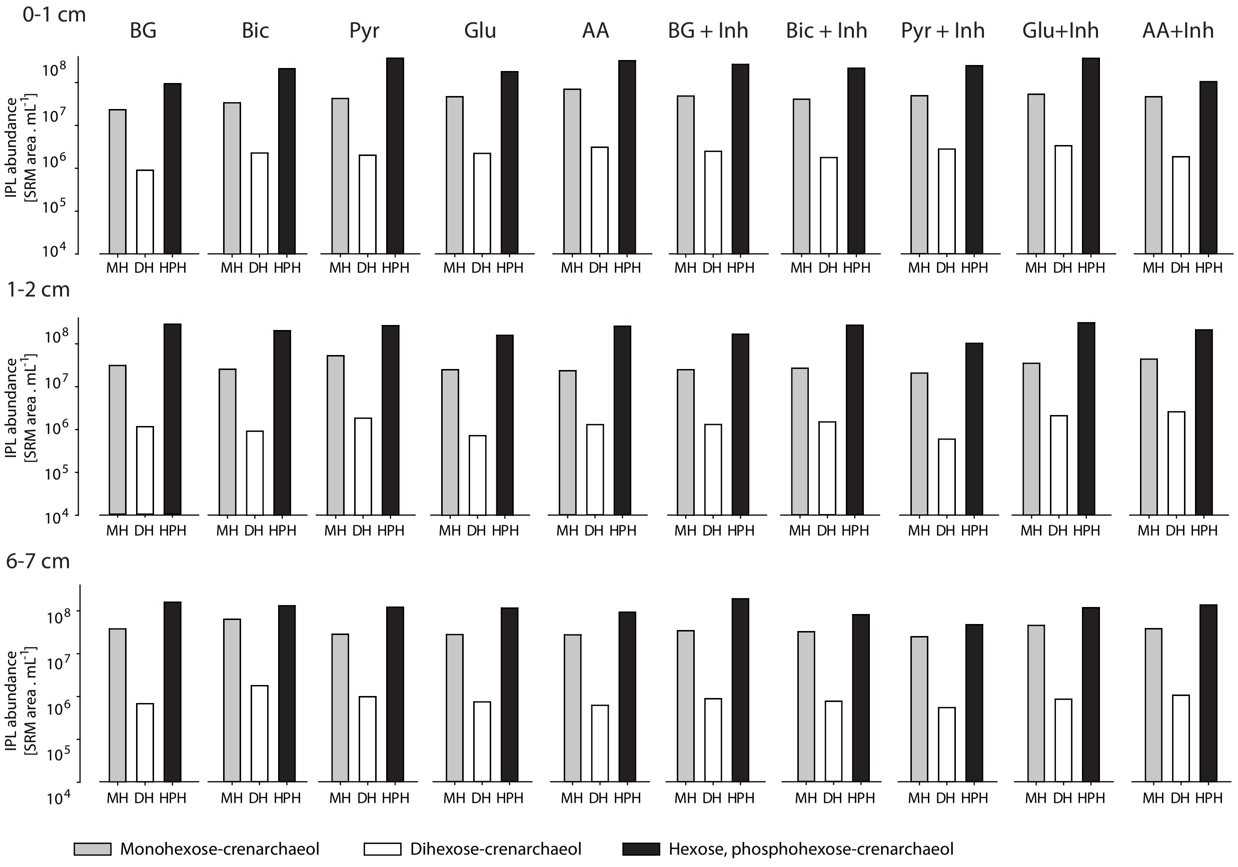

4.2 Activity indicators and label uptake during incubation

Several parameters can be monitored during the incubation experiments to cast hints on sedimentary microbial activities stimulated by the addition of substrates. During incubation, a decrease of oxygen penetration depths would indicate an increased aerobic metabolism at the surface, utilizing oxygen and preventing it from penetrating deeper, which was expected in the slices where organic carbon was added. However, at station 1, this was not observed and oxygen penetration depths only decreased in the background core (Table 8.2). This could be due to the aeration carried out by bubbling air into the bottom water of the core, and oxygen penetrating deeper into the sandy sediment. However, the cores from station 2 showed a decrease of oxygen penetration depth after incubation, except for the core incubated with pyruvate and inhibitor. Also the cores from station 3, i.e. those where oxygen penetration depth could be measured, showed a decrease, indicating that the oxygen was consumed upon incubation, independent of the type of substrate added to the cores. Ammonia and nitrite concentrations in the bottom water showed no changes during the incubations, but nitrate concentrations were, at station 2 and station 3, below detection limit after 6 and 5 days, respectively, suggesting consumption of nitrate (Table 8.2). This may indicate a strong contribution of denitrification to organic carbon processing in these sediments. The increase in $\delta^{13}C$ of the DIC in the bottom water of all cores compared to the background cores (Table 8.2) clearly showed that the organic substrates added were respired. Indeed, the strong labeling of the PLFAs at station 3 indicated that the organic substrates were readily taken up by bacteria, and potentially non-photosynthetic eukaryotes, and incorporated into their biomass.

For archaeal lipids, however, there are no indications of any substantial uptake of ^{13}C-label. IPL-GDGT abundances did not substantially change upon incubation, suggesting that Thaumarchaeota abundances did not change (Fig. 8.5 showing an average of all incubated cores, with standard deviations). However, this could also indicate that the majority of IPLs in these sediments were fossil (cf. Schouten et al., 2010; Logemann et al., 2011; Lengger et al., 2012b) and not part of living Thaumarchaeota, and thus not affected at all by the incubation. This could include HPH-GDGTs as well, though it is also possible that the bias during analysis, i.e. loss during silica column chromatography (cf. Lengger et al., 2012b), resulted in an underrepresentation of HPH-GDGT-derived biphytanes measured by irmGC-MS. Importantly, in nearly all of the incubation experiments, the $\delta^{13}C$ values of all measured biphytanes changed by less than 2 ‰ and sometimes even decreased in ^{13}C-content compared to the background values (Fig. 8.9). In some of the experiments, mainly at station 1, a slight enrichment in the tricyclic biphytane of up to 4 ± 2 ‰ was observed though this difference is not statistically significant for individual experiments. Furthermore, the bicyclic biphytane, also predominantly derived from crenarchaeol, shows in general lower ^{13}C-enrichments than the tricyclic biphytane and also no statistically significant enrichments for individual experiments. Thus, there is no evidence for substantial uptake of ^{13}C-label in archaeal GDGTs, like is observed for the PLFA.

This apparent lack of uptake could be due to three reasons. Firstly, it is possible that the Thaumarchaeota were active, but the substrates were not taken up. However, in case of the bicarbonate incubations this is unlikely as, in water incubations as well as enrichment cultures – including those of sedimentary Thaumarchaeota - it has been shown to be readily incorporated into biphytanes (Wuchter et al., 2003; Park et al., 2010; Pitcher et al., 2011a). Secondly, it is possible that most of the IPLs measured (i.e. MH- and DH-GDGTs, assuming the chromatographic discrimination against the HPH-GDGTs) are fossil, and thus only a very small amount of these IPLs are part of live and active sedimentary Thaumarchaeota. Finally, it is also possible that a higher proportion of the IPLs are part of sedimentary Thaumarchaeota, but that their metabolism and growth rates are so slow (as opposed to Thaumarchaeota in sea water and enrichment cultures), that no incorporation could be detected over the time scales investigated. These options are discussed in further detail below.

4.3 Estimating growth rates of Thaumarchaeota and turnover rates of IPL-GDGTs

To investigate whether growth rates as well as degradation rates of IPL-GDGTs were responsible for the apparent lack of substantial ^{13}C-labeling, we used data from our experiments to estimate minimal growth rates and the turnover time of IPL-GDGTs. The largest labeling was found at station 1 in the sandy sediment, indicating that Thaumarchaeota may have been active there. If a labeling of 2 ‰ of biphytanes is assumed, this can be converted to growth rates by using a formula used for growth of phytoplankton based on the isotope dilution theory of Laws (1984; Eq. 1), with μ representing the growth rate, t_{inc} the incubation time, P^* the atom%-excess of the product, in our case the biphytane, and A^* the atom%-excess of the substrate added (cf. alkenone lipids for eustigmatophyte algae; Popp et al., 2006) :

$$\mu = -\frac{1}{t_{inc}} . \ln\left(1 - \frac{P^*}{A^*}\right) \qquad \text{(Eq. 1)}$$

Unfortunately, as natural concentrations of the added substrates were not determined, A* could not be calculated for the incubation experiments with pyruvate, glucose and amino acids. In the bicarbonate experiments, we calculated A* based on the amount of added 99%-labeled DIC and natural sy^{13}C and concentration of DIC (Table 8.2). For P* we used the highest enrichment observed s at 6-7 depth with no inhibitor, i.e. 4 ‰. This gives an estimate of the maximum μ calculated to be 6.3 ×10^{-4} d^{-1}, corresponding to a generation time of 3 yrs. Clearly for the other bicarbonate experiments, generation times will be much higher (e.g. for a 2 ‰ enrichment, 9 yr). Interestingly, growth rates as low as estimated here have been predicted by Valentine (2007), who stated that the archaeal domain, other than bacteria and eukaryotes, has adapted to low energy conditions and is thus characterized by the exceptional ability to live in low energy environments and is not quick in adapting to settings with higher concentrations of available carbon and redox substrates. However, this has not been observed for pelagic Thaumarchaeota as SIP experiments showed a substantial enrichment in ^{13}C in IPL-GDGTs (Wuchter et al., 2003; Pitcher et al., 2011a). Indeed, the generation times calculated from enriched North Sea water labeling experiments conducted by Wuchter et al. (2003; *A**=5%; *P**=0.46% - 400 ‰ enrichment) and Pitcher et al. (2011a; *A**=9%; *P**=0.07 % – 44 ‰ enrichment) were at least an order of magnitude lower – 50 and 88 d, respec-

Table 8.4. δ^{13}C values of fatty acids measured in the 0-1 cm slice in cores from station 3, incubated without inhibitor, for 5 days.

	δ^{13}C ‰			
Fatty acid	**BG**	**Bic**	**Glu**	**AA**
$C_{16:0}$	-25.5 ± 0.2	-25.3 ± 0.6	20.6 ± 0.5	30.0 ± 3.9
$C_{18:0}$	-24.6*	-24.5 ± 0.2	66.2 ± 0.4	63.1 ± 2.1

*Single measurement

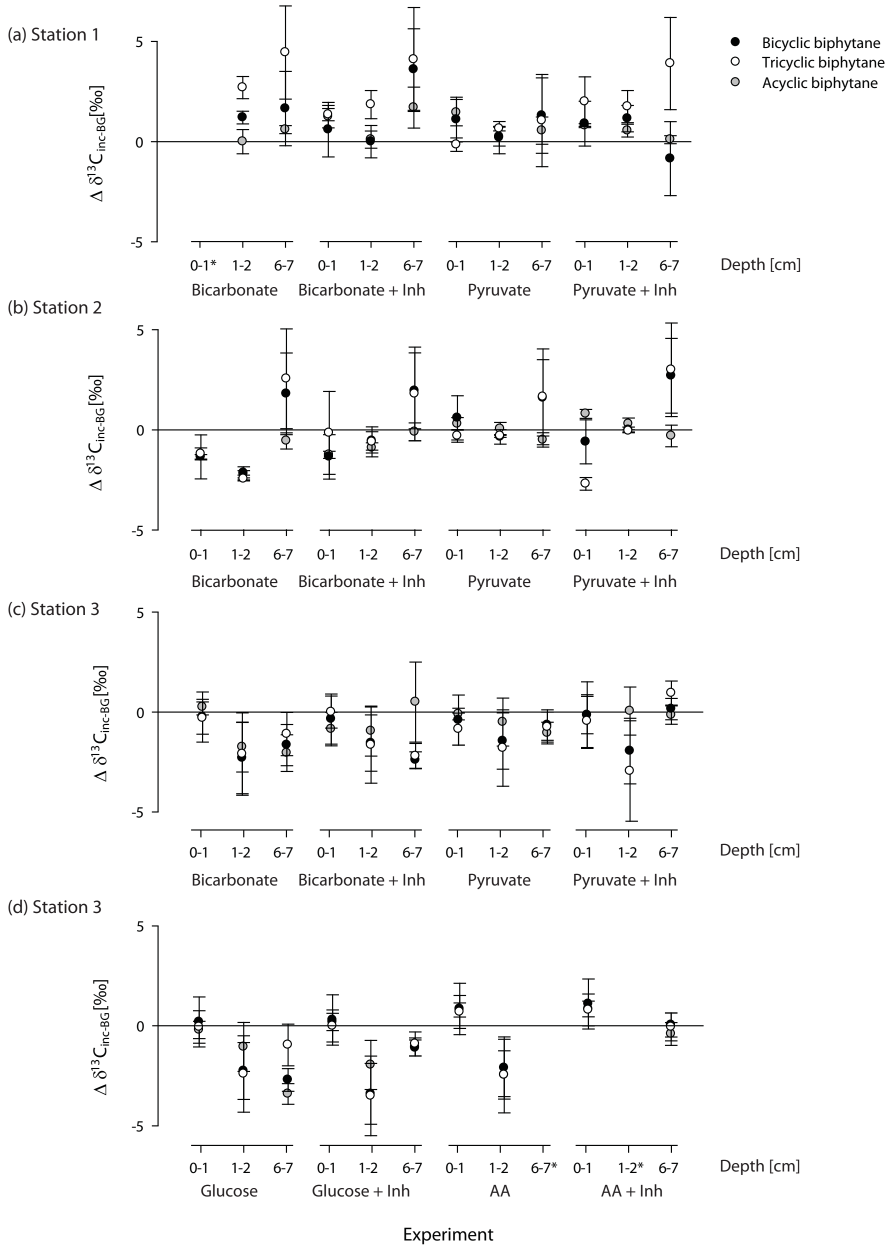

Figure 8.9. Difference inδ^{13}C-values ($\Delta\delta^{13}C_{inc\text{-}bg}$) of the acyclic, bicyclic and tricyclic biphytanes in ‰ in the cores incubated with labeled substrate versus the δ^{13}C-values in the background cores (incubated with and without inhibitor) at station 1 (a), station 2 (b) and station 3 (c) from the cores incubated with bicarbonate and pyruvate, with and without inhibitor, and the cores incubated with glucose and amino acids with and without inhibitor, at station 3 (d).

tively, than observed here. Also sedimentary Thaumarchaeota have been shown to incorporate ^{13}C from bicarbonate in enrichment cultures, resulting in biphytanes with ^{13}C contents as high as 50 at% (Park et al., 2010).

The calculations above assume exponential growth of sedimentary Thaumarchaeota and an immediate translation of this signal into the lipid pool. If, on the other hand, steady state conditions are assumed, i.e. cell numbers and lipid concentrations are not increasing but remain constant, the turnover time for the sedimentary lipid pool t_{to} can be calculated according to Lin et al. (2012) :

$$t_{to} = \frac{A^* . t_{inc}}{P^*} \qquad \text{(Eq. 2)}$$

Using Eq. 2, the turnover time of IPL-crenarchaeol in sediments would thus be at least ~4 yrs based on the 4 ‰ enrichment of the tricyclic biphytane in the bicarbonate incubation experiment. Since labeling was not detected in the other sediments, this turnover time estimate is likely to be a minimal estimate. This large turnover time is not an unusual postulate for thaumarchaeal lipids in sediments, as also Lin et al. (2012) found very low ^{13}C incorporation rates of labeled glucose into sugar moieties of glycosidic GDGTs over >400 d and used these to estimate turnover times of diglycosyl-lipids of 1,700 – 20,500 years. This is in strong contrast to GDGTs in the water column: Using the SIP data of Wuchter et al. (2003) and Pitcher et al. (2011a) from incubations of North Sea water, we obtained t_{to} of 76 and 128 d, respectively, for the thaumarchaeal GDGTs.

One possible reason for the slow label incorporation rates is that the incubations were performed shipboard at atmospheric pressure on cores from 200 to 500 m depth and thus the change in the pressure upon recovery of the sediment cores could have caused rupture of the cells. However, if our results are compared to the *in situ*-incubations carried out by Takano et al. (2010), it is obvious that *in situ*-incubations did not result in significant incorporation into the biphytanyl chains either. Another possibility, as suggested ibid., is that biphytanyl chains are not or hardly produced by sedimentary Thaumarchaeota, but recycled, and the sugar headgroups and/or the glycerol are only newly generated and ^{13}C-labeled. However, as also the incorporation into the sugar headgroups of GDGTs, as reported by Lin et al. (2012), is similarly low, it suggests that there is indeed a lack of, or only very slow, ^{13}C-uptake into IPL-

GDGTs. It seems that stable carbon isotope probing is most likely not the method of choice for thaumarchaeal activity measurements in sediments, where conditions are favorable for preservation of fossil GDGTs providing a large background signal. In the water column, however, where growth of Thaumarchaeota is faster and lipids are likely degraded on shorter time scales, due to the abundant presence of oxygen and lack of mineral matrix protection (Keil et al., 1994; Hedges and Keil, 1995), stable isotope incubations are useful for determining activities of Thaumarchaeota. In sediments that contain a high proportion of fossil IPL-GDGTs which are not part of live Archaea, the incorporation of ^{13}C into the lipids of the few active Thaumarchaeota is probably not enough to change the δ^{13}C of the IPL-GDGTs to a significant degree over the commonly used time scales of SIP experiments.

5 CONCLUSIONS

Incubations of sediment cores from the Iceland Shelf were used in order to determine the metabolism of sedimentary Thaumarchaeota. Thaumarchaeal IPLs were present in sediment cores recovered from the Iceland Shelf and the presence of labile IPL-biomarkers for Thaumarchaeota, such as HPH-crenarchaeol, suggested the presence of living Thaumarchaeota. However, incubations with ^{13}C-labeled substrates bicarbonate, pyruvate, glucose and amino acids did not result in any substantial incorporation of the ^{13}C into the biphytanyl chains of these lipids. Turnover times and generation times of thaumarchaeal lipids were estimated to be at least several years suggesting slow growth of sedimentary Thaumarchaeota in contrast to other sedimentary organisms, as well as a slow degradation of IPL-GDGTs, in contrast to bacterial or eukaryotic PLFAs.

Acknowledgements. The authors would like to thank the Master and crew of the R/V Pelagia and the participants of the Long Chain Diols Cruise 64PE341, in particular M. Baas, S. Rampen, M. Besseling, L. Handley and W. Lenthe, as well as the NIOZ technical department (Y. Witte, J. Schilling). We would also like to thank L. Moodley, H.T.S. Boschker, L. Pozzato, J. Middelburg, G. Duineveld and M. Lavaleye for helpful advice in planning the experiments and K. Koho / Utrecht University and L. Stal and N. Bale for providing equipment. We are grateful for analytical assistance to J. van Ooijen, S. Crayford, A. Mets, M. Verweij and J. Ossebaar. S.K.L. was funded by a studentship from the Darwin Center for Biogeosciences to S. S. This is a publication of the Darwin Center for Biogeosciences.

REFERENCES

Abell, G.C.J., Banks, J., Ross, D.J., Keane, J.P., Robert, S.S., Revill, A.T., Volkman, J.K., 2011. Effects of estuarine sediment hypoxia on nitrogen fluxes and ammonia oxidizer gene transcription. *FEMS Microbiology Ecology* **75**, 111-122.

Agogué, H., Brink, M., Dinasquet, J., Herndl, G.J., 2008. Major gradients inputatively nitrifying and non-nitrifying Archaea in the deep North Atlantic. *Nature* **456**, 788-791.

Aitchison, J., 1981. A new approach to null correlations of proportions. *Journal of the International Association for Mathematical Geology* **13**, 175-189.

Albers, S.-V., Meyer, B.H., 2011. The archaeal cell envelope. *Nature Reviews Microbiology* **9**, 414-427.

Alonso-Sáez, L., Waller, A.S., Mende, D.R., Bakker, K., Farnelid, H., Yager, P.L., Lovejoy, C., Tremblay, J.-É., Potvin, M., Heinrich, F., Estrada, M., Riemann, L., Bork, P., Pedrós-Alió, C., Bertilsson, S., 2012. Role for urea in nitrification by polar marine Archaea. *Proceedings of the National Academy of Sciences USA* **109**, 17989-17994.

Baker, B.J., Lesniewski, R.A., Dick, G.J., 2012. Genome-enabled transcriptomics reveals archaeal populations that drive nitrification in a deep-sea hydrothermal plume. *The ISME Journal* **6**, 2269-2279.

Bauersachs, T., Speelman, E.N., Hopmans, E.C., Reichart, G.-J., Schouten, S., Sinninghe Damsté, J.S., 2010. Fossilized glycolipids reveal past oceanic N_2 fixation by heterocystous cyanobacteria. *Proceedings of the National Academy of Sciences USA* **107**, 19190-19194.

Beman, J.M., Francis, C.A., 2006. Diversity of ammonia-oxidizing archaea and bacteria in the sediments of a hypernutrified subtropical estuary: Bahía del Tóbari, Mexico. *Applied and Environmental Microbiology* **72**, 7767-7777.

Beman, J.M., Popp, B.N., Francis, C.A., 2008. Molecular and biogeochemical evidence for ammonia oxidation by marine Crenarchaeota in the Gulf of California. *The ISME Journal* **2**, 429-441.

Berg, I.A., Kockelkorn, D., Buckel, W., Fuchs, G., 2007. A 3-Hydroxypropionate/4-hydroxybutyrate autotrophic carbon dioxide assimilation pathway in Archaea. *Science* **318**, 1782-1786.

Biddle, J.F., Lipp, J.S., Lever, M.A., Lloyd, K.G., Sørensen, K.B., Anderson, R., Fredricks, H.F., Elvert, M., Kelly, T.J., Schrag, D.P., Sogin, M.L., Brenchley, J.E., Teske, A., House, C.H., Hinrichs, K.-U., 2006. Heterotrophic Archaea dominate sedimentary subsurface ecosystems off Peru. P*roceedings of the National Academy of Sciences USA* **103**, 3846-3851.

Bijl, P.K., Schouten, S., Sluijs, A., Reichart, G.-J., Zachos, J.C., Brinkhuis, H., 2009. Early Palaeogene temperature evolution of the southwest Pacific Ocean. *Nature* **461**, 776-779.

Bligh, E.G., Dyer, W.J., 1959. A rapid method of total lipid extraction and purification. *Canadian Journal of Biochemistry and Physiology* **37**, 911-917.

Blumenberg, M., Seifert, R., Reitner, J., Pape, T., Michaelis, W., 2004. Membrane lipid patterns typify distinct anaerobic methanotrophic consortia. *Proceedings of the National Academy of Sciences USA* **101**, 11111-11116.

Boetius, A., Lochte, K., 2000. Regional variation of total microbial biomass in sediments of the deep Arabian Sea. *Deep Sea Research Part II: Topical Studies in Oceanography* **47**, 149-168.

Boetius, A., Ravenschlag, K., Schubert, C.J., Rickert, D., Widdel, F., Gieseke, F., Amann, R., Jørgensen, B.B., Witte, U., Pfannkuche, O., 2000. A marine microbial consortium apparently mediating anaerobic oxidation of methane. *Nature* **407**, 623-626.

Bolhuis, H., Stal, L.J., 2011. Analysis of bacterial and archaeal diversity in coastal microbial mats using massive parallel 16S rRNA gene tag sequencing. *The ISME Journal* **5**, 1701-1712.

Bouma, A.H., 1962. *Sedimentology of some flysch deposits: A graphic approach to facies interpretation.* Elsevier Pub. Co., Amsterdam, New York.

Brassell, S.C., Eglinton, G., Marlowe, I.T., Pflaumann, U., Samthein, M., 1986. Molecular stratigraphy: a new tool for climatic assessment. *Nature* **320**, 129-133.

Brochier-Armanet, C., Boussau, B., Gribaldo, S., Forterre, P., 2008. Mesophilic crenarchaeota: proposal for a third archaeal phylum, the Thaumarchaeota. *Nature Reviews Microbiology* **6**, 245-252.

Brocks, J.J., Logan, G.A., Buick, R., Summons, R.E., 1999. Archean molecular fossils and the early rise of eukaryotes. *Science* **285**, 1033-1036.

Buckley, D.E., Cranston, R.E., 1988. Early diagenesis in deep sea turbidites: The imprint of paleo-oxidation zones. *Geochimica et Cosmochimica Acta* **52**, 2925-2939.

Burd, A.B., Hansell, D.A., Steinberg, D.K., Anderson, T.R., Arístegui, J., Baltar, F., Beaupré, S.R., Buesseler, K.O., Dehairs, F., Jackson, G.A., Kadko, D.C., Koppelmann, R., Lampitt, R.S., Nagata, T., Reinthaler, T., Robinson, C., Tamburini, C., Tanaka, T., 2010. Assessing the apparent imbalance between geochemical and biochemical indicators of meso- and bathypelagic biological activity: What the @$#! is wrong with present calculations of carbon budgets? *Deep Sea Research Part II: Topical Studies in Oceanography* **57**, 1557-1571.

Burdige, D.J., 2007. Preservation of organic matter in marine sediments: Controls, mechanisms, and an imbalance in sediment organic carbon budgets? *Chemical Reviews* **107**, 467-485.

Caffrey, J.M., Bano, N., Kalanetra, K., Hollibaugh, J.T., 2007. Ammonia oxidation and ammonia-oxidizing bacteria and archaea from estuaries with differing histories of hypoxia. *The ISME Journal* **1**, 660-662.

Cao, H., Hong, Y., Li, M., Gu, J.-D., 2011. Phylogenetic diversity and ecological pattern of ammonia-oxidizing Archaea in the surface sediments of the Western Pacific. *Microbial Ecology* **62**, 813-823.

Cavicchioli, R., 2006. Cold-adapted archaea. *Nature Reviews Microbiology* **4**, 331-343.

Chen, X.-P., Zhu, Y.-G., Xia, Y., Shen, J.-P., He, J.-Z., 2008. Ammonia-oxidizing archaea: important players in paddy rhizosphere soil? *Environmental Microbiology* **10**, 1978-1987.

Church, M.J., Wai, B., Karl, D.M., DeLong, E.F., 2009. Abundances of crenarchaeal amoA genes and transcripts in the Pacific Ocean. *Environmental Microbiology* **12**, 679-688.

Coolen, M.J.L., Abbas, B., van Bleijswijk, J., Hopmans, E.C., Kuypers, M.M.M., Wakeham, S.G., Sinninghe Damsté, J.S., 2007. Putative ammonia-oxidizing Crenarchaeota in suboxic waters of the Black Sea: a basin-wide ecological study using 16S ribosomal and functional genes and membrane lipids. *Environmental Microbiology* **9**, 1001-1016.

Cowie, G., Calvert, S., de Lange, G., Keil, R., Hedges, J., 1998. Extents and implications of organic matter alteration at oxidation fronts in turbidites from the Madeira Abyssal Plain. In: *Proceedings of the Ocean Drilling Program, Scientific Results Leg 157*. US Government Printing Office, Washington DC, pp. 581-589.

Cowie, G.L., Hedges, J.I., Prahl, F.G., de Lange, G.J., 1995. Elemental and major biochemical changes across an oxidation front in a relict turbidite: An oxygen effect. *Geochimica et Cosmochimica Acta* **59**, 33-46.

Cowie, G.L., Levin, L.A., 2009. Benthic biological and biogeochemical patterns and processes across an oxygen minimum zone (Pakistan Margin, NE Arabian Sea). *Deep Sea Research Part II: Topical Studies in Oceanography* **56**, 261-270.

D'Hondt, S.L., Jørgensen, B.B., Miller, D.J., et al., 2003. *Proceedings of the Ocean Drilling Program, Initial Reports.* Ocean Drilling Program, College Station, TX.

Dang, H., Luan, X.-W., Chen, R., Zhang, X., Guo, L., Klotz, M.G., 2010. Diversity, abundance and distribution of amoA-encoding archaea in deep-sea methane seep sediments of the Okhotsk Sea. *FEMS Microbiology Ecology* **72**, 370-385.

de la Torre, J.R., Walker, C.B., Ingalls, A.E., Könneke, M., Stahl, D.A., 2008. Cultivation of a thermophilic ammonia oxidizing archaeon synthesizing crenarchaeol. *Environmental Microbiology* **10**, 810-818.

De Lange, G.J., 1992. Distribution of exchangeable, fixed, organic and total nitrogen in interbedded turbiditic/pelagic sediments of the Madeira Abyssal Plain, eastern North Atlantic. *Marine Geology* **109**, 95-114.

de Rosa, M., Gambacorta, A., 1988. The lipids of archaebacteria. *Progress in Lipid Research* **27**, 153-175.

DeLong, E.F., 1992. Archaea in coastal marine environments. *Proceedings of the National Academy of Sciences USA* **89**, 5685-5689.

DeLong, E.F., King, L.L., Massana, R., Cittone, H., Murray, A., Schleper, C., Wakeham, S.G., 1998. Dibiphytanyl ether lipids in nonthermophilic crenarchaeotes. *Applied and Environmental Microbiology* **64**, 1133-1138.

Denman, K.L., Brasseur, G., Chidthaisong, A., Ciais, P., Cox, P.M., Dickinson, R.E., Hauglustaine, D., Heinze, C., Holland, E., Jacob, D., Lohmann, U., Ramachandran, S., da Silva Dias, P.L., Wofsy, S.C., Zhang, X., 2007. Couplings between changes in the climate system and biogeochemistry. In: *Climate change 2007: The physical science basis. Contribution of working group I to the fourth assessment report of the Intergovernmental Panel on Climate Change.* Cambridge University Press, Cambridge, United Kingdom and New York, NY, USA, pp. 499-587.

Enge, A.J., Nomaki, H., Ogawa, N.O., Witte, U., Moeseneder, M.M., Lavik, G., Ohkouchi, N., Kitazato, H., Kucera, M., Heinz, P., 2011. Response of the benthic foraminiferal community to a simulated short-term phytodetritus pulse in the abyssal North Pacific. *Marine Ecology Progress Series* **438**, 129-142.

Erguder, T.H., Boon, N., Wittebolle, L., Marzorati, M., Verstraete, W., 2009. Environmental factors shaping the ecological niches of ammonia-oxidizing archaea. *FEMS Microbiology Reviews* **33**, 855-869.

Forster, A., Schouten, S., Baas, M., Sinninghe Damsté, J.S., 2007. Mid-Cretaceous (Albian-Santonian) sea surface temperature record of the tropical Atlantic Ocean. *Geology* **35**, 919-922.

Francis, C.A., Roberts, K.J., Beman, J.M., Santoro, A.E., Oakley, B.B., 2005. Ubiquity and diversity of ammonia-oxidizing archaea in water columns and sediments of the ocean. *Proceedings of the National Academy of Sciences USA* **102**, 14683-14688.

Fuhrman, J.A., McCallum, K., Davies, A.A., 1992. Novel major archaebacterial group from marine plankton. *Nature* **356**, 148-149.

Fuhrman, J.A., Davis, A.A., 1997. Widespread archaea and novel bacteria from the deep sea as shown by 16S rRNA gene sequences. *Marine Ecology Progress Series* **150**, 275-285.

Gabriel, J.L., Chong, P.L.G., 2000. Molecular modeling of archaebacterial bipolar tetraether lipid membranes. *Chemistry and Physics of Lipids* **105**, 193-200.

Gliozzi, A., Rolandi, R., de Rosa, M., Gambacorta, A., 1983. Monolayer black membranes from bipolar lipids of archaebacteria and their temperature-induced structural changes. *The Journal of Membrane Biology* **75**, 45-56.

Grasshoff, K., Kremlin, K., Ehrhardt, M., 1983. *Methods of seawater analysis.* Verlag Chemie GmbH, Weinheim.

Guckert, J.B., Antworth, C.P., Nichols, P.D., White, D.C., 1985. Phospholipid, ester-linked fatty acid profiles as reproducible assays for changes in prokaryotic community structure of estuarine sediments. *FEMS Microbiology Ecology* **31**, 147-158.

Gutiérrez, D., Bouloubassi, I., Sifeddine, A., Purca, S., Goubanova, K., Graco, M., Field, D., Méjanelle, L., Velazco, F., Lorre, A., Salvatteci, R., Quispe, D., Vargas, G., Dewitte, B., Ortlieb, L., 2011. Coastal cooling and increased productivity in the main upwelling zone off Peru since the mid-twentieth century. *Geophysical Research Letters* **38**, L07603.

Hallam, S.J., Mincer, T.J., Schleper, C., Preston, C.M., Roberts, K., Richardson, P.M., DeLong, E.F., 2006a. Pathways of carbon assimilation and ammonia oxidation suggested by environmental genomic analyses of marine Crenarchaeota. *PLoS Biology* **4**, 0520-0536.

Hallam, S.J., Konstantinidis, K.T., Putnam, N., Schleper, C., Watanabe, Y., Sugahara, J., Preston, C., de la Torre, J., Richardson, P.M., DeLong, E.F., 2006b. Genomic analysis of the uncultivated marine crenarchaeote *Cenarchaeum symbiosum*. *Proceedings of the National Academy of Sciences USA* **103**, 18296-18301.

Hartnett, H.E., Keil, R.G., Hedges, J.I., Devol, A.H., 1998. Influence of oxygen exposure time on organic carbon preservation in continental margin sediments. *Nature* **391**, 572-574.

Harvey, H.R., Fallon, R.D., Patton, J.S., 1986. The effect of organic matter and oxygen on the degradation of bacterial membrane lipids in marine sediments. *Geochimica et Cosmochimica Acta* **50**, 795-804.

Hatzenpichler, R., Lebedeva, E.V., Spieck, E., Stoecker, K., Richter, A., Daims, H., Wagner, M., 2008. A moderately thermophilic ammonia-oxidizing crenarchaeote from a hot spring. *Proceedings of the National Academy of Sciences USA* **105**, 2134-2139.

Hatzenpichler, R., 2012. Diversity, physiology and niche differentiation of ammonia-oxidizing archaea. *Applied and Environmental Microbiology* **78**, 7501-7510.

Hedges, J.I., Keil, R.G., 1995. Sedimentary organic matter preservation: an assessment and speculative synthesis. *Marine Chemistry* **49**, 81-115.

Hedges, J.I., Sheng Hu, F., Devol, A.H., Hartnett, H.E., Tsamakis, E., Keil, R.G., 1999. Sedimentary organic matter preservation: a test for selective degradation under oxic conditions. *American Journal of Science* **299**, 529-555.

Helder, W., de Vries, R., 1979. An automatic phenol-hypochlorite method for the determination of ammonia in sea- and brackish waters. *Netherlands Journal of Sea Research* **13**, 154-160.

Herndl, G.J., Reinthaler, T., Teira, E., van Aken, H., Veth, C., Pernthaler, A., Pernthaler, J., 2005. Contribution of *Archaea* to total prokaryotic production in the deep Atlantic Ocean. *Applied and Environmental Microbiology* **71**, 2303-2309.

Hershberger, K.L., Barns, S.M., Reysenbach, A.-L., Dawson, S.C., Pace, N.R., 1996.

Wide diversity of Crenarchaeota. *Nature* **384**, 420.

Hoefs, M.J.L., Schouten, S., de Leeuw, J.W., King, L.L., Wakeham, S.G., Sinninghe Damsté, J.S., 1997. Ether lipids of planktonic Archaea in the marine water column. *Applied and Environmental Microbiology* **63**, 3090-3095.

Hoefs, M.J.L., Rijpstra, W.I.C., Sinninghe Damsté, J.S., 2002. The influence of oxic degradation on the sedimentary biomarker record I: Evidence from Madeira Abyssal Plain turbidites. *Geochimica et Cosmochimica Acta* **66**, 2719-2735.

Hopmans, E.C., Weijers, J.W.H., Schefuß, E., Herfort, L., Sinninghe Damsté, J.S., Schouten, S., 2004. A novel proxy for terrestrial organic matter in sediments based on branched and isoprenoid tetraether lipids. *Earth and Planetary Science Letters* **224**, 107-116.

Huguet, C., Cartes, J.E., Sinninghe Damsté, J.S., Schouten, S., 2006a. Marine crenarchaeotal membrane lipids in decapods: Implications for the TEX_{86} paleothermometer. *Geochemistry Geophysics Geosystems* **7**, 1-12.

Huguet, C., Kim, J.-H., Sinninghe Damsté, J.S., Schouten, S., 2006b. Reconstruction of sea surface temperature variations in the Arabian Sea over the last 23 kyr using organic proxies (TEX_{86} and $U^{K'37}$). *Paleoceanography* **21**, PA3003.

Huguet, C., Hopmans, E.C., Febo-Ayala, W., Thompson, D.H., Sinninghe Damsté, J.S., Schouten, S., 2006c. An improved method to determine the absolute abundance of glycerol dibiphytanyl glycerol tetraether lipids. *Organic Geochemistry* **37**, 1036-1041.

Huguet, C., Schimmelmann, A., Thunell, R., Lourens, L.J., Sinninghe Damsté, J.S., Schouten, S., 2007. A study of the TEX_{86} paleothermometer in the water column and sediments of the Santa Barbara Basin, California. *Paleoceanography* **22**, PA3203.

Huguet, C., de Lange, G.J., Gustafsson, Ö., Middelburg, J.J., Sinninghe Damsté, J.S., Schouten, S., 2008. Selective preservation of soil organic matter in oxidized marine sediments (Madeira Abyssal Plain). *Geochimica et Cosmochimica Acta* **72**, 6061-6068.

Huguet, C., Kim, J.-H., de Lange, G.J., Sinninghe Damsté, J.S., Schouten, S., 2009. Effects of long term oxic degradation on the $U^{K'}_{37}$, TEX_{86} and BIT organic proxies. *Organic Geochemistry* **40**, 1188-1194.

Huguet, C., Martens-Habbena, W., Urakawa, H., Stahl, D.A., Ingalls, A.E., 2010a. Comparison of extraction methods for quantitative analysis of core and intact polar glycerol dialkyl glycerol tetraethers (GDGTs) in environmental samples. *Limnology and Oceanography: Methods* **8**, 127-145.

Huguet, C., Urakawa, H., Martens-Habbena, W., Truxal, L., Stahl, D.A., Ingalls, A.E., 2010b. Changes in intact membrane lipid content of archaeal cells as an indication of metabolic status. *Organic Geochemistry* **41**, 930-934.

Ingalls, A.E., Shah, S.R., Hansman, R.L., Aluwihare, L.I., Santos, G.M., Druffel, E.R.M., Pearson, A., 2006. Quantifying archaeal community autotrophy in the mesopelagic ocean using natural radiocarbon. *Proceedings of the National Academy of Sciences USA* **103**, 6442-6447.

IPCC Core Writing Team, 2007. *Contribution of Working Groups I, II and III to the Fourth Assessment Report of the Intergovernmental Panel on Climate Change*. IPCC, Geneva, Switzerland.

Jansen, E., Overpeck, J., Briffa, K.R., Duplessy, J.-C., Joos, F., Masson-Delmotte, V., Olago, D., Otto-Bliesner, B., Peltier, W.R., Rahmstorf, S., Ramesh, R., Raynaud, D., Rind, D., Solomina, O., Villalba, R., Zhang, D., 2007. Paleoclimate. In: *Climate Change 2007: The physical science basis.* Cambridge University Press, Cambrige, United Kingdom and New York, NY, USA, pp. 433-497.

Jenkyns, H.C., Schouten-Huibers, L., Schouten, S., Sinninghe Damsté, J.S., 2012. Warm Middle Jurassic-Early Cretaceous high-latitude sea-surface temperature from the Southern Ocean. *Climate of the Past* **8**, 215-226.

Jensen, M.M., Lam, P., Revsbech, N.P., Nagel, B., Gaye, B., Jetten, M.S.M., Kuypers, M.M.M., 2011. Intensive nitrogen loss over the Omani Shelf due to anammox coupled with dissimilatory nitrite reduction to ammonium. *The ISME Journal* **5**, 1660-1670.

Jiang, H., Dong, H., Ji, S., Ye, Y., Wu, N., 2007. Microbial diversity in the deep marine sediments from the Qiongdongnan Basin in South China Sea. *Geomicrobiology Journal* **24**, 505-517.

Jung, M.Y., Park, S.-J., Min, D., Kim, J.-S., Rijpstra, W.I.C., Sinninghe Damsté, J.S., Kim, G.-J., Madsen, E.L., Rhee, S.-K., 2011. Enrichment and characterization of an autotrophic ammonia-oxidizing archaeon of Mesophilic Crenarchaeal Group I.1a from an agricultural soil. *Applied and Environmental Microbiology* **77**, 8635-8647.

Kaneko, M., Kitajima, F., Naraoka, H., 2011. Stable hydrogen isotope measurement of archaeal ether-bound hydrocarbons. *Organic Geochemistry* **42**, 166-172.

Karner, M.B., DeLong, E.F., Karl, D.M., 2001. Archaeal dominance in the mesopelagic zone of the Pacific Ocean. *Nature* **409**, 507-510.

Kates, M., Yengoyan, L.S., Sastry, G.N., 1965. A diether analog of phosphatidyl glycerophosphate in Halobacterium cutirubrum. *Biochimica et Biophysica Acta-Molecular and Cell Biology of Lipids* **98**, 252-268.

Keil, R.G., Montluçon, D.B., Prahl, F.G., Hedges, J.I., 1994. Sorptive preservation of labile organic matter in marine-sediments. *Nature* **370**, 549-552.

Kennett, J.P., Stott, L.D., 1991. Abrupt deep-sea warming, palaeoceanographic changes and benthic extinctions at the end of the Palaeocene. *Nature* **353**, 225-229.

Kim, J.-G., Jung, M.-Y., Park, S.-J., Rijpstra, W.I.C., Sinninghe Damsté, J.S., Madsen, E.L., Min, D., Kim, J.-S., Kim, G.-J., Rhee, S.-K., 2012a. Cultivation of a highly enriched ammonia-oxidizing archaeon of thaumarchaeotal group I.1b from an agricultural soil. *Environmental Microbiology* **14**, 1528-1543.

Kim, J.-H., Schouten, S., Hopmans, E.C., Donner, B., Sinninghe Damsté, J.S., 2008. Global sediment core-top calibration of the TEX_{86} paleothermometer in the ocean. *Geochimica et Cosmochimica Acta* **72**, 1154-1173.

Kim, J.-H., Huguet, C., Zonneveld, K.A.F., Versteegh, G.J.M., Roeder, W., Sinninghe Damsté, J.S., Schouten, S., 2009. An experimental field study to test the stability of lipids used for the TEX_{86} and $U^{K'}{}_{37}$ palaeothermometers. *Geochimica et Cosmochimica Acta* **73**, 2888-2898.

Kim, J.-H., van der Meer, J., Schouten, S., Helmke, P., Willmott, V., Sangiorgi, F., Koç, N., Hopmans, E.C., Sinninghe Damsté, J.S., 2010. New indices and calibrations derived from the distribution of crenarchaeal isoprenoid tetraether lipids: Implications for past sea surface temperature reconstructions. *Geochimica et Cosmochimica Acta* **74**, 4639-4654.

Kim, J.-H., Romero, O.E., Lohmann, G., Donner, B., Laepple, T., Haam, E., Sinninghe Damsté, J.S., 2012b. Pronounced subsurface cooling of North Atlantic waters off Northwest Africa during Dansgaard-Oescher interstadials. *Earth and Planetary Science Letters* **339-340**, 95-102.

Köchling, T., Lara-Martín, P., González-Mazo, E., Amils, R., Sanz, J.L., 2011. Microbial community composition of anoxic marine sediments in the Bay of Cádiz (Spain). *International Microbiology* **14**, 143-154.

Koga, Y., Nishihara, M., Morii, H., Akagawa-Matsushita, M., 1993. Ether polar lipids of methanogenic bacteria: structures, comparative aspects, and biosyntheses. *Microbiological Reviews* **57**, 164-182.

Koga, Y., Morii, H., 2005. Recent advances in structural research on ether lipids from archaea including comparative and physiological aspects. *Bioscience Biotechnology and Biochemistry* **69**, 2019-2034.

Koga, Y., Nakano, M., 2008. A dendrogram of archaea based on lipid component parts composition and its relationship to rRNA phylogeny. *Systematic and Applied Microbiology* **31**, 169-182.

Koho, K.A., Nierop, K.G.J., Moodley, L., Middelburg, J.J., Pozzato, L., Soetaert, K., van der Plicht, J., Reichart, G.-J., 2012. Microbial bioavailability regulates organic matter preservation in marine sediments. *Biogeosciences Discussions* **9**, 13187-13210.

Könneke, M., Bernhard, A.E., de la Torre, J.R., Walker, C.B., Waterbury, J.B., Stahl, D.A., 2005. Isolation of an autotrophic ammonia-oxidizing marine archaeon. *Nature* **437**, 543-546.

Könneke, M., Lipp, J.S., Hinrichs, K.-U., 2012. Carbon isotope fractionation by the marine ammonia-oxidizing archaeon *Nitrosopumilus maritimus*. *Organic Geochemistry* **48**, 21-24.

Kraal, P., Slomp, C.P., Reed, D.C., Reichart, G.J., Poulton, S.W., 2012. Sedimentary phosphorus and iron cycling in and below the oxygen minimum zone of the Northern Arabian Sea. *Biogeosciences Discussions* **9**, 3829-3880.

Kubo, K., Lloyd, K.G., Biddle, J.F., Amann, R., Teske, A., Knittel, K., 2012. Archaea of the Miscellaneous Crenarchaeotal Group are abundant, diverse and widespread in marine sediments. *The ISME Journal* **6**, 1949-1965.

Kuypers, M.M.M., Blokker, P., Erbacher, J., Kinkel, H., Pancost, R.D., Schouten, S., Sinninghe Damsté, J.S., 2001. Massive expansion of marine archaea during a Mid-Cretaceous oceanic anoxic event. *Science* **293**, 92-94.

Langworthy, T.A., Smith, P.F., Mayberry, W.R., 1972. Lipids of *Thermoplasma acidophilum*. *Journal of Bacteriology* **112**, 1193-1200.

Langworthy, T.A., Mayberry, W.R., Smith, P.F., 1974. Long-chain glycerol diether and polyol dialkyl glycerol triether lipids of *Sulfolobus acidocaldarius*. *Journal of Bacteriology* **119**, 106-116.

Langworthy, T.A., 1977. Long-chain diglycerol tetraethers from *Thermoplasma acidophilum*. *Biochimica et Biophysica Acta (BBA) - Lipids and Lipid Metabolism* **487**, 37-50.

Law, G.T.W., Shimmield, T.M., Shimmield, G.B., Cowie, G.L., Breuer, E.R., Harvey, S.M., 2009. Manganese, iron and sulphur cycling on the Pakistan margin. *Deep Sea Research Part II: Topical Studies in Oceanography* **56**, 305-323.

Laws, E.A., 1984. Improved estimates of phytoplankton carbon based on ^{14}C incorporation into Chlorophyll *a*. *Journal of Theoretical Biology* **110**, 425-434.

Lebaron, P., Servais, P., Agogué, H., Courties, C., Joux, F., 2001. Does the high nucleic acid content of individual bacterial cells allow us to discriminate between active cells and inactive cells in aquatic Systems? *Applied and Environmental Microbiology* **67**, 1775-1782.

Leininger, S., Urich, T., Schloter, M., Schwark, L., Qi, J., Nicol, G.W., Prosser, J.I., Schuster, S.C., Schleper, C., 2006. Archaea predominate among ammonia-oxidizing prokaryotes in soils. *Nature* **442**, 806-809.

Lengger, S.K., Hopmans, E.C., Sinninghe Damsté, J.S., Schouten, S., 2012a. Comparison of extraction and work up techniques for analysis of core and intact polar tetraether lipids from sedimentary environments. *Organic Geochemistry* **47**, 34-40.

Lengger, S.K., Hopmans, E.C., Reichart, G.-J., Nierop, K.G.J., Sinninghe Damsté, J.S., Schouten, S., 2012b. Intact polar and core glycerol dibiphytanyl glycerol tetraether lipids in the Arabian Sea oxygen minimum zone: II. Selective preservation and degradation in sediments and consequences for the TEX$_{86}$. *Geochimica et Cos-*

mochimica Acta **98**, 244-258.

Lin, Y.S., Lipp, J.S., Elvert, M., Holler, T., Hinrichs, K.-U., 2013. Assessing production of the ubiquitous archaeal diglycosyl tetraether lipids in marine subsurface sediment using intramolecular stable isotope probing. *Environmental Microbiology* **15**, 1634-46.

Lipp, J.S., Morono, Y., Inagaki, F., Hinrichs, K.-U., 2008. Significant contribution of Archaea to extant biomass in marine subsurface sediments. *Nature* **454**, 991-994.

Lipp, J.S., Hinrichs, K.-U., 2009. Structural diversity and fate of intact polar lipids in marine sediments. *Geochimica et Cosmochimica Acta* **73**, 6816-6833.

Liu, X., Lipp, J.S., Hinrichs, K.-U., 2011. Distribution of intact and core GDGTs in marine sediments. *Organic Geochemistry* **42**, 368-375.

Liu, X.-L., Lipp, J.S., Simpson, J.H., Lin, Y.S., Summons, R.E., Hinrichs, K.-U., 2012. Mono- and dihydroxyl glycerol dibiphytanyl glycerol tetraethers in marine sediments: Identifications of both core and intact polar lipid forms. *Geochimica et Cosmochimica Acta* **89**, 102-115.

Liu, Z., Pagani, M., Zinniker, D., DeConto, R., Huber, M., Brinkhuis, H., Shah, S.R., Leckie, R.M., Pearson, A., 2009. Global cooling during the Eocene-Oligocene climate transition. *Science* **323** , 1187-1189.

Logemann, J., Graue, J., Köster, J., Engelen, B., Rullkötter, J., Cypionka, H., 2011. A laboratory experiment of intact polar lipid degradation in sandy sediments. *Biogeosciences* **8**, 2547-2560.

Lomstein, B.A., Langerhuus, A.T., D‘Hondt, S., Jørgensen, B.B., Spivack, A.J., 2012. Endospore abundance, microbial growth and necromass turnover in deep sub-seafloor sediment. *Nature* **484**, 101-104.

Lopes dos Santos, R.A., Prange, M., Castañeda, I.S., Schefuß, E., Mulitza, S., Schulz, M., Niedermeyer, E.M., Sinninghe Damsté, J.S., Schouten, S., 2010. Glacial-interglacial variability in Atlantic meridional overturning circulation and thermocline adjustments in the tropical North Atlantic. *Earth and Planetary Science Letters* **300**, 407-414.

Luna, G.M., Manini, E., Danovaro, R., 2002. Large fraction of dead and inactive bacteria in coastal marine sediments: Comparison of protocols for determination and ecological significance. *Applied and Environmental Microbiology* **68**, 3509-3513.

Macalady, J.L., Vestling, M.M., Baumler, D., Boekelheide, N., Kaspar, C.W., Banfield, J.F., 2004. Tetraether-linked membrane monolayers in Ferroplasma spp: a key to survival in acid. *Extremophiles* **8**, 411-419.

Madigan, M., Martinko, J.M., Parker, J., 2000. *Brock biology of microorganisms*. Prentice Hall, Upper Saddle River, NJ.

Martens-Habbena, W., Berube, P.M., Urakawa, H., de la Torre, J.R., Stahl, D.A., 2009. Ammonia oxidation kinetics determine niche separation of nitrifying Archaea and Bacteria. *Nature* **461**, 976-979.

Mayer, L.M., 1994. Surface area control of organic carbon accumulation in continental shelf sediments. *Geochimica et Cosmochimica Acta* **58**, 1271-1284.

Mayer, L.M., Schick, L.L., Hardy, K.R., Wagai, R., McCarthy, J., 2004. Organic matter in small mesopores in sediments and soils. *Geochimica et Cosmochimica Acta* **68**, 3863-3872.

McGregor, H.V., Dupont, l., Stuut, J.-B.W., Kuhlmann, H., 2009. Vegetation change, goats, and religion: a 2000-year history of land use in southern Morocco. *Quaternary Science Reviews* **28**, 1434-1448.

Meehl, G.A., Stocker, T.F., Collins, W.D., Friedlingstein, P., Gaye, A.T., Gregory, J.M., Kitoh, A., Knutti, R., Murphy, J.M., Noda, A., Raper, S.C.B., Watterson, I.G., Weaver, A.J., Zaho, Z.-C., 2007. Global climate projections. In: *Climate Change 2007: The physical science basis. Contribution of working group I to the fourth assessment report of the Intergovernmental Panel on Climate Change*. Cambridge University Press, Cambridge, United Kingdom and New York, NY, USA, pp. 663-745.

Middelburg, J.J., 1989. A simple rate model for organic matter decomposition in marine sediments. *Geochimica et Cosmochimica Acta* **53**, 1577-1581.

Moeseneder, M.M., Smith Jr., K.L., Ruhl, H.A., Jones, D.O.B., Witte, U., Prosser, J.I., 2012. Temporal and depth-related differences in prokaryotic communities in abyssal sediments associated with particulate organic carbon flux. *Deep Sea Research Part I* **70**, 26-35.

Moldowan, J.M., Dahl, J., Huizinga, B.J., Fago, F.J., Hickey, L.J., Peakman, T.M., Taylor, D.W., 1994. The molecular fossil record of Oleanane and its relation to Angiosperms. *Science* **265**, 768-771.

Moodley, L., Middelburg, J.J., Boschker, H.T.S., Duineveld, G.C.A., Pel, R., Herman, P.M.J., Heip, C.H.R., 2002. Bacteria and Foraminifera: key players in a short-term deep-sea benthic response to phytodetritus. *Marine Ecology Progress Series* **236**, 23-29.

Moodley, L., Middelburg, J.J., Soetaert, K., Boschker, H.T.S., Herman, P.M.J., Heip, C.H.R., 2005. Similar rapid response to phytodetritus deposition in shallow and deep-sea sediments. *Journal of Marine Research* **63**, 457-469.

Murphy, J., Riley, J.P., 1962. A modified single solution method for the determination of phosphate. *Analytica Chimica Acta* **27**, 31-36.

Mußmann, M., Brito, I., Pitcher, A., Sinninghe Damsté, J.S., Hatzenpichler, R., Richter, A., Nielsen, J.L., Nielsen, P.H., Müller, A., Daims, H., Wagner, M., Head, I.M., 2011. Thaumarchaeotes abundant in refinery nitrifying sludges express amoA but are not obligate autotrophic ammonia oxidizers. *Proceedings of the National Academy of Sciences USA* **108**, 16771-16776.

Nakanishi, T., Yamamoto, M., Irino, T., Tada, R., 2012. Distribution of glycerol dialkyl glycerol tetraethers, alkenones and polyunsaturated fatty acids in suspended particulate organic matter in the East China Sea. *Journal of Oceanography* **68**, 959-970.

Oba, M., Sakata, S., Tsunogai, U., 2006. Polar and neutral isopranyl glycerol ether lipids as biomarkers of archaea in near-surface sediments from the Nankai. *Organic Geochemistry* **37**, 1643-1654.

Olson, D.B., Hitchcock, G.L., Fine, R.A., Warren, B.A., 1993. Maintenance of the low-oxygen layer in the central Arabian Sea. *Deep Sea Research Part II: Topical Studies in Oceanography* **40**, 673-685.

Ouverney, C.C., Fuhrman, J.A., 2000. Marine planktonic archaea take up amino acids. *Applied and Environmental Microbiology* **66**, 4829-4833.

Pancost, R.D., Hopmans, E.C., Sinninghe Damsté, J.S., the Medinaut Shipboard Scientific Party., 2001. Archaeal lipids in Mediterranean cold seeps: Molecular proxies for anaerobic methane oxidation. *Geochimica et Cosmochimica Acta* **65**, 1611-1627.

Park, B.-J., Park, S.-J., Yoon, D.-N., Schouten, S., Sinninghe Damsté, J.S., Rhee, S.-K., 2010. Cultivation of autotrophic ammonia-axidizing archaea from marine sediments in coculture with sulfur-oxidizing bacteria. *Applied and Environmental Microbiology* **76**, 7575-7587.

Park, S.-J., Park, B.-J., Rhee, S.-K., 2008. Comparative analysis of archaeal 16S rRNA and *amoA* genes to estimate the abundance and diversity of ammonia-oxidizing archaea in marine sediments. *Extremophiles* **12**, 605-615.

Paulmier, A., Ruiz-Pino, D., 2009. Oxygen minimum zones (OMZs) in the modern ocean. *Progress in Oceanography* **80**, 113-128.

Pearson, A., McNichol, A.P., Benitez-Nelson, B.C., Hayes, J.M., Eglinton, T.I., 2001. Origins of lipid biomarkers in Santa Monica Basin surface sediment: A case study using compound-specific δ^{14}C analysis. *Geochimica et Cosmochimica Acta* **65**, 3123-3137.

Peters, K.E., Walters, C.C., Moldowan, J.M., 2004. T*he Biomarker Guide: Biomarkers and isotopes in the environment and human history.* Cambridge University Press, Cambridge, United Kingdom and New York, NY, USA.

Peterse, F., Kim, J.-H., Schouten, S., Klitgaard Kristensen, D., Koç, N., Sinninghe Damsté, J.S., 2009. Constraints on the application of the MBT/CBT palaeothermometer at high latitude environments (Svalbard, Norway). *Organic Geochemistry* **40**, 692-699.

Peterse, F., Hopmans, E.C., Schouten, S., Mets, A., Rijpstra, W.I.C., Sinninghe

Damsté, J.S., 2011. Identification and distribution of intact polar branched tetraether lipids in peat and soils. *Organic Geochemistry* **42**, 1007-1015.

Peterse, F., van der Meer, J., Schouten, S., Weijers, J.W.H., Fierer, N., Jackson, R.B., Kim, J.-H., Sinninghe Damsté, J.S., 2012. Revised calibration of the MBT-CBT paleotemperature proxy based on branched tetraether membrane lipids in surface soils. *Geochimica et Cosmochimica Acta* **96**, 215-229.

Pitcher, A., Schouten, S., Sinninghe Damsté, J.S., 2009a. In situ production of Crenarchaeol in two California hot springs. *Applied and Environmental Microbiology* **75**, 4443-4451.

Pitcher, A., Hopmans, E.C., Schouten, S., Sinninghe Damsté, J.S., 2009b. Separation of core and intact polar archaeal tetraether lipids using silica columns: Insights into living and fossil biomass contributions. *Organic Geochemistry* **40**, 12-19.

Pitcher, A., Rychlik, N., Hopmans, E.C., Spieck, E., Rijpstra, W.I.C., Ossebaar, J., Schouten, S., Wagner, M., Sinninghe Damsté, J.S., 2010. Crenarchaeol dominates the membrane lipids of *Candidatus* Nitrososphaera gargensis, a thermophilic Group I.1b Archaeon. *The ISME Journal* **4**, 542-552.

Pitcher, A., Wuchter, C., Siedenberg, K., Schouten, S., Sinninghe Damsté, J.S., 2011a. Crenarchaeol tracks winter blooms of ammonia-oxidizing Thaumarchaeota in the coastal North Sea. *Limnology and Oceanography* **56**, 2308-2318.

Pitcher, A., Hopmans, E.C., Villanueva, L., Reichart, G.-J., Schouten, S., Sinninghe Damsté, J.S., 2011b. Niche segregation of Ammonia-oxidizing Archaea and Anammox bacteria in the Arabian Sea oxygen minimum zone. *The ISME Journal* **5**, 1896-1904.

Pitcher, A., Hopmans, E.C., Mosier, A.C., Park, S.-J., Rhee, S.-K., Francis, C.A., Schouten, S., Sinninghe Damsté, J.S., 2011c. Core and intact polar glycerol dibiphytanyl glycerol tetraether lipids of ammonia-oxidizing archaea enriched from marine and estuarine sediments. *Applied and Environmental Microbiology* **77**, 3468-3477.

Popp, B.N., Bidigare, R.R., Deschenes, B., Laws, E.A., Prahl, F.G., Tanimoto, J.K., Wallsgrove, R.J., 2006. A new method for estimating growth rates of alkenone-producing haptophytes. *Limnology and Oceanography: Methods* **4**, 114-129.

Powell, A.J., Dodge, J.D., Lewis, J., 1990. Late Neogene to Pleistocene palynological facies of the Peruvian continental margin upwelling, Leg 112. *Proceedings of the Ocean Drilling Program, Scientific Results* **112**, 297-321.

Pozzato, L., Van Oevelen, D., Moodley, L., Soetaert, K., Middelburg, J.J., 2013. Carbon processing at the deep-sea floor of the Arabian Sea oxygen minimum zone: a tracer approach. *Journal of Sea Research* **78**, 45-58.

Prahl, F.G., Wakeham, S., 1987. Calibration of unsaturation patterns in long-chain ketone compositions for palaeotemperature assessment. *Nature* **330**, 367-369.

Prahl, F.G., de Lange, G.J., Scholten, S., Cowie, G.L., 1997. A case of post-depositional aerobic degradation of terrestrial organic matter in turbidite deposits from the Madeira Abyssal Plain. *Organic Geochemistry* **27**, 141-152.

Preston, C.M., Wu, K.Y., Molinski, T.F., DeLong, E.F., 1996. A psychrophilic crenarchaeon inhabits a marine sponge: *Cenarchaeum symbiosum* gen. nov., sp. nov. *Proceedings of the National Academy of Sciences USA* **93**, 6241-6246.

Pross, J., Contreras, L., Bijl, P.K., Greenwood, D.R., Bohaty, S.M., Schouten, S., Bendle, J.A., Röhl, U., Tauxe, L., Raine, J.I., Huck, C.E., van de Flierdt, T., Jamieson, S.S.R., Stickley, C.E., van de Schootbrugge, B., Escutia, C., Brinkhuis, H., Integrated Ocean Drilling Program Expedition 318 Scientists, 2012. Persistent near-tropical warmth on the Antarctic continent during the early Eocene epoch. *Nature* **488**, 73-77.

Reimers, C.E., 1987. An *in situ* microprofiling instrument for measuring interfacial pore water gradients: methods and oxygen profiles from the North Pacific Ocean. *Deep-Sea Research Part A-Oceanographic Research Papers* **34**, 2019-2021.

Reimers, C.E., Jahnke, R.A., McCorkle, D.C., 1992. Carbon fluxes and burial rates over the continental slope and rise off central California with implications for the global carbon cycle. *Global Biogeochemical Cycles* **6**, 199-224.

Reinthaler, T., van Aken, H.M., Herndl, G.J., 2010. Major contribution of autotrophy to microbial carbon cycling in the deep North Atlantic‘s interior. *Deep Sea Research Part II: Topical Studies in Oceanography* **57**, 1572-1580.

Revsbech, N.P., 1989. An oxygen microsensor with a guard cathode. *Limnology and Oceanography* **34**, 474-478.

Revsbech, N.P., Larsen, L.H., Gundersen, J., Dalsgaard, T., Ulloa, O., Thamdrup, B., 2009. Determination of ultra-low oxygen concentrations in oxygen minimum zones by the STOX sensor. *Limnology and Oceanography: Methods* **7**, 371-381.

Roussel, E.G., Sauvadet, A.-L., Chaduteau, C., Fouquet, Y., Charlou, J.-L., Prieur, D., Cambon Bonavita, M.-A., 2009. Archaeal communities associated with shallow to deep subseafloor sediments of the New Caledonia Basinemi. *Environmental Microbiology* **11**, 2446-2462.

Schleper, C., Holben, W., Klenk, H.-P., 1997. Recovery of Crenarchaeotal ribosomal DNA sequences from freshwater-lake sediments. *Applied and Environmental Microbiology* **63**, 321-323.

Schleper, C., 2007. Diversity of uncultivated Archaea: perspectives from microbial ecology and metagenomics. In: *Archaea: evolution, physiology, and molecular biology*. Blackwell Publishing Ltd, Malden (MA), Oxford, Carlton, pp. 39-50.

Schouten, S., Hoefs, M.J.L., Koopmans, M.P., Bosch, H.-J., Sinninghe Damsté, J.S., 1998. Structural characterization, occurrence and fate of archaeal ether-bound acyclic and cyclic biphytanes and corresponding diols in sediments. *Organic Geo-*

chemistry **29**, 1305-1319.

Schouten, S., Hopmans, E.C., Pancost, R.D., Sinninghe Damsté, J.S., 2000. Widespread occurrence of structurally diverse tetraether membrane lipids: Evidence for the ubiquitous presence of low-temperature relatives of hyperthermophiles. *Proceedings of the National Academy of Sciences USA* **97**, 14421-14426.

Schouten, S., Hopmans, E.C., Schefuß, E., Sinninghe Damsté, J.S., 2002. Distributional variations in marine crenarchaeotal membrane lipids: a new tool for reconstructing ancient sea water temperatures? *Earth and Planetary Science Letters* **204**, 265-274.

Schouten, S., Hopmans, E.C., Sinninghe Damsté, J.S., 2004. The effect of maturity and depositional redox conditions on archaeal tetraether lipid palaeothermometry. *Organic Geochemistry* **35**, 567-571.

Schouten, S., Forster, A., Panoto, F.E., Sinninghe Damsté, J.S., 2007a. Towards calibration of the TEX_{86} palaeothermometer for tropical sea surface temperatures in ancient greenhouse worlds. *Organic Geochemistry* **38**, 1537-1546.

Schouten, S., Huguet, C., Hopmans, E.C., Kienhuis, M.V.M., Sinninghe Damsté, J.S., 2007b. Analytical methodology for TEX_{86} paleothermometry by high-performance liquid chromatography/atmospheric pressure chemical ionization-mass spectrometry. *Analytical Chemistry* **79**, 2940-2944.

Schouten, S., Hopmans, E.C., Baas, M., Boumann, H., Standfest, S., Könneke, M., Stahl, D.A., Sinninghe Damsté, J.S., 2008. Intact membrane lipids of „*Candidatus* Nitrosopumilus maritimus," a cultivated representative of the cosmopolitan mesophilic group I crenarchaeota. *Applied and Environmental Microbiology* **74**, 2433-2440.

Schouten, S., Middelburg, J.J., Hopmans, E.C., Sinninghe Damsté, J.S., 2010. Fossilization and degradation of intact polar lipids in deep subsurface sediments: A theoretical approach. *Geochimica et Cosmochimica Acta* **74**, 3806-3814.

Schouten, S., Pitcher, A., Hopmans, E.C., Villanueva, L., van Bleijswijk, J., Sinninghe Damsté, J.S., 2012. Intact polar and core glycerol dibiphytanyl glycerol tetraether lipids in the Arabian Sea oxygen minimum zone: I. Selective preservation and degradation in the water column and consequences for the TEX_{86}. *Geochimica et Cosmochimica Acta* **98**, 228-243.

Schouten, S., Hopmans, E.C., Sinninghe Damsté, J.S., 2013. The organic geochemistry of glycerol dialkyl glycerol tetraether lipids: A review. *Organic Geochemistry* **54**, 19-61.

Schubotz, F., Wakeham, S.G., Lipp, J.S., Fredricks, H.F., Hinrichs, K.-U., 2009. Detection of microbial biomass by intact polar membrane lipid analysis in the water column and surface sediments of the Black Sea. *Environmental Microbiology* **11**, 2720-2734.

Shah, S.R., Mollenhauer, G., Ohkouchi, N., Eglinton, T., Pearson, A., 2008. Origins of archaeal tetraether lipids in sediments: Insights from radiocarbon analysis. *Geochimica et Cosmochimica Acta* **72**, 4577-4594.

Sinninghe Damsté, J.S., Rijpstra, W.I.C., Reichart, G.-J., 2002a. The influence of oxic degradation on the sedimentary biomarker record II. Evidence from Arabian Sea sediments. *Geochimica et Cosmochimica Acta* **66**, 2737-2754.

Sinninghe Damsté, J.S., Schouten, S., Hopmans, E.C., van Duin, A.C.T., Geenevasen, J.A.J., 2002b. Crenarchaeol: the characteristic core glycerol dibiphytanyl glycerol tetraether membrane lipid of cosmopolitan pelagic crenarchaeota. *Journal of Lipid Research* **43**, 1641-1651.

Sinninghe Damsté, J.S., Rijpstra, W.I.C., Hopmans, E.C., Prahl, F.G., Wakeham, S.G., Schouten, S., 2002c. Distribution of membrane lipids of planktonic *Crenarchaeota* in the Arabian Sea. *Applied and Environmental Microbiology* **68**, 2997-3002.

Sinninghe Damsté, J.S., Rijpstra, W.I.C., Hopmans, E.C., Jung, M.Y., Kim, J.G., Rhee, S.K., Stieglmeier, M., Schleper, C., 2012. Intact polar and core dibiphytanyl glycerol tetraether lipids of group I. 1a and I. 1b thaumarchaeota in soil. *Applied and Environmental Microbiology* **78**, 6866-6874.

Skilbeck, C.G., Fink, D., 2006. Data report: Radiocarbon dating and sedimentation rates for Holocene upper Pleistocene sediments, eastern equatorial Pacific and Peru continental margin. In: *Proceedings of the Ocean Drilling Program, Scientific Results*, **201**. Ocean Drilling Program, College Station, TX, pp. 1-15.

Sluijs, A., Schouten, S., Pagani, M., Woltering, M., Brinkhuis, H., Sinninghe Damsté, J.S., Dickens, G.R., Huber, M., Reichart, G.-J., Stein, R., Matthiessen, J., Lourens, L.J., Pedentchouk, N., Backman, J., Moran, K., & the Expedition 302 Scientists, 2006. Subtropical Arctic Ocean temperatures during the Palaeocene/Eocene thermal maximum. *Nature* **441**, 610-613.

Smith, R.W., Bianchi, T.S., Li, X., 2012. A re-evaluation of the use of branched GDGTs as terrestrial biomarkers: Implications for the BIT Index. *Geochimica et Cosmochimica Acta* **80**, 14-29.

Spang, A., Hatzenpichler, R., Brochier-Armanet, C., Rattei, T., Tischler, P., Spieck, E., Streit, W., Stahl, D.A., Wagner, M., Schleper, C., 2010. Distinct gene set in two different lineages of ammonia-oxidizing archaea supports the phylum Thaumarchaeota. *Trends in Microbiology* **18**, 331-340.

Stahl, D.A., de la Torre, J.R., 2012. Physiology and diversity of ammonia-oxidizing Archaea. *Annual Review of Microbiology* **66**, 83-101.

Stevenson, P.L., 1978. A case for bacterial dormancy in aquatic systems. *Microbial Ecology* **4**, 127-133.

Sturt, H.F., Summons, R.E., Smith, K., Elvert, M., Hinrichs, K.-U., 2004. Intact polar membrane lipids in prokaryotes and sediments deciphered by high-performance liquid chromatography/electrospray ionization multistage mass spectrometry - new biomarkers for biogeochemistry and microbial ecology. *Rapid Communications in Mass Spectrometry* **18**, 617-628.

Takano, Y., Chikaraishi, Y., Ogawa, N.O., Nomaki, H., Morono, Y., Inagaki, F., Kitazato, H., Hinrichs, K.-U., Ohkouchi, N., 2010. Sedimentary membrane lipids recycled by deep-sea benthic archaea. *Nature Geoscience* **3**, 858-861.

Tjallingii, R., Röhl, U., Kölling, M., Bickert, T., 2007. Influence on the water content on X-ray fluorescence core-scanning measurements in soft marine sediments. *Geochemistry Geophysics Geosystems* **8**, Q02004.

Tourna, M., Stieglmeier, M., Spang, A., Könneke, M., Schintlmeister, A., Urich, T., Engel, M., Schloter, M., Wagner, M., Richter, A., Schleper, C., 2011. Nitrosospahera viennensis, an ammonia oxidizing archaeon from soil. *Proceedings of the National Academy of Sciences USA* **108**, 8420-8425.

Turich, C., Freeman, K.H., Bruns, M.A., Conte, M., Jones, A.D., Wakeham, S.G., 2007. Lipids of marine Archaea: Patterns and provenance in the water-column and sediments. *Geochimica et Cosmochimica Acta* **71**, 3272-3291.

Valentine, D.L., 2007. Adaptations to energy stress dictate the ecology and evolution of the Archaea. *Nature Reviews Microbiology* **5**, 316-323.

van der Weijden, C.H., Reichart, G.-J., Visser, H.J., 1999. Enhanced preservation of organic matter in sediments deposited within the oxygen minimum zone in the northeastern Arabian Sea. *Deep Sea Research Part I* **46**, 807-830.

van Mooy, B., Fredricks, H.F., Pedler, B.E., Dyhrman, S.T., Karl, D.M., Koblížek, M., Lomas, M.W., Mincer, T.J., Moore, L.R., Moutin, T., Rappé, M.S., Webb, E.A., 2009. Phytoplankton in the ocean use non-phosphorous lipids in response to phosphorus scarcity. *Nature* **458**, 69-72.

Vetriani, C., Jannasch, H.W., MacGregor, B.J., Stahl, D.A., Reysenbach, A.-L., 1999. Population structure and phylogenetic characterization of marine benthic archaea in deep-sea sediments. *Applied and Environmental Microbiology* **65**, 4375-4384.

Wakeham, S.G., Lewis, C.M., Hopmans, E.C., Schouten, S., Sinninghe Damsté, J.S., 2003. Archaea mediate anaerobic oxidation of methane in deep euxinic waters of the Black Sea. *Geochimica et Cosmochimica Acta* **67**, 1359-1374.

Walker, C.B., de la Torre, J.R., Klotz, M.G., Urakawa, H., Pinel, N., Arp, D.J., Brochier-Armanet, C., Chain, P.S.G., Chan, P.P., Gollabgir, A., Hemp, J., Hügler, M., Könneke, M., Shin, M., Lawton, T.J., Lowe, T., Martens-Habbena, W., Sayavedra-Soto, L.A., Lang, D., Sievert, S.M., Rosenzweig, A.C., Manning, G., Stahl, D.A., 2010. *Nitrosopumilus maritimus* genome reveals unique mechanisms for nitrification and autotrophy in globally distributed marine crenarchaea. *Proceedings of the National Academy of Sciences USA* **107**, 8818-8823.

Wang, P., Xiao, X., Wang, F., 2005. Phylogenetic analysis of Archaea in the deep-sea sediments of west Pacific Warm Pool. *Extremophiles* **9**, 209-217.

Wang, P., Li, T., Hu, A., Wei, Y., Guo, W., Jiao, N., Zhang, C., 2010. Community structure of archaea from deep-sea sediments of the South China Sea. *Microbial Ecology* **60**, 796-806.

Weaver, P.P.E., Kuijpers, A., 1983. Climatic control of turbidite deposition during the last 200,000 years on the Madeira Abyssal Plain. *Nature* **306**, 360-363.

Weaver, P.P.E., Buckley, D.E., Kuijpers, A., 1989. Geological investigations of ESOPE cores from the Madeira Abyssal Plain. In: *Geoscience Investigations of Two North Atlantic Abyssal Plains - The ESOPE International Expedition. OECD/NEA-Seabed Working group.* Commission of European Communities Joint Research Centre, Ispra, pp. 535-555.

Weijers, J.W.H., Schouten, S., Spaargaren, O.C., Sinninghe Damsté, J.S., 2006. Occurrence and distribution of tetraether membrane lipids in soils: Implications for the use of the TEX_{86} proxy and the BIT index. *Organic Geochemistry* **37**, 1680-1693.

Weijers, J.W.H., Schouten, S., van den Donker, J.C., Hopmans, E.C., Sinninghe Damsté, J.S., 2007. Environmental controls on bacterial tetraether membrane lipid distribution in soils. *Geochimica et Cosmochimica Acta* **71**, 703-713.

Weijers, J.W.H., Panoto, E., van Bleijswijk, J., Schouten, S., Rijpstra, W.I.C., Balk, M., Stams, A.J.M., Sinninghe Damsté, J.S., 2009. Constraints on the biological surce(s) of the orphan branched tetraether membrane lipids. *Geomicrobiology Journal* **26**, 402-414.

Weijers, J.W.H., Lim, K.L., Aquilina, A., Sinninghe Damsté, J.S., Pancost, R.D., 2011. Biogeochemical controls on glycerol dialkyl glycerol tetraether lipid distributions in sediments characterized by diffusive methane flux. *Geochemistry Geophysics Geosystems* **12**, Q10010.

Weltje, G.J., Tjallingii, R., 2008. Calibration of XRF core scanners for quantitative geochemical logging of sediment cores: Theory and application. *Earth and Planetary Science Letters* **274**, 423-438.

White, D.C., Davis, W.M., Nickels, J.S., King, J.D., Bobbie, R.J., 1979. Determination of the sedimentary microbial biomass by extractible lipid phosphate. *Oecologia* **40**, 51-62.

White, D.C., Stair, J.O., Ringelberg, D.B., 1996. Quantitative comparisons of in situ microbial biodiversity by signature biomarker analysis. *Journal of Industrial Microbiology* **17**, 185-196.

White, D.C., Ringelberg, D.B., 1998. Signature lipid biomarker analysis. In: *Techniques in Microbial Ecology*. Oxford University Press, New York, pp. 255-259.

Witte, U., Wenzhöfer, f., Sommer, S., Boetius, A., Heinz, P., Aberle, N., Sand, M., Cremer, A., Abraham, W.-R., Jørgensen, B.B., Pfannkuche, O., 2003. In situ experimental evidence of the fate of a phytodetritus pulse at the abyssal sea floor. *Nature* **424**, 763-766.

Woese, C.R., Fox, G.E., 1977. Phylogenetic structure of the prokarytic domain: The primary kingdoms. *Proceedings of the National Academy of Sciences USA* **74**, 5088-5090.

Wuchter, C., Schouten, S., Boschker, H.T.S., Sinninghe Damsté, J.S., 2003. Bicarbonate uptake by marine Crenarchaeota. *FEMS Microbiology Letters* **219**, 203-207.

Wuchter, C., Schouten, S., Coolen, M.J.L., Sinninghe Damsté, J.S., 2004. Temperature-dependent variation in the distribution of tetraether membrane lipids of marine Crenarchaeota: Implications for TEX_{86} paleothermometry. *Paleoceanography* 19, PA4028.

Wuchter, C., Schouten, S., Wakeham, S.G., Sinninghe Damsté, J.S., 2005. Temporal and spatial variation in tetraether membrane lipids of marine Crenarchaeota in particulate organic matter: Implications for TEX_{86} paleothermometry. *Paleoceanography* **20**, PA3013.

Wuchter, C., Schouten, S., Wakeham, S.G., Sinninghe Damsté, J.S., 2006a. Archaeal tetraether membrane lipid fluxes in the northeastern Pacific and the Arabian Sea: Implications for TEX_{86} paleothermometry. *Paleoceanography* **21**, PA4208.

Wuchter, C., Abbas, B., Coolen, M.J.L., Herfort, L., van Bleijswijk, J., Timmers, P., Strous, M., Teira, E., Herndl, G.J., Middelburg, J.J., Schouten, S., Sinninghe Damsté, J.S., 2006b. Archaeal nitrification in the ocean. *Proceedings of the National Academy of Sciences USA* **103**, 12317-12322.

Wyrtki, K., 1971. *Oceanographic Atlas of the International Indian Ocean Expedition*. USGPO, Washington.

Wyrtki, K., 1973. Physical Geography of the Indian Ocean. In: *The Biology of the Indian Ocean*. Springer, Berlin, pp. 18-36.

Zachos, J.C., Röhl, U., Schellenberg, S.A., Sluijs, A., Hodell, D.A., Kelly, D.C., Nicolo, M., Raffi, I., Lourens, L.J., McCarren, H., Kroon, D., 2005. Rapid acidification of the ocean during the Paleocene-Eocene Thermal Maximum. *Science* **308**, 1611-1615.

Zell, C., Kim, J.-H., Moreira-Turcq, P., Abril, G., Hopmans, E.C., Bonnet, M.-P., Lima Sobrinho, R., Sinninghe Damsté, J.S., 2013. Disentangling the origins of branched tetraether lipids and crenarchaeol in the lower Amazon River: Implications for GDGT-based proxies. *Limnology and Oceanography* **58**, 000.

Zink, K.-G., Wilkes, H., Disko, U., Elvert, M., Horsfield, B., 2003. Intact phospholipids - microbial „life markers“ in marine deep subsurface sediments. *Organic Geochemistry* **34**, 755-769.

SUMMARY

Paleoclimate reconstructions are vital for climate modelling and climate change predictions. Paleotemperature, an important variable in paleoclimate determinations, can be reconstructed using proxies. Some of them rely on specific organic compounds, so-called biomarker lipids. One of these organic paleotemperature proxies is the TEX_{86}, a ratio of different glycerol dibiphytanyl glycerol tetraether (GDGT) lipids produced by Thaumarchaeota. These archaea constitute a phylum whose members are ubiquitous in the environment, and are the second most abundant micro-organisms in the ocean. Their cell membranes mainly consist of GDGT-core lipids (CL) with attached polar head groups (also called intact polar lipid-GDGTs; IPL-GDGTs). IPL-GDGTs are often used as biomarkers for live Archaea due to the labile bonds between the head groups and the lipids, whose cleavage constitutes the first step in lipid diagenesis, leaving the more stable CL-GDGTs. Thaumarchaeal GDGTs contain different numbers of cyclopentyl or cyclohexyl moieties, and their relative proportions are dependent on the growth temperature. After cell death, IPL-GDGTs are transformed into CL- GDGTs which are exported from the water column to the sea floor and preserved over long timescales – up to hundreds of Myrs – and thus provide information about past sea surface temperatures. However, sedimentary Archaea producing the same GDGTs or differential degradation of GDGT isomers in the sediment could alter the original GDGT-distribution stored in the sedimentary archive and thus bias paleotemperature assessments.

In this thesis, the effect of post-depositional processes on biomarkers and proxies was investigated, specifically on the GDGT-distribution and the TEX_{86}. The applicability of IPL-GDGTs as biomarkers for live Archaea was critically assessed and the contribution of live Archaea to the sedimentary IPL-GDGT pool was studied. First, several extraction methods were tested, and experiments showed that Bligh-Dyer extractions were most capable of extracting all IPL-GDGTs, including relatively polar ones, such as those with a hexose, phosphohexose head group. However, further sample processing such as column chromatography can result in a reduction of the latter IPLs by up to 80%. Based on the results, a modified Bligh–Dyer extraction with as little further treatment as possible was used in the thesis to allow measurement of the full range of IPL-GDGTs in sediments, and silica column chromatography was additionally used for quantification of GDGTs derived from IPL-GDGTs and of CL-GDGTs.

Determination of IPL-GDGT concentrations in surface sediments from the Arabian Sea and a 186 mbsf core from the Peru Margin, showed that glycosidic IPL-GDGTs are preserved over geological time scales (Myr). IPL-GDGTs with a phosphate head group, however, were degraded much faster (within 7 kyr). Previously reported measurements of archaeal biomass in deeply buried sediments were based mainly on glycosidic GDGTs and are thus probably substantially overestimating of the actual number of live archaeal cells. Some sedimentary in situ production, based on the presence of sub-surface (~1 cmbsf) peaks of the phosphate-containing IPL-GDGTs was found. However, it was also observed that these IPL-GDGTs were more labile, probably due to a lack of matrix protection, and did not accumulate as IPL-GDGTs or CL-GDGTs. The minor amounts of in situ production in sediments were not influencing the TEX_{86} of the CL-GDGTs. The TEX_{86} of individual IPL-GDGTs showed differences dependent on the head group, with the highest TEX_{86} values in the dihexose-GDGTs, and the lowest values in the hexose, phosphohexose-GDGTs. These differences were universally observed in sediments, water column samples, and enrichment cultures, suggesting that they occur already upon IPL-assembly in the archaeal cell. Differences in degradation rates between thedifferent IPL-GDGTs and the differences in TEX_{86} per head group can cause small changes in IPL-derived TEX_{86} values upon progressing degradation, i.e. the hexose, phosphohexose-GDGTs with lower TEX_{86} values are degraded first resulting in slightly higher IPL-derived TEX_{86} values compared to CL-TEX_{86}, in accordance with other studies. A slight decrease of TEX_{86} with increasing oxygen exposure time and increasing water depth was found in the Arabian Sea. This trend could be explained with in situ production in the water column, as it was also observed in suspended particulate matter from the overlying water column.

In order to determine sedimentary in situ production, incubation studies with ^{13}C-labeled substrates were performed. The substrates used were phytodetritus from *Thalassiosira* diatoms, bicarbonate, pyruvate, glucose and mixed amino acids. However, no incorporation of ^{13}C-label was observed in the phytodetritus, glucose and amino acid labeling experiments, and no enrichment higher than 3‰ could be detected in the isoprenoid chains of any of the GDGT lipids when bicarbonate or pyruvate was used. This is in contrast to bacterial phospholipid fatty acids, which were shown to be substantially enriched in ^{13}C after incubation with labeled organic compounds. This suggests that sedimentary Thaumarchaeota are mainly autotrophic and only play a minor direct role in benthic organic carbon processing. The low incorporation rates suggest a low activity of Thaumarchaeota in marine sediments and/or a low turnover rate of thaumarchaeal IPL-GDGTs due to their low degradation rates, as a high background concentration of fossil IPL-GDGTs could mask the labeling. This also suggests that IPL-GDGTs are not as suitable for stable isotope probing experiments as bacterial phospholipids.

Thus, the work in this thesis has shown that some IPL-GDGTs can be preserved over geological time scales and are thus not an accurate measure for live archaeal biomass. Cell numbers and activity of sedimentary Thaumarchaeota based on glycosidic IPL-GDGT measurements may thus have previously been overestimated. In situ production might occur in sediments in small numbers, but is not large enough to significantly affect the TEX_{86}. In conclusion, post-depositional processes have, in the settings investigated, no impact on the functioning of the TEX_{86} as a paleotemperature proxy.

SAMENVATTING

Paleoklimaatreconstructies zijn essentieel voor het testen van klimaatmodellen en dus voor het voorspellen van toekomstige klimaatveranderingen. De paleotemperatuur, een belangrijke parameter in paleoklimaatbepalingen, kan met behulp van zogenaamde proxies worden gereconstrueerd. Sommige proxies zijn gebaseerd op specifieke organische stoffen, zogenaamde biomarker lipiden. Één van deze organische paleotemperatuurproxies is de tetraether index, TEX_{86}, een ratio van verschillende glycerol dibifytanyl glycerol tetraether (GDGT) lipiden, geproduceerd door Thaumarchaeota. Dit type archaea is alomtegenwoordig in het milieu als nitrificeerder en vormt de op één na in aantal belangrijkste groep microörganismen in de oceaan. Hun celmembraan bestaat voornamelijk uit GDGTs (zogenaamde 'core' lipiden, CL), met daaraan gebonden polaire kopgroepen (ook wel intacte polaire lipiden-GDGTs genoemd; IPL-GDGTs). IPL-GDGTs worden vaak als biomarker voor levende archaea gebruikt omdat de labiele binding tussen lipiden en kopgroepen snel na de dood van de archaea verbroken wordt. Hierdoor blijven de stabielere CL-GDGTs over. GDGTs in de celmembranen van Thaumarchaeota vertonen variatie in het aantal cyclopentyl- en cyclohexylgroepen, waarbij er meer ringen aanwezig zijn bij een hogere groeitemperatuur. Na de celdood worden IPL-GDGTs afgebroken tot CL-GDGTs en worden zij naar de zeebodem getransporteerd, waar zij gedurende langere perioden – tot wel honderden miljoenen jaren – bewaard kunnen blijven. De CL-GDGT distributie in oude sedimenten kan op deze manier de temperatuur van vroegere tijden reflecteren. Sedimentaire archaea, die dezelfde GDGTs produceren, of selectieve degradatie van specifieke GDGTs in het sediment, kunnen echter de originele GDGT-distributie in het sedimentaire archief veranderen en daardoor paleotemperatuurbepalingen beïnvloeden.

In het onderzoek beschreven in dit proefschrift werd de invloed van sedimentaire processen op GDGTs en de TEX_{86} proxy onderzocht. De toepassing van IPL-GDGTs als biomarkers voor levende archaea is kritisch geëvalueerd, alsmede de bijdrage van levende archaea aan de hoeveelheid sedimentaire IPL-GDGTs. In het eerste gedeelte van het proefschrift wordt het testen van extractiemethoden beschreven, waarbij aangetoond wordt dat Bligh-Dyer extractie de meest geschikte methode voor volledige extractie van IPL-GDGTs is, met inbegrip van IPL-GDGTs met sterk polaire kopgroepen, zoals hexose, fosfohexose GDGTs. De volgende stap in de opwerkingsmethode van GDGTs, de kolomscheiding, kan leiden tot een reductie in concentratie van sommige IPLs tot wel 80%. Om dit te vermijden werd er in dit onderzoek een Bligh–Dyer extractie toegepast met zo min mogelijke opeenvolgende opwerkingstappen om het verlies aan IPL-GDGTs sterk te beperken. Daartoe werd een silica kolomscheiding toegepast om GDGTs van IPLs en CL-GDGTs te scheiden en als aparte groepen te kunnen kwantificeren.

Door de bepaling van IPL-GDGT concentraties in sedimenten van een 186 m lange boorkern van de kustzone van Peru werd ondekt dat glycosidische IPL-GDGTs over langdurige tijdsperioden (miljoenen jaren) gepreserveerd kunnen worden. Daarentegen bleek dat IPL-GDGTs met een fosfaat-kopgroep in oppervlaktesedimenten van de Arabische Zee relatief snel (binnen zevenduizend jaar) werden afgebroken. Gepubliceerde schattingen van het aantal levende archaeale cellen in diepe mariene sedimenten zijn grotendeels op de concentratie van glycosidische IPL-GDGTs gebaseerd en overschatten daarom waarschijnlijk het aantal levende archaeale cellen. Maxima in concentraties van fosfaat-bevattende IPL-GDGTs vlak onder het sediment-wateroppervlak toonden aan dat er ook sprake is van benthische in-situ productie van nitrificerende Thaumarchaeota. Deze benthisch geproduceerde IPL-GDGTs zijn echter relatief labiel en worden snel afgebroken, waarschijnlijk door het ontbreken van matrixbescherming. De geringe hoeveelheid in-situ productie in sedimenten beïnvloedt daarom niet het oorspronkelijke TEX_{86} signaal van de CL-GDGTs.

De TEX_{86} –waarden van verschillende groepen van IPL-GDGTs verschilden afhankelijk van de kopgroep, met de hoogste TEX_{86} waarden voor de dihexose-GDGTs, en de laagste waarden voor de hexose, fosfohexose-GDGTs. Deze verschillen werden zowel in sedimenten, gesuspendeerd materiaal in de waterkolom, als in verrijkingsculturen van Thaumarchaeota waargenomen. Dit geeft aan dat deze verschillen reeds tijdens de biosynthese optreden. Verschillen in degradatiesnelheid tussen de verschillende IPL-GDGTs en de verschillen in TEX_{86} per IPL componentklasse kunnen tot kleine veranderingen in de TEX_{86} -waarde van IPL-GDGTs leiden; de hexose, fosfohexose-GDGTs met een lagere TEX_{86} waarde worden eerst afgebroken, resulterend in een hogere IPL-TEX_{86} waarde vergeleken met die van de CL-GDGTs. Deze verschillen zijn al eerder gerapporteerd. In de Arabische Zee dalen de TEX_{86} waarden van CL-GDGTs? met met toenemende waterdiepte. Dit kan verklaard worden met een toenemende bijdrage van GDGTs uit het diepere gedeelte van de waterkolom.

Om de omvang van de sedimentaire in-situ productie van GDGTs vast te stellen werden incubaties met ^{13}C-gelabelde substraten uitgevoerd. De gebruikte substraten zijn fytodetritus van *Thalassiosira* diatomeeën, bicarbonaat, pyruvaat, glucose en een mengsel van aminozuren. Er werd geen inbouw van het ^{13}C-label waargenomen in de experimenten waar fytodetritus, glucose en aminozuren gebruikt werden, terwijl in de experimenten met bicarbonaat en pyruvaat een verrijking van <3 ‰ werd gevonden. Bacteriële fosfolipiden, daarentegen, waren na verloop van de incubatie met organische substraten aanzienlijk verrijkt in ^{13}C. Dit geeft aan dat sedimentaire Thaumarchaeota voornamelijk autotroof zijn en maar een kleine rol spelen in de benthische verwerking van organische koolstof. De lage gemeten inbouwsnelheid van ^{13}C toont aan dat Thaumarchaeota in mariene sedimenten niet erg actief zijn of dat hun lipiden een lage omzettingssnelheid hebben. Dit laatste zou verklaard kunnen worden door hun lage degradatiesnelheid, waardoor er een hoge achtergrondconcentratie van fossiele IPL-GDGTs aanwezig is die het signaal van de nieuw geproduceerde, ^{13}C-gelabelde lipiden verdunnen. Archaeale IPL-GDGTs zijn dus minder goed bruikbaar voor stabiele isotopen inbouw-experimenten, in tegenstelling tot hun bacteriële equivalenten.

De resultaten beschreven in dit proefschrift laten zien dat sommige IPL-GDGTs over geologische tijdschalen kunnen worden gepreserveerd. Zij zijn dus niet goed bruikbaar als 'biomarker' voor levende Archaea. Eerdere bepalingen van het aantal levende archaeale cellen in diepe mariene sedimenten gebaseerd op de concentratie van glycosidische IPL-GDGTs hebben zeer waarschijnlijk tot een overschatting geleid. In-situ productie van kleine hoeveelheden GDGTs in sedimenten is mogelijk, maar niet belangrijk genoeg om de TEX_{86} te beïnvloeden. Uiteindelijk oefenen postdepositionele processen dus geen grote invloed uit op de toepassing van de TEX_{86} als paleotemperatuurproxy.

ACKNOWLEDGEMENTS

I have just told my new colleagues, whilst extracting mussel tissue, that what I enjoy most about my new position is the way we share the burden, the workload, the highs and the lows of the project we are in. In comparison, it makes a PhD seem like a long single-handed circumnavigation of the globe, with all the ups and downs lived through mainly by myself. But when I think back, it fills me with warmth to remember how there was always someone there to share the good and the bad times, to give me all the help I needed and to teach me how to do science.

Usually, this was Stefan. I could not have wished for a better supervisor and throughout those years, I always knew that I could walk into your office with any problem, question, and news (good or bad!). Thank you for being so understanding and encouraging. Jaap, you too, with your busy schedule, always had time for me when I needed it. I learned from both of you not only about data interpretation, methods and science, but also about science politics, people skills and lab management. Thank you especially for the hard work you put in when I bombarded you with drafts in the last months! Ellen, I did not only learn everything about HPLC from you, but you are also one of the best paper, poster and talk-editors. I won't forget how you were my replacement-mother when I had surgery, and how much it helped to have someone around to talk to - from woman to woman.

At this point, I would also like to thank the reading committee - Jan de Leeuw, Chuanlun Zhang, Tim Eglington and Jack Middelburg.

I really need to thank some inspirational people in my earlier science education – most of all my maths teacher Prof. Wieser, and Prof. Kopetzky, my female physics teacher, who, when I told her I was not confident about taking up a science subject at an engineering university because my maths wasn't good enough, kindly pointed out that all the boys in my year who scored lower on maths than me were planning on taking on engineering. And who supplied me with the calming mantra: "Die anderen kochen auch nur mit Wasser", meaning "Don't worry, we all put our pants on the same way". I had some great teachers in my university times as well, and the best one was probably my MSc-Thesis supervisor, Dave Cullen, whose playful approach to science I truly admire. If I ever get a spare ticket for an Antarctic cruise, I'll try to get you on board! Also thanks to Steve Rowland, who gave me a good reason (and a deadline) to finish, and to his group who has welcomed me so kindly in Plymouth.

When I was being interviewed for this PhD position, Stefan asked me what I thought

about lab work. I said “It’s usually repetitive and pretty boring, but it feels good to get the data, and, weirdly, I kind of enjoy it.” I have never enjoyed lab work as much as at the NIOZ, which is due to its incredibly well organized lab and all the fantastic people working there permanently. I would like to thank Marianne for everything she does in the lab (I didn’t realize HOW much I would miss you in the new lab!) and for instructing me when I first arrived. Thanks to Jort for all the instrument instructions, TOC measurement help, the HPLC-MS and GC-IRMS – and all the fun times we had with the gas bench, as well as Michiel and Monique for teaching me a lot about GC and helping me out with it. Thank you, Irene, for teaching me procedures and for pondering over mass spectra and extraction techniques with me; Anchelique, for putting up with me and sorting out the freeze drier after it spit oil across the room when I “refilled” it; Denise and Jord B. for being such fun “across bench neighbours”. Sharyn, thanks for all the help with analysis, planning and preparation, in your sediment – then – nutrients function! Mariska, you were a fantastic student, thanks for all the great work and the fun evenings we shared - with the most hilarious incidents. It was a pleasure to lend you my lab bench and “supervise” you! Marcel, I truly enjoyed our nerdy science talks and and shared love for isotopes, I will miss working with you around in the downstairs lab. Thanks for all the advice! Also Laura, I aspire to be as hard working and switched on as you are at one point in my career. It is also so easy to talk to you about anything, and sometimes I think that I should have followed all the advice you gave me on those long Switzerland evenings.

I had the pleasure to participate in two research cruises during my project, both on the R/V Pelagia, and I would like to thank the crew for all the effort they made and all the fun we had, that, especially the more steady crew and officers – Bert, Klaas, Freddy, and Corky. I had a wonderful time in the warm and calm Arabian Sea, and a great time in the beautiful waters of the North Sea and on the Iceland Shelf. I would like to thank everybody who helped me, as a newbie, on the PASOM cruise: Lara, Leon, Peter, Martin, Anne, Karoliina, Klaas and chief-scientist Gert-Jan. On my second cruise, I had a tight schedule, and there were many people who helped me out incessantly with the crazy amounts of work I had scheduled in. Thanks above all Yvonne, Marc, Luke, Sebastiaan, Marianne, Walther, Henk, Leon and Jan Dirk. Jack Middelburg, you were a great advisor along the way, and Lara, I enjoyed having you as a partner-PhD.

Coming back to Texel and the NIOZ has always felt like a warm, big hug, and this

is mainly because of the wonderful people there. All the support staff were always really helpful – Joke and Jolanda, Bert and Nelleke, Hilde, Ruud D. and W., and all the others. Thanks to the past and present PhD students and post-docs of the BGC department (and adopted) for the cakes and coffee breaks: Petra, Raquel, Darci, Isla, Francien, Joost, Thorsten, Angela, Arjan, Claudia, Cindy, Sebastian, Yvonne, Sandra, Elisabeth, Lisa, Martina and Daniela; Sebastian, Nicole, Rob, Eli, Veronica, Kim, Els, Luke, Cecile, Dave, John, Rachel, Santi, Nikki, Libby. Francien, thank you for all the motivational emails and for being such an inspirational example in about everything. Also thanks to all the fun students and guests we had at the department – Sylvia, Kevin, Laura Buckles, Kasia, Lara, Hendrik, Elizabeth J. and D., Sabrina and Amber.

Offices at the NIOZ are so special, as, by sharing only with two or three, you get the opportunity to bond! Rob, thank you for being the best office mate one can imagine (I told you many times already). It was a pleasure sharing with you for two years. Being able to understand Northerners won't really help me much in the South-West now, but you never know when it will come in handy to have mastered comprehending you. I never told you though how much I enjoyed watching a lovely romance evolve – but am truly happy that it grew such wonderful fruit. Also thanks to my office mates for the first months, Elda and Antje, who taught me many things about Texel, the NIOZ, and life in general. Thank you Elda for getting me involved with the sailing course on the island. Dave, I really hope that one day you will be happy with who and where you are, confident in your abilities and proud of your achievements. Martina, thanks for all the hugs and all the understanding, and for bearing with all my lab instructions. I enjoyed passing my knowledge on!

I was blessed to live in the most wonderful house I can imagine – and with so many housemates over the years! Potvis 6 friends, Charlie and Catarina, Arno and Lesley, Cornelia and Olga, thank you for all the shared dinners, the shared moaning, the shared drinks, the science talks, the politics talks, for putting up with me, my schedule, and my spice and alcohol shelf. I miss you all so bad, especially my long-term housemates Arno and Catarina. Also thanks to all the other Potvis inhabitants. Though there were quite a lot of long term residents there (Kate, Jez and Izzy, Lisa and Eli, Elisabeth, Jaime and Matias, Jenny, Viola, Hans, Anja, Santi, Amanda and Michiel and many others), the fun of the Potvis clearly also consisted in spending time with all the short-term residents – you know who you are!

When I was a child, I was obsessed with the long white beaches of the North Sea shores. As I arrived on Texel, it felt surreal to live in this beautiful place, and like I had always been longing for the beautiful light and the great skies. Texel has tried me and thrown the most terrible weather at me, and admittedly, there was a point when I did cave in – but looking back at the four years I spent there, I can only say that there wasn't a better place for me to be. Having travelled for years, it was one of the first places that made me feel like home – mainly because of all the lovely Texelaars. Understandably, people on Texel are sometimes reluctant to warm up to people staying for a short amount of time – it is hard to see them leave again. However, there were so many people who made me feel incredibly welcome: Everybody from the Youth Sailing Course, the surfers, windsurfers and kitesurfers and their extended circle of friends, the 12 Balcken-crew, the Texelaars working at the NIOZ, and the wonderful family Witte, who were always exceptionally warm and welcoming (and let me cuddle their cute little lambs).

I have also been fortunate to make a lot of friends on Texel. You know that your friends are true friends when they are with you in the good times and the bad times. There came a time when I realized that all those people I had been drinking and having fun with for years were also there to give me a hug, to cheer me on, to distract me or to just listen. Thank you, Lennart, Richard, Kristina, Anouk, Meinard and Rachel, Thalia and Leon, Allert, Matthijs, Anja, Michiel, Andreas, Tristan, Jenny, Ingmar, Maarten and Pedro.

Cees, thanks for being my first friend on Texel, for being my virtual running mate and for all the good talks we had. Your socializing skills and friend number on Texel are yet unrivalled for a NIOZ person. Craig, you are the most loyal friend one can imagine. Thanks for all the drinking evenings and fun times in Texel and Den Helder, for recruiting me as a friend for your then-girlfriend-soon-to-be-wife, for all the gossiping together, for all the hugs and your support. I won't thank you for introducing me to “headbangers”. Yvo, thanks for being so fun, happy and social, for making my friend Nicole so happy, for all the beach evenings and for the hugs which always came at the right time (like that one on the ferry), and for calling a taxi for me when I fell off my bike. Paul, you are great to talk to as you have a deep insight in human nature. Thanks for all the fun dancing, the laughs, the great music, the shared love of Iceland, the gin and tonics, the rum and ginger beers and the sake. Maybe not for the sake. We share memories of some iconic nights - thanks for being there for me.

Nicole, Julie, Darci, Juliane – I miss you so bad around here, I can't even tell you. I might be bad at keeping in touch, but I am thinking of you all the time. Juliane, you are the most inspiring, tough, sporty, smart, stunning girl I can imagine. I enjoyed "kind of" living with you and your endless supply of tasty sugary treats (I still wonder how you can be so slim despite of being constantly surrounded by sweets), and am really happy that we got so close during the past year. Nicole, I have no words for how much fun you brought to our lives. You brought Texel and its people even closer to our hearts. I love seeing how your life is just pure joy. It is amazing how much you care for your friends, and how you want them to be the best they can be. You really saved me. Thank you. And thanks for making me not only feel welcome on Texel, but also in my new home Plymouth! Julie, when I first met you, I was … impressed. But I didn't know that I and the mental girl would become such good friends (and what a loyal one you are!). You are the most organized, caring and selfless person I know – and when I heard that you would become a mum, I had not a single doubt that you would be the best mum ever (which you are). I actually cried when I got the news that Lauren was born (and that she was ginger). You are probably also the only person in the world who can extract age-old DNA from rocks! Be proud of it. Darci, you were my PhD-buddy, and we share so many precious memories. Through you, I have become so much more confident, open and content with myself. Your way of seeing the good sides in everyone (but not letting anyone screw with you either) is exemplary, and is why everyone loves you (except for the odd one or two weirdos who don't!). What I love most about the friendship with every single one of you is that we can all be truly ourselves, without hiding anything, and that is just beautiful.

An important aspect of my relationship with Texel was that I felt the need to leave and meet other people once in a while. I was lucky to make some lovely friends throughout the Netherlands, who would sail with me and teach me to sail and to speak Dutch: Bedankt vooral Esther en Han, maar ook Xavier, Frits, Koen, Elise, Rosa, Mark, Sytze, Carmen, Wilbert, Jenneke, Rosanne en alle Schuiters, CW en Anne, and also the international sailors – especially the Hamburgers, Christian and Niels. Elisabeth, thanks for keeping my home country alive in me, and for all the sailing fun. On to some more in Plymouth soon! Kayakpolo met de Odysseus club was geweldig – ik had helaas veel te weinig tijd om te trainen, sorry Djurre! De WEX heft mijn liefde voor de Waddeneilanden nog sterker gemaakt, en ik had het heel erg naar mijn zin tijdens het excursie geven, wandelen, fietsen, borrelen en dansen. Met jullie allen voelde ik me echt thuis in Nederland. Cornelia, thank you and Frank

for setting me up with not only a house in Leiden, but also with a circle of friends and a housemate which was this wonderful lady, Alexandra – who is a descendant of Amazons and Argonauts! You didn't know me at all before, Alexandra, and yet you had to bear living with me in the last three months of writing up my thesis to the soundtrack of Kill Bill, Les Misérables and Awolnation, and, to be honest, I probably couldn't have done it without you. Thanks for all the talks, shared laughter, and for getting me out of the house once in a while.

During all this time, I enjoyed travelling around to visit my old friends at home and in Europe – Katharina and Andreas, Steffi, Marion, Pernilla, Pelle and Mike, Giacomo, and my friends from the Vulcanus in Japan-programme. You are the kind of friends I don't see for a long time, but everytime we are together it feels like we have never been apart. Dasselbe gilt für meine Familie – ich halte es nur so leicht aus, so weit weg von Zuhause zu sein, weil ich so starke Wurzeln dort habe. Ich vermisse euch alle sehr und bedaure es furchtbar, dass ich nicht mehr an eurem Leben teilhaben kann und Annika, Alexandra, Lily und Leo nicht aufwachsen sehe. Meine Wände sind aber mit Zeichungen gepflastert! Und mit Tante Adis Karten! Grandma and Grandpa, I inherited determination and die-hard work ethics from you as the probably the most characteristic trait. Oma und Opa, von euch habe ich eindeutig die Entschlossenheit geerbt – steirischer und Waldviertler Sturschädel. Danke für die Unterstützung, Oma, und es tut mir leid, dass ich keinen Doktorhut bekomme! I was lucky to have an uncle who was a computer geek and left me his leftover computers early on – I probably owe all my IT skills to that Amiga 5000. Ich hatte das Glück, einen Computer-Geek als Onkel zu haben, der mir seine alten Geräte überliess. Die meisten meiner Computerfähigkeiten sind wahrscheinlich auf den Amiga 5000 zurückzuführen. Of course though, I owe most to my parents, who have continuously supported me in everything I showed an interest in, funded my studies and loved me unconditionally. Am meisten Dank schulde ich natürlich meinen Eltern, die mich immer in allen Interessen und (fast allen) Verrücktheiten gefördert haben, mich finanziell und emotionell unterstützt habe, und immer so furchtbar stolz auf mich sind.

Ich hab euch alle sehr lieb.

CURRICULUM VITAE

SABINE KERSTIN LENGGER was born on 22 April 1983 in Leoben, Austria. During her years of high school education at the BG & BRG I Leoben, her career wishes oscillated between becoming a scientist or a politician. She decided that obtaining the skills of a scientist clearly required more specific training, and studied for an MSc degree in Technical Chemistry, with a specialization in Biochemistry, at Graz University of Technology. A course in Arctic Microbiology on Svalbard gave her a taste of the exciting life of an environmental (marine) scientist. After an Erasmus year at the Universidad de Oviedo in Spain, an internship in Japan and writing her MSc thesis at Cranfield University, UK, in Environmental Diagnostics, she undertook a PhD at the Royal NIOZ Netherlands Institute for Sea Research on Texel in Marine Organic Biogeochemistry. She has recently joined the Petroleum and Environmental Geochemistry Group at the University of Plymouth, UK, as as post-doctoral research fellow to work within the ERC-funded *Outreach* project.